Arming Antibodies for Cancer Therapy: Transglutaminase-Mediated Toxin Conjugation

TECHNISCHE
UNIVERSITÄT
DARMSTADT

Vom Fachbereich Chemie
der Technischen Universität Darmstadt

zur Erlangung des Grades
Doctor rerum naturalium
(Dr. rer. nat)

Dissertation

Von

M.Sc. Ludwig Lukas Deweid
aus Pfungstadt

Referent:	Prof. Dr. Harald Kolmar
Korreferentin:	Prof. Dr. Beatrix Süß

Darmstadt 2020

Deweid, Ludwig Lukas: Arming Antibodies for Cancer Therapy: Transglutaminase-Mediated Toxin Conjugation

Darmstadt, Technische Universität Darmstadt

Jahr der Veröffentlichung der Dissertation auf TUprints: 2020

URN: urn:nbn:de:tuda-tuprints-114410

URL: https://tuprints.ulb.tu-darmstadt.de/id/eprint/11441

Tag der Einreichung: 2. Dezember 2020

Tag der mündlichen Prüfung: 3. Februar 2020

Veröffentlicht unter CC BY-NC-ND 4.0 International

https://creativecommons.org/licenses/

Die vorliegende Arbeit wurde unter der Leitung von Herr Prof. Dr. Harald Kolmar am Clemens-Schöpf-Institut für Organische Chemie und Biochemie der Technischen Universität Darmstadt von August 2016 bis August 2019 angefertigt.

Publications Derived From This Work

Research Articles

Deweid L, Parisien A, Bitsch S, Lafontaine K, Sagamanova I, Charette A, Kolmar H and Pelletier J (2020) Glutamine Scanning Towards Transglutaminase-Mediated Modification of an Antibody Fragment Crystallisable. *Manuscript prepared but submission postponed*.

Schneider H, Yanakieva D, Macarron A, **Deweid L**, Becker B, Englert S, Avrutina O and Kolmar H (2019) TRAIL-inspired multivalent dextran conjugates efficiently induce apoptosis upon DR5 receptor clustering. *ChemBioChem.* 20 (24), 3006-3012.

Ebenig A*, Juettner N. E*, **Deweid L***, Avrutina O, Fuchsbauer H-L and Kolmar H (2019) Efficient Site-Specific Antibody-Drug Conjugation by Engineering a Nature-Derived Recognition Tag for Microbial Transglutaminase. *ChemBioChem*. 20 (18), 2411-2419.

Dickgiesser S, **Deweid L**, Kellner R, Kolmar H and Nicolas R (2019) Site-Specific Antibody-Drug Conjugation Using Microbial Transglutaminase. *Methods in Molecular Biology*. 2012, 135-149.

Deweid L, Avrutina O and Kolmar H (2019) Tailoring Activity and Selectivity of Microbial Transglutaminase. *Methods in Molecular Biology*. 2012, 151-169.

Schneider H, **Deweid L**, Pirzer T, Yanakieva D, Englert S, Becker B, Avrutina O and Kolmar H (2019) Dextramabs: A Novel Format of Antibody-Drug Conjugates Featuring a Multivalent Polysaccharide Scaffold. *ChemistryOpen*. 8 (3), 354-357.

Deweid L, Neureiter L, Englert S, Schneider H, Deweid J, Yanakieva D, Sturm J, Bitsch S, Christmann A, Avrutina O, Fuchsbauer H-L and Kolmar H (2018) Directed Evolution of a Bond-Forming Enzyme: Ultrahigh-Throughput Screening of Microbial Transglutaminase Using Yeast Surface Display. *Chemistry: a European Journal*. 24 (57), 15195-15200.

Review Articles

Schneider H*, **Deweid L***, Avrutina O and Kolmar H (2020) Recent Progress in Transglutaminase-mediated Assembly of Antibody-Drug Conjugates. *Analytical Biochemistry*.
DOI: https://doi.org/10.1016/j.ab.2020.113615

Deweid L, Avrutina O and Kolmar H (2019) Microbial Transglutaminase for Biotechnological and Biomedical Engineering. *Biological Chemistry*. 400 (3), 257-274.

*These authors contributed equally to this work

Contributions to Conferences

Poster

Deweid L, Ebenig A, Juettner N. E, Lafontaine K, Avrutina O, Fuchsbauer H-L, Pelletier J and Kolmar H (2019) Efficient Site-Specific Antibody-Drug Conjugation by Engineering of Different Recognition Motifs for Microbial Transglutaminase. *Proteo, 19th Annual Symposium*, Quebec City, Canada.

Deweid L and Kolmar H (2018) A Novel Ultra-High Throughput Screen for Microbial Transglutaminase Activity. *Novel Enzymes 2018*, Darmstadt, Germany.

Deweid L and Kolmar H (2018) A Novel Ultra-High Throughput Screen for Microbial Transglutaminase Activity. *Protein Engineering Summit Europe*, Lisbon, Portugal.

Deweid L, Neureiter L, Hinz S, Gülzow F, Brenner L, Ulitzka M, Siegmund V, Valldorf B, Dickgießer S, Christmann A and Kolmar H (2017) Microbial transglutaminases as versatile tools for orthogonal protein conjugation – expanding the toolbox of available biocatalysts. *GdCh Wissenschaftsforum Chemie*, Berlin, Germany.

Lectures

Poster flash talk in the context of the poster session (2018) *Novel Enzymes 2018*, Darmstadt, Germany.

Awards and Scholarships

Scholarships

Fonds de recherche du Québec - Nature et technologies (FRQNT) travel scholarship awarded from the strategic cluster Centre in Green Chemistry and Catalysis (CGCC).

Table of Content

Publications Derived From This Work ii

Contributions to Conferences iii

Awards and Scholarships iii

Table of Content iv

1……Zusammenfassung und Wissenschaftlicher Erkenntnisgewinn 1

2……Scientific Novelty and Significance 4

3……Individuelle Beiträge zum Kumulativen Teil der Dissertation 7

4……Introduction 12

4.1. Cancer – an Overview 12

4.2. Antibodies for Cancer Treatment 14

4.3. Antibody-Drug Conjugates 16

4.4. *Streptomyces mobaraensis* Microbial Transglutaminase 20

4.4.1. Transglutaminase-Mediated Construction of Antibody-Drug Conjugates 23

4.5. Yeast Surface Display 25

5……Objective 28

6……References 31

7……Cumulative Section 39

7.1. Microbial Transglutaminase for Biotechnological and Biomedical Engineering 39

7.2. Directed Evolution of a Bond-Forming Enzyme: Ultrahigh-Throughput Screening of Microbial Transglutaminase Using Yeast Surface Display 58

7.3. Tailoring Activity and Selectivity of Microbial Transglutaminase 80

7.4. Recent Progress in Transglutaminase-Mediated Assembly of Antibody-Drug Conjugates 100

7.5. Efficient Site-Specific Antibody-Drug Conjugation by Engineering of a Nature-Derived Recognition Tag for Microbial Transglutaminase 101

7.6. Glutamine Scanning Towards Transglutaminase-Mediated Modification of an Antibody Fragment Crystallisable 151

8……Danksagung 159

9……Affirmations 161

1. Zusammenfassung und Wissenschaftlicher Erkenntnisgewinn

Die Anzahl an Krebsdiagnosen weltweit steigt stetig und Wissenschaftler verschiedener Disziplinen sind dadurch gefordert, innovative, effiziente und patientenfreundliche Therapien zu entwickeln. Unter anderem erwiesen sich Antikörper-Wirkstoff-Konjugate (ADCs) als eine vielversprechende Strategie zur Behandlung von Krebs, welche durch die Konjugation von potenten, organischen Molekülen an tumour-spezifische Immunglobuline generiert werden. In den letzten Jahrzehnten wurde eine Vielzahl chemischer und enzymatischer Methoden entwickelt, um die präzise Modifikation von Antikörpern zu ermöglichen. Das Enzym mikrobielle Transglutaminase (mTG) aus *Streptomyces mobaraensis*, welches natürlicherweise Isopeptidbindungen zwischen Glutamin- und Lysinseitenketten bildet, wurde unlängst für die Erzeugung von ADCs verwendet. Leider können natürlich vorkommende Aminosäuren humaner Antikörpern jedoch nicht mittels mTG-adressiert werden. Diese Einschränkung kann umgangen werden indem entweder peptidische Erkennungssequenzen auf genetischer Ebene in die natürliche Sequenz des Antikörpers eingefügt werden oder die Zuckerseitenkette der CH2-Domäne entfernt wird, wodurch Gln295 als Markierungsstelle verfügbar wird. Diese Arbeit beschäftigt sich mit der Optimierung der mTG-vermittelten Katalyse für die effiziente und schnelle Erzeugung von ADCs, wobei sowohl das eingesetzte Enzym als, auch der adressierte Antikörper modifiziert werden. Zu diesem Zweck wurden drei verschiedene Studien durchgeführt:

(1) Mikrobielle Transglutaminase ist ein nützliches Werkzeug für die Vernetzung unterschiedlichster Zielmoleküle, da es stabile Isopeptidbindungen zwischen Glutaminresten und primären Aminen bilden kann. Ein Zugang zu maßgeschneiderten Transglutaminasen wäre jedoch wünschenswert, da die bis heute nicht vollständig verstandene Substratspezifität des Enzymes zu heterogener Produktbildung führen kann. Dieser Teil der vorliegenden Arbeit konzentriert sich auf die Entwicklung eines Verfahrens zur Optimierung von mTG mittels Hefeoberflächendisplay (YSD) und fluoreszenzaktivierter Zellsortierung (FACS), um Varianten mit erhöhter Aktivität und veränderter Substratspezifität aus einem großen Spektrum zufallsmäßig generierter Mutanten, zu identifizieren. Aufgrund seiner intrazellulären Toxizität wurde mTG als inaktives Zymogen auf der Oberfläche von *Saccharomyces cerevisiae* Zellen präsentiert, welches anschließend durch Zugabe unterschiedlicher Proteasen in das reife Enzym umgewandelt wurde. Nach Zugabe des biotinylierten Glutamin-Donor-Peptids LLQG, katalysiert das oberflächenverankerte Enzym die Transamidierung des supplementierten Substrats an räumlich verfügbaren Lysinresten und ermöglicht so die Identifizierung aktiver Varianten aus einer Mischung mit inaktiven Varianten. Anschließend wurde eine randomisierte Bibliothek mit 3×10^8 verschiedenen Mutanten erzeugt. Nach fünf Runden FACS-Durchmusterung gegen das Substrat Biotin-GSGLLQG wurden 150 einzelne Klone auf der Oberfläche von Hefezellen analysiert und mit dem Wildtyp-Enzym verglichen. Nach rekombinanter Expression zeigten sechs Mutanten einen verbesserten Umsatz des

entsprechenden Peptids in einem HPLC-basierten Assay. Des Weiteren, markierte die dreifach Mutante R5.2 (S2G/R15C/M234L) den therapeutischen Antikörper Trastuzumab, welcher eine LLQG Erkennungssequenz trug, effizienter als die Wildtyp-Referenz. Durch optimierte Transglutaminasen mit erhöhter katalytischer Leistung könnten die Kopplungseffizienz und die Ausbeuten bei der ortsspezifischen Konstruktion von Antikörper-Wirkstoff-Konjugaten verbessert und dadurch deren Produktionskosten gesenkt werden.

(2) Neben der Optimierung des verwendeten Enzyms kann ebenfalls die genetisch inkorporierte mTG-Erkennungssequenz verbessert werden, um eine effizientere Katalyse zu erreichen. Die Reaktivität des Enzyms wird durch die Ladung und die Polarität der Aminosäuren, die das adressierte Glutamin umgeben, sowie der räumlichen Anordnung dieser Sequenz innerhalb des Zielproteins, beeinflusst. In früheren Arbeiten konnten Siegmund und Kollegen zeigen, dass natürliche Glutamin-Donor-Stellen intrinsischer mTG-Substrate nachgeahmt werden können um die Modifikation von therapeutischen Antikörpern mittels mTG zu ermöglichen. In diesem Teil der vorliegenden kumulativen Arbeit sollen Erkennungssequenzen, die die effiziente Markierung von Antikörpern ermöglichen, von den intrinsischen mTG-Substraten Dispase-Autolyse-induzierendes Protein (DAIP) und Streptomyces-Papain-Inhibitor (SPI$_P$) abgeleitet werden. Zu diesem Zweck wurden Sequenzen, die vom Gln6 des SPI$_P$, sowie von Gln39 und Gln298 des DAIP abstammen, mittels mikrowellenunterstützter Fmoc-Festphasenpeptidsynthese (SPPS) als Oligopeptide synthetisiert, und ihre Umsetzung durch mTG mit verschiedenen Linkersubstraten bestimmt. Nach der *C*-terminalen Fusion der jeweiligen Sequenzen an die schwere Kette des HER2-targetierenden Antikörpers Trastuzumab, wurde die mTG-vermittelte Modifikation der resultierenden Konstrukte mit dem Modellsubstrat *N*-(Biotinyl) Cadaverin (MBC) untersucht. Die von SPI$_P$ abgeleitete Sequenz DIPIGQGMTG (SPI7G) zeigte in vorhergegangenen Experimenten eine hohe Reaktivität und wurde aufgrund dessen für die Erzeugung eines ADC durch chemo-enzymatische zweischritt-Synthese, ausgewählt. Die *C*-terminal modifizierten Antikörper wurden in einer zeitlich stark begrenzen Reaktion mittels mTG mit *N*-[(1R,8S,9s)-bicyclo[6.1.0]non-4-in-9-ylmethyloxycarbonyl]-1,8-diamino-3,6-dioxaoctan (NH$_2$-PEG$_2$-BCN) modifiziert. Anschließend wurden die BCN-modifizierten Antikörper mittels SPAAC (strain-promoted alkine-azide cycloaddition) mit dem zytotoxischen Wirkstoff Monomethylauristatin E (MMAE) ausgerüstet, um das Wachstum HER2-überexprimierender Brustkrebszellen selektiv zu hemmen. Aufgrund der verbesserten Markierungseffizienz, war ein ADC der ausgehend von der neu identifizierten Sequenz SPI7G zusammengesetzter wurde, wesentlich wirksamer gegen HER2-positive SKBR3-Zellen als eine Referenz mit dem herkömmlichen LLQG-Motiv. Es konnte gezeigt werden, dass intrinsische mTG-Substrate einfach als Quelle für potente Erkennungssequenzen genutzt werden können. Innerhalb einer stark eingeschränkten Reaktionszeit von 1 h, wurde die neue Sequenz SPI7G am *C*-Terminus der schweren Kette von Trastuzumab, fünffach effizienter mit dem Molekül NH$_2$-PEG$_2$-BCN modifiziert als der LLQG-

markierte Referenzantikörper. Für die mTG-vermittelte Erzeugung von ADCs werden typischerweise Reaktionszeiten von $>16\,\mathrm{h}$ angewandt wobei es zu unerwünschten Schädigungen durch lange thermische Belastung, und somit Verringerung der Ausbeute kommen kann. Eine verkürzte Reaktionszeit, die durch effizientere Erkennungssequenzen ermöglicht wird, könnte diese Gefahr minimieren und somit den gesamten Prozess der mTG-vermittelten ADC Generierung verbessern.

(3) Der Einbau von spezifischen mTG-Erkennungssequenzen in das Grundgerüst von Antikörpern ist eine bewährte Methode für deren Markierung mit unterschiedlichen Zielmolekülen. Längere Sequenzen können jedoch die intrinsische Stabilität des Antikörpers beeinträchtigen und eine Immunantwort des Patienten während der Behandlung auslösen. In diesem Teil der vorliegenden kumulativen Arbeit wurden verschiedene Positionen eines humanen IgG Fc (fragment crystallisable) untersucht um Positionen zu identifizieren, die nach Austausch gegen Glutamin eine Markierung mittels mTG ermöglichen. Durch den Austausch einer einzelnen Aminosäure soll das potenzielle Risiko von Immunogenität und Instabilität im Vergleich zu langen Erkennungssequenzen, verringert werden. Zuerst wurde eine einfache Strategie für die rekombinante Expression des Antikörper Fc in *E. coli*-Zellen etabliert. Das Fragment wurde in ausreichenden Mengen durch Ni^{2+}-Affinitätschromatographie gereinigt und mittels nichtreduzierender SDS-PAGE, Thermal Shift Assays und Flüssigchromatographie-gekoppelter Massenspektrometrie hinsichtlich seiner strukturellen Integrität untersucht. Mithilfe von ortsgerichteter Mutagenese wurden Glutamin-Austausche innerhalb des Fc eingeführt und deren Markierung durch mTG in einem Fluoreszenz-basierten Assay untersucht. Von den 30 untersuchten Positionen wurden zwei Varianten (I253Q und Y296Q) mit einem fluoreszierenden Amin-Substrat durch mTG markiert. Diese vielversprechenden Ergebnisse müssen im Kontext eines vollständigen Antikörpers bestätigt werden, um ihren Nutzen für die mTG-vermittelte Konstruktion von ADCs zu belegen.

2. Scientific Novelty and Significance

The growing number of malignant cancer cases worldwide is an enormous threat for modern society. Therefore, the efforts of scientists from various research fields are focused on the development of efficient and viable therapeutic approaches. Recently, site-specific conjugation of highly potent organic compounds to tumour-binding immunoglobulins towards antibody-drug conjugates (ADCs) emerged as a promising strategy for the treatment of cancer. To allow for the precise modification of antibodies, multiple chemical and enzymatic methodologies have been developed within the last decades. Among them, application of microbial transglutaminase (mTG) from *Streptomyces mobaraensis* represents a promising approach. This enzyme that natively catalyses formation of isopeptide bonds between glutamine and lysine side chains, has been recently used for the assembly of ADCs. Although native residues within human antibodies cannot be employed in mTG catalysis, incorporation of reactive peptidyl linker sequences or truncation of the CH2 glycan to expose Gln295 were shown to overcome this limitation. In the present work, we focused on improving the performance of mTG catalysis towards efficient and rapid generation of ADCs by engineering both the enzyme and the targeted immunoglobulin. To that end, three independent studies were conducted:

(1) Microbial transglutaminase is a useful tool for the crosslinking of diverse molecules due to its ability to form stable isopeptide bonds between proteinaceous glutamine residues and primary amines. However, tailoring of transglutaminase is desired because the substrate indiscrimination of mTG can lead to heterogeneous product formation. In this part of my thesis, we aimed at the development of a molecular platform for the engineering of transglutaminase towards altered activity and selectivity by yeast surface display (YSD) in combination with fluorescence-activated cell sorting (FACS). Due to its intracellular cytotoxicity, mTG was displayed on the surface of *Saccharomyces cerevisiae* cells as an inactive zymogen. The precursor was converted into the mature enzyme by the addition of different proteases and a biotinylated glutamine-donor peptide LLQG was added. The surface-anchored enzyme catalyses the respective transamidation of the supplemented substrate at available lysine residues, thus enabling the identification of active variants. We demonstrated that genotype-phenotype correlation is provided and constructed a randomised library comprising 3×10^8 different mutants. After five rounds of FACS-screening against biotin-GSGLLQG, 150 individual clones were analysed on the surface of yeast cells and compared to the wildtype enzyme. Upon recombinant expression, six mutants revealed improved consumption of the corresponding peptide in an HPLC-controlled assay and a triple mutant R5.2 (S2G/R15C/M234L) labelled LLQG-tagged therapeutic antibody trastuzumab more efficiently compared to the wildtype counterpart. Site-specific conjugation mediated by mutant transglutaminases with elevated catalytic performance might improve coupling efficiency and increase yields upon the construction of antibody-drug conjugates.

(2) In addition to enzyme optimization, improvement of catalytic efficiency can be achieved upon engineering of the genetically incorporated mTG recognition sequence. The reactivity of the enzyme is influenced by charge and polarity of the amino acids surrounding the addressed glutamine as well as by the spatial arrangement of the targeted protein. In previous work, Siegmund *et al*. demonstrated that mimicking glutamine-donor sites of natural mTG substrates is a fruitful approach to yield peptidyl-linker sequences, which mediate proper modification by the enzyme. We aimed at the identification of novel recognition sequences derived from intrinsic mTG substrates dispase-autolysis inducing protein (DAIP) and *Streptomyces* papain inhibitor (SPI_P) towards efficient modification of therapeutic antibodies. To that end, sequences derived from Gln6 of SPI_P as well as Gln39 and Gln298 of DAIP were synthesized as oligopeptides by microwave-assisted Fmoc solid-phase peptide synthesis (SPPS) and their reactivity in mTG-mediated conjugation of different linker substrates was determined. Upon *C*-terminal fusion of the respective sequences to the heavy chain of HER2-targeting antibody trastuzumab, mTG-promoted modification of the resulting constructs with model substrate *N*-(biotinyl)cadaverine (MBC) was investigated. Having demonstrated high reactivity in preliminary experiments, SPI_P-derived sequence DIPIGQGMTG (SPI7G) was chosen for the assembly of an ADC in a twostep chemo-enzymatic approach. Engineered antibodies were labelled with *N*-[(1*R*,8*S*,9s)-bicyclo[6.1.0]non-4-yn-9-ylmethyloxycarbonyl]-1,8-diamino-3,6-dioxaoctane (NH_2-PEG_2-BCN) by mTG within a drastically shortened reaction time. Subsequently, BCN-modified monoclonal antibodies (mAb) were armed with the cytotoxic agent monomethyl auristatin E (MMAE) for selective growth inhibition of HER2-overexpressing breast cancer cells by strain-promoted alkyne-azide cycloaddition (SPAAC). Due to the superior labelling efficiency, an ADC assembled from the newly identified sequence SPI7G was significantly more potent on HER2-positive SKBR3-cells compared to a conventional LLQG-motif. We were able to show that intrinsic mTG substrates can be rapidly harnessed as a source of potent bioconjugation tags. Within a short reaction time of 1 h, a novel sequence SPI7G outperformed the conventional tag LLQG when located at the *C*-terminus of the heavy chain of trastuzumab. Such a short reaction time minimizes the risk of yield-limiting protein denaturation that often occurs during commonly applied overnight reactions.

(3) Incorporation of specific mTG recognition tags into the framework of antibodies proved to be a powerful approach for their labelling. However, longer sequences may interfere with the antibody's intrinsic stability and trigger the patient's immune response during treatment. We investigated different positions of a human IgG Fc (fragment crystallisable) to identify sites that allow for mTG-mediated labelling upon single residue substitution to reduce undesired immunogenicity and instability risks. In a first step, a straightforward strategy for the recombinant expression of the Fc in *E. coli* cells was established. The fragment was purified by Ni^{2+}-affinity chromatography in sufficient yields and analysed by non-reducing SDS-PAGE, thermal shift assays and liquid chromatography-mass spectrometry (LC-

MS) regarding dimeric assembly and native disulfide formation. Site-directed mutagenesis was used to specifically introduce glutamine substitutions within the Fc and the mutants were screened for labelling by mTG in a rapid fluorescent assay. Out of 30 analysed positions, two mutations, namely I253Q and Y296Q were efficiently labelled with a fluorescent amine substrate by mTG. These promising results need to be further confirmed in the context of a full-length antibody to study their usefulness for the mTG-mediated construction of ADCs.

3. Individuelle Beiträge zum Kumulativen Teil der Dissertation

1) **Deweid L**, Avrutina O and Kolmar H (2019) Microbial Transglutaminase for Biotechnological and Biomedical Engineering. *Biological Chemistry*. 400 (3), 257-274.

Beiträge von Lukas Deweid

- Initiale Idee und Literaturrecherche.

- Schriftliche Ausarbeitung des Reviews und Anfertigung aller darin enthaltenen Abbildungen.

Der Anteil von Lukas Deweid an genanntem Projekt belief sich auf insgesamt 85%. Die verbleibenden 15% verteilen sich auf O. Avrutina und H. Kolmar, die das Manuskript gelesen und konstruktiv korrigiert haben.

2) **Deweid L**, Neureiter L, Englert S, Schneider H, Deweid J, Yanakieva D, Sturm J, Bitsch S, Christmann A, Avrutina O, Fuchsbauer H-L and Kolmar H (2018) Directed Evolution of a Bond-Forming Enzyme: Ultrahigh-Throughput Screening of Microbial Transglutaminase Using Yeast Surface Display. *Chemistry: a European Journal*. 24 (57), 15195-15200.

Beiträge von Lukas Deweid

- Initiale Idee und Projektplanung zusammen mit H. Kolmar.

- Durchführung des Großteiles der Experimente.

- Verfassen des Manuskripts und Anfertigung aller darin enthaltenen Abbildungen.

Der Anteil von Lukas Deweid an genanntem Projekt belief sich auf insgesamt 75%. Die verbleibenden 25% verteilen sich auf L. Neureiter, S. Englert, H. Schneider, J. Deweid, D. Yanakieva, J. Sturm, S. Bitsch und A. Christmann für ihre Beteiligung am Experimentalteil sowie O. Arutina, H.-L. Fuchsbauer und H. Kolmar für Projektkoordination und Unterstützung beim Verfassen des Manuskripts.

3) **Deweid L**, Avrutina O and Kolmar H (2019) Tailoring Activity and Selectivity of Microbial Transglutaminase. *Methods in Molecular Biology*. 2012, Enzyme-Mediated Ligation Methods, 151-169.

Beiträge von Lukas Deweid

- Entwicklung der im Manuskript erläuterten Methoden.

- Verfassung des Manuskripts und Anfertigung aller darin enthaltenen Abbildungen.

Der Anteil von Lukas Deweid an genanntem Projekt belief sich auf insgesamt 85%. Die verbleibenden 15% verteilen sich auf O. Avrutina und H. Kolmar, die das Manuskript gelesen und konstruktiv korrigiert haben.

4) Schneider H*, **Deweid L***, Avrutina O and Kolmar H (2020) Recent Progress in Transglutaminase-Mediated Assembly of Antibody-Drug Conjugates. *Analytical Biochemistry. Accepted for publication.*

DOI: https://doi.org/10.1016/j.ab.2020.113615

*Diese Autoren haben gleichermaßen zu diesem Projekt beigetragen.

Beiträge von Lukas Deweid

- Initiale Idee und Literaturrecherche.

- Schriftliche Ausarbeitung des Reviews und Anfertigung darin enthaltener Abbildungen zusammen mit H. Schneider.

Der Anteil von Lukas Deweid an genanntem Projekt belief sich auf insgesamt 40%. Der Beitrag von H. Schneider als Co-Autor belief sich ebenfalls auf 40%. Die verbleibenden 20% verteilen sich auf O. Avrutina und H. Kolmar für ihre Unterstützung bei der Ausarbeitung des Manuskripts und der Anfertigung der Abbildungen. Das genannte Manuskript soll auf Einladung im Rahmen des Special Issues „Transglutaminases in Translation – Novel Tools and Methods Impacting on Diagnostics and Therapeutics“ in *Analytical Biochemistry* veröffentlicht werden.

5) Ebenig A*, Juettner N. E*, **Deweid L***, Avrutina O, Fuchsbauer H-L and Kolmar H (2019) Efficient Site-Specific Antibody-Drug Conjugation by Engineering a Nature-Derived Recognition Tag for Microbial Transglutaminase. *ChemBioChem*. 20 (18), 2411-2419.

* Diese Autoren haben gleichermaßen zu diesem Projekt beigetragen.

Beiträge von Lukas Deweid

- Durchführung der peptid-basierten Kinetiken.

- Erzeugung und Analytik der gezeigten Antikörper-Wirkstoff Konjugate.

- Verfassen des Manuskripts und Anfertigung von darin enthaltenen Abbildungen.

Der Anteil von Lukas Deweid an genanntem Projekt belief sich auf insgesamt 30% für die durchgeführten Experimente und die Beteiligung an der schriftlichen Ausarbeitung des Manuskripts. Der Beitrag von A. Ebenig und N. E. Juettner als Co-Autoren belief sich ebenfalls auf 30%. Die verbleibenden 10% verteilen sich auf O. Avrutina, H.-L. Fuchsbauer und H. Kolmar für die Koordination des Projekts sowie kritisches Lesen und korrigieren des Manuskripts.

6) **Deweid L**, Parisien A, Bitsch S, Lafontaine K, Sagamanova I, Charette A, Kolmar H and Pelletier J (2020) Glutamine Scanning Towards Transglutaminase-Mediated Modification of an Antibody Fragment Crystallisable. *Manuscript prepared but submission postponed*.

Beiträge von Lukas Deweid

- Initiation der internationalen Kooperation zwischen den Arbeitsgruppen Prof. J. Pelletier (Université de Montréal) und Prof. H. Kolmar (TU Darmstadt) sowie Organisation und Durchführung des informationellen und personellen Austausches zwischen den Instituten.

- Projektplanung zusammen mit J. Pelletier und H. Kolmar.

- Durchführung der initialen Experimente

- Schriftliche Ausarbeitung des Manuskripts und Anfertigung aller darin enthaltenen Abbildungen.

Der Anteil von Lukas Deweid an genanntem Projekt belief sich auf insgesamt 70%. Die verbleibenden 30% verteilen sich auf A. Parisien, S. Bitsch, K. Lafontaine und I. Sagamanova für ihre Unterstützung bei der Durchführung der Experimente, sowie A. Charette, J. Pelletier und H. Kolmar für die Koordination des Projekts und das kritische Lesen des Manuskripts. Die im Manuskript dargelegten Daten stellen einen signifikanten Erkenntnisgewinn gegenüber konventionellen Methoden zur Transglutamianse-vermittelten Modifikation von humanen Antikörpern dar. Von einer Veröffentlichung selbiger wurde jedoch bisher abgesehen, um in folgenden Experimenten wissenschaftlich hochwertigere Daten zu generieren. Zusätzlich soll dabei die Beziehung zwischen den Arbeitsgruppen Pelletier und Kolmar durch weiteren personellen Austausch gefestigt werden. Eine Veröffentlichung erfolgt nicht vor Einreichung der vorliegenden Thesis.

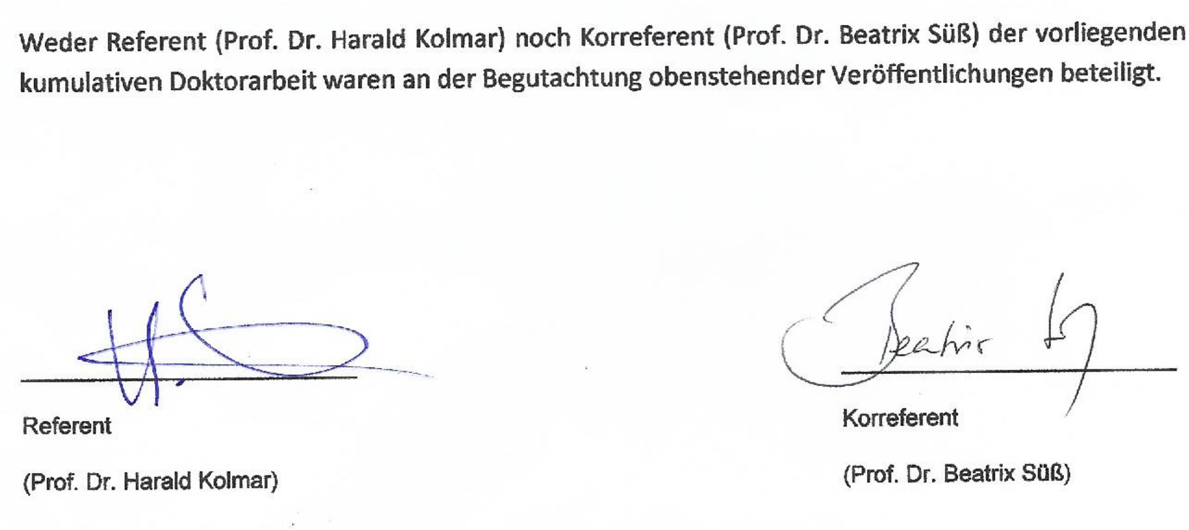

Weder Referent (Prof. Dr. Harald Kolmar) noch Korreferent (Prof. Dr. Beatrix Süß) der vorliegenden kumulativen Doktorarbeit waren an der Begutachtung obenstehender Veröffentlichungen beteiligt.

Beatrix

Referent

(Prof. Dr. Harald Kolmar)

Korreferent

(Prof. Dr. Beatrix Süß)

Des Weiteren bestätige ich, Ludwig Lukas Deweid, die Richtigkeit der obenstehenden prozentualen Angaben zur Beteiligung an sämtlichen genannten Veröffentlichungen, und erkläre nicht an der Begutachtung selbiger beteiligt gewesen zu sein.

Datum:

Unterschrift:

Ludwig Lukas Deweid

4. Introduction

The vast majority of human cells are constantly dividing to induce tissue growth and prevent age-dependent malfunction. Though all cells - with only few exceptions - carry identical copies of the genome, their lifespan varies from days to years, depending on the function of the respective cell. While fat cells, adipocytes, for instance last approximately 10 years,[1, 2] enterocytes of the small intestine renew themselves every 3-4 days.[3] This simplified example demonstrates that cell division is a very tightly regulated process, which comprises numerous genetic and physiological parameters. If a normal gene that is involved in differentiation- or growth-regulating pathways (proto-oncogene) is damaged by a mutagenic agent, it might become tumourigenic and promote unregulated proliferation (oncogene).[4] A single cell repairs on average ~20,000 potentially mutagenic DNA damages (hydrolysis, oxidation and methylation) plus 100,000 – 1,000,000 polymerase-induced replication errors per day.[5] Overburden of this highly-efficient machinery can result in unregulated cell division and upregulated tissue growth, having drastic effects on the entire organism. Abnormal cell division is a symptom shared by all subtypes of cancer; the corresponding genotypes can be however diverse since multiple genes are involved in growth regulation. Moreover, phenotypes of tumour cells often vary between subclasses. Consequently, the term "cancer" should be seen as a kind of headline that summarizes different diseases with multiple causes rather than a solitaire illness with a defined pattern of symptoms. To date, approximately 800 varying subtypes of cancer that differ in genotype, phenotype and the location of the affected organ are assumed.[6] One can easily imagine that the treatment of such a plethora of diseases by a single agent that spares healthy cells, like in the concept of "magic bullet" by Paul Ehrlich, is illusive.[7] Nevertheless, the modern research does not dissuade itself from envisioning fruitful approaches to provide access to more effective and patient-friendly therapeutic options.

4.1. Cancer – an Overview

The history of cancer dates back to prehistoric times when dinosaurs have populated the planet. Benign tumours could be detected in different samples of the family *Hadrosauridae* as well as malignant tumours in *Edmontosaurus*, a species of the same family that has lived approximately 70 million years ago.[8] The oldest written documentation of cancer in humans is presented in ancient Egyptian papyri (Edwin Smith and Georg Ebers papyri) from 1500 – 1600 BC. These transcripts are based on records from the 27th century BC and describe primeval methods of treatment, including what is believed to be the first mentioning of breast cancer.[9] Though roughly 4,700 years have passed since that time, curing cancer still remains a demanding challenge for physicians, oncologists and biologists around the globe. In 2018, approximately 18.1 million new patients worldwide were diagnosed with cancer while 9.6 million cancer-related deaths were registered and recent studies estimate that ~600,000 US citizens are about to pass away as a result of cancer in 2019.[10, 11] In men, 14.5% of 9.5 million new cases are lung cancer, followed by prostate (13.5%) and colorectal tumours (10.9%). In women, the most frequently affected organs are breasts, colorectum and lungs comprising 24.2%, 9.5% and 8.4% of 8.6 million new cases, respectively. Global incidence numbers are constantly rising (Figure 1) and the reasons therefore are diverse but include aging and growth of the population, an increasingly unhealthy lifestyle of tobacco and alcohol abuse, physical inactivity, obesity and poor diet, as well as incautious reproduction pattern that promote viral infections.[10, 12] Regardless, survival rates are improving as a consequence of gained knowledge of cancer mechanisms, awareness and elucidation campaigns, progress in diagnosis and constant development of novel therapeutic options.[13-15]

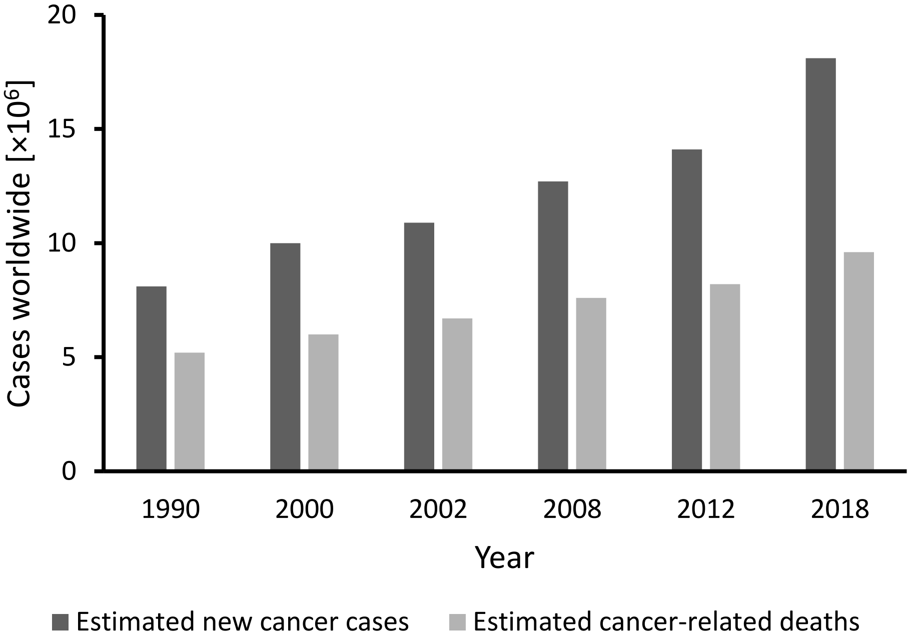

Figure 1: Estimated numbers of new cases und cancer-related deaths worldwide according to the American Cancer Society, Atlanta, USA and the International Agency for Research on Cancer, Lyon, France from 1990-2018.[10, 12, 16-19]. Of note, time scale is not linear.

Being already mentioned around 400 BC by the “father of medicine”, Greek physician Hippocrates of Kos, surgery remained the predominant option for cancer treatment until the recently discovered X-ray radiation gave rise to radiotherapy at the end of the 19th century.[9, 20] Ionizing radiation is locally applied to cause deathful DNA damage within tumour cells while intending to spare healthy surrounding tissue.[21] However, surgery and radiotherapy were limited to solid tumours and their success rates plateaued due to irrepressible micrometastases.[22, 23] During the 1940s and 1950s, often in World War II-related programs, a plethora of chemotherapeutic drugs such as alkylating agents (nitrogen mustard, chlorambucil, cyclophosphamide), folate antagonists (methotrexate) or nucleotide analogous (5-fluorouracil, 6-mercaptopurine) were synthesised and promising results were achieved in the treatment of leukemia and lymphomas.[22, 23] In the 1960s, a synergistic effect was observed applying surgery, radio- or chemotherapy in combination leading to the invention of adjuvant cancer treatments.[23] Chemotherapy is still an important option for the treatment of cancer today even though drastic side-effects for the patient may occur due to the drugs' unspecific mode of action. Chemotherapeutic agents are not able to discriminate between healthy and malignant cells. They interfere with cell division and kill tumour cells due to their rapidly dividing nature. Unfortunately, quickly dividing healthy cells are equally affected leading to undesired side-effects including nausea and vomiting, hair loss, cognitive dysfunction (CRCI; chemotherapy-related cognitive impairment), fatigue, sexual dysfunction or infertility.[24-26] In general terms, chemotherapeutic drugs possess a remarkable cytotoxicity but suffer from low target specificity during oncological application, which rises a demand for more patient-friendly therapeutic options.

4.2. Antibodies for Cancer Treatment

Antibodies comprise a class of proteins that are secreted by B-lymphocytes and mostly plasma cells as a part of the adaptive immune response in vertebrates.[27] These glycoproteins are also called immunoglobulins and can be divided into five different isotypes according to their structure and function during immune response (IgA, IgD, IgE, IgG and IgM). IgG antibodies, the most predominantly found isotype in human serum, are involved in the elimination of pathogens such as microbes and viruses.[28] They are heterotetrameric molecules that consist of two heavy (H) and light (L) chains covalently linked via four intermolecular disulfide bridges within the hinge region (see Figure 2). Possessing a Y-shaped pattern, their "arms" are referred to as Fabs (fragment antigen binding) while the "stem" is called Fc (fragment crystallisable). Located within the Fab of an IgG, six hypervariable areas (three per chain) called complementarity-determining regions (CDRs) assemble the antibody's paratope, which mediates binding to the targeted molecule - the antigen. Consequently, IgG antibodies comprise two paratopes (one per Fab) and are therefore bivalent molecules. Once the IgG has bound to its antigen, the effector function of the Fc triggers the host's immune system. Complexing of complement-activation protein C1q induces the classical pathway of the complement system and finally leads to the formation of the membrane attack complex (MAC) that perforates the pathogen's cell membrane.[28] Additionally, phagocytes are attracted that eliminate the target by phagocytosis (CDC; complement-dependent cytotoxicity).[29]

By binding of the Fc to the Fcγ-receptor III (CD16), IgGs recruit effector cells such as natural killer cells (NK cells) to lyse the pathogen by secreting perforin, granzymes, tumour necrosis factor α (TNF-α) and interferon γ (IFN-γ) in a process called antibody-dependent cell-mediated cytotoxicity (ADCC).[30, 31] The Fc portion of an IgG consists exclusively of the constant CH2 and CH3 domains of the heavy chain and possesses a single *N*-glycosylation at Asn297 (see Figure 2), which stabilises the antibody and participates in binding to different receptors.[32] Besides triggering the immune system to lyse pathogens, antibodies are able to directly neutralize infectious bodies or toxins. By binding to proteins or domains that are crucial for cell penetration, antibodies are able to suppress their pathogenic character and mediate degradation.

Even though their precise target recognition and the ability to induce different parts of the immune defence have been to that time unknown, antibodies were used already in the 1890s to treat diphtheria by transferring blood of immunized animals.[22, 33] Within the following century, their remarkable features raised strong interest in view of applications in medicine, especially in tumour therapy.

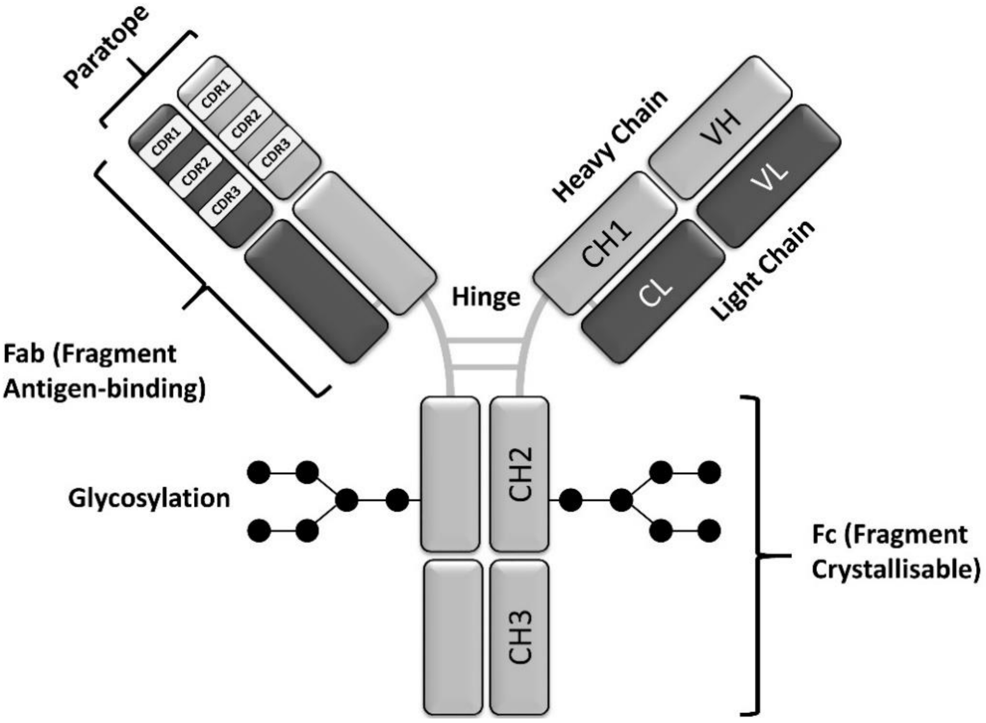

Figure 2: Schematic illustration of a human full-length IgG antibody. IgGs are heterotetrameric glycoproteins consisting of two identical heavy and light chains that are covalently linked via disulfide-bridges within their hinge region. The Fab fragment mediates binding to the respective antigen and comprises three complementarity-determining region (CDRs) per chain that assemble the antibody's paratope. *N*-glycosylation of the Fc at Asn297 contributes to the effector function and binding to different receptors of immune cells.

The groundbreaking invention of hybridoma technology in 1975 has laid the cornerstone for the development of therapeutic antibodies for cancer treatment. Till that day, polyclonal antibodies binding different epitopes of an antigen were obtained from immunized animals such as mouse, rat, sheep or goat. Milstein and Köhler have immortalized murine B-cells by fusion to myeloma cells to yield hybrid cells secreting monoclonal antibodies (mAb) in high yields, which were able to bind to a single epitope.[34] However, poor results were obtained from initial clinical trials due to the intrinsic immunogenicity of mouse/rat antibodies caused by their large size and dissenting glycosylation pattern.[22]

The massive progress in genetic engineering at the end of the 20th century opened avenues for the approval of the first anti-tumour mAb, CD-20 targeting rituximab, by the Food and Drug Administration (FDA).[22, 35] At the end of 2018, a total of >80 antibody-based therapeutics have been approved for various applications including immunosuppression, treatment of cancer, autoimmune diseases and viral infections. Moreover, 570 are currently in ongoing clinical trials of different stages.[36] These numbers impressively illustrate the huge potential of mAb biotherapeutics, and a plethora of studies have demonstrated their beneficial effect for the treatment of different diseases. However, especially in solid tumours, the effect of mAbs as a single agent is often limited due to their low potency, slow tissue penetration and the development of resistance pathways.[37, 38] Consequently, mAbs are often applied in adjuvant therapy in combination with surgery, chemo- or radiotherapy.[38]

4.3. Antibody-Drug Conjugates

State-of-the-art therapeutic options for cancer treatment have obvious advantages and disadvantages. Radiotherapy and surgical excision of cancerous tissue are straightforward methodologies but are incapable of treating micrometastases and are limited to accessible, solid tumours.[22] Chemotherapeutic drugs are highly cytotoxic. Though they have achieved good results in the treatment of hematologic cancers, their unspecific mode of action leads to high systemic toxicity and severe side-effects for the patient. Therapeutic antibodies are remarkably precise towards their respective target protein, which reduces off-target activity, but they suffer from comparably low potency.[38]

Antibody-drug conjugates (ADCs) intend to overcome the limitations of conventional chemotherapeutics and monoclonal antibodies by combining the benefits of both well-established strategies. In this class of molecules, small cytotoxic compounds are covalently linked to a tumour-targeting antibody via a chemical linker (Figure 3). In the context of an ADC, the antibody functions as a vehicle that transports its payload to the tumour environment. Upon binding to a cell-surface antigen, usually an overexpressed receptor, the ADC is internalized through receptor-mediated endocytosis. The formed endosome fuses with the late lysosome where the antibody is degraded and the payload is released to exhibit its cytotoxic action. Once released from the ADC, hydrophobic drugs may pass through membranes and harm neighboring cells by bystander killing (Figure 4). This effect can be beneficial for the targeting of inhomogeneous cancers and locally inaccessible cells but might cause adverse effects by damaging healthy tissue.[39] Since ADCs are designed to be stable in circulation and release their payload preferably in tumour tissue, unspecific off-target toxicity is reduced, which results in an improved therapeutic index of the drug. However, besides payload-mediated cell killing, ADCs can also execute anti-tumour activity by inducing ADCC or CDC and receptor blocking based on the mechanism of the parent antibody.[40, 41]

In general, ADCs comprise a targeting antibody, a chemical linker entity and a cytotoxic agent (Figure 3). The suitable monoclonal antibody should possess certain biophysical properties and be highly specific for its target. Usually, antigens that are massively overexpressed on malignant cells but almost absent on normal tissue are preferred as targets to spare healthy cells. However, ADC efficiency does not correlate directly with the copy number of the addressed antigen since further properties such as the internalization rate contribute therein.[42] Recent studies have demonstrated that careful fine-tuning of an ADC also allows for the targeting of antigens such as Trop-2 (trophoblast cell-surface antigen 2; M1S1) or EGFR (epidermal growth factor receptor) that are expressed on both cancerous and healthy cells (for further details also see Section 7.4 of this work).[40, 43]

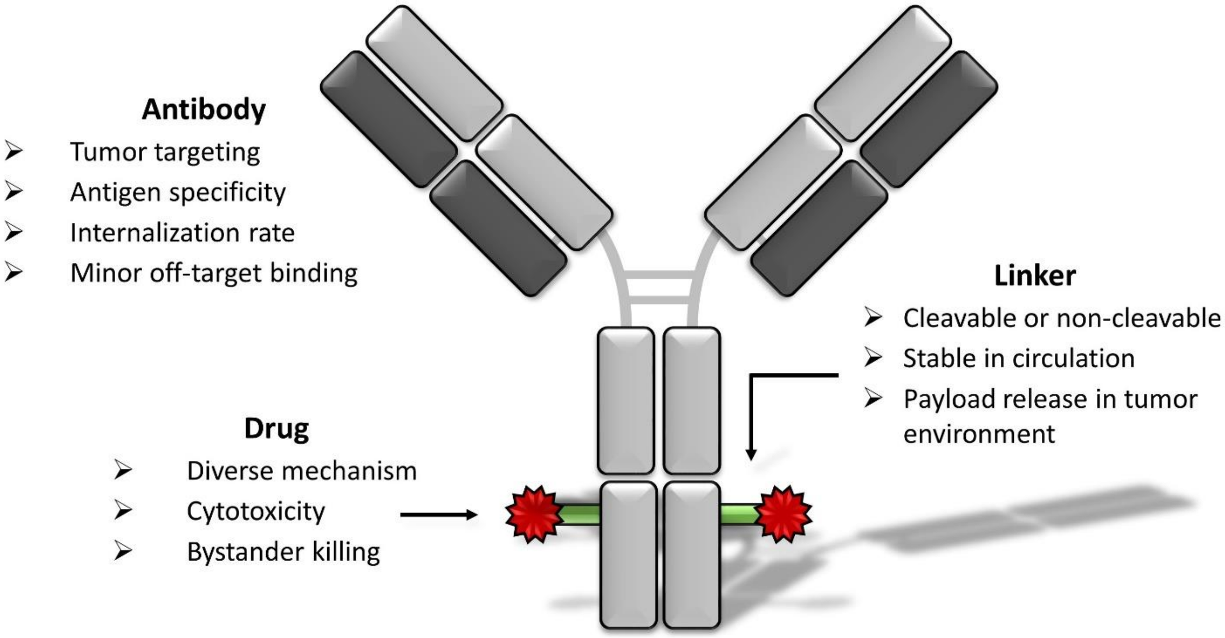

Figure 3: Schematic depiction of antibody-drug conjugates and key properties of the corresponding moieties. The tumour-binding antibody is supposed to comprise good biophysical properties and high target specificity. It functions as a vehicle that transports its warhead to the tumour but can still exhibit ADCC, CDC and neutralization according to the parental antibody's mode of action.[40, 41] The chemical linker covalently links the targeting moiety to the payload and is designed to be stable in circulation to prevent systemic toxicity. Cleavable linkers release their cargo protease- or pH-dependently in the tumour environment while non-cleavable linkers rely on intracellular degradation of the mAb. The cytotoxic drug mediates cell killing according to its mode of action. Upon lysis of the targeted cell, bystander killing of neighboring cells can be exhibited: an effect that can be beneficial for targeting of inhomogeneous tumours.[39]

The chemical linker that covalently connects the antibody and its payload is supposed to be stable in circulation to prevent premature drug release and mediate warhead liberation upon tumour accumulation. Linker chemistry can be chosen according to the cleavable or non-cleavable character of a linker. Non-cleavable linkers are thought to be more stable in circulation and the cargo is released after intracellular degradation of the antibody.[44, 45] Cleavable linkers are less stable and may suffer from partial drug loss. However, they provide rapid release of the drug under particular conditions. To that end, different approaches were developed including pH-sensitive hydrazone linkers that decompose in the acidic microenvironment of the lysosome,[45, 46] disulfide-containing linkers that are reduced in the cytosol, and oligopeptides such as valine-citruline (Val-Cit) or PVGLIG that are intra- or extracellularly cleaved by proteases cathepsin B (CatB) or matrix metalloproteinase-2 (MMP-2), respectively.[45, 47-49] Moreover, polarity of the utilized linker should be considered because an elevated hydrophobicity might prompt aggregation, resulting in hepatotoxicity and accelerated degradation.[42]

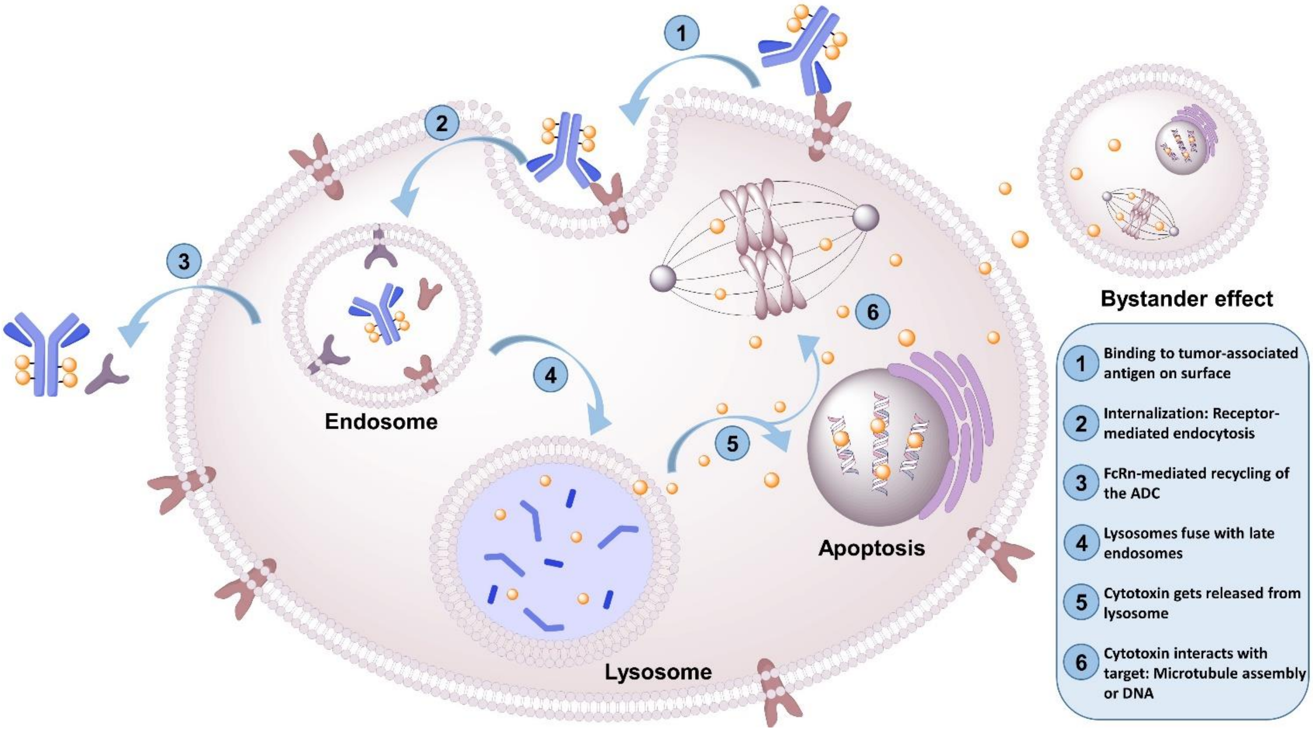
1
2
3
Endosome
4
Lysosome
5
6
Apoptosis
Bystander effect
1 Binding to tumor-associated antigen on surface
2 Internalization: Receptor-mediated endocytosis
3 FcRn-mediated recycling of the ADC
4 Lysosomes fuse with late endosomes
5 Cytotoxin gets released from lysosome
6 Cytotoxin interacts with target: Microtubule assembly or DNA

Figure 4: Internalization of antibody-drug conjugates through receptor-mediated endocytosis. A tumour-specific ADC binds to an overexpressed receptor and is internalized through endocytosis. The endosome fuses with the late lysosome, leading to degradation of the ADC. The cytotoxic cargo is released and exhibits potent cell killing by interfering with DNA or microtubule assembly.[148]

To mediate efficient anti-tumour activity, different warheads can be installed. Thus, antimitotic agents such as maytansinoides or auristatin analogues interfere with mitotic spindles by suppressing tubulin polymerisation, leading to apoptosis of the cell.[50] Duocarmycins and pyrrolobenzodiazepines are small molecules secreted by *Streptomyces* species that specifically bind to the minor groove of the DNA and exhibit potent cell killing by alkylation of adenine at N3[51] and guanine at C2 position, respectively.[52] Calicheamicins are DNA-damaging probes that cause lethal DNA double-strand breaks by a unique mode of action.[50]Amanitins are fungus-derived toxins that mediate cells death by extremely potent inhibition of RNA polymerase II, while camptothecins are plant alkaloids that bind to DNA topoisomerase I to initiate apoptosis.[50]

80 ADCs are currently in clinical trials.[53] Five ADCs and one fragment variable (Fv) drug conjugate (moxetumomab pasudotox[54]) are authorized by regulatory agencies for the treatment of solid and hematologic malignancies (Table 1). Conventionally, ADC assembly is based on the reactivity of intrinsic lysine or cysteine residues towards organic compounds. Hence, activated carboxylic acids are utilized to form amide bonds at solvent-exposed lysine side chains while maleimides are employed to modify thiol groups of cysteines upon reduction of interchain disulfide bonds under mild conditions.[42] Wang *et al.* demonstrated that approximately 40 sites of an anti-CD56 antibody are modified when lysine residues are addressed[55] and more recent studies by Kim *et al.* showed that 70 out of 92 available sites (88 lysine residues plus 4 *N*-terminal primary amines) of FDA-approved trastuzumab emtansine that comprises an average drug-to-antibody ratio (DAR) of 3.5 were coupled to antimitotic DM1.[56] Assuming distribution to 40 different positions, more than 10^6 potential conjugates could be formed. When addressing the eight interchain hinge cysteines of IgGs by partial reduction, this number drastically drops but still comprises a variable stoichiometry of >100 species.[57] This statistically distributed attachment of payloads results in the formation of a heterogeneous population that contains multiple species with different ligation sites and variable DARs of 0-8, all possessing potentially varying pharmacokinetic properties.[56]

Table 1: Overview of ADCs and Fv-drug conjugates currently approved for the treatment of different cancers. Unlike conventional ADCs, moxetumomab pasudotox does not comprise a full-length IgG but consists of a murine immunoglobulin variable domain (Fv). The CD22-targeting Fv is genetically fused to a truncated variant of *Pseudomonas* exotoxin PE38 and recombinantly expressed in *E. coli* cells. [54]

Drug (Trade name)	Cancer	Conjugation strategy	Linker Chemistry	Warhead	Ref.
Gemtuzumab ozogamicin (Mylotarg)	CD33-positive acute myeloid leukemia	Amide (lysine)	Hydrazone (pH-labile)	Calicheamicin	[58, 59]
Brentuximab vedotin (Adcetris)	CD30-positive Hodgkin lymphoma and ALCL	Thiol-maleimide (native cysteine)	Val-Cit-PABC (CatB-cleavable)	Monomethyl auristatin E	[60-62]
Trastuzumab emtansine (Kadcyla)	HER2-positive breast cancer	Amide (lysine)	SMCC (non-cleavable)	DM1	[56, 63]
Inotuzumab ozogamicin (Besponsa)	CD22-positive B-cell precursor acute lymphoblastic leukemia	Amide (lysine)	Hydrazone (pH-labile)	Calicheamicin	[64]
Polatuzumab vedotin (Polivy)	CD79b-positive diffuse large B-cell lymphoma	Thiol-maleimide (engineered cysteine)	Val-Cit-PABC (CatB-cleavable)	Monomethyl auristatin E	[65-67]
Moxetumomab pasudotox (Lumoxiti)	CD22-positive hairy cell leukaemia	Genetic fusion	-	Truncated *Pseudomonas* exotoxin PE38	[54]

Abbreviations: ALCL - anaplastic large cell lymphoma; CatB – cathepsin B; Fv - fragment variable; PABC - *p*-aminobenzyloxycarbonyl; SMCC - succinimidyl-4-(*N*-maleimidomethyl)cyclohexane-1-carboxylate

In addition to the above-described features, different studies found that conjugation site and homogeneity of payload attachment influence the therapeutic index and efficiency of the ADC.[57, 68, 69] In a pioneering study by Junutula *et al.*, a site-specifically assembled ADC of near-homogeneous nature revealed diminished clearance, reduced systemic toxicity and a notably improved therapeutic index in rats and cynomolgus monkeys compared to its conventionally produced counterpart.[57] To allow for the precise modification of antibodies at selected sites, numerous bioorthogonal chemical and enzymatic labelling methodologies have been to date developed, among them THIOMAB-technology[57], conjugation under catalysis with sortase A,[70] formylglycine-generating enzyme[71] or phosphopantetheinyl transferase,[72] as well as glyco-engineering[73, 74] and ribosomal incorporation of unnatural amino acids.[75, 76]

The majority of ADCs currently in clinical trials are constructed by randomly distributed conjugation to multiple available sites of the parental antibody. However, a pronounced shift towards more homogeneous conjugates was observed. In 2017, 15% of clinical trials investigated site-specifically assembled ADCs, which represents a three-fold increase within the previous four years.[77, 78] This trend is confirmed by the first approval of a site-specifically assembled ADC polatuzumab vedotin by the FDA in 2019 (Table 1).[65-67]

4.4. *Streptomyces mobaraensis* Microbial Transglutaminase

Transglutaminases (TGases) are protein-glutamine γ-glutamyltransferases (EC 2.3.2.13), present in multiple different species including mammals, invertebrates,[79] plants,[80] fungi[81] and microorganisms.[82] In nature, they primarily catalyse an acyl-transfer reaction under ammonia release to form intra- or intermolecular isopeptide bonds. Typically, the γ-carboxamide function of protein- or peptide-bound glutamines servers as an acyl-donor, while the ε-amino group of lysine residues acts as the acyl-acceptor, to form a stable γ-glutamyl-ε-lysine linkage (Figure 5C).[83] Other primary amines can also act as acyl-acceptors, leading to the incorporation of different amines into the targeted protein. In the absence of primary amines, water serves as the acyl acceptor, resulting in the deamidation of glutamine into glutamic acid.[79] Interestingly, the attachment of ω-hydroxyceramide to involucrin of human keratinocytes through esterification has been demonstrated as an additional mechanism of transglutaminase 1.[84]

In humans, eight different transglutaminases and an additional catalytically inactive one are known to date.[79] These Ca^{2+}-dependent enzymes contribute to various physiological processes including blood coagulation, bone tissue formation, hematopoiesis, spermatogenesis, membrane building and cell apoptosis. To date, not all of their biological functions have been discovered.[79, 85, 86]

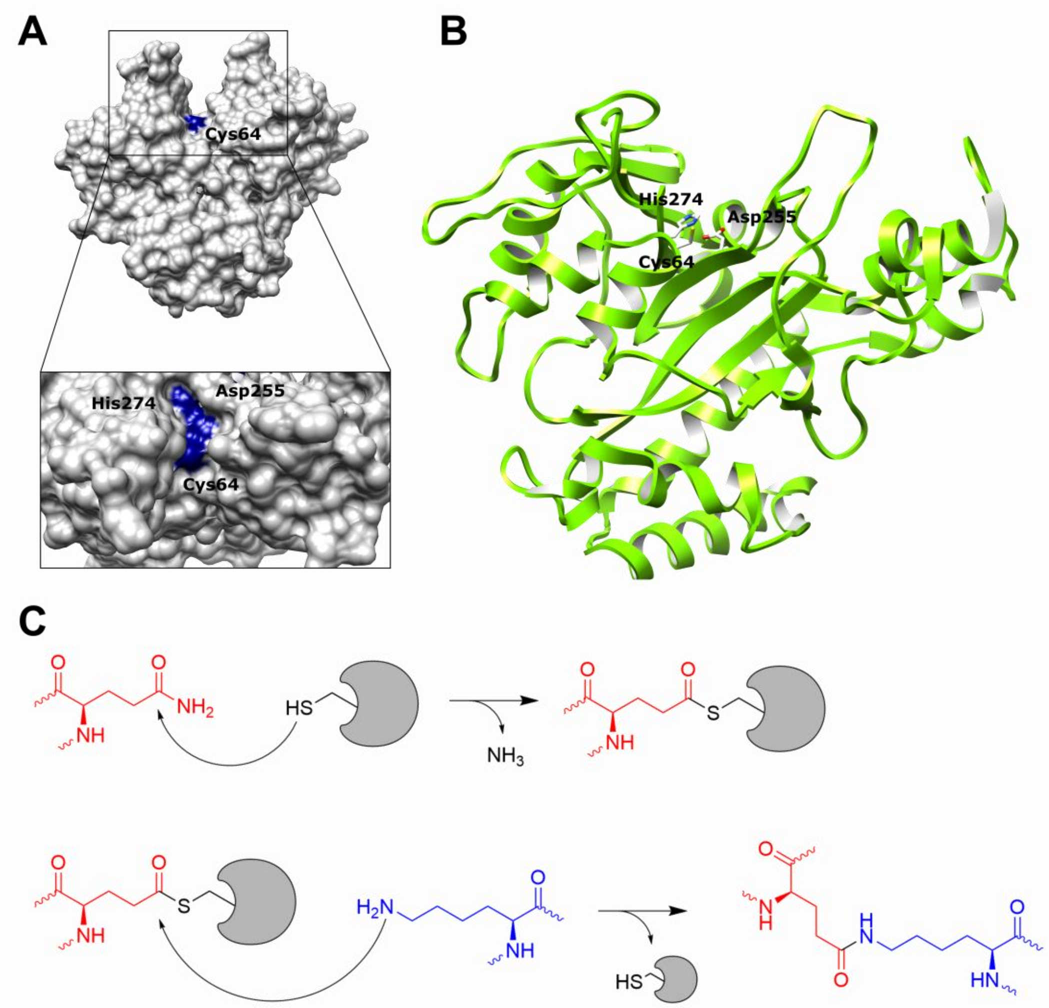

Figure 5: Structure (PDB:1IU4) and catalytic action of microbial transglutaminase. (**A**) Molecular surface of the enzyme. Catalytic triad Cys64, Asp255 and His274 (highlighted in blue) is buried at the bottom of the active site cleft (inlet). (**B**) Ribbon structure of the enzyme. (**C**) Mechanism of the catalysed transamidation according to Kashiwagi *et al.*: Cys64 nucleophilically attacks the γ-carboxamide group of the acyl-donor (red) to form a thioester and release ammonia as a side-product. The ε-amino group of lysine serves as the acyl-acceptor (blue) and a side-chain isopeptide bond is formed while Cys64 is regenerated.[87] Figure adapted with permission from Deweid *et al.*[88]

Besides eukaryotic TGases, numerous functional homologous of bacterial origin are described.[89, 90] The most relevant one derived from the soil bacterium *Streptomyces mobaraensis* (hereafter referred to as microbial transglutaminase; mTG), was initially discovered at the end of the 1980s and used as a tool for food-processing industry, which remains one of its major applications today.[91-93] mTG is produced as a catalytically inactive zymogen that is extracellularly processed by TAMP (transglutaminase-activating metalloprotease)[94] and SM-TAP (*Streptomyces mobaraensis* tripeptidyl aminopeptidase).[95] Conventionally, the mature enzyme is purified from the culture broth of *S. mobaraensis* by ion exchange chromatography.[96] In addition, multiple strategies for its recombinant expression in *E. coli* that apply commercially available proteases to truncate the inhibitory propeptide, have been developed.[97-99] The active enzyme is a monomeric 331 residue polypeptide chain of 37,842 kDa.[91] mTG activity is independent of regulation by Ca^{2+} or GTP[100] and its optimal temperature and pH conditions were found to be 50 °C and pH 6-7 in an assay employing CBZ-glutaminylglycine (Z-Gln-Gly) and hydroxylamine as substrates within 10 min.[92] It operates on a catalytic triad consisting of Cys64, Asp255 and His274 that is buried at the bottom of the active site cleft (Figure 5A and B) and a cysteine protease-like mechanism is assumed.[87] Releasing ammonia as a side-product, catalytic Cys64 forms a reactive thioester with the γ-carboxamide of the targeted acyl-donor. Negatively charged Asp255 then subtracts a proton from the approaching acyl-acceptor, which then nucleophilically attacks the thioester to release Cys64 and form the corresponding reaction product.[87] Interestingly, a recent study by Juettner *et al*. demonstrated that acyl-donor substrates are likely to undergo conformational changes therein. The same study provided evidence that the concept of an "approaching" acyl-acceptor during protein-protein crosslinking might be questionable, since structural conditions indicate a pre-assembly of reaction partners.[101]

The detailed substrate specificity of mTG is still a matter of investigations but is influenced by the flexibility of the addressed sites, the polarity of the neighboring amino acids as well as the structural arrangement of the targeted protein.[101, 102] Generally, the enzyme is quite promiscuous towards its acyl-acceptor substrate and transamidates multiple different primary amines.[103, 104] The choice of a corresponding acyl-donor on the other hand is more stringent and different library screening approaches were employed to identify consensus sequences that are well tolerated.[105-107] The enriched peptidic motifs however hardly matched the sequence environment found in modified sites of native mTG substrates. Investigating acyl-donor sites of intrinsic mTG substrates DAIP (dispase autolysis-inducing protein) and SPI_P (*Streptomyces* papain inhibitor protein), the group of Fuchsbauer proposed that neighboring small residues of polar, hydrophobic or uncharged nature are preferred over bulky and aromatic residues, while the charged ones are strongly unfavored.[108, 109]

Besides its application as food additive, mTG's crosslinking ability quickly raised interest for the post-translational modification of proteins in biotechnological and pharmaceutical research (Figure 6). Different groups successfully applied mTG for the assembly of multifunctional hybrids consisting of two or more proteins such as a targeting moiety (e.g. single-chain variable fragment; scFv) and fluorescent proteins.[110, 111] The attachment of polyethylene glycol (PEG) to proteinaceous drugs is a common strategy to prevent their clearance by renal filtration, leading to an increased half-life *in vivo* and more patient-friendly therapeutic options due to less frequent administration.[112] To that end, different pharmaceutically relevant proteins including hGh (human growth hormone),[113] interleukin-2[114] and salmon calcitonin[115] were PEGylated applying mTG catalysis. Covalent linkage of proteins and nucleic acids is a potent strategy to combine the advantages of both molecules for medical, diagnostic and research purposes and the groups of Kamiya and Goto developed different approaches that employed mTG therefore.[116, 117] mTG was also applied to covalently immobilize degradation-prone and cost-intensive proteins on solid-support to increase their stability and facilitate their reuse.[118, 119] Further details about the versatile applications of mTG in biotechnology can be found in the section 7.1 of this work.

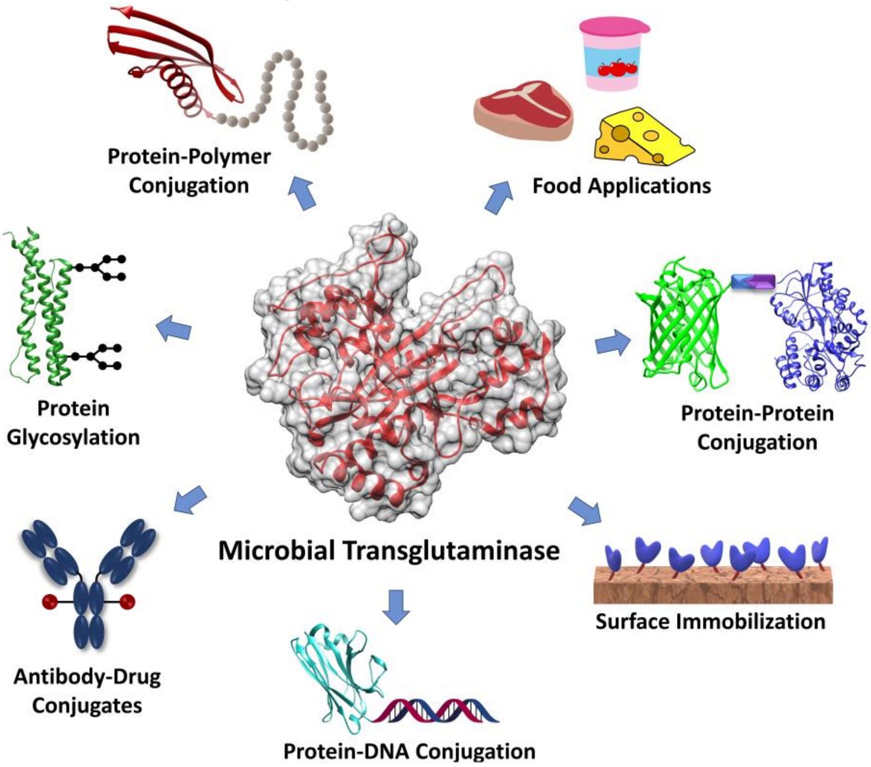
Protein-Polymer Conjugation
Food Applications
Protein Glycosylation
Protein-Protein Conjugation
Microbial Transglutaminase
Antibody-Drug Conjugates
Surface Immobilization
Protein-DNA Conjugation

Figure 6: Overview of industrial and technological application of microbial transglutaminase. mTG is massively applied in food-processing industry but also emerged as a versatile tool in biotechnology for the crosslinking of various molecules. See also section 7.1 and 7.4 for further details on the different approaches.[148]

4.4.1. Transglutaminase-Mediated Construction of Antibody-Drug Conjugates

Antibody-drug conjugates are hybrid macromolecules that attempt to minimize the side-effects of conventional chemotherapy by tumour-specific guidance of the drug to the targeted site of action. For that purpose, myriad ligation strategies were developed and different studies demonstrated that site-specific methodologies are favoured compared to non-directed ones because their homogeneous products comprise beneficial pharmacological properties (see section 4.3). To that end, multiple studies harnessed the ability of mTG to address the chemically almost inert γ-carboxamide group of glutamines for the assembly of ADCs. Full-length human IgG antibodies comprise ~60 glutamine residues but none of them serves as a substrate for mTG.[100, 120] However, different methodologies to overcome this limitation were developed (see Figure 7). The Schibli group recognized that removal of the Fc glycan moiety exposes Gln295 as a suitable site for transamidation and argued that an increased flexibility of the Fc's C/E loop (Gln295–Thr299) accounted for their observations. They demonstrated that either enzymatic truncation by glycosidase PNGaseF or genetic substitution of *N*-glycosylation site Asn297 against alanine (N297A) gave rise to homogeneous ADCs with a DAR of 2.[121] Moreover, mutation N297Q introduced an additional acyl-donor site for the assembly of potent DAR 4 ADCs with convenient pharmacokinetics and therapeutic indexes.[121, 122] This straightforward methodology was adapted by many groups and represents a key technology for the site-specific assembly of ADCs, mediated by mTG.[123, 124] One major benefit in comparison with conventional conjugation enzymes such as *Staphylococcus aureus* sortase A is that mTG activity is not limited to terminal sites but can address internal residues.[125] Strop *et al*. took advantage of this capability and engineered a short tetrameric recognition sequence LLQG at ~90 positions of an anti-EGFR antibody to identify sites that provide efficient conjugation.[69] In a further approach, they combined the identified sites for the generation of ADCs with different DARs (2, 4, 6 and 8) and compared their homogeneous constructs with a reference assembled by conventional maleimido-thiol chemistry to demonstrate improved therapeutic indexes of site-specifically assembled conjugates.[68] Besides glycan removal to expose Gln295, incorporation of specific peptidyl-linker sequences outlines another key technology for the mTG-assisted construction of ADCs with a defined DAR.

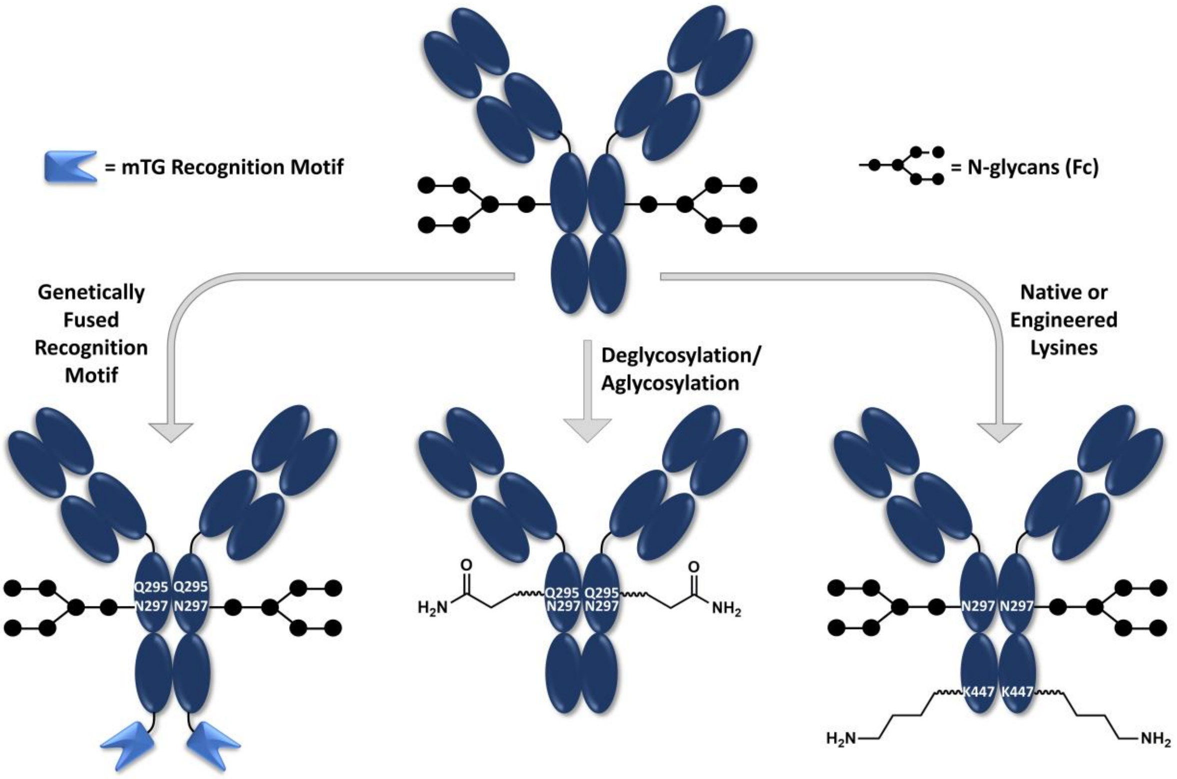
= mTG Recognition Motif
= N-glycans (Fc)
Genetically Fused Recognition Motif
Deglycosylation/ Aglycosylation
Native or Engineered Lysines
Q295 Q295
N297 N297
O
H2N
NH2
K447 K447

Figure 7: mTG-mediated assembly of homogeneous ADCs. Native IgG antibodies lack suitable sites for transamidation even though they comprise multiple surface-exposed glutamine and lysine residues (**top**). This limitation can be overcome by genetic incorporation of acyl-donor sequences (**left**); enzymatic or genetic removal of the Fc glycosylation to expose Gln295 for transamidation (**middle**); incorporation of acyl-acceptor sites or additional *C*-terminal amino acids to spare Lys447 from processing by carboxypeptidase B (**right**).[148]

The previously described strategies employed the utilized antibody solely as the acyl-donor of the catalysed reaction and synthesized the attached payload with a corresponding acyl-acceptor. However, only a few studies demonstrated the reversed approach: utilizing the targeted antibody as the acyl-acceptor. Spidel *et al*. investigated different chimeric, humanized and fully human immunoglobulins and recognized that none of the approximately 80 present lysines is modified by mTG. Upon engineering of an acyl-acceptor tag at the *C*-terminus of the heavy chain, they observed efficient transamidation of terminal Lys447. Encouraged by these results, they demonstrated that incorporation of a non-basic amino acid prevents Lys447 from cleavage by carboxypeptidase B during production in mammalian cell lines HEK293 and CHO. Moreover, they screened for sites that allowed for transamidation after their substitution against lysine and identified residues that were well tolerated.[126] Further details on the different strategies that allow for the transglutaminase-mediated construction of ADCs and multiple examples of their use are summarized in section 7.4 of this work.

4.5. Yeast Surface Display

Nature shaped its biomolecules over billions of years by Darwinian evolution but applications in biotechnology to solve modern day issues requires evolution at a more rapid pace.[127] Recently awarded with the Nobel Prize in chemistry in 2018, the concept of directed evolution mimics this process in a test tube. Directed evolution massively accelerates the evolutionary progress to months instead of millennia, leading to improved biomolecules that are applied in the treatment of cancer, the generation of biofuels or as laundry detergent.[128] Conceptually, the protein of interest is mutated applying one out of different techniques such as error-prone PCR, gene-shuffling or site-saturation mutagenesis to construct a randomised library that comprises multiple variants with varying characteristics.[129] The obtained library is then screened for mutants with desired properties such as improved binding affinity,[130] thermal-[131] or solvent-stability,[132] altered substrate specificity,[133] elevated catalytic turnover[134] or co-factor independency.[135]

This screening process is often associated with the search for a needle in a haystack because one has to isolate the very few promising candidates from a pool of millions to billions of non- or dysfunctional variants.[127] To facilitate this process, different molecular display technologies were developed that couple the investigated protein's phenotype to its corresponding genotype to enable DNA sequencing of enriching mutants (genotype-phenotype linkage). During host-free *in vitro* display methods ribosomal- or mRNA-display, genotype-phenotype linkage is achieved by either trapping of the prolonging polypeptide chain and the coding mRNA within the ribosomal complex or covalent linkage of both molecules, respectively. Upon binding of the complex to an immobilized target, non-functional variants are washed away, followed by elution of the binding mutants and their analysis by sequencing.[136, 137]

In vivo display technologies such as phage-,[138] bacterial-[139] or mammalian-display[140] rely on the genetic fusion of the protein of interest to a host protein that anchors it on the surface of the cell. The fusion protein is typically plasmid-encoded and transformation of the respective host results in a library of different cells that all carry the genetic information for a single mutant of the protein, fused to the surface anchor. After continues cycles of isolation and regrowing, cells that bear mutants with favoured characteristics are enriched.

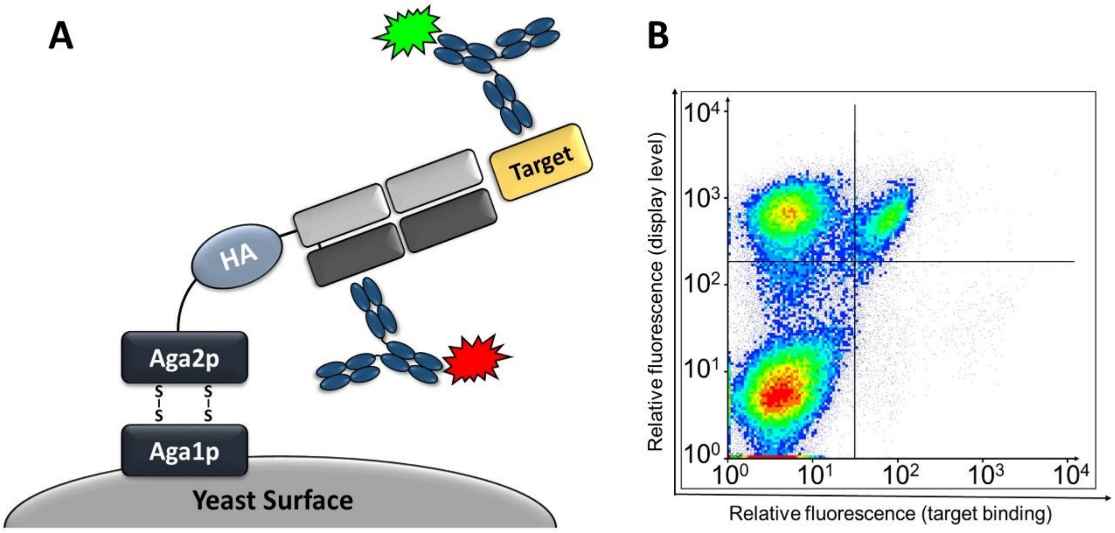

Figure 8: Yeast surface display of an antibody Fab fragment. (**A**)The investigated Fab is displayed on the surface of *S. cerevisiae* cells by genetic fusion to the Aga2p, which forms two disulfide bridges with the cell wall-anchored Aga1p. Surface display level of the Fab is visualized by a light chain specific, fluorescently labelled antibody, while binding to the targeted antigen is visualized by a target-specific antibody. Additionally, terminal or internal epitope tags such as HA or Myc can be incorporated to verify surface display of the fusion protein. (**B**) Schematic flow cytometry image of a randomised library. Cells in the upper right quadrant exhibit both, surface display of the investigated protein and binding to the targeted antigen. Figure adapted with permission from Deweid *et al.*[141]

Display of protein libraries on the cell surface of eukaryotic baker's yeast *Saccharomyces cerevisiae* (yeast surface display) as pioneered by Boder and Wittrup in 1997, is a powerful *in vivo* display technology for the engineering of binding moieties and enzymes.[142, 143] In combination with immunofluorescent staining and fluorescence-activated cell sorting (FACS), yeast surface display allows for the ultra-high throughput screening of tailor-made biomolecules from a randomised library. The investigated protein is genetically fused to the Aga2p subunit of the *a*-agglutinin mating complex and covalently linked to the surface-anchored Aga1p domain via two disulfide bridges (see Figure 8A). Aga1p is encoded in the yeast genome while the Aga2p-fusion protein on the other hand is plasmid encoded. However, both genes are under the control of the galactose-inducible GAL1 promotor, leading to surface display of the complex when gene expression is triggered by growing the yeast cells in galactose-containing medium. Surface display level of the fusion protein is visualized by fluorescently labelled antibodies that are specific for the investigated protein or genetically incorporated epitope tags such as HA (YPYDVPDYA) or Myc (EQKLISEEDL). Binding to the addressed antigen is visualized by either fluorescent labelling of the target or application of target-specific detection antibodies (Figure 8A). Yeast cells that comprise both characteristics (surface display and target binding) can be discriminated from non-binding ones and enriched over multiple screening rounds by fluorescence-activated cell sorting (Figure 8B).

In comparison to phage- or bacterial display, yeast surface display benefits from its near-human glycosylation and an intrinsic machinery of chaperones and foldases (unfolded protein response) that ensures correct folding of the polypeptide and prevents enrichment of misfolded mutants. Moreover, the application of FACS technology offers an online quality control of the screening process that is not compatible with phage-display. The size of yeast libraries (10^9) is usually smaller than that of phage- or bacterial libraries (10^{12}-10^{14}) due to the efficiency of yeast transformation during library construction. Additionally, the maximal sorting rate of ~50,000 cells per second of the FACS device, technically limits the throughput of larger libraries.[144] Nevertheless, yeast surface display in combination with FACS represents a robust and straightforward technology for the engineering of biomolecules towards improved characteristics.

5. Objective

The quest for novel, more efficient anti-tumour therapeutics continues. To address this challenge, antibody-drug conjugates that harness the remarkable target-specificity of monoclonal antibodies to transport a cytotoxin specifically to the tumour site have been developed. Regulatory approval of five (six, including moxetumomab pasudotox) different ADCs for the treatment of solid and hematologic malignancies underlines the potential of this class of molecules (see Section 4.3 and Table 1). However, multiple studies demonstrated that site-specific attachment of the warhead to the carrier antibody bears certain advantages over the conjugation strategies of most ADCs that are currently undergoing clinical trials. Besides others, microbial transglutaminase from *Streptomyces mobaraensis* was recently employed for the synthesis of homogeneous ADCs. Therein, the absence of native transamidation sites within human IgG antibodies was overcome by different strategies that all comprise certain advantages and disadvantages. Enzymatic deglycosylation to expose Gln295 can be applied to any purified antibody without previous genetic engineering but removal of the Fc-glycan might cause aggregation and increase thermal lability.[145] Incorporation of specific recognition motifs is a flexible strategy that allows for modification at desired sites of the mAb. However, genetic manipulation is required and incorporated tags might interfere with the antibody's intrinsic stability.

The engineering of an mTG mutant with altered substrate specificity that is capable of transamidating unmodified, native IgG antibodies could overcome the need for glycan truncation or tag incorporation to facilitate the construction of homogeneous ADCs. Even though the enzyme is massively used for biotechnological purposes, its engineering is barely described in the per-reviewed literature. However, engineering of mTG towards elevated thermal stability,[131, 146] increased activity[134] and redirected substrate recognition[133] are reported. These approaches utilized multi titer plate-based screening assays with a laborious throughput of <25,000 variants. One aspect of this thesis focuses on the establishment of an ultra-high throughput screening assay based on yeast surface display for the engineering of mTG (see section 7.2) and provides detailed protocols therefore (see section 7.3). To that end, mTG should be displayed on the surface of yeast cells as an inactive precursor that is converted into the mature enzyme by proteolytic cleavage upon surface display. Genotype-phenotype correlation has to be demonstrated to prove that active variants can be discriminated from inactive ones. To demonstrate that improved mTG mutants can be isolated by the established assay, a randomised library is constructed and screened by FACS to isolate mutants with elevated catalytic activity towards a short biotinylated acyl-donor peptide. The enriched mutants have to be purified from *E. coli* cells and compared to the wildtype enzyme in terms of activity towards the utilized peptide and a therapeutic antibody, tagged with the respective acyl-donor sequence. A screening assay for mTG based on yeast surface display would allow for the rapid and convenient isolation of mutants with tailor-made properties for different applications.

Both well-established strategies for the mTG-mediated assembly of ADCs (glycan truncation and tag incorporation) employ reaction times of ~16 h[69, 122] that can prompt undesired aggregation leading to inefficient product formation (unpublished results). Highly efficient labelling within short reaction times could minimize this risk during ADC construction. In previous research, Siegmund *et al*. demonstrated that grafting the amino acid pattern and mimicking the corresponding spatial arrangement of native transamidation sites of intrinsic mTG substrate DAIP, is a suitable strategy to derive a novel acyl-donor recognition tag.[120] Encouraged by these findings, the second part of this thesis focuses on the identification of recognitions sequences from mTG substrates DAIP and SPI$_P$ for the efficient construction of ADCs. Different acyl-donor sites should be mimicked by solid-phase peptide synthesis and their turnover by mTG investigated in an HPLC-based assay to predetermine promising hit sequences. Upon genetic incorporation into therapeutic antibody trastuzumab, attachment of different acyl-acceptor substrates to the engineered tags has to be analysed. The most potent sequence as determined in previous experiments will be utilized for the construction of an ADC and compared to conventionally applied sequence LLQG. Analysis by hydrophobic interaction chromatography and *in vitro* cells killing assays will reveal the degree of conjugation and the potency of the resulting conjugate.

Engineering of recognitions sequences into the scaffold of IgG antibodies is a powerful methodology to enable their labelling by mTG. However, incorporation of longer tags at internal positions can interfere with the antibody's intrinsic stability and cause a response of the patient's immune system upon intravenous administration.[126, 147] Single amino acid substitutions that allow for the efficient labelling of antibodies would reduce this risk of immunogenicity and diminished antibody stability compared to incorporated tag sequences.[126] In the third part of this thesis, we intend to identify positions of a human IgG Fc that can be substituted against glutamine and transamidated by mTG. 30 amino acids of the Fc moiety will be solitarily exchanged against glutamine residues by site-directed mutagenesis and a protocol for the recombinant expression in *E. coli* has to be established. In comparison to production in mammalian hosts, purification from bacterial sources rapidly offers high yields at low costs. However, the correct assembly of a disulfide-containing dimeric Fc portion in *E. coli* is not trivial. Non-reducing SDS-PAGE, thermal shift assays and LC-MS analysis have to be performed to validate proper dimerization, thermal stability and native disulfide-bridge formation of the Fc. The purified Fc mutants will be characterized towards their labelling by mTG in a straight-forward fluorescent assay based on non-reducing SDS-PAGE. Identified hits have to be validated in the context of an antibody purified from mammalian cells to verify the effect of posttranslational modifications that are not provided by prokaryotic hosts, and the tetrameric arrangement of the full-length antibody on conjugation efficiency. Efficient ligation of payloads to a defined site of an Fc, enabled by substitution of a single residue against glutamine, would be of great value for the mTG-mediated construction of ADCs, since minimal tag incorporation reduces immunogenicity and instability risks.

In summary, the presented work aimed at the optimization of mTG-mediated construction of homogeneous ADCs. Existing methodologies should be improved for more convenient and efficient conjugation. Moreover, an ultra-high throughput screening assay based on yeast surface display should be established to provide an access to engineered mTG variants with tailor-made properties.

6. References

(1) Arner, P., Bernard, S., Salehpour, M., Possnert, G., Liebl, J., Steier, P., Buchholz, B. A., Eriksson, M., Arner, E., Hauner, H., Skurk, T., Ryden, M., Frayn, K. N., and Spalding, K. L. (2011) Dynamics of human adipose lipid turnover in health and metabolic disease. *Nature 478* (7367), 110-113.

(2) Spalding, K. L., Arner, E., Westermark, P. O., Bernard, S., Buchholz, B. A., Bergmann, O., Blomqvist, L., Hoffstedt, J., Naslund, E., Britton, T., Concha, H., Hassan, M., Ryden, M., Frisen, J., and Arner, P. (2008) Dynamics of fat cell turnover in humans. *Nature 453* (7196), 783-787.

(3) Li, H. J., Ray, S. K., Singh, N. K., Johnston, B., and Leiter, A. B. (2011) Basic helix-loop-helix transcription factors and enteroendocrine cell differentiation. *Diabetes Obes Metab 13*, 5-12.

(4) Anderson, M. W., Reynolds, S. H., You, M., and Maronpot, R. M. (1992) Role of proto-oncogene activation in carcinogenesis. *Environ Health Perspect 98*, 13-24.

(5) Preston, B. D., Albertson, T. M., and Herr, A. J. (2010) DNA replication fidelity and cancer. *Semin Cancer Biol 20* (5), 281-293.

(6) Song, Q., Merajver, S. D., and Li, J. Z. (2015) Cancer classification in the genomic era: five contemporary problems. *Hum Genomics 9*, 27.

(7) Tan, S. Y., and Grimes, S. (2010) Paul Ehrlich (1854-1915): man with the magic bullet. *Singapore Med J 51* (11), 842-843.

(8) Rothschild, B. M., Tanke, D. H., Helbling, M., 2nd, and Martin, L. D. (2003) Epidemiologic study of tumors in dinosaurs. *Naturwissenschaften 90* (11), 495-500.

(9) Faguet, G. B. (2015) A brief history of cancer: age-old milestones underlying our current knowledge database. *Int J Cancer 136* (9), 2022-2036.

(10) Bray, F., Ferlay, J., Soerjomataram, I., Siegel, R. L., Torre, L. A., and Jemal, A. (2018) Global cancer statistics 2018: GLOBOCAN estimates of incidence and mortality worldwide for 36 cancers in 185 countries. *CA Cancer J Clin 68* (6), 394-424.

(11) Siegel, R. L., Miller, K. D., and Jemal, A. (2019) Cancer statistics, 2019. *CA Cancer J Clin 69* (1), 7-34.

(12) Torre, L. A., Bray, F., Siegel, R. L., Ferlay, J., Lortet-Tieulent, J., and Jemal, A. (2015) Global cancer statistics, 2012. *CA Cancer J Clin 65* (2), 87-108.

(13) Allemani, C., Matsuda, T., Di Carlo, V., Harewood, R., Matz, M., Niksic, M., Bonaventure, A., Valkov, M., Johnson, C. J., Esteve, J., Ogunbiyi, O. J., Azevedo, E. S. G., Chen, W. Q., Eser, S., Engholm, G., Stiller, C. A., Monnereau, A., Woods, R. R., Visser, O., Lim, G. H., Aitken, J., Weir, H. K., Coleman, M. P., and Group, C. W. (2018) Global surveillance of trends in cancer survival 2000-14 (CONCORD-3): analysis of individual records for 37 513 025 patients diagnosed with one of 18 cancers from 322 population-based registries in 71 countries. *Lancet 391* (10125), 1023-1075.

(14) Hiom, S. C. (2015) Diagnosing cancer earlier: reviewing the evidence for improving cancer survival. *Br J Cancer 112 Suppl 1*, S1-5.

(15) Brenner, H. (2002) Long-term survival rates of cancer patients achieved by the end of the 20th century: a period analysis. *Lancet 360* (9340), 1131-1135.

(16) Jemal, A., Bray, F., Center, M. M., Ferlay, J., Ward, E., and Forman, D. (2011) Global cancer statistics. *CA Cancer J Clin 61* (2), 69-90.

(17) Parkin, D. M., Bray, F., Ferlay, J., and Pisani, P. (2005) Global cancer statistics, 2002. *CA Cancer J Clin 55* (2), 74-108.

(18) Parkin, D. M. (2001) Global cancer statistics in the year 2000. *Lancet Oncol 2* (9), 533-543.

(19) Parkin, D. M., Pisani, P., and Ferlay, J. (1999) Global cancer statistics. *CA Cancer J Clin 49* (1), 33-64, 31.

(20) Leszczynski, K., and Boyko, S. (1997) On the controversies surrounding the origins of radiation therapy. *Radiother Oncol 42* (3), 213-217.

(21) Baskar, R., Lee, K. A., Yeo, R., and Yeoh, K. W. (2012) Cancer and radiation therapy: current advances and future directions. *Int J Med Sci 9* (3), 193-199.

(22) Arruebo, M., Vilaboa, N., Saez-Gutierrez, B., Lambea, J., Tres, A., Valladares, M., and Gonzalez-Fernandez, A. (2011) Assessment of the evolution of cancer treatment therapies. *Cancers (Basel) 3* (3), 3279-3330.

(23) DeVita, V. T., Jr., and Chu, E. (2008) A history of cancer chemotherapy. *Cancer Res 68* (21), 8643-8653.

(24) Cascella, M., Di Napoli, R., Carbone, D., Cuomo, G. F., Bimonte, S., and Muzio, M. R. (2018) Chemotherapy-related cognitive impairment: mechanisms, clinical features and research perspectives. *Recenti Prog Med 109* (11), 523-530.

(25) Schover, L. R., van der Kaaij, M., van Dorst, E., Creutzberg, C., Huyghe, E., and Kiserud, C. E. (2014) Sexual dysfunction and infertility as late effects of cancer treatment. *EJC Suppl 12* (1), 41-53.

(26) Kayl, A. E., and Meyers, C. A. (2006) Side-effects of chemotherapy and quality of life in ovarian and breast cancer patients. *Curr Opin Obstet Gynecol 18* (1), 24-28.

(27) Alberts, B., Johnson, A., Lewis, J., Raff, M., Roberts, K., and Walter, P. (2002) *Molecular Biology of the Cell. 4th edition*, Garland Science, New York.

(28) Vidarsson, G., Dekkers, G., and Rispens, T. (2014) IgG subclasses and allotypes: from structure to effector functions. *Front Immunol 5*, 520.

(29) Zipfel, P. F., and Skerka, C. (2009) Complement regulators and inhibitory proteins. *Nat Rev Immunol 9* (10), 729-740.

(30) Wang, W., Erbe, A. K., Hank, J. A., Morris, Z. S., and Sondel, P. M. (2015) NK Cell-Mediated Antibody-Dependent Cellular Cytotoxicity in Cancer Immunotherapy. *Front Immunol 6*, 368.

(31) Bryceson, Y. T., March, M. E., Ljunggren, H.-G., and Long, E. O. (2006) Synergy among receptors on resting NK cells for the activation of natural cytotoxicity and cytokine secretion. *Blood 107* (1), 159-166.

(32) Subedi, G. P., and Barb, A. W. (2015) The Structural Role of Antibody N-Glycosylation in Receptor Interactions. *Structure 23* (9), 1573-1583.

(33) Llewelyn, M. B., Hawkins, R. E., and Russell, S. J. (1992) Discovery of antibodies. *Bmj 305* (6864), 1269-1272.

(34) Köhler, G., and Milstein, C. (1975) Continuous cultures of fused cells secreting antibody of predefined specificity. *Nature 256* (5517), 495.

(35) Nixon, A. E., Sexton, D. J., and Ladner, R. C. (2014) Drugs derived from phage display: from candidate identification to clinical practice. *MAbs 6* (1), 73-85.

(36) Kaplon, H., and Reichert, J. M. (2019) Antibodies to watch in 2019. *MAbs 11* (2), 219-238.

(37) Cruz, E., and Kayser, V. (2019) Monoclonal antibody therapy of solid tumors: clinical limitations and novel strategies to enhance treatment efficacy. *Biologics 13*, 33-51.

(38) Bhutani, D., and Vaishampayan, U. N. (2013) Monoclonal antibodies in oncology therapeutics: present and future indications. *Expert Opin Biol Ther 13* (2), 269-282.

(39) Marcucci, F., Caserta, C. A., Romeo, E., and Rumio, C. (2019) Antibody-Drug Conjugates (ADC) Against Cancer Stem-Like Cells (CSC)-Is There Still Room for Optimism? *Front Oncol 9*, 167.

(40) Wong, O. K., Tran, T. T., Ho, W. H., Casas, M. G., Au, M., Bateman, M., Lindquist, K. C., Rajpal, A., Shelton, D. L., Strop, P., and Liu, S. H. (2018) RN765C, a low affinity EGFR antibody drug conjugate with potent anti-tumor activity in preclinical solid tumor models. *Oncotarget 9* (71), 33446-33458.

(41) Nejadmoghaddam, M. R., Minai-Tehrani, A., Ghahremanzadeh, R., Mahmoudi, M., Dinarvand, R., and Zarnani, A. H. (2019) Antibody-Drug Conjugates: Possibilities and Challenges. *Avicenna J Med Biotechnol 11* (1), 3-23.

(42) Tsuchikama, K., and An, Z. (2018) Antibody-drug conjugates: recent advances in conjugation and linker chemistries. *Protein Cell 9* (1), 33-46.

(43) Strop, P., Tran, T. T., Dorywalska, M., Delaria, K., Dushin, R., Wong, O. K., Ho, W. H., Zhou, D., Wu, A., Kraynov, E., Aschenbrenner, L., Han, B., O'Donnell, C. J., Pons, J., Rajpal, A., Shelton, D. L., and Liu, S. H. (2016) RN927C, a Site-Specific Trop-2 Antibody-Drug Conjugate (ADC) with Enhanced Stability, Is Highly Efficacious in Preclinical Solid Tumor Models. *Mol Cancer Ther 15* (11), 2698-2708.

(44) DeVay, R. M., Delaria, K., Zhu, G., Holz, C., Foletti, D., Sutton, J., Bolton, G., Dushin, R., Bee, C., Pons, J., Rajpal, A., Liang, H., Shelton, D., Liu, S. H., and Strop, P. (2017) Improved Lysosomal Trafficking Can Modulate the Potency of Antibody Drug Conjugates. *Bioconjug Chem 28* (4), 1102-1114.

(45) Ritchie, M., Tchistiakova, L., and Scott, N. (2013) Implications of receptor-mediated endocytosis and intracellular trafficking dynamics in the development of antibody drug conjugates. *MAbs 5* (1), 13-21.

(46) Hamann, P. R., Hinman, L. M., Beyer, C. F., Lindh, D., Upeslacis, J., Flowers, D. A., and Bernstein, I. (2002) An anti-CD33 antibody-calicheamicin conjugate for treatment of acute myeloid leukemia. Choice of linker. *Bioconjug Chem 13* (1), 40-46.

(47) Thornlow, D. N., Cox, E. C., Walker, J. A., Sorkin, M., Plesset, J. B., DeLisa, M. P., and Alabi, C. A. (2019) Dual Site-Specific Antibody Conjugates for Sequential and Orthogonal Cargo Release. *Bioconjug Chem 30* (6), 1702-1710.

(48) Chau, Y., Tan, F. E., and Langer, R. (2004) Synthesis and characterization of dextran-peptide-methotrexate conjugates for tumor targeting via mediation by matrix metalloproteinase II and matrix metalloproteinase IX. *Bioconjug Chem 15* (4), 931-941.

(49) Doronina, S. O., Toki, B. E., Torgov, M. Y., Mendelsohn, B. A., Cerveny, C. G., Chace, D. F., DeBlanc, R. L., Gearing, R. P., Bovee, T. D., Siegall, C. B., Francisco, J. A., Wahl, A. F., Meyer, D. L., and Senter, P. D. (2003) Development of potent monoclonal antibody auristatin conjugates for cancer therapy. *Nat Biotechnol 21* (7), 778-784.

(50) Chari, R. V., Miller, M. L., and Widdison, W. C. (2014) Antibody-drug conjugates: an emerging concept in cancer therapy. *Angew Chem Int Ed Engl 53* (15), 3796-3827.

(51) Boger, D. L., and Johnson, D. S. (1995) CC-1065 and the duocarmycins: unraveling the keys to a new class of naturally derived DNA alkylating agents. *Proc Natl Acad Sci U S A 92* (9), 3642-3649.

(52) Mantaj, J., Jackson, P. J., Rahman, K. M., and Thurston, D. E. (2017) From Anthramycin to Pyrrolobenzodiazepine (PBD)-Containing Antibody-Drug Conjugates (ADCs). *Angew Chem Int Ed Engl 56* (2), 462-488.

(53) Coats, S., Williams, M., Kebble, B., Dixit, R., Tseng, L., Yao, N. S., Tice, D. A., and Soria, J. C. (2019) Antibody-Drug Conjugates: Future Directions in Clinical and Translational Strategies to Improve the Therapeutic Index. *Clin Cancer Res 25* (18), 5441-5448.

(54) Dhillon, S. (2018) Moxetumomab Pasudotox: First Global Approval. *Drugs 78* (16), 1763-1767.

(55) Wang, L., Amphlett, G., Blattler, W. A., Lambert, J. M., and Zhang, W. (2005) Structural characterization of the maytansinoid-monoclonal antibody immunoconjugate, huN901-DM1, by mass spectrometry. *Protein Sci 14* (9), 2436-2446.

(56) Kim, M. T., Chen, Y., Marhoul, J., and Jacobson, F. (2014) Statistical modeling of the drug load distribution on trastuzumab emtansine (Kadcyla), a lysine-linked antibody drug conjugate. *Bioconjug Chem 25* (7), 1223-1232.

(57) Junutula, J. R., Raab, H., Clark, S., Bhakta, S., Leipold, D. D., Weir, S., Chen, Y., Simpson, M., Tsai, S. P., Dennis, M. S., Lu, Y., Meng, Y. G., Ng, C., Yang, J., Lee, C. C., Duenas, E., Gorrell, J., Katta, V., Kim, A., McDorman, K., Flagella, K., Venook, R., Ross, S., Spencer, S. D., Lee Wong, W., Lowman, H. B., Vandlen, R., Sliwkowski, M. X., Scheller, R. H., Polakis, P., and Mallet, W. (2008) Site-specific conjugation of a cytotoxic drug to an antibody improves the therapeutic index. *Nat Biotechnol 26* (8), 925-932.

(58) Jen, E. Y., Ko, C. W., Lee, J. E., Del Valle, P. L., Aydanian, A., Jewell, C., Norsworthy, K. J., Przepiorka, D., Nie, L., Liu, J., Sheth, C. M., Shapiro, M., Farrell, A. T., and Pazdur, R. (2018) FDA Approval: Gemtuzumab Ozogamicin for the Treatment of Adults with Newly Diagnosed CD33-Positive Acute Myeloid Leukemia. *Clin Cancer Res 24* (14), 3242-3246.

(59) Hamann, P. R., Hinman, L. M., Hollander, I., Beyer, C. F., Lindh, D., Holcomb, R., Hallett, W., Tsou, H. R., Upeslacis, J., Shochat, D., Mountain, A., Flowers, D. A., and Bernstein, I. (2002) Gemtuzumab ozogamicin, a potent and selective anti-CD33 antibody-calicheamicin conjugate for treatment of acute myeloid leukemia. *Bioconjug Chem 13* (1), 47-58.

(60) D'Atri, V., Fekete, S., Stoll, D., Lauber, M., Beck, A., and Guillarme, D. (2018) Characterization of an antibody-drug conjugate by hydrophilic interaction chromatography coupled to mass spectrometry. *J Chromatogr B Analyt Technol Biomed Life Sci 1080*, 37-41.

(61) Ansell, S. M. (2014) Brentuximab vedotin. *Blood 124* (22), 3197-3200.

(62) Senter, P. D., and Sievers, E. L. (2012) The discovery and development of brentuximab vedotin for use in relapsed Hodgkin lymphoma and systemic anaplastic large cell lymphoma. *Nat Biotechnol 30* (7), 631.

(63) Verma, S., Miles, D., Gianni, L., Krop, I. E., Welslau, M., Baselga, J., Pegram, M., Oh, D.-Y., Diéras, V., and Guardino, E. (2012) Trastuzumab emtansine for HER2-positive advanced breast cancer. *New Engl J Med 367* (19), 1783-1791.

(64) DiJoseph, J. F., Armellino, D. C., Boghaert, E. R., Khandke, K., Dougher, M. M., Sridharan, L., Kunz, A., Hamann, P. R., Gorovits, B., Udata, C., Moran, J. K., Popplewell, A. G., Stephens, S., Frost, P., and Damle, N. K. (2004) Antibody-targeted chemotherapy with CMC-544: a CD22-targeted immunoconjugate of calicheamicin for the treatment of B-lymphoid malignancies. *Blood 103* (5), 1807-1814.

(65) Deeks, E. D. (2019) Polatuzumab Vedotin: First Global Approval. *Drugs 79* (13), 1467-1475.

(66) Dornan, D., Bennett, F., Chen, Y., Dennis, M., Eaton, D., Elkins, K., French, D., Go, M. A., Jack, A., Junutula, J. R., Koeppen, H., Lau, J., McBride, J., Rawstron, A., Shi, X., Yu, N., Yu, S. F., Yue, P., Zheng, B., Ebens, A., and Polson, A. G. (2009) Therapeutic potential of an anti-CD79b antibody-drug conjugate, anti-CD79b-vc-MMAE, for the treatment of non-Hodgkin lymphoma. *Blood 114* (13), 2721-2729.

(67) Kim, E. G., and Kim, K. M. (2015) Strategies and Advancement in Antibody-Drug Conjugate Optimization for Targeted Cancer Therapeutics. *Biomol Ther (Seoul) 23* (6), 493-509.

(68) Strop, P., Delaria, K., Foletti, D., Witt, J. M., Hasa-Moreno, A., Poulsen, K., Casas, M. G., Dorywalska, M., Farias, S., Pios, A., Lui, V., Dushin, R., Zhou, D., Navaratnam, T., Tran, T. T., Sutton, J., Lindquist, K. C., Han, B., Liu, S. H., Shelton, D. L., Pons, J., and Rajpal, A. (2015) Site-specific conjugation improves therapeutic index of antibody drug conjugates with high drug loading. *Nat Biotechnol 33* (7), 694-696.

(69) Strop, P., Liu, S. H., Dorywalska, M., Delaria, K., Dushin, R. G., Tran, T. T., Ho, W. H., Farias, S., Casas, M. G., Abdiche, Y., Zhou, D., Chandrasekaran, R., Samain, C., Loo, C., Rossi, A., Rickert, M., Krimm, S., Wong, T., Chin, S. M., Yu, J., Dilley, J., Chaparro-Riggers, J., Filzen, G. F., O'Donnell, C. J., Wang, F., Myers, J. S., Pons, J., Shelton, D. L., and Rajpal, A. (2013) Location matters: site of conjugation modulates stability and pharmacokinetics of antibody drug conjugates. *Chem Biol 20* (2), 161-167.

(70) Beerli, R. R., Hell, T., Merkel, A. S., and Grawunder, U. (2015) Sortase Enzyme-Mediated Generation of Site-Specifically Conjugated Antibody Drug Conjugates with High In Vitro and In Vivo Potency. *PLoS One 10* (7), e0131177.

(71) Drake, P. M., Albers, A. E., Baker, J., Banas, S., Barfield, R. M., Bhat, A. S., de Hart, G. W., Garofalo, A. W., Holder, P., Jones, L. C., Kudirka, R., McFarland, J., Zmolek, W., and Rabuka, D. (2014) Aldehyde tag coupled with HIPS chemistry enables the production of ADCs conjugated site-specifically to different antibody regions with distinct in vivo efficacy and PK outcomes. *Bioconjug Chem 25* (7), 1331-1341.

(72) Grunewald, J., Klock, H. E., Cellitti, S. E., Bursulaya, B., McMullan, D., Jones, D. H., Chiu, H. P., Wang, X., Patterson, P., Zhou, H., Vance, J., Nigoghossian, E., Tong, H., Daniel, D., Mallet, W., Ou, W., Uno, T., Brock, A., Lesley, S. A., and Geierstanger, B. H. (2015) Efficient Preparation of Site-Specific Antibody-Drug Conjugates Using Phosphopantetheinyl Transferases. *Bioconjug Chem 26* (12), 2554-2562.

(73) Zhou, Q., Stefano, J. E., Manning, C., Kyazike, J., Chen, B., Gianolio, D. A., Park, A., Busch, M., Bird, J., and Zheng, X. (2014) Site-specific antibody–drug conjugation through glycoengineering. *Bioconjug Chem 25* (3), 510-520.

(74) Li, X., Fang, T., and Boons, G. J. (2014) Preparation of well-defined antibody-drug conjugates through glycan remodeling and strain-promoted azide-alkyne cycloadditions. *Angew Chem Int Ed Engl 53* (28), 7179-7182.

(75) Hallam, T. J., Wold, E., Wahl, A., and Smider, V. V. (2015) Antibody conjugates with unnatural amino acids. *Mol Pharm 12* (6), 1848-1862.

(76) Axup, J. Y., Bajjuri, K. M., Ritland, M., Hutchins, B. M., Kim, C. H., Kazane, S. A., Halder, R., Forsyth, J. S., Santidrian, A. F., Stafin, K., Lu, Y., Tran, H., Seller, A. J., Biroc, S. L., Szydlik, A., Pinkstaff, J. K., Tian, F., Sinha, S. C., Felding-Habermann, B., Smider, V. V., and Schultz, P. G. (2012) Synthesis of site-specific antibody-drug conjugates using unnatural amino acids. *Proc Natl Acad Sci U S A 109* (40), 16101-16106.

(77) Drake, P. M., and Rabuka, D. (2017) Recent Developments in ADC Technology: Preclinical Studies Signal Future Clinical Trends. *BioDrugs 31* (6), 521-531.

(78) Beck, A., Goetsch, L., Dumontet, C., and Corvaia, N. (2017) Strategies and challenges for the next generation of antibody-drug conjugates. *Nat Rev Drug Discov 16* (5), 315-337.

(79) Lorand, L., and Graham, R. M. (2003) Transglutaminases: crosslinking enzymes with pleiotropic functions. *Nat Rev Mol Cell Biol 4* (2), 140-156.

(80) Serafini-Fracassini, D., Della Mea, M., Tasco, G., Casadio, R., and Del Duca, S. (2009) Plant and animal transglutaminases: do similar functions imply similar structures? *Amino Acids 36* (4), 643-657.

(81) Ruiz-Herrera, J., Iranzo, M., Elorza, M. V., Sentandreu, R., and Mormeneo, S. (1995) Involvement of transglutaminase in the formation of covalent cross-links in the cell wall of Candida albicans. *Arch Microbiol 164* (3), 186-193.

(82) Zhu, Y., and Tramper, J. (2008) Novel applications for microbial transglutaminase beyond food processing. *Trends Biotechnol 26* (10), 559-565.

(83) Griffin, M., Casadio, R., and Bergamini, C. M. (2002) Transglutaminases: nature's biological glues. *Biochem J 368* (Pt 2), 377-396.

(84) Nemes, Z., Marekov, L. N., Fesus, L., and Steinert, P. M. (1999) A novel function for transglutaminase 1: attachment of long-chain omega-hydroxyceramides to involucrin by ester bond formation. *Proc Natl Acad Sci U S A 96* (15), 8402-8407.

(85) Fesus, L., Thomazy, V., Autuori, F., Ceru, M. P., Tarcsa, E., and Piacentini, M. (1989) Apoptotic hepatocytes become insoluble in detergents and chaotropic agents as a result of transglutaminase action. *FEBS Lett 245* (1-2), 150-154.

(86) Fesus, L., Thomazy, V., and Falus, A. (1987) Induction and activation of tissue transglutaminase during programmed cell death. *FEBS Lett 224* (1), 104-108.

(87) Kashiwagi, T., Yokoyama, K., Ishikawa, K., Ono, K., Ejima, D., Matsui, H., and Suzuki, E. (2002) Crystal structure of microbial transglutaminase from Streptoverticillium mobaraense. *J Biol Chem 277* (46), 44252-44260.

(88) Deweid, L., Avrutina, O., and Kolmar, H. (2019) Microbial transglutaminase for biotechnological and biomedical engineering. *Biol Chem 400* (3), 257-274.

(89) Rachel, N. M., and Pelletier, J. N. (2013) Biotechnological applications of transglutaminases. *Biomolecules 3* (4), 870-888.

(90) Milani, A., Vecchietti, D., Rusmini, R., and Bertoni, G. (2012) TgpA, a protein with a eukaryotic-like transglutaminase domain, plays a critical role in the viability of Pseudomonas aeruginosa. *PLoS One 7* (11), e50323.

(91) Yokoyama, K., Nio, N., and Kikuchi, Y. (2004) Properties and applications of microbial transglutaminase. *Appl Microbiol Biotechnol 64* (4), 447-454.

(92) Ando, H., Adachi, M., Umeda, K., Matsuura, A., Nonaka, M., Uchio, R., Tanaka, H., and Motoki, M. (1989) Purification and characteristics of a novel transglutaminase derived from microorganisms. *Agric Biol Chem 53* (10), 2613-2617.

(93) Kieliszek, M., and Misiewicz, A. (2014) Microbial transglutaminase and its application in the food industry. A review. *Folia Microbiol (Praha) 59* (3), 241-250.

(94) Zotzel, J., Keller, P., and Fuchsbauer, H. L. (2003) Transglutaminase from Streptomyces mobaraensis is activated by an endogenous metalloprotease. *Eur J Biochem 270* (15), 3214-3222.

(95) Zotzel, J., Pasternack, R., Pelzer, C., Ziegert, D., Mainusch, M., and Fuchsbauer, H. L. (2003) Activated transglutaminase from Streptomyces mobaraensis is processed by a tripeptidyl aminopeptidase in the final step. *Eur J Biochem 270* (20), 4149-4155.

(96) Gerber, U., Jucknischke, U., Putzien, S., and Fuchsbauer, H. L. (1994) A rapid and simple method for the purification of transglutaminase from Streptoverticillium mobaraense. *Biochem J 299 (Pt 3)*, 825-829.

(97) Sommer, C., Hertel, T. C., Schmelzer, C. E., and Pietzsch, M. (2012) Investigations on the activation of recombinant microbial pro-transglutaminase: in contrast to proteinase K, dispase removes the histidine-tag. *Amino acids 42* (2-3), 997-1006.

(98) Marx, C. K., Hertel, T. C., and Pietzsch, M. (2008) Purification and activation of a recombinant histidine-tagged pro-transglutaminase after soluble expression in Escherichia coli and partial characterization of the active enzyme. *Enzyme Microb Technol 42* (7), 568-575.

(99) Marx, C. K., Hertel, T. C., and Pietzsch, M. (2007) Soluble expression of a pro-transglutaminase from Streptomyces mobaraensis in Escherichia coli. *Enzyme Microb Technol 40* (6), 1543-1550.

(100) Strop, P. (2014) Versatility of microbial transglutaminase. *Bioconjug Chem 25* (5), 855-862.

(101) Juettner, N. E., Schmelz, S., Kraemer, A., Knapp, S., Becker, B., Kolmar, H., Scrima, A., and Fuchsbauer, H. L. (2018) Structure of a glutamine donor mimicking inhibitory peptide shaped by the catalytic cleft of microbial transglutaminase. *FEBS J 285* (24), 4684-4694.

(102) Spolaore, B., Raboni, S., Ramos Molina, A., Satwekar, A., Damiano, N., and Fontana, A. (2012) Local unfolding is required for the site-specific protein modification by transglutaminase. *Biochemistry 51* (43), 8679-8689.

(103) Gundersen, M. T., Keillor, J. W., and Pelletier, J. N. (2014) Microbial transglutaminase displays broad acyl-acceptor substrate specificity. *Appl Microbiol Biotechnol 98* (1), 219-230.

(104) Ohtsuka, T., Sawa, A., Kawabata, R., Nio, N., and Motoki, M. (2000) Substrate specificities of microbial transglutaminase for primary amines. *J Agric Food Chem 48* (12), 6230-6233.

(105) Malesevic, M., Migge, A., Hertel, T. C., and Pietzsch, M. (2015) A fluorescence-based array screen for transglutaminase substrates. *Chembiochem 16* (8), 1169-1174.

(106) Lee, J. H., Song, C., Kim, D. H., Park, I. H., Lee, S. G., Lee, Y. S., and Kim, B. G. (2013) Glutamine (Q)-peptide screening for transglutaminase reaction using mRNA display. *Biotechnol Bioeng 110* (2), 353-362.

(107) Sugimura, Y., Yokoyama, K., Nio, N., Maki, M., and Hitomi, K. (2008) Identification of preferred substrate sequences of microbial transglutaminase from Streptomyces mobaraensis using a phage-displayed peptide library. *Arch Biochem Biophys 477* (2), 379-383.

(108) Juettner, N. E., Schmelz, S., Bogen, J. P., Happel, D., Fessner, W. D., Pfeifer, F., Fuchsbauer, H. L., and Scrima, A. (2018) Illuminating structure and acyl donor sites of a physiological transglutaminase substrate from Streptomyces mobaraensis. *Protein Sci. 27* (5), 910-922.

(109) Fiebig, D., Schmelz, S., Zindel, S., Ehret, V., Beck, J., Ebenig, A., Ehret, M., Frols, S., Pfeifer, F., Kolmar, H., Fuchsbauer, H. L., and Scrima, A. (2016) Structure of the Dispase Autolysis-inducing Protein from Streptomyces mobaraensis and Glutamine Cross-linking Sites for Transglutaminase. *J Biol Chem 291* (39), 20417-20426.

(110) Bhokisham, N., Pakhchanian, H., Quan, D., Tschirhart, T., Tsao, C. Y., Payne, G. F., and Bentley, W. E. (2016) Modular construction of multi-subunit protein complexes using engineered tags and microbial transglutaminase. *Metab Eng 38*, 1-9.

(111) Kamiya, N., Takazawa, T., Tanaka, T., Ueda, H., and Nagamune, T. (2003) Site-specific cross-linking of functional proteins by transglutamination. *Enzyme Microb Technol 33* (4), 492-496.

(112) Dozier, J. K., and Distefano, M. D. (2015) Site-Specific PEGylation of Therapeutic Proteins. *Int J Mol Sci 16* (10), 25831-25864.

(113) da Silva Freitas, D., Mero, A., and Pasut, G. (2013) Chemical and enzymatic site specific PEGylation of hGH. *Bioconjug Chem 24* (3), 456-463.

(114) Sato, H., Hayashi, E., Yamada, N., Yatagai, M., and Takahara, Y. (2001) Further studies on the site-specific protein modification by microbial transglutaminase. *Bioconjug Chem 12* (5), 701-710.

(115) Mero, A., Schiavon, M., Veronese, F. M., and Pasut, G. (2011) A new method to increase selectivity of transglutaminase mediated PEGylation of salmon calcitonin and human growth hormone. *J Control Release 154* (1), 27-34.

(116) Takahara, M., Wakabayashi, R., Minamihata, K., Goto, M., and Kamiya, N. (2017) Primary Amine-Clustered DNA Aptamer for DNA-Protein Conjugation Catalyzed by Microbial Transglutaminase. *Bioconjug Chem 28* (12), 2954-2961.

(117) Takahara, M., Hayashi, K., Goto, M., and Kamiya, N. (2016) Enzymatic conjugation of multiple proteins on a DNA aptamer in a tail-specific manner. *Biotechnol J 11* (6), 814-823.

(118) Li, T., Li, C., Quan, D. N., Bentley, W. E., and Wang, L. X. (2018) Site-specific immobilization of endoglycosidases for streamlined chemoenzymatic glycan remodeling of antibodies. *Carbohydr Res 458-459*, 77-84.

(119) Yu, C. M., Zhou, H., Zhang, W. F., Yang, H. M., and Tang, J. B. (2016) Site-specific, covalent immobilization of BirA by microbial transglutaminase: A reusable biocatalyst for in vitro biotinylation. *Anal Biochem 511*, 10-12.

(120) Siegmund, V., Schmelz, S., Dickgiesser, S., Beck, J., Ebenig, A., Fittler, H., Frauendorf, H., Piater, B., Betz, U. A., Avrutina, O., Scrima, A., Fuchsbauer, H. L., and Kolmar, H. (2015) Locked by Design: A Conformationally Constrained Transglutaminase Tag Enables Efficient Site-Specific Conjugation. *Angew Chem Int Ed Engl 54* (45), 13420-13424.

(121) Jeger, S., Zimmermann, K., Blanc, A., Grunberg, J., Honer, M., Hunziker, P., Struthers, H., and Schibli, R. (2010) Site-specific and stoichiometric modification of antibodies by bacterial transglutaminase. *Angew Chem Int Ed Engl 49* (51), 9995-9997.

(122) Lhospice, F., Bregeon, D., Belmant, C., Dennler, P., Chiotellis, A., Fischer, E., Gauthier, L., Boedec, A., Rispaud, H., Savard-Chambard, S., Represa, A., Schneider, N., Paturel, C., Sapet, M., Delcambre, C., Ingoure, S., Viaud, N., Bonnafous, C., Schibli, R., and Romagne, F. (2015) Site-Specific Conjugation of Monomethyl Auristatin E to Anti-CD30 Antibodies Improves Their Pharmacokinetics and Therapeutic Index in Rodent Models. *Mol Pharm 12* (6), 1863-1871.

(123) Anami, Y., Xiong, W., Gui, X., Deng, M., Zhang, C. C., Zhang, N., An, Z., and Tsuchikama, K. (2017) Enzymatic conjugation using branched linkers for constructing homogeneous antibody-drug conjugates with high potency. *Org Biomol Chem 15* (26), 5635-5642.

(124) Puthenveetil, S., Musto, S., Loganzo, F., Tumey, L. N., O'Donnell, C. J., and Graziani, E. (2016) Development of Solid-Phase Site-Specific Conjugation and Its Application toward Generation of Dual Labeled Antibody and Fab Drug Conjugates. *Bioconjug Chem 27* (4), 1030-1039.

(125) Antos, J. M., Ingram, J., Fang, T., Pishesha, N., Truttmann, M. C., and Ploegh, H. L. (2017) Site-Specific Protein Labeling via Sortase-Mediated Transpeptidation. *Curr Protoc Protein Sci 89*, 15 13 11-15 13 19.

(126) Spidel, J. L., Vaessen, B., Albone, E. F., Cheng, X., Verdi, A., and Kline, J. B. (2017) Site-Specific Conjugation to Native and Engineered Lysines in Human Immunoglobulins by Microbial Transglutaminase. *Bioconjug Chem 28* (9), 2471-2484.

(127) Jackel, C., Kast, P., and Hilvert, D. (2008) Protein design by directed evolution. *Annu Rev Biophys 37*, 153-173.

(128) Paria, D., and Venugopalan, P. L. (2019) Controlling Evolution: The Nobel Prize in Chemistry 2018. *IEEE Pulse 10* (4), 12-16.

(129) Neylon, C. (2004) Chemical and biochemical strategies for the randomization of protein encoding DNA sequences: library construction methods for directed evolution. *Nucleic Acids Res 32* (4), 1448-1459.

(130) Bogen, J. P., Hinz, S. C., Grzeschik, J., Ebenig, A., Krah, S., Zielonka, S., and Kolmar, H. (2019) Dual Function pH Responsive Bispecific Antibodies for Tumor Targeting and Antigen Depletion in Plasma. *Front Immunol 10*, 1892.

(131) Buettner, K., Hertel, T. C., and Pietzsch, M. (2012) Increased thermostability of microbial transglutaminase by combination of several hot spots evolved by random and saturation mutagenesis. *Amino Acids 42* (2-3), 987-996.

(132) Chen, K., and Arnold, F. H. (1993) Tuning the activity of an enzyme for unusual environments: sequential random mutagenesis of subtilisin E for catalysis in dimethylformamide. *Proc Natl Acad Sci U S A 90* (12), 5618-5622.

(133) Zhao, X., Shaw, A. C., Wang, J., Chang, C. C., Deng, J., and Su, J. (2010) A novel high-throughput screening method for microbial transglutaminases with high specificity toward Gln141 of human growth hormone. *J Biomol Screen 15* (2), 206-212.

(134) Yokoyama, K., Utsumi, H., Nakamura, T., Ogaya, D., Shimba, N., Suzuki, E., and Taguchi, S. (2010) Screening for improved activity of a transglutaminase from Streptomyces mobaraensis created by a novel rational mutagenesis and random mutagenesis. *Appl Microbiol Biotechnol 87* (6), 2087-2096.

(135) Hirakawa, H., Ishikawa, S., and Nagamune, T. (2015) Ca2+ -independent sortase-A exhibits high selective protein ligation activity in the cytoplasm of Escherichia coli. *Biotechnol J 10* (9), 1487-1492.

(136) Pluckthun, A. (2012) Ribosome display: a perspective. *Methods Mol Biol 805*, 3-28.

(137) Zahnd, C., Amstutz, P., and Pluckthun, A. (2007) Ribosome display: selecting and evolving proteins in vitro that specifically bind to a target. *Nat Methods 4* (3), 269-279.

(138) McCafferty, J., Griffiths, A. D., Winter, G., and Chiswell, D. J. (1990) Phage antibodies: filamentous phage displaying antibody variable domains. *Nature 348* (6301), 552-554.

(139) Wentzel, A., Christmann, A., Adams, T., and Kolmar, H. (2001) Display of passenger proteins on the surface of Escherichia coli K-12 by the enterohemorrhagic E. coli intimin EaeA. *J Bacteriol 183* (24), 7273-7284.

(140) Ho, M., and Pastan, I. (2009) Mammalian cell display for antibody engineering. *Methods Mol Biol 525*, 337-352, xiv.

(141) Deweid, L., Neureiter, L., Englert, S., Schneider, H., Deweid, J., Yanakieva, D., Sturm, J., Bitsch, S., Christmann, A., Avrutina, O., Fuchsbauer, H. L., and Kolmar, H. (2018) Directed Evolution of a Bond-Forming Enzyme: Ultrahigh-Throughput Screening of Microbial Transglutaminase Using Yeast Surface Display. *Chem Eur J 24* (57), 15195-15200.

(142) Konning, D., and Kolmar, H. (2018) Beyond antibody engineering: directed evolution of alternative binding scaffolds and enzymes using yeast surface display. *Microb Cell Fact 17* (1), 32.

(143) Boder, E. T., and Wittrup, K. D. (1997) Yeast surface display for screening combinatorial polypeptide libraries. *Nat Biotechnol 15* (6), 553-557.

(144) Cherf, G. M., and Cochran, J. R. (2015) Applications of Yeast Surface Display for Protein Engineering. *Methods Mol Biol 1319*, 155-175.

(145) Reusch, D., and Tejada, M. L. (2015) Fc glycans of therapeutic antibodies as critical quality attributes. *Glycobiology 25* (12), 1325-1334.

(146) Marx, C. K., Hertel, T. C., and Pietzsch, M. (2008) Random mutagenesis of a recombinant microbial transglutaminase for the generation of thermostable and heat-sensitive variants. *J Biotechnol 136* (3-4), 156-162.

(147) Terpe, K. (2003) Overview of tag protein fusions: from molecular and biochemical fundamentals to commercial systems. *Appl Microbiol Biotechnol 60* (5), 523-533.

(148) Schneider, H., Deweid L., Avrutina O. and Kolmar H. (2020) Recent Progress in Transglutaminase-mediated Assembly of Antibody-Drug Conjugates. *Analytical Biochemistry*. DOI: https://doi.org/10.1016/j.ab.2020.113615

7. Cumulative Section

7.1. Microbial Transglutaminase for Biotechnological and Biomedical Engineering

Title:

Microbial Transglutaminase for Biotechnological and Biomedical Engineering

Authors:

Lukas Deweid, Olga Avrutina and Harald Kolmar

Bibliographic data:

Biological Chemistry

Volume 400, Issue 3, Pages 257-274

Article first published online: 6th Oct 2018

DOI: https://doi.org/10.1515/hsz-2018-0335

Copyright: 2019 Walter de Gruyter GmbH, Berlin/Boston. Reproduced with permission.

Contributions by Lukas Deweid:

- Initial idea and performed literature research
- Preparation of the manuscript and all included graphical material
- Revised the manuscript

DE GRUYTER Biol. Chem. 2018; aop

Review

Lukas Deweid, Olga Avrutina and Harald Kolmar*

Microbial transglutaminase for biotechnological and biomedical engineering

https://doi.org/10.1515/hsz-2018-0335
Received August 7, 2018; accepted September 4, 2018

Abstract: Research on bacterial transglutaminase dates back to 1989, when the enzyme has been isolated from *Streptomyces mobaraensis*. Initially discovered during an extensive screening campaign to reduce costs in food manufacturing, it quickly appeared as a robust and versatile tool for biotechnological and pharmaceutical applications due to its excellent activity and simple handling. While pioneering attempts to make use of its extraordinary cross-linking ability resulted in heterogeneous polymers, currently it is applied to site-specifically ligate diverse biomolecules yielding precisely modified hybrid constructs comprising two or more components. This review covers the extensive and rapidly growing field of microbial transglutaminase-mediated bioconjugation with the focus on pharmaceutical research. In addition, engineering of the enzyme by directed evolution and rational design is highlighted. Moreover, cumbersome drawbacks of this technique mainly caused by the enzyme's substrate indiscrimination are discussed as well as the ways to bypass these limitations.

Keywords: antibody-drug conjugates; bioconjugation; microbial transglutaminase; protein labeling; protein PEGylation.

Introduction

Protein engineering by post-translational modification towards the generation of multifunctional conjugates is of particular importance for biomolecular and pharmaceutical research as the resulting constructs have recently found application in the field of cancer treatment (Sau et al., 2017), molecular diagnostics (Trads et al., 2017) and tailoring of therapeutics, e.g. improvement of their in-patient stability (Hu et al., 2016). Commonly used methods to generate bioconjugates, namely genetic fusion or chemical ligation, suffer from a number of drawbacks. While the genetic strategy is typically limited to the scope of proteinogenic amino acids, the chemical one either yields heterogeneous conjugates if multiple functional groups are addressed or requires orthogonally reactive sites in the target protein (Hermanson, 2013). With its stringent substrate specificity and remarkable activity, enzyme-promoted bioconjugation provides a viable alternative to the common methods of protein labeling. Enzymes can be easily isolated from cell culture, are cost-effective, environmentally friendly and allow avoiding organic solvents and harmful chemicals. No wonder that to date diverse enzymes have been applied to site-specific protein modifications, with microbial transglutaminase (mTG) from *Streptomyces mobaraensis* being among the favored candidates (Rashidian et al., 2013).

Transglutaminases comprise a class of protein-glutamine γ-glutamyltransferases (EC 2.3.2.13), bond-forming enzymes that catalyze the attachment of primary amines to protein- or peptide-bound γ-carboxamides under ammonia release (Griffin et al., 2002). In nature, this transamidation involves the glutamine side chains as acyl donors, and the ε-amino groups of lysines as acyl acceptors resulting in stable inter or intramolecular γ-glutamyl-ε-lysine isopeptide linkage (Figure 1).

In eukaryotes, transglutaminases are found in many phylogenetic taxonomic groups, including plants, animals and fungi (Folk and Cole, 1966; Bech et al., 1996; Serafini-Fracassini et al., 2009), where they participate in various physiological and cellular processes, among them wound healing (Verderio et al., 2004), male sperm maturation (Porta et al., 1986), apoptotic death pathways (Autuori et al., 1998), macrophage endocytosis (Davies and Murtaugh, 1984) or cell-matrix assembly (Zemskov et al., 2006). Furthermore, prokaryotic transglutaminases have been found in microorganisms, where they are involved in

---

***Corresponding author: Harald Kolmar,** Institute for Organic Chemistry and Biochemistry, Technische Universität Darmstadt, Alarich-Weiss-Straße 4, D-64287 Darmstadt, Germany, e-mail: Kolmar@Biochemie-TUD.de
Lukas Deweid and Olga Avrutina: Institute for Organic Chemistry and Biochemistry, Technische Universität Darmstadt, Alarich-Weiss-Straße 4, D-64287 Darmstadt, Germany

Bereitgestellt von | Universitaets- und Landesbibliothek Darmstadt
Angemeldet | kolmar@biochemie-tud.de Autorenexemplar
Heruntergeladen am | 08.10.18 09:21

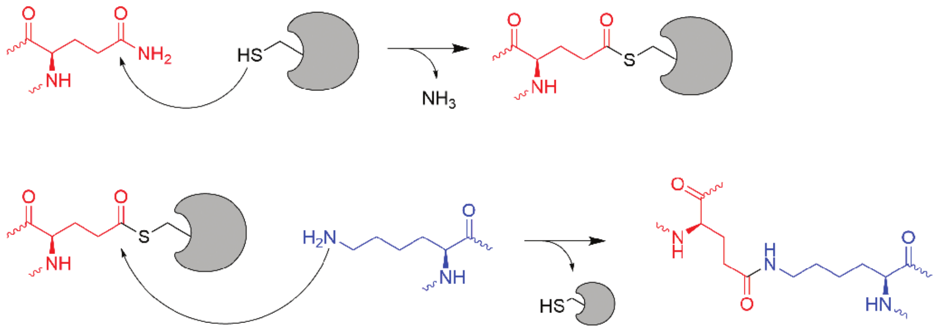

Figure 1: Mechanism of mTG-catalyzed isopeptide bond formation between protein-bound glutamine and lysine residues according to Kashiwagi et al. (2002).

sporulation (Kobayashi et al., 1998) and the formation of aerial hyphae (Chen et al., 2010; Zindel et al., 2016). Since its isolation from *S. mobaraensis* in 1989 (Ando et al., 1989), transglutaminase production has been discovered in other strains, e.g. *Streptomyces hygroscopicus* (Cui et al., 2008), *Streptomyces ladakanum* (Ho et al., 2000), *Streptomyces libani* (Umezawa et al., 2002), *S. platensis*, *Streptomyces sioyaensis*, *Streptomyces nigrescens* (Bech et al., 2000) and *Streptoverticillium cinnamoneum* (Duran et al., 1998). In addition to *Streptomycetes*, transglutaminases from *Pseudomonas aeruginosa* (Milani et al., 2012), *Bacillus subtilis* (Kobayashi et al., 1998), *Escherichia coli* (Schmidt et al., 1998), *Physarum polycephalum* (Klein et al., 1992) and a variety of other microorganisms have been identified and characterized (Kim et al., 2000; Bourneow et al., 2012).

Microbial transglutaminase from *S. mobaranesis* is widely used in the food industry and material science, where it is applied to the manufacturing of reconstructed meat, texturizing of dairy products, such as cheese or yoghurt, and stabilization of wool and leather goods (Kieliszek and Misiewicz, 2014; Tesfaw and Assefa, 2014; Romeih and Walker, 2017; Santhi et al., 2017; Taghi Gharibzahedi et al., 2018). Compared to their eukaryotic counterparts, bacterial transglutaminases possess a number of obvious advantages like small size, cofactor independency, improved performance, high stability and reduced deamination activity. Therefore, they evoked interest in the field of biochemical applications and have recently become one of the most frequently used tools for site-specific bioconjugation. In biotechnology and pharmaceutical research, mTG's ability to catalyze protein cross-linkage is used to produce stable conjugates comprising various functional biomolecules and to immobilize desired payloads onto different surfaces (Rachel and Pelletier, 2013; Strop, 2014). Due to the numerous varying applications of mTG, different process-related grades of the enzyme are currently commercially available. For biotechnological approaches, the usage of highly purified enzyme is recommended to avoid the disturbing side-reactions of impurities. Herein, we focus on recent achievements in the field of microbial transglutaminase-mediated bioconjugation and highlight its features for the generation of homogeneous biopharmaceutics. Its advantages over comparable biocatalysis and chemical modification strategies will be discussed as well as its disadvantages often induced by the non-transparent substrate preference.

Protein structure and substrate preference

Within the last three decades, microbial transglutaminase from *S. mobaraensis* has been intensively studied and thoroughly characterized. The enzyme is secreted from the cytoplasm of its host as a 406 residues zymogen bearing an *N*-terminal prepro-sequence consisting of an 18 amino acids signal peptide and a 57 residues fragment suppressing enzymatic activity to avoid intracellular crosstalk (Washizu et al., 1994; Yang et al., 2011). Extracellulary, the zymogen is processed by an endogenous metalloprotease called TGase-activating protease (TAMEP) and a tripeptidyl aminopeptidase (SM-TAP) (Zotzel et al., 2003a). Interestingly, SM-TAP procession is not essential for activity as TAMEP-treated and fully processed zymogen exhibits similar catalytic activity (Zotzel et al., 2003b). The mature enzyme is a monomeric 37.9 kDa polypeptide with an isoelectric point of 8.0 (Pasternack et al., 1998). Its catalytic activity is independent form Ca^{2+} and has its optimum at 50°C and pH 6–7 remaining rather stable in a pH range from 5 to 9 (Ando et al., 1989). Published in 2002, its crystal structure revealed that the mature enzyme adapts a disk-like shape with a ~16 Å deep cleft that holds the

Bereitgestellt von | Universitaets- und Landesbibliothek Darmstadt
Angemeldet | kolmar@biochemie-tud.de Autorenexemplar
Heruntergeladen am | 08.10.18 09:21

catalytic triad of Cys64, Asp255 and His274 at its bottom (Figure 2) (Kashiwagi et al., 2002). Residues essential for substrate recognition and catalytic activity have been determined by three-dimensional docking simulation and alanine mutagenesis scanning (Tagami et al., 2009). An overview of currently available crystal structures of microbial transglutaminases is given in Table 1. Interestingly, mTG shares neither sequential nor overall homology with eukaryotic transglutaminases but its active site coincides with that of factor XIII-like transglutaminase. This eukaryotic transglutaminase is Ca^{2+}-dependent and is operated by a catalytic triad of Cys-His-Asp that rearranges that of mTG (Cys-Asp-His) supporting the hypothesis that both enzymes evolved from convergent evolution (Kanaji et al., 1993; Kashiwagi et al., 2002).

In post-translational bioconjugation, site-specific derivatization of the desired target protein at a solitary position is strongly desired. Therefore, for a biocatalytic process knowledge on the substrate recognition is indispensable to predict potential conjugation sites. In the case of microbial transglutaminase, many attempts have been undertaken to address this challenge. In 1996, Nonaka and coworkers investigated mTG's acyl-acceptor specificity upon catalytic tethering of various lysine-bearing dipeptides to α_{s1}-casein and found that all of them were accepted by mTG. Though no clear trend concerning the nature of neighboring amino acids was observed, hydrophobic residues Ile, Trp and Leu seemed to impair catalytic performance (Nonaka et al., 1996). Two decades later, Malesevic et al. established a synthetic library of tripeptides on a cellulose membrane to examine the influence of the surrounding amino acids at −1 and +1 position to the reactive residue. Coupling of a fluorescently labeled acyl donor confirmed the promiscuity of mTG concerning the acyl acceptor. Interestingly, the tripeptides having an aromatic residue or an additional lysine adjacent to the addressable amine showed better performance in mTG-catalyzed couplings. In contrast, anionic neighbors of the respective lysine compromised mTG activity (Malesevic et al., 2015).

Obviously, mTG chooses its acyl-acceptor substrate nearly promiscuous. Therefore, numerous primary amines besides its typical lysine substrate were examined in order to expand the scope of reactive handles.

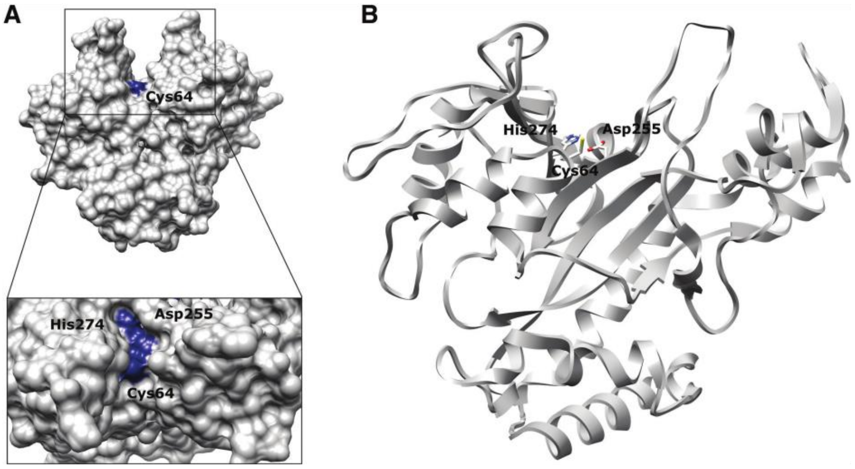

Figure 2: Crystal structure of microbial transglutaminase derived from PDB:1IU4.
(A) Front view: molecular surface of the active enzyme. Inlet: top view: The ~16 Å deep active site cleft buries the catalytic residues Cys64, Asp255 and His274 (highlighted in blue). (B) Ribbon drawing of the enzyme.

Table 1: Available crystal structures of microbial transglutaminases on the RCSB Protein Data Base.

Enzyme	Size (kDa)	Organism	RCSB PDB entry
Pro-mTG	42.5	*Streptomyces mobaraensis*	3IU0
mTG	37.9	*Streptomyces mobaraensis*	1IU4
Tgl	28	*Bacillus subtilis*	4P8I
KalbTG	26.4	*Kutzneria albida*	5M6Q
Cytotoxic necrotizing factor 1 catalytic domain	32.6	*Escherichia coli*	1HQ0

Bereitgestellt von | Universitaets- und Landesbibliothek Darmstadt
Angemeldet | kolmar@biochemie-tud.de Autorenexemplar
Heruntergeladen am | 08.10.18 09:21

It has been shown that mTG tolerates aliphatic amines (the primary ones are preferred), carboxyterminal esters of amino acids, pentyl- and hexylamine-tethered sugar derivatives (Ohtsuka et al., 2000a) and, surprisingly, small unbranched amines bearing π-electron systems in close proximity. Thus, excellent conversion was achieved for nitrile-, alkyne- and azide-decorated primary amines enabling new perspectives for the efficient introduction of ‘clickable’ moieties in natural biomolecules (Gundersen et al., 2014; Oteng-Pabi et al., 2014; Rachel and Pelletier, 2016).

Acyl-donor recognition is more stringent. Many attempts have been made to identify amino acid patterns which can facilitate mTG-mediated labeling. Thus, initial studies by Ohtsuka et al. revealed that leucine and bulky residues in close proximity to the addressable glutamine generally accelerate mTG performance (Ohtsuka et al., 2000b). Further results obtained from a phage-displayed peptide library reported by Sugimura et al. confirmed these findings. Indeed, it was found that aromatic amino acids Trp, Phe and Tyr at the –3 to –5 position to the reactive glutamine, as well as arginine and hydrophobic residues at the +1 and +2 as well –1 and –2 position support mTG catalysis (Sugimura et al., 2008). An mRNA-displayed peptide library constructed by Lee et al. barely yielded conserved motifs recognized by mTG. At the –3 position, Arg was predominant while at +1 position Gln and Pro appeared repeatedly (Lee et al., 2013). However, both screening attempts succeeded in identifying peptidic sequences that mediated efficient and site-specific modification when genetically fused to model proteins. Moreover, results from a fluorescent peptide array screen developed by Malesevic and colleagues are in good accordance with those obtained from phage display (Malesevic et al., 2015).

Besides the properties of the surrounding amino acids in view of their charge and polarity, substrate recognition of mTG is assumed to be affected by the tertiary structure of the targeted protein. In 2012, Spolaore et al. postulated that local unfolding and chain flexibility are key factors for substrate recognition as unstructured regions of investigated model proteins were well conjugated (Spolaore et al., 2012). On the contrary, Rachel et al. demonstrated that mTG-mediated transamidation within well-defined secondary structure elements is feasible by incorporating highly reactive glutamine residues into α-helices and β-sheets of the B1 domain of protein G (Rachel et al., 2017).

Recently, Fiebig and coworkers identified dispase autolysis-inducing protein (DAIP) from *S. mobaraensis* as an intrinsic substrate for mTG. Five cross-linked Gln residues were investigated concerning their reactivity in mTG-catalyzed couplings. However, amino acids neighboring reactive glutamines neither possessed a distinct consensus sequence nor reassembled the motifs predicted by library screening. Those findings led the authors to the hypothesis that Gln residues flanked by small, polar, hydrophobic and/or uncharged amino acids are preferred over the bulky, aromatic and charged ones (Fiebig et al., 2016). These assumptions were confirmed in further studies by Juettner et al. who investigated the Gln6 acyl-donor site (the only reactive one out of three surface exposed glutamines) of another physiological substrate, *Streptomyces* papain inhibitory protein (SPI_p), by mutagenesis of neighboring Lys7. Indeed, replacement of surface-exposed residues offsite the glutamine (Q6) flanking region of the SPI_p, which are believed to contribute in mTG recognition, for arginine or anionic amino acids influenced reactivity of the enzyme. Surprisingly, charge inversion of ionic residues accelerated SPI_p modification in all cases and comparable results were observed when uncharged residues where substituted for acidic or basic ones. These results gave rise to the hypothesis that mTG-mediated modification of proteinaceous substrates is determined by site- and orientation-specific conditions due to the surface and structural properties of the substrate (Juettner et al., 2018).

Summarizing the above highlighted studies, current knowledge of mTG substrate recognition is rather vague, especially considering its acyl-acceptor repertoire. A number of excellent screening strategies have to date been applied to shed light on this issue (Sugimura et al., 2008; Lee et al., 2013; Malesevic et al., 2015). However, the mTG subsite specificity on a peptidic level seems to differ from that observed for the full-size folded proteins, where altered substrate preference could emerge due to unpredictable accessibility of potentially addressable sites. Though Maullu et al. successfully forecasted potential conjugation sites for mTG in human granulocyte colony-stimulating factor (G-CSF) by combining MS simulation and molecular docking (Maullu et al., 2009), predicting sites for modification in novel target proteins remains difficult, especially when crystal structures are not available. Surprisingly, some proteins like human growth hormone (hGH) bear two or more addressable glutamines that were labeled to an unequal extent (Buchardt et al., 2010), while others like human immunoglobulin G1 (IgG1) lack suitable glutamines for transamidation, hence, no mTG-assisted modification could be achieved (Jeger et al., 2010). It should be noted that in the case of unequally labeled conjugate expensive and laborious purification is required. In addition, when unexpectedly addressable acyl donors

Bereitgestellt von | Universitaets- und Landesbibliothek Darmstadt
Angemeldet | kolmar@biochemie-tud.de Autorenexemplar
Heruntergeladen am | 08.10.18 09:21

and acceptors are located within the same target, an uncontrolled polymerization of starting material can occur, leading to drastic decreases in coupling efficiency. As a consequence, sites of modification within novel targets need careful case-specific evaluation to guarantee orthogonality of the mTG-catalyzed acyl transfer. How scientists overcame these major drawbacks and made use of the enzyme's extraordinary substrate specificity will be presented in the following sections.

Biotechnological applications

Protein-protein conjugates

Dual-functional fusion proteins are of particular importance for essential immunochemical assays, among them Western blotting and enzyme-linked immunosorbent assay (ELISA). However, genetic fusion of the respective counterparts suffers from poor yields when hybrid molecules of large size are assembled. To that end, mTG catalysis was considered as a method of choice for the preparation of protein-protein conjugates. In 2000, Bechtold et al. have demonstrated that coupling of two functional proteins, soybean peroxidase and protein G, at intrinsic lysine and glutamine sites is feasible. However, only a minor amount of desired conjugate was yielded, that possessed a heterogeneous distribution of constituents; moreover, the sites of conjugation were not investigated (Bechtold et al., 2000). Later, mTG-mediated conjugation of avidin with G-CSF revealed Lys127 as major ligation site, while modification at two additional positions of this protein, namely Gln126 and Lys58, was negligible. As a consequence, only desired conjugates were obtained, without further polymerization (Spolaore et al., 2014). This finding opened the door for straightforward preparation of avidin conjugates which are widely used in different biomedical, especially diagnostic, applications (Wilchek and Bayer, 1990; Lesch et al., 2010).

When intrinsic residues within the desired protein lack mTG recognition, the respective tags can be introduced upon recombinant production at either terminal or internal sites. Thus, incorporation of acyl-donor and -acceptor sequences LLQG and KGK (see Table 2, entry **6** and **14**), respectively, in the monomeric subunits of the 'sweet protein' monellin enabled their covalent linkage that accounted for the enhanced thermal stability of the dimer (Ota et al., 1999). Since these pioneering attempts, various novel recognition motifs for efficient crosslinking have been utilized in a broad range of applications. Frequently used acyl-donor and -acceptor sequences are overviewed in Table 2. Exemplarily, a single-chain variable fragment specific for anti-hen egg white lysozyme was ligated with bacterial alkaline phosphatase (AP) (Takazawa et al., 2004) or enhanced yellow fluorescent protein (Kamiya et al., 2003a). A *camelid* variable heavy-chain domain-only antibody specific for human tumor necrosis factor was dimerized and even multimerized through recombinantly incorporated specific peptidyl linkers, which resulted in improved *in vitro* activity (Plagmann et al., 2009). Surprisingly, *N*-terminal pentaglycyl motifs as an amine component were found to mediate protein modification upon mTG as demonstrated through crosslinking of enhanced green fluorescent protein (eGFP) and dihydrofolate reductase (Tanaka et al., 2005). Recently, multifunctional protein complexes of three subunits were engineered using peptidyl linker sequences. Having applied this strategy, Bhokisham et al. succeed in the coupling of quorum sensing synthases S-ribosylhomocysteinase and S-adenosylhomocysteine nucleosidase to protein G and demonstrated functionality of the formed trimer. Interestingly, the sequential attachment of the reaction partners occurred on solid support, which enabled careful optimization of reaction stoichiometry. The precise choice of a recognition tag locus allowed to minimize undesired multimerization (Bhokisham et al., 2016).

Protein-oligonucleotide conjugates

Covalent coupling of nucleic acid macromolecules, DNA or RNA, to proteins became a powerful approach in modern molecular biology, pharmacy and material science due to the variable functions of both components. Protein-oligonucleotide conjugates emerged as versatile tools for valuable analytic and medical applications such as drug delivery (Mascini et al., 2012), molecular diagnostics (Niemeyer et al., 2003; Adler, 2010), and surface immobilization (Wacker and Niemeyer, 2004). Traditional protein-oligonucleotide ligation relies on chemical techniques that address umpteen functional groups of the desired target protein and is often accompanied by a partial functional loss due to treatment of the protein with organic solvent or steric hindrance within the resulting conjugate. Obviously, site-specific coupling is favored to avoid modification of residues that are essential for protein function. To that end, innovative strategies that rely on microbial transglutaminase were developed in the laboratory of Kamiya and Goto. In initial attempts, aminated DNA showing poor reactivity towards mTG was chemically attached to the standard acyl-donor substrate

Bereitgestellt von | Universitaets- und Landesbibliothek Darmstadt
Angemeldet | kolmar@biochemie-tud.de Autorenexemplar
Heruntergeladen am | 08.10.18 09:21

Table 2: Summary of commonly used peptidyl-linker sequences that facilitate modification by microbial transglutaminase.

Entry	Sequence	Acyl-site	Origin	Demonstrated target	Reference
1	MKHK(GS)	Acceptor	Horse heart myoglobin	*Escherichia coli* alkaline phosphatase; eGFP	(Tominaga et al., 2004, 2007; Abe et al., 2010; Takahara et al., 2016)
2	MRHKGS	Acceptor	Horse heart myoglobin	eGFP	(Abe et al., 2011)
3	TKHKIP	Acceptor	Horse heart myoglobin	*Escherichia coli* alkaline phosphatase	(Takazawa et al., 2004)
4	KETAAAAFERAHMDS	Acceptor	Ribonuclease S-peptide	Enhanced yellow fluorescent protein (eYFP)	(Kamiya et al., 2003a)
5	IRINKGPGRAFVT/ IRINRGPGKAFVT	Acceptor	V3 loop of HIV-1 IIIB gp 120 protein	*Escherichia coli* alkaline phosphatase	(Mori et al., 2011)
6	KGK	Acceptor		Monellin	(Ota et al., 1999)
7	NH_2-GGGGG	Acceptor		eGFP	(Tanaka et al., 2005)
8	KETAAAKFERQHMDS	Acceptor + Donor	Ribonuclease S-peptide	eGFP; eBFP; camelidae anti-human TNF TrpV_HH	(Kamiya et al., 2003b; Plagmann et al., 2009)
9	PLAQSH	Donor	Horse heart myoglobin	Anti hen-egg lysozyme scFv	(Kamiya et al., 2003a; Takazawa et al., 2004)
10	RLQQG	Donor	mRNA-display library	DsRed	(Lee et al., 2013)
11	WALQRPYTLTES/ YELQRPYHSELP/ WALQRPHYSYPD	Donor	Phage-display library	Glutathion-S-transferase	(Sugimura et al., 2008)
12	EQKLISEEDL	Donor	c-Myc epitope commonly used for immunostaining	Fab-fragments; Nanobody; affibody; dihydrofolatereductase	(Tanaka et al., 2005; Dennler et al., 2015)
13	LQSP	Donor	Focused, synthetic peptide library	Fluorescent peptides	(Caporale et al., 2015)
14	LLQG(A)	Donor		Several immunglobulins; eGFP; glutathion-S-transferase Q207A; monellin	(Ota et al., 1999; Tanaka et al., 2007; Strop et al., 2013)
15	MLAQGS	Donor		*Escherichia coli* alkaline phosphatase; *Escherichia coli* biotin ligase (BirA)	(Moriyama et al., 2011; Yu et al., 2016)
16	FYPLQMRG	Donor		eGFP	(Takahara et al., 2017)
17	GECTYFQAY GCTE	Donor	Dispase-autolysis inducing protein	Therapeutic antibody cetuximab	(Siegmund et al., 2015)

N-benzyloxycarbonyl-L-glutaminylglycine (Z-Gln-Gly, Z-QG) and further coupled to AP (Figure 3, left) (Tominaga et al., 2007). Later, they identified polymerases that are capable of incorporating Z-QG-modified desoxyribonucleotides (dNTPs) in DNA and labeled the resulting strand with multiple copies of a thermostable AP from *Pyrococcus furiosus* (Figure 3, center) (Kitaoka et al., 2011). Another methodology invented by the same group relies on the template-independent incorporation of transglutaminase-applicable dNTPs by a terminal desoxynucleotidyl transferase (Figure 3, right). Thus, a thrombin-binding aptamer was coupled to multiple AP molecules and functionality of the complex was verified in a sandwich enzyme-linked aptamer assay (Takahara et al., 2013, 2016). Using a similar strategy, a c-Met binding aptamer was recently attached to eGFP and potential of the resulting bifunctional construct for molecular drug delivery was clearly demonstrated by binding to c-Met-overexpressing cells (Takahara et al., 2017).

Transglutaminase-mediated surface immobilization

Immobilization on a solid support is a widely-used technique to increase stability of labile and cost-intensive enzymes and enable their reuse. For this application

Bereitgestellt von | Universitaets- und Landesbibliothek Darmstadt
Angemeldet | kolmar@biochemie-tud.de Autorenexemplar
Heruntergeladen am | 08.10.18 09:21

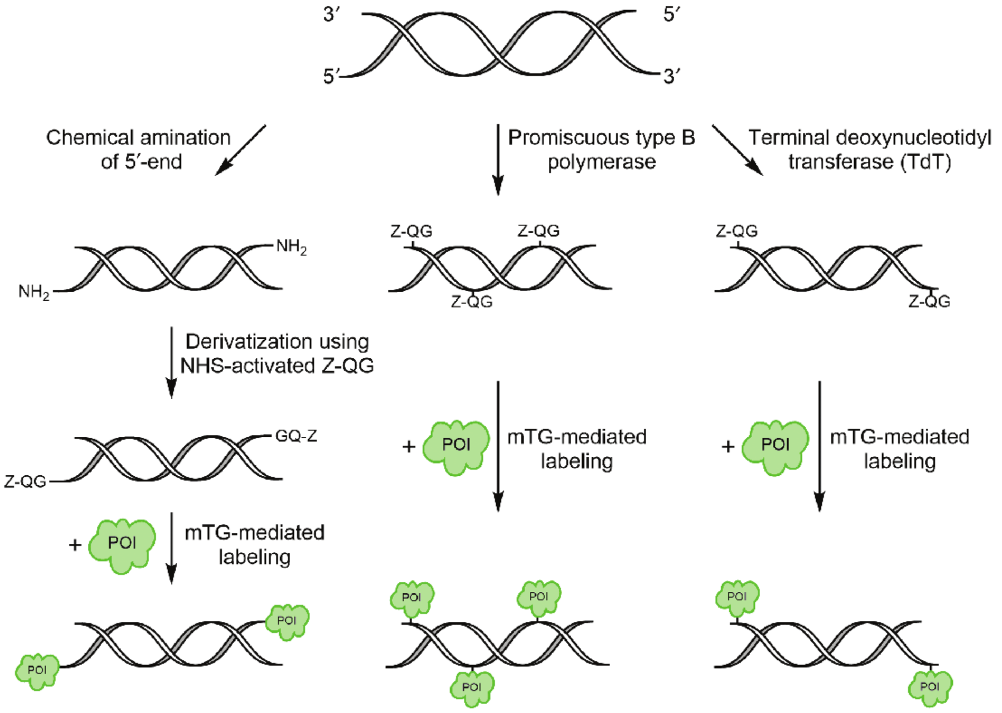
3′
5′
5′
3′
Chemical amination of 5′-end
Promiscuous type B polymerase
Terminal deoxynucleotidyl transferase (TdT)
NH$_2$
NH$_2$
Z-QG
Z-QG
Z-QG
Z-QG
Z-QG
Derivatization using NHS-activated Z-QG
GQ-Z
Z-QG
+ POI
mTG-mediated labeling
+ POI
mTG-mediated labeling
+ POI
mTG-mediated labeling
POI

Figure 3: Overview of chemical and enzymatic methodologies that allow for the construction of protein-oligonucleotide conjugates by microbial transglutaminase.
Abbreviation used: POI, protein of interest.

site-specific modification is desired as well, especially when instable targets are addressed. Compared to the harsh conditions often applied upon chemical immobilization, enzymatic catalysis has an obvious advantage due to fast and selective performance in aqueous media under mild conditions. To that end, microbial transglutaminase was used to immobilize model proteins AP and eGFP at various modified surfaces to demonstrate feasibility of this approach. While AP was coupled to aminated magnetic particles (Moriyama et al., 2011) and casein-coated agarose beads (Tominaga et al., 2005), eGFP was immobilized at a chemically treated glass surface (Tanaka et al., 2008) and at polystyrene coated with β-casein (Tanaka et al., 2007).

BirA, a biotin ligase from *E. coli*, frequently used for *in vivo* and *in vitro* biotinylation of recombinant proteins, was immobilized at amine-modified magnetic beads by mTG-promoted condensation. While manufacturing of the recombinant enzyme for large-scale protein purification is cost-intensive, and recovery of the catalyst is cumbersome, immobilized BirA exhibited >95% activity after 10 rounds of recycling. Moreover, separation from the reaction mixture was straightforward (Yu et al., 2016).

Widely used for various applications, antibodies contain a conserved *N*-glycosylation site within their F$_c$-region and usually comprise a heterogeneous mixture of different glycoforms when purified from cell culture. Engineering of F$_c$-glycans is a viable strategy to tailor the properties of these multifaceted biomolecules, e.g. by truncation or remodeling of the attached oligosaccharide. Recently, mTG catalysis was applied by Li and colleagues to couple endoglycosidase S2 (Endo-S2) from *Streptococcus pyogenes* and its glycosynthase mutant D184M (Endo-S2D184M) onto aminated agarose beads. They demonstrated that immobilized Endo-S2 is capable of truncating the F$_c$-glycan of therapeutic antibodies rituximab and trastuzumab while its mutant Endo-S2 D184M was able to restore the cleaved sugar chain towards a mono-substituted homogeneous glycoform (Li et al., 2018).

Noteworthy, though all of the examined proteins possessed intrinsic residues within the wildtype sequences that theoretically could be recognized by mTG, no transglutaminase activity was observed at those sites. In all the cases, site-specific immobilization was achieved through incorporation of specific peptidyl linker sequences that mediated crosslinking by mTG (Table 2, entries **1**, **14** and **15**).

Bereitgestellt von | Universitaets- und Landesbibliothek Darmstadt
Angemeldet | kolmar@biochemie-tud.de Autorenexemplar
Heruntergeladen am | 08.10.18 09:21

Pharmaceutical applications

Protein-polymer conjugation

PEGylation, the post-translational attachment of polyethylene glycol to small protein-based drugs is a powerful technique in modern medicine to improve the pharmacokinetic properties of a pharmacophore. PEGylated pharmaceutics usually reveal diminished renal clearance and reduced immunogenicity compared to their non-PEGylated counterparts due to an enlarged hydrodynamic radius and higher conformational stability (Dozier and Distefano, 2015). As a consequence of increased bioavailability, daily intravenous administration can be adjusted to a more patient-friendly frequency (Lawrence and Price, 2016). Especially in pharmaceutical research, tightly controlled conjugation strategies are of prime importance because modification at binding interfaces or active-site residues might affect the *in vivo* functions. Undesired side reactivity during conjugation results in a heterogeneous mixture of products with potentially altered pharmacokinetic profiles making it difficult to guarantee batch-to-batch stability which is required when new biological entities are licensed by the Food and Drug Administration (FDA). Otherwise, complicated and cost-intensive separation from the side-products is necessary. Nevertheless, PEGlayted proteins manufactured by chemical derivatization, namely G-CSF (Neulasta®), interferon-α-2b (PegIntron®), hGH (Somavert®) and others successfully reached the world market (Dozier and Distefano, 2015). Compared to chemical modification, the site-selectivity of microbial transglutaminase is sufficient to access PEGylated custom derivatives of various proteinaceous drugs without compromising their properties. Sato et al. used mTG in pioneering site-specific conjugation of PEG-12000 to Gln74 of human interleukin-2 under preservation of bioactivity and decreased secretion of the active drug (Sato et al., 2001). Since then, mTG has been used for the PEGylation of pharmaceutically relevant proteins, among them human G-CSF (Scaramuzza et al., 2012; Mero et al., 2016), cytochrome *c* (Zhou et al., 2016), interferon α-2b (Spolaore et al., 2016) and β-1a (Spolaore et al., 2018), salmon calcitonin (sCT) (Mero et al., 2011) and hGH (Buchardt et al., 2010; da Silva Freitas et al., 2013; Grigoletto et al., 2016).

As mentioned above, substrate selectivity of mTG is sometimes difficult to comprehend; while some target proteins possess more than one transamidation site, others remain unaddressed. For example, in hGH several residues (Gln40 and Gln141) are mTG-reactive (Buchardt et al., 2010; da Silva Freitas et al., 2013; Grigoletto et al., 2016). This observation was first described by Mero et al. who coupled monodisperse *Boc*-protected aminoPEG to model proteins hGH, G-CSF and horse heart apomyoglobin and used the sensitivity of mass spectrometry to identify the modified residues (Mero et al., 2009). In their further studies, organic solvents were used to influence the substrate specificity of mTG towards hGH and sCT. Mass-spectrometric analysis and size exclusion chromatography have clearly revealed that modification of hGH in the presence of 50% (v/v) ethanol yielded exclusively mono-PEGylated product at Gln141. Moreover, the conjugation of sCT to Gln20 was successfully directed by the addition of 30% (v/v) DMSO, 50% (v/v) ethanol or 60% (v/v) methanol (Mero et al., 2011).

Covalent immobilization of mTG to a solid support was found to be another suitable approach to manipulate its subsite specificity. Recently, Grigoletto and coworkers coupled mTG to agarose beads through its *N*-terminus by reductive alkylation and examined its activity and substrate specificity in the bound state. The immobilized enzyme possessed diminished enzymatic activity and changed kinetic parameters (most likely as a result of chemical treatment) but appeared more site-selective with respect to PEGylation of α-lactalbumin and G-CSF. In the case of α-lactalbumin, substrate specificity was driven towards selective modification of a single glutamine out of four possible residues addressed by the unbound enzyme. When G-CSF served as a target, site-selectivity towards Gln135 remained; moreover, undesired deamination was decreased (Grigoletto et al., 2017).

Besides PEGylation, other polymeric molecules have been utilized for mTG-mediated protein conjugation. Hydroxyethyl starch (HES), a biodegradable alternative to PEG, was chemically modified to serve as an acyl donor/acceptor and successfully ligated to monodansyl cadaverine. However, coupling of HES to model protein *N*,*N*-dimethylcasein led to heterogeneous polymerization due to multiple acceptable acyl-donor/acceptor sites within the addressed target protein (Besheer et al., 2009). In 2011, Abe et al. used mTG to couple MRHKGS-tagged eGFP to lipid-modified peptide GGGSLLQG and demonstrated that the hydrophobic tail of the eGFP-C18 conjugate anchored the hybrid molecule at the cell membrane of B16 melanoma cells (Abe et al., 2011). Moreover, mTG was shown to be capable of catalyzing its acyl-transfer reaction between acyl-donor molecules and aminated oligosaccharides. Bovine trypsin was coupled to putrescin (1,4-diaminobutane)-derivatized dextran, carboxy-methylcellulose and Ficoll resulting in enhanced thermostability. Interestingly, the glycosylated enzyme revealed to be more resistant to autolytic degradation and

Bereitgestellt von | Universitaets- und Landesbibliothek Darmstadt
Angemeldet | kolmar@biochemie-tud.de Autorenexemplar
Heruntergeladen am | 08.10.18 09:21

action of anionic detergent SDS (Villalonga et al., 2006). Similar results were obtained when bovine liver catalase was modified with aminated dextran. The protein-polymer conjugate showed increased enzymatic activity and enhanced stability at 55°C. Its pharmacokinetic properties were also positively influenced as the glycosylated enzyme possesses 2.5-fold increased plasma half-life and three-fold reduced clearance after intravenous administration in rats (Valdivia et al., 2006). Noteworthy, glycosylation of trypsin and catalase was obtained by transamidation of intrinsic carboxamide functions. Even though an average distribution of conjugated oligosaccharides per protein was calculated from the colorimetric quantification of d-glucose units, a precise identification of modified residues is lacking.

Antibody-drug conjugates

Cancer as the second leading cause of death in the USA is a major health threat for modern society and a challenging task for medical and pharmaceutical research (Siegel et al., 2016). Antibody-drug conjugates (ADCs) are promising agents for the treatment of tumors because they combine benefits of two different well-established strategies. In these constructs, a chemotherapeutic is covalently linked to an immunoglobulin to enlarge the respective therapeutic window by combining the potency of organic toxins and the target specificity of antibodies. Recently, ADCs Besponsa® (Inotuzumab-ozogamicin) (Shor et al., 2015; Lamb, 2017) and Mylotarg® (Gemtuzumab-ozogamicin) (Appelbaum and Bernstein, 2017; Lamba et al., 2017) from Pfizer have been launched to the marked and joined Kadcyla® (Trastuzumab-emtansine) (Niculescu-Duvaz, 2010; LoRusso et al., 2011) from Roche and Adcetris® (Brentuximab-vedotin) (Senter and Sievers, 2012; Yi et al., 2017) from Seattle Genetics. More than 60 ADCs were in ongoing clinical trials in 2017 underlining the importance of these novel drugs (Beck et al., 2017). The therapeutic index of an ADC is stipulated by certain factors depending on the choice of target, linker chemistry and the toxicity of a payload. The respective topics are detailed in many excellent current reviews (Behrens and Liu, 2014; Jain et al., 2015; Kline et al., 2015; Schumacher et al., 2016; Beck et al., 2017; Drake and Rabuka, 2017; Sau et al., 2017; Tsuchikama and An, 2018). Multiple studies consistently reported significantly improved pharmacokinetics, superior efficacy and reduced off-target toxicity of ADCs when warheads are site-selectively and not randomly ligated (Figure 4) (Junutula et al., 2008; Behrens et al., 2015; Bryant et al., 2015). To date, the majority of ADCs in the clinical pipeline (as well as those already approached by the FDA) are assembled by a random modification of intrinsic lysines or cysteines. Recently, as the landscape of ADC field has been shifted towards site-specific modification at defined positions, a number of respective chemical and enzymatic approaches has been developed (Drake and Rabuka, 2017).

From a chemical point of view, antibodies are absolutely unfavorable targets as they lack orthogonally addressable functionalities. Nonetheless, chemical approaches to modify antibodies site-selectively were developed including engineering of additional cysteine (THIOMAB technology) (Junutula et al., 2008; Shen et al., 2012; Shinmi et al., 2016; Dimasi et al., 2017) or selenocysteine residues (Li et al., 2017), re-bridging of naturally occurring cysteines (Behrens et al., 2015; Bryant et al., 2015), redox-based methionine bioconjugation (Lin et al., 2017), incorporation of unnatural amino acids (Axup et al., 2012; Zimmerman et al., 2014; VanBrunt et al., 2015), glyco-engineering (Li et al., 2014; Zhou et al., 2014; van Geel et al., 2015) and metallopeptide-based catalysis (Ohata and Ball, 2017) as well as ADCs derived from auto-catalytic antibodies (Nanna et al., 2017). Moreover, the subsite-specificity of some enzymes, among them sortase A (Chen et al., 2016; Xu et al., 2017), SpyLigase (Siegmund et al., 2016), formylglycine-generating enzyme (Drake et al., 2014), phosphopantetheinyl transferase (Grunewald et al., 2015), tubulin tyrosine ligase (Schumacher et al., 2015, 2016) and mushroom tyrosinase (Bruins et al., 2017) were successfully recruited for site-selective ADC generation. Microbial transglutaminase has been shown to be incapable of labeling glutamines in native human IgG1 antibodies efficiently, even though multiple surface-exposed Gln sites were available (Mindt et al., 2007). However, incorporation of a specific recognition tag proved to be a powerful strategy to overcome this limitation. Researchers at Rinat-Pfizer systematically placed the transglutaminase recognition sequence LLQGA (Table 2, entry **14**) at various surface-exposed regions of an anti-epidermal growth factor receptor antibody and thus identified 12 positions within the light or heavy chain which facilitated highly-efficient labeling by mTG. They transferred their findings to an anti-M1S1 antibody and examined potency of MMAD (monomethyl dolastatin 10)-armed IgGs in xenograft mouse models and *in vitro* cell-killing assays. The constructs showed toxicity similar to that of an antibody modified by conventional cysteine conjugation, but pharmacokinetic studies revealed that the site of conjugation significantly influences whole body clearance. In addition, species-dependent difference in mice and rat was observed that is in-line with previous

Bereitgestellt von | Universitaets- und Landesbibliothek Darmstadt
Angemeldet | kolmar@biochemie-tud.de Autorenexemplar
Heruntergeladen am | 08.10.18 09:21

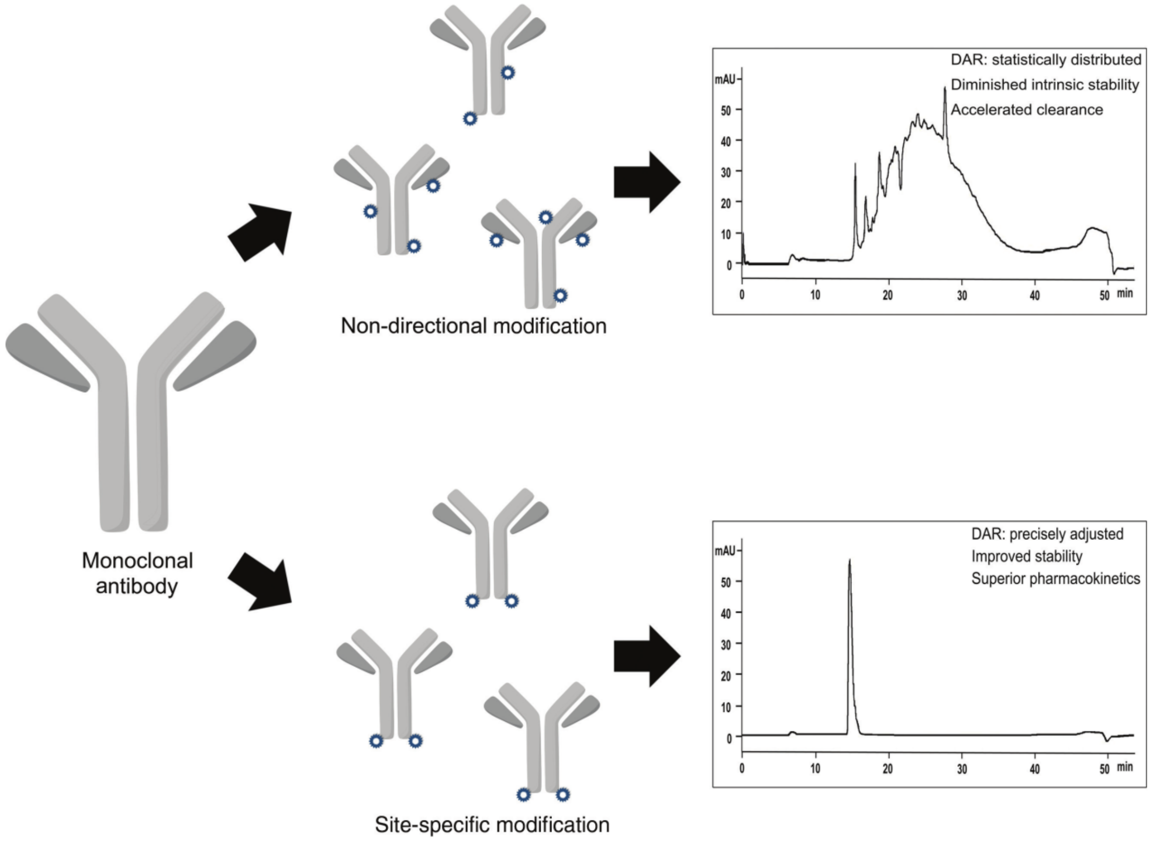
DAR: statistically distributed
Diminished intrinsic stability
Accelerated clearance
mAU
50
40
30
20
10
0
0
10
20
30
40
50
min
Non-directional modification
Monoclonal antibody
DAR: precisely adjusted
Improved stability
Superior pharmacokinetics
Site-specific modification

Figure 4: Schematic comparison of site-specifically and non-directionally manufactured antibody-drug conjugates. Hydrophobic interaction chromatography visualizes the impact of the utilized methodology on the homogeneity of the assembled ADC. Non-directional methodologies generate a heterogeneous product with statistically distributed coupling sites and a fluctuating hydrophobic profile. On the contrary, site-specific conjugation ensures reproducible hydrophobic properties by restricting antibody modification onto distinct positions. Abbreviations used: DAR, drug-to-antibody ratio; ADC, antibody-drug conjugate.

observations (Strop et al., 2013). Further studies demonstrated that ADCs constructed in a site-specific manner by mTG have superior pharmacokinetics compared to conventional cysteine-conjugated ADCs, underlining the benefits of selective strategies over statistical ones (Dorywalska et al., 2015; Strop et al., 2015).

We have recently derived a novel recognition motif for mTG from its natural substrate. The Gln298-containing region of DAIP was mimicked and grafted at the heavy chain of therapeutic antibody cetuximab with its native loop covalently locked by incorporation of an intramolecular cysteine bridge. The conformationally constrained recognition motif was shown to mediate superior labeling over a linear control, making it a suitable tag for the generation of homogeneous ADCs (Siegmund et al., 2015).

Researchers of the Schibli group discovered that removal of the F$_C$-glycan from the C$_2$H domain of antibodies exposes Gln295 as potential site for transamidation by mTG. They showed that enzymatic truncation of the F$_C$-glycan by PNGase F and genetic substitution of Asn297 by Gln facilitates the efficient generation of homogeneous ADCs with a defined drug-to-antibody ratio (DAR) of 2 and 4, respectively (Jeger et al., 2010). Interestingly, Farias et al. found that native antibodies purified from cell culture were also labeled at Gln295 to a lower extent, most likely as a result of incomplete glycosylation (Farias et al., 2014). Moreover, a chemo-enzymatic methodology based on the aglycosylation of Asn297 was established, relying on mTG-directed incorporation of an aminated azide that can be further selectively modified by highly efficient strain-promoted alkyne-azide cycloaddition (Dennler et al., 2014). An anti-CD30 antibody armed using this technique showed higher tumor uptake, reduced off-target activity and significant increase in the maximal tolerated dose in mouse models compared to commercially available ADC Adcetris® (Lhospice et al., 2015). Anami et al. extended this chemo-enzymatic strategy using synthetic branched linkers containing two alkyne-reactive handles

Bereitgestellt von | Universitaets- und Landesbibliothek Darmstadt
Angemeldet | kolmar@biochemie-tud.de Autorenexemplar
Heruntergeladen am | 08.10.18 09:21

for the generation of ADCs with defined DARs of 4 (Anami et al., 2017). Aglycosylation of liberated Gln295 enabling transamidation in combination with well-established maleimide-thiol coupling to engineered cysteines was recently used by Puthenveetil et al. to yield dual-functionalized derivatives of a therapeutic antibody trastuzumab. The authors demonstrated both strategies as being suitable to modify protein A-captured antibodies, making the construction of single- and dual-functionalized ADCs more straightforward (Puthenveetil et al., 2016).

Though aglycosylation of Asn297 opened the door for various innovative techniques, discussion concerning the eliminated F_c-glycan is necessary. Glycosylation of immunoglobulins is essential to trigger effector cells of the human immune defence to eliminate pathogens through various cellular pathways – an effect that is employed in the treatment of tumors with therapeutic antibodies (Smith, 2015). This benefit can be neglected in the context of ADCs as they mediate efficient tumor suppression by a cytotoxic warhead. However, the contribution of F_c-glycans to pharmacodynamics and pharmacokinetics is still under discussion (Reusch and Tejada, 2015). The remarkably long half-life (approximately 21 days for typical IgG1 molecules; Mould and Sweeney, 2007) of IgGs is achieved through recycling mediated by the neonatal F_c receptor and is believed to be glycosylation-independent (Jefferis, 2012). Compared to their native counterparts, glyco-deficient IgG1 molecules showed similar antigen binding, plasma clearance and serum half-life in rats and mice, but showed increased thermal and proteolytic lability and pronounced tendency to pH-induced aggregation (Tao and Morrison, 1989; Zheng et al., 2011; Hristodorov et al., 2013). Therefore, careful evaluation of ADCs manufactured by transamidation of aglycosylated antibodies is necessary to ensure stability of the resulting construct.

In addition to multiple non-reactive glutamines, antibodies possess surface-exposed lysines that can act as potential acyl-acceptors for mTG. Researchers from Morphotek Inc. recognized that *C*-terminal incorporation of a single amino acid at the heavy chain of antibodies prohibits clipping of Lys447 which is normally processed by an endogenous carboxypeptidase. Within their study, only Lys447 appeared reactive towards mTG. Besides Lys447, multiple sites for the incorporation of reactive lysines were screened, which allowed for the construction of stable ADCs with a defined DAR (Spidel et al., 2017). Spycher et al. immobilized mTG on glass microbeads and observed, consistent with others, that surface-bound mTG exhibits more selective substrate recognition compared to its soluble counterpart (Grigoletto et al., 2017). While the unbound enzyme utilizes Lys288/290 and Lys340 as acyl-acceptors to an unequal extent, the immobilized one exclusively addresses Lys340 of antibody cAC10, most likely as a result of steric hindrance. These findings in combination with aglycosylation of Asn297 were used to construct dual-functional ADCs comprising a fluorescent handle and a metal chelator for *in vivo* tumor imaging and radiotherapy, respectively (Spycher et al., 2017).

To date, transglutaminases have been isolated from various bacterial strains besides *S. mobaraensis*. Wojtek and co-workers from Roche recently identified a highly interesting mTG species from *Kutzneria albida* (KalbTG) (Steffen et al., 2017). Sequence alignment with *S. mobaraensis* transglutaminase revealed 30% coverage with conserved areas within the enzyme's active site making KalbTG a potential transglutaminase. Production of soluble and active KalbTG in *E. coli* cells was established and the corresponding crystal structure was obtained. Moreover, substrate specificity of the smallest (26 kDa) transglutaminase known to date was identified using a novel ultra-dense peptide array technology. Interestingly, consensus sequences that mediated efficient transamidation by KalbTG clearly differed from those identified for mTG. They demonstrated orthogonality of both enzymes by incorporating specific recognition motifs of the corresponding transglutaminases to a 7 kDa model peptide as well as its dual labeling with different fluorescent handles. Though no ADCs were constructed in the scope of this study, it has been shown that KalbTG does not recognize the typical recognition motif LLQGA (Table 2, entry **14**) at the heavy chain of human antibodies. This finding opened the door for the development of dual-functionalized ADCs employing orthogonal transglutaminases.

Engineering of microbial transglutaminase

Though mTG has been already used in a vast number of applications in pharmaceutic and biotechnological research, only a scanty amount of scientific publications covers the challenging field of its engineering. Directed evolution of a biocatalyst requires efficient recombinant expression that enables the coverage of a statistically relevant number of mutants to identify those with altered properties. Engineering of mTG is hindered by the intracellular toxicity of the mature enzyme in bacterial hosts, resulting in poor product yields for high-throughput screening. Therefore, troublesome proteolytic activation of the inactive zymogen is necessary. In 2008, Marx et al. established a microtiter plate-based assay that allowed for the screening of randomized transglutaminase libraries. After screening of 5500 clones, mutants with increased

Bereitgestellt von | Universitaets- und Landesbibliothek Darmstadt
Angemeldet | kolmar@biochemie-tud.de Autorenexemplar
Heruntergeladen am | 08.10.18 09:21

thermostability/heat-sensitivity were isolated. A single amino acid substitution (S2P) resulted in a 270% increased stability at 60°C and a ~two-fold elevated specific activity at 37°C (Sommer et al., 2011). A thermo-sensitive enzyme bearing point mutation G25S exhibited specific activity at 40°C comparable to the wildtype enzyme, but was revealed to be significantly less active at temperatures of 50°C and above. Interestingly, all amino acid substitutions identified in this screening approach as responsible for altered thermal properties were located within the *N*-terminal region (Asp1-Asn32) or at the bottom of the active-site cleft (Marx et al., 2008). Saturation-site mutagenesis of previously identified hotspots and gene shuffling were performed in continuative studies to further increase the thermal stability of mTG. As a result, triple and quadruple mutants were isolated which possessed a temperature optimum of 60°C, that is 10°C higher compared to the wildtype enzyme, as well as variants with 12- and 10-fold higher half-life at 60 and 50°C, respectively (Buettner et al., 2012). In 2010, Yokoyama et al. developed an agar plate-based screening in *Corynebacterium glutamicum* for the optimization of mTG. They screened 24 000 colonies and identified 10 that bore mutant enzymes with increased specific activity, among them a single S199A mutant that exhibited 1.7-fold elevated activity over the wildtype protein. In addition, a strategy based on rational design called 'water accessible surface hot-space region-oriented mutagenesis (WASH-ROM)' was developed. Here, 40 out of 90 surface-exposed amino acid residues within a 15 Å range from the active site Cys64 were mutated based on their accessibility to water molecules. A focused library comprising 151 mutant enzymes yielded 32 variants with increased catalytic performance, with the most promising one, Y75F, being 1.5-fold more potent than the wildtype enzyme (Yokoyama et al., 2010). By combining previously identified mutations beneficial for enzymatic activity and thermostability, variants were obtained exhibiting up to 2.2-fold elevated specific activity and 24.8-fold increased half-life at 60°C (Mu et al., 2018).

The relatively wide range of transglutaminase-acceptable substrates sometimes causes difficulties when multiple sites are addressed within the same target protein, like in hGH that possesses two glutamine residues, Gln40 and Gln141, which are modified by mTG. The group of Jing Su from Novo Nordisk overcame these limitations by engineering mTG from *S. ladakanum* towards the exclusive recognition of Gln141. Saturation-site mutagenesis of residues Y62 and Y75, which are known to affect catalytic activity, was performed and the resulting library members were screened for the incorporation of tritium-labeled (2,3-^{3}H)-putrescine into hGH mutants Q40N and Q141N. Five candidates that modified hGH Q40N and simultaneously lacked recognition of the Q141N mutant were isolated and were shown to be highly selective for Gln141 of wildtype hGH. Within their study, the authors succeeded in reprogramming the specificity of a microbial transglutaminase, enabling the engineering of mutants with desired characteristics (Zhao et al., 2010).

Within recent research of our own group, a novel ultra-high throughput screen for microbial transglutaminase based on yeast surface display (YSD) has been developed. YSD in combination with fluorescence-activated cell sorting (FACS) appeared to be a powerful tool for the tailoring of mutant proteins with improved properties as its high throughput of ~50 000 cells per second enables the screening of large libraries (Cherf and Cochran, 2015). However, evolving enzymes by YSD remains challenging because attachment of a reaction product to the yeast cell is required to discriminate cells bearing inactive and improved variants. We displayed inactive pro-mTG on the surface of yeast cells to overcome its intracellular cytotoxicity by recombinant fusion to the Aga2p protein. Cells displaying the inactive precursor were incubated with human enterokinase to convert the surface-bound zymogen into the active enzyme by cleaving of an engineered DDDDK site at the interface of the inhibitory propeptide and a mature enzyme. When enterokinase-treated cells were incubated in the presence of an *N*-terminally biotinylated peptide with a sequence GSGLLQG derived from the commonly used recognition motif LLQG (Table 2, entry **14**) and the mature enzyme catalyzed its coupling to available lysine residues, thus enabling discrimination of the corresponding cell by fluorescent staining. We demonstrated that genotype-phenotype correlation was given by separating mTG-bearing cells from the non-related ones by FACS and screened a randomized library of $3 \cdot 10^8$ members for mutants with improved recognition of peptide biotin-GSGLLQG-NH_2. Though enriched mutants possessed only minor improvements in kinetic parameters K_M and k_{cat}/K_M, a triple mutant S2G, R15C and M234L showed superior labeling of LLQG-tagged therapeutic antibody trastuzumab (Deweid et al., 2018).

Conclusions

Microbial transglutaminase from *S. mobaraensis* emerged as a versatile tool for enzymatic bioconjugation due to its high catalytic activity and stable performance in various media over a wide pH range. Various studies demonstrated its usage for the generation of bifunctional

Bereitgestellt von | Universitaets- und Landesbibliothek Darmstadt
Angemeldet | kolmar@biochemie-tud.de Autorenexemplar
Heruntergeladen am | 08.10.18 09:21

conjugates. Enzymes in general possess superior selectivity over chemical ligation and mostly recognize a specific amino acid pattern, while chemical strategies rely on the high reactivity of organic compounds towards functional groups within the desired target. In proteins multiple copies of amino acid are present resulting in the statistical distribution of payload at all available side chain residues. In contrast, functionalization of the desired molecule by an enzymatic catalyst leads to a less frequent modification, in the best-case scenario to a mono-conjugated target. As most proteins lack specific recognition pattern within their native structure, motifs that mediate enzymatic catalysis are recombinantly introduced. Many enzymes commonly used for enzymatic bioconjugation suffer from low catalytic performance, requirement of relatively large recognition motifs or the restriction of tag locus to terminal sites (Hermanson, 2013; Rashidian et al., 2013). Microbial transglutaminase, on the other hand, possess comparably promiscuous selectivity that can be a gift or a curse depending on the addressed target. For many protein targets, it allows for the conjugation at intrinsic residues of proteins and therefore preserves the native structure of the target as internally or terminally introduced tags may impair global folding. However, precise identification of conjugation site should be undertaken to avoid modification at functional sites of the target protein such as binding interfaces or catalytic residues. When intrinsic residues that mediate mTG recognition are absent, relatively small recognition motifs can be incorporated at either terminal or internal sites, enabling the tight control of conjugation site to modulate stability and functionality of the resulting conjugate. The downsides of its incompletely understood substrate specificity are obviously discernible when multiple reactive sites are located within the addressed target. Troublesome multi-functionalization and polymerization reduce coupling efficiency and require laborious purification of the desired mono-conjugate. Alternatively, reactive residues can be removed by residue replacement in the target protein (e.g. Q for N).

Besides its extensive usage in food manufacturing industry, multiple recent achievements concerning microbial transglutaminase-mediated bioconjugation contributed to pharmaceutic and biomedical research, e.g. in the development of ADCs, tailoring of bioactive drugs through PEGylation, or molecular diagnostics. Its high catalytic activity and feasible handling are making it a powerful component of the bioconjuagtion toolbox as demonstrated in various excellent reports. Though its idiosyncratic substrate selectivity should be kept in mind, especially when orthogonality is needed.

Acknowledgments: This work was supported by the NANOKAT II grant from the BMBF (Bundesministerium für Bildung und Forschung, Funder Id: 10.13039/501100002347) and by DFG, Funder Id: 10.13039/501100001659, priority program 1623.

References

Abe, H., Goto, M., and Kamiya, N. (2010). Enzymatic single-step preparation of multifunctional proteins. Chem. Commun. (Camb.). *46*, 7160–7162.

Abe, H., Goto, M., and Kamiya, N. (2011). Protein lipidation catalyzed by microbial transglutaminase. Chemistry *17*, 14004–14008.

Adler, M. (2010). Properties and potential of protein-DNA conjugates for analytic applications. In: Oxford Handbook of Nanoscience and Technology: Volume 2: Materials: Structures, Properties and Characterization Techniques, A.V. Narlikar and Y.Y. Fu, eds. (Oxford, England: Oxford University Press), pp. 891–923.

Anami, Y., Xiong, W., Gui, X., Deng, M., Zhang, C.C., Zhang, N., An, Z., and Tsuchikama, K. (2017). Enzymatic conjugation using branched linkers for constructing homogeneous antibody-drug conjugates with high potency. Org. Biomol. Chem. *15*, 5635–5642.

Ando, H., Adachi, M., Umeda, K., Matsuura, A., Nonaka, M., Uchio, R., Tanaka, H., and Motoki, M. (1989). Purification and characteristics of a novel transglutaminase derived from microorganisms. Agric. Biol. Chem. *53*, 2613–2617.

Appelbaum, F.R. and Bernstein, I.D. (2017). Gemtuzumab ozogamicin for acute myeloid leukemia. Blood *130*, 2373–2376.

Autuori, F., Farrace, M.G., Oliverio, S., Piredda, L., and Piacentini, M. (1998). "Tissue" transglutaminase and apoptosis. Adv Biochem. Eng. Biotechnol. *62*, 129–136.

Axup, J.Y., Bajjuri, K.M., Ritland, M., Hutchins, B.M., Kim, C.H., Kazane, S.A., Halder, R., Forsyth, J.S., Santidrian, A.F., and Stafin, K. (2012). Synthesis of site-specific antibody-drug conjugates using unnatural amino acids. Proc. Natl. Acad. Sci. USA *109*, 16101–16106.

Bech, L., Rasmussen, G., Halkier, T., Okada, M., Andersen, L.N., Kauppinen, M.S., and Sandal, T. (1996). Transglutaminases from oomycetes. In: WO1996022366 A1.

Bech, L., Halkier, T., Rasmussen, G., and Schafer, T. (2000). Microbial transglutaminases, their production and use. In: US6100053A.

Bechtold, U., Otterbach, J.T., Pasternack, R., and Fuchsbauer, H.L. (2000). Enzymic preparation of protein G-peroxidase conjugates catalysed by transglutaminase. J. Biochem. *127*, 239–245.

Beck, A., Goetsch, L., Dumontet, C., and Corvaia, N. (2017). Strategies and challenges for the next generation of antibody-drug conjugates. Nat. Rev. Drug. Discov. *16*, 315–337.

Behrens, C.R. and Liu, B. (2014). Methods for site-specific drug conjugation to antibodies. mAbs *6*, 46–53.

Behrens, C.R., Ha, E.H., Chinn, L.L., Bowers, S., Probst, G., Fitch-Bruhns, M., Monteon, J., Valdiosera, A., Bermudez, A., Liao-Chan, S., et al. (2015). Antibody-drug conjugates (ADCs) derived from interchain cysteine cross-linking demonstrate improved homogeneity and other pharmacological properties over conventional heterogeneous ADCs. Mol. Pharm. *12*, 3986–3998.

Bereitgestellt von | Universitaets- und Landesbibliothek Darmstadt
Angemeldet | kolmar@biochemie-tud.de Autorenexemplar
Heruntergeladen am | 08.10.18 09:21

Besheer, A., Hertel, T.C., Kressler, J., Mader, K., and Pietzsch, M. (2009). Enzymatically catalyzed HES conjugation using microbial transglutaminase: proof of feasibility. J. Pharm. Sci. *98*, 4420–4428.

Bhokisham, N., Pakhchanian, H., Quan, D., Tschirhart, T., Tsao, C.Y., Payne, G.F., and Bentley, W.E. (2016). Modular construction of multi-subunit protein complexes using engineered tags and microbial transglutaminase. Metab. Eng. *38*, 1–9.

Bourneow, C., Benjakul, S., Sumpavapol, P., and Aran, H. (2012). Isolation and cultivation of transglutaminase-producing bacteria from seafood processing factories. Innov. Rom. Food. Biotechnol. *10*, 28.

Bruins, J.J., Westphal, A.H., Albada, B., Wagner, K., Bartels, L., Spits, H., van Berkel, W.J.H., and van Delft, F.L. (2017). Inducible, site-specific protein labeling by tyrosine oxidation-strain-promoted (4 + 2) cycloaddition. Bioconjug. Chem. *28*, 1189–1193.

Bryant, P., Pabst, M., Badescu, G., Bird, M., McDowell, W., Jamieson, E., Swierkosz, J., Jurlewicz, K., Tommasi, R., Henseleit, K., et al. (2015). In vitro and in vivo evaluation of cysteine rebridged trastuzumab-MMAE antibody drug conjugates with defined drug-to-antibody ratios. Mol. Pharm. *12*, 1872–1879.

Buchardt, J., Selvig, H., Nielsen, P.F., and Johansen, N.L. (2010). Transglutaminase-mediated methods for site-selective modification of human growth hormone. Biopolymers *94*, 229–235.

Buettner, K., Hertel, T.C., and Pietzsch, M. (2012). Increased thermostability of microbial transglutaminase by combination of several hot spots evolved by random and saturation mutagenesis. Amino Acids *42*, 987–996.

Caporale, A., Selis, F., Sandomenico, A., Jotti, G.S., Tonon, G., and Ruvo, M. (2015). The LQSP tetrapeptide is a new highly efficient substrate of microbial transglutaminase for the site-specific derivatization of peptides and proteins. Biotechnol. J. *10*, 154–161.

Chen, K., Liu, S., Ju, X., Ma, T., Zhang, D., Du, G., and Chen, J. (2010). Effect of transglutaminase-gene disruption in *Streptomyces hygroscopicus* on cell differentiation. Acta Microbiol. Sin. *50*, 1626–1632.

Chen, L., Cohen, J., Song, X., Zhao, A., Ye, Z., Feulner, C.J., Doonan, P., Somers, W., Lin, L., and Chen, P.R. (2016). Improved variants of SrtA for site-specific conjugation on antibodies and proteins with high efficiency. Sci. Rep. *6*, 31899.

Cherf, G.M. and Cochran, J.R. (2015). Applications of yeast surface display for protein engineering. Methods Mol. Biol. *1319*, 155–175.

Cui, L., Du, G., Zhang, D., and Chen, J. (2008). Thermal stability and conformational changes of transglutaminase from a newly isolated *Streptomyces hygroscopicus*. Bioresour. Technol. *99*, 3794–3800.

da Silva Freitas, D., Mero, A., and Pasut, G. (2013). Chemical and enzymatic site specific PEGylation of hGH. Bioconjug. Chem. *24*, 456–463.

Davies, P.J. and Murtaugh, M.P. (1984). Transglutaminase and receptor-mediated endocytosis in macrophages and cultured fibroblasts. Mol. Cell Biochem. *58*, 69–77.

Dennler, P., Chiotellis, A., Fischer, E., Bregeon, D., Belmant, C., Gauthier, L., Lhospice, F., Romagne, F., and Schibli, R. (2014). Transglutaminase-based chemo-enzymatic conjugation approach yields homogeneous antibody-drug conjugates. Bioconjug. Chem. *25*, 569–578.

Dennler, P., Bailey, L.K., Spycher, P.R., Schibli, R., and Fischer, E. (2015). Microbial transglutaminase and c-myc-tag: a strong couple for the functionalization of antibody-like protein scaffolds from discovery platforms. Chembiochem *16*, 861–867.

Deweid, L., Neureiter, L., Englert, S., Schneider, H., Deweid, J., Yanakieva, D., Sturm, J., Bitsch, S., Christmann, A., Avrutina, O., et al. (2018). Directed evolution of a bond-forming enzyme: ultrahigh-throughput screening of microbial transglutaminase using yeast surface display. Chem. Eur. J. 10.1002/chem.201803485.

Dimasi, N., Fleming, R., Zhong, H., Bezabeh, B., Kinneer, K., Christie, R.J., Fazenbaker, C., Wu, H., and Gao, C. (2017). Efficient preparation of site-specific antibody-drug conjugates using cysteine insertion. Mol. Pharm. *14*, 1501–1516.

Dorywalska, M., Strop, P., Melton-Witt, J.A., Hasa-Moreno, A., Farias, S.E., Galindo Casas, M., Delaria, K., Lui, V., Poulsen, K., Loo, C., et al. (2015). Effect of attachment site on stability of cleavable antibody drug conjugates. Bioconjug. Chem. *26*, 650–659.

Dozier, J.K. and Distefano, M.D. (2015). Site-specific PEGylation of therapeutic proteins. Int. J. Mol. Sci. *16*, 25831–25864.

Drake, P.M. and Rabuka, D. (2017). Recent developments in ADC technology: preclinical studies signal future clinical trends. BioDrugs *31*, 521–531.

Drake, P.M., Albers, A.E., Baker, J., Banas, S., Barfield, R.M., Bhat, A.S., de Hart, G.W., Garofalo, A.W., Holder, P., Jones, L.C., et al. (2014). Aldehyde tag coupled with HIPS chemistry enables the production of ADCs conjugated site-specifically to different antibody regions with distinct in vivo efficacy and PK outcomes. Bioconjug. Chem. *25*, 1331–1341.

Duran, R., Junqua, M., Schmitter, J.M., Gancet, C., and Goulas, P. (1998). Purification, characterisation, and gene cloning of transglutaminase from *Streptoverticillium cinnamoneum* CBS 683.68. Biochimie *80*, 313–319.

Farias, S.E., Strop, P., Delaria, K., Galindo Casas, M., Dorywalska, M., Shelton, D.L., Pons, J., and Rajpal, A. (2014). Mass spectrometric characterization of transglutaminase based site-specific antibody-drug conjugates. Bioconjug. Chem. *25*, 240–250.

Fiebig, D., Schmelz, S., Zindel, S., Ehret, V., Beck, J., Ebenig, A., Ehret, M., Frols, S., Pfeifer, F., Kolmar, H., et al. (2016). Structure of the dispase autolysis-inducing protein from *Streptomyces mobaraensis* and glutamine cross-linking sites for transglutaminase. J. Biol. Chem. *291*, 20417–20426.

Folk, J.E. and Cole, P.W. (1966). Mechanism of action of guinea pig liver transglutaminase. I. Purification and properties of the enzyme: identification of a functional cysteine essential for activity. J. Biol. Chem. *241*, 5518–5525.

Griffin, M., Casadio, R., and Bergamini, C.M. (2002). Transglutaminases: nature's biological glues. Biochem. J. *368*, 377–396.

Grigoletto, A., Mero, A., Zanusso, I., Schiavon, O., and Pasut, G. (2016). Chemical and enzymatic site specific PEGylation of hGH: the stability and in vivo activity of PEG-N-terminal-hGH and PEG-Gln141-hGH conjugates. Macromol. Biosci. *16*, 50–56.

Grigoletto, A., Mero, A., Yoshioka, H., Schiavon, O., and Pasut, G. (2017). Covalent immobilisation of transglutaminase: stability and applications in protein PEGylation. J. Drug. Target. *25*, 856–864.

Grunewald, J., Klock, H.E., Cellitti, S.E., Bursulaya, B., McMullan, D., Jones, D.H., Chiu, H.P., Wang, X., Patterson, P., Zhou, H., et al. (2015). Efficient preparation of site-specific antibody-drug conjugates using phosphopantetheinyl transferases. Bioconjug. Chem. *26*, 2554–2562.

Gundersen, M.T., Keillor, J.W., and Pelletier, J.N. (2014). Microbial transglutaminase displays broad acyl-acceptor substrate specificity. Appl. Microbiol. Biotechnol. *98*, 219–230.

Hermanson, G.T. (2013). Bioconjugate Techniques (Cambridge, MA, USA: Academic Press).

Bereitgestellt von | Universitaets- und Landesbibliothek Darmstadt
Angemeldet | kolmar@biochemie-tud.de Autorenexemplar
Heruntergeladen am | 08.10.18 09:21

Ho, M.L., Leu, S.Z., Hsieh, J.F., and Jiang, S.T. (2000). Technical approach to simplify the purification method and characterization of microbial transglutaminase produced from *Streptoverticillium ladakanum*. J. Food Sci. *65*, 76–80.

Hristodorov, D., Fischer, R., Joerissen, H., Muller-Tiemann, B., Apeler, H., and Linden, L. (2013). Generation and comparative characterization of glycosylated and aglycosylated human IgG1 antibodies. Mol. Biotechnol. *53*, 326–335.

Hu, Q.Y., Berti, F., and Adamo, R. (2016). Towards the next generation of biomedicines by site-selective conjugation. Chem. Soc. Rev. *45*, 1691–1719.

Jain, N., Smith, S.W., Ghone, S., and Tomczuk, B. (2015). Current ADC linker chemistry. Pharm. Res. *32*, 3526–3540.

Jefferis, R. (2012). Isotype and glycoform selection for antibody therapeutics. Arch. Biochem. Biophys. *526*, 159–166.

Jeger, S., Zimmermann, K., Blanc, A., Grunberg, J., Honer, M., Hunziker, P., Struthers, H., and Schibli, R. (2010). Site-specific and stoichiometric modification of antibodies by bacterial transglutaminase. Angew. Chem. Int. Ed. *49*, 9995–9997.

Juettner, N.E., Schmelz, S., Bogen, J.P., Happel, D., Fessner, W.D., Pfeifer, F., Fuchsbauer, H.L., and Scrima, A. (2018). Illuminating structure and acyl donor sites of a physiological transglutaminase substrate from *Streptomyces mobaraensis*. Protein Sci. *27*, 910–922.

Junutula, J.R., Raab, H., Clark, S., Bhakta, S., Leipold, D.D., Weir, S., Chen, Y., Simpson, M., Tsai, S.P., Dennis, M.S., et al. (2008). Site-specific conjugation of a cytotoxic drug to an antibody improves the therapeutic index. Nat. Biotechnol. *26*, 925–932.

Kamiya, N., Takazawa, T., Tanaka, T., Ueda, H., and Nagamune, T. (2003a). Site-specific cross-linking of functional proteins by transglutamination. Enzyme Microb. Technol. *33*, 492–496.

Kamiya, N., Tanaka, T., Suzuki, T., Takazawa, T., Takeda, S., Watanabe, K., and Nagamune, T. (2003b). S-peptide as a potent peptidyl linker for protein cross-linking by microbial transglutaminase from *Streptomyces mobaraensis*. Bioconjug. Chem. *14*, 351–357.

Kanaji, T., Ozaki, H., Takao, T., Kawajiri, H., Ide, H., Motoki, M., and Shimonishi, Y. (1993). Primary structure of microbial transglutaminase from *Streptoverticillium* sp. strain s-8112. J. Biol. Chem. *268*, 11565–11572.

Kashiwagi, T., Yokoyama, K., Ishikawa, K., Ono, K., Ejima, D., Matsui, H., and Suzuki, E. (2002). Crystal structure of microbial transglutaminase from Streptoverticillium mobaraense. J. Biol. Chem. *277*, 44252–44260.

Kieliszek, M. and Misiewicz, A. (2014). Microbial transglutaminase and its application in the food industry. A review. Folia Microbiol. (Praha). *59*, 241–250.

Kim, H.-S., Jung, S.-H., Lee, I.-S., and Yu, T.-S. (2000). Production and characterization of a novel microbial transglutaminase from *Actinomadura* sp. T-2. J. Microbiol. Biotechnol. *10*, 187–194.

Kitaoka, M., Tsuruda, Y., Tanaka, Y., Goto, M., Mitsumori, M., Hayashi, K., Hiraishi, Y., Miyawaki, K., Noji, S., and Kamiya, N. (2011). Transglutaminase-mediated synthesis of a DNA-(enzyme)n probe for highly sensitive DNA detection. Chemistry *17*, 5387–5392.

Klein, J.D., Guzman, E., and Kuehn, G.D. (1992). Purification and partial characterization of transglutaminase from *Physarum polycephalum*. J. Bacteriol. *174*, 2599–2605.

Kline, T., Steiner, A.R., Penta, K., Sato, A.K., Hallam, T.J., and Yin, G. (2015). Methods to make homogenous antibody drug conjugates. Pharm. Res. *32*, 3480–3493.

Kobayashi, K., Suzuki, S.I., Izawa, Y., Miwa, K., and Yamanaka, S. (1998). Transglutaminase in sporulating cells of *Bacillus subtilis*. J. Gen. Appl. Microbiol. *44*, 85–91.

Lamb, Y.N. (2017). Inotuzumab ozogamicin: first global approval. Drugs *77*, 1603–1610.

Lamba, J.K., Chauhan, L., Shin, M., Loken, M.R., Pollard, J.A., Wang, Y.C., Ries, R.E., Aplenc, R., Hirsch, B.A., Raimondi, S.C., et al. (2017). CD33 splicing polymorphism determines gemtuzumab ozogamicin response in de novo acute myeloid leukemia: report from randomized phase III children's oncology group trial AAML0531. J. Clin. Oncol. *35*, 2674–2682.

Lawrence, P.B. and Price, J.L. (2016). How PEGylation influences protein conformational stability. Curr. Opin. Chem. Biol. *34*, 88–94.

Lee, J.H., Song, C., Kim, D.H., Park, I.H., Lee, S.G., Lee, Y.S., and Kim, B.G. (2013). Glutamine (Q)-peptide screening for transglutaminase reaction using mRNA display. Biotechnol. Bioeng. *110*, 353–362.

Lesch, H.P., Kaikkonen, M.U., Pikkarainen, J.T., and Yla-Herttuala, S. (2010). Avidin-biotin technology in targeted therapy. Expert Opin. Drug. Deliv. *7*, 551–564.

Lhospice, F., Bregeon, D., Belmant, C., Dennler, P., Chiotellis, A., Fischer, E., Gauthier, L., Boedec, A., Rispaud, H., Savard-Chambard, S., et al. (2015). Site-specific conjugation of monomethyl auristatin E to anti-CD30 antibodies improves their pharmacokinetics and therapeutic index in rodent models. Mol. Pharm. *12*, 1863–1871.

Li, X., Fang, T., and Boons, G.J. (2014). Preparation of well-defined antibody–drug conjugates through glycan remodeling and strain-promoted azide–alkyne cycloadditions. Angew. Chem. Int. Ed. *53*, 7179–7182.

Li, X., Nelson, C.G., Nair, R.R., Hazlehurst, L., Moroni, T., Martinez-Acedo, P., Nanna, A.R., Hymel, D., Burke, T.R., Jr., and Rader, C. (2017). Stable and potent selenomab-drug conjugates. Cell Chem. Biol. *24*, 433–442 e436.

Li, T., Li, C., Quan, D.N., Bentley, W.E., and Wang, L.X. (2018). Site-specific immobilization of endoglycosidases for streamlined chemoenzymatic glycan remodeling of antibodies. Carbohydr. Res. *458–459*, 77–84.

Lin, S., Yang, X., Jia, S., Weeks, A.M., Hornsby, M., Lee, P.S., Nichiporuk, R.V., Iavarone, A.T., Wells, J.A., Toste, F.D., et al. (2017). Redox-based reagents for chemoselective methionine bioconjugation. Science *355*, 597–602.

LoRusso, P.M., Weiss, D., Guardino, E., Girish, S., and Sliwkowski, M.X. (2011). Trastuzumab emtansine: a unique antibody-drug conjugate in development for human epidermal growth factor receptor 2-positive cancer. Clin. Cancer Res. *17*, 6437–6447.

Malesevic, M., Migge, A., Hertel, T.C., and Pietzsch, M. (2015). A fluorescence-based array screen for transglutaminase substrates. Chembiochem *16*, 1169–1174.

Marx, C.K., Hertel, T.C., and Pietzsch, M. (2008). Random mutagenesis of a recombinant microbial transglutaminase for the generation of thermostable and heat-sensitive variants. J. Biotechnol. *136*, 156–162.

Mascini, M., Palchetti, I., and Tombelli, S. (2012). Nucleic acid and peptide aptamers: fundamentals and bioanalytical aspects. Angew. Chem., Int. Ed. Engl. *51*, 1316–1332.

Maullu, C., Raimondo, D., Caboi, F., Giorgetti, A., Sergi, M., Valentini, M., Tonon, G., and Tramontano, A. (2009). Site-directed enzymatic PEGylation of the human granulocyte colony-stimulating factor. FEBS J. *276*, 6741–6750.

Bereitgestellt von | Universitaets- und Landesbibliothek Darmstadt
Angemeldet | kolmar@biochemie-tud.de Autorenexemplar
Heruntergeladen am | 08.10.18 09:21

Mero, A., Spolaore, B., Veronese, F.M., and Fontana, A. (2009). Transglutaminase-mediated PEGylation of proteins: direct identification of the sites of protein modification by mass spectrometry using a novel monodisperse PEG. Bioconjug. Chem. *20*, 384–389.

Mero, A., Schiavon, M., Veronese, F.M., and Pasut, G. (2011). A new method to increase selectivity of transglutaminase mediated PEGylation of salmon calcitonin and human growth hormone. J. Control. Release *154*, 27–34.

Mero, A., Grigoletto, A., Maso, K., Yoshioka, H., Rosato, A., and Pasut, G. (2016). Site-selective enzymatic chemistry for polymer conjugation to protein lysine residues: PEGylation of G-CSF at lysine-41. Polym. Chem. *7*, 6545–6553.

Milani, A., Vecchietti, D., Rusmini, R., and Bertoni, G. (2012). TgpA, a protein with a eukaryotic-like transglutaminase domain, plays a critical role in the viability of *Pseudomonas aeruginosa.* PLoS One *7*, e50323.

Mindt, T.L., Jungi, V., Wyss, S., Friedli, A., Pla, G., Novak-Hofer, I., Grünberg, J., and Schibli, R. (2007). Modification of different IgG1 antibodies via glutamine and lysine using bacterial and human tissue transglutaminase. Bioconjug. Chem. *19*, 271–278.

Mori, Y., Goto, M., and Kamiya, N. (2011). Transglutaminase-mediated internal protein labeling with a designed peptide loop. Biochem. Biophys. Res. Commun. *410*, 829–833.

Moriyama, K., Sung, K., Goto, M., and Kamiya, N. (2011). Immobilization of alkaline phosphatase on magnetic particles by site-specific and covalent cross-linking catalyzed by microbial transglutaminase. J. Biosci. Bioeng. *111*, 650–653.

Mould, D.R. and Sweeney, K.R. (2007). The pharmacokinetics and pharmacodynamics of monoclonal antibodies-mechanistic modeling applied to drug development. Curr. Opin. Drug Discov. Dev. *10*, 84–96.

Mu, D., Lu, J., Shu, C., Li, H., Li, X., Cai, J., Luo, S., Yang, P., Jiang, S., and Zheng, Z. (2018). Improvement of the activity and thermostability of microbial transglutaminase by multiple-site mutagenesis. Biosci. Biotechnol. Biochem. *82*, 106–109.

Nanna, A.R., Li, X., Walseng, E., Pedzisa, L., Goydel, R.S., Hymel, D., Burke, T.R., Jr., Roush, W.R., and Rader, C. (2017). Harnessing a catalytic lysine residue for the one-step preparation of homogeneous antibody-drug conjugates. Nat. Commun. *8*, 1112.

Niculescu-Duvaz, I. (2010). Trastuzumab emtansine, an antibody-drug conjugate for the treatment of HER2+ metastatic breast cancer. Curr. Opin. Mol. Ther. *12*, 350–360.

Niemeyer, C.M., Wacker, R., and Adler, M. (2003). Combination of DNA-directed immobilization and immuno-PCR: very sensitive antigen detection by means of self-assembled DNA-protein conjugates. Nucleic Acids Res. *31*, e90.

Nonaka, M., Matsuura, Y., and Motoki, M. (1996). Incorporation of lysine-and lysine dipeptides into α s1-Casein by Ca^{2+}-independent microbial transglutaminase. Biosci. Biotechnol. Biochem. *60*, 131–133.

Ohata, J. and Ball, Z.T. (2017). A hexa-rhodium metallopeptide catalyst for site-specific functionalization of natural antibodies. J. Am. Chem. Soc. *139*, 12617–12622.

Ohtsuka, T., Sawa, A., Kawabata, R., Nio, N., and Motoki, M. (2000a). Substrate specificities of microbial transglutaminase for primary amines. J. Agric. Food Chem. *48*, 6230–6233.

Ohtsuka, T., Ota, M., Nio, N., and Motoki, M. (2000b). Comparison of substrate specificities of transglutaminases using synthetic peptides as acyl donors. Biosci. Biotechnol. Biochem. *64*, 2608–2613.

Ota, M., Sawa, A., Nio, N., and Ariyoshi, Y. (1999). Enzymatic ligation for synthesis of single-chain analogue of monellin by transglutaminase. Biopolymers *50*, 193–200.

Oteng-Pabi, S.K., Pardin, C., Stoica, M., and Keillor, J.W. (2014). Site-specific protein labelling and immobilization mediated by microbial transglutaminase. Chem. Commun. (Camb.) *50*, 6604–6606.

Pasternack, R., Dorsch, S., Otterbach, J.T., Robenek, I.R., Wolf, S., and Fuchsbauer, H.L. (1998). Bacterial pro-transglutaminase from *Streptoverticillium mobaraense*-purification, characterisation and sequence of the zymogen. Eur. J. Biochem. *257*, 570–576.

Plagmann, I., Chalaris, A., Kruglov, A.A., Nedospasov, S., Rosenstiel, P., Rose-John, S., and Scheller, J. (2009). Transglutaminase-catalyzed covalent multimerization of *Camelidae* anti-human TNF single domain antibodies improves neutralizing activity. J. Biotechnol. *142*, 170–178.

Porta, R., Esposito, C., De Santis, A., Fusco, A., Iannone, M., and Metafora, S. (1986). Sperm maturation in human semen: role of transglutaminase-mediated reactions. Biol. Reprod. *35*, 965–970.

Puthenveetil, S., Musto, S., Loganzo, F., Tumey, L.N., O'Donnell, C.J., and Graziani, E. (2016). Development of solid-phase site-specific conjugation and its application toward generation of dual labeled antibody and fab drug conjugates. Bioconjug. Chem. *27*, 1030–1039.

Rachel, N.M. and Pelletier, J.N. (2013). Biotechnological applications of transglutaminases. Biomolecules *3*, 870–888.

Rachel, N.M. and Pelletier, J.N. (2016). One-pot peptide and protein conjugation: a combination of enzymatic transamidation and click chemistry. Chem. Commun. (Camb.) *52*, 2541–2544.

Rachel, N.M., Quaglia, D., Levesque, E., Charette, A.B., and Pelletier, J.N. (2017). Engineered, highly reactive substrates of microbial transglutaminase enable protein labeling within various secondary structure elements. Protein Sci. *26*, 2268–2279.

Rashidian, M., Dozier, J.K., and Distefano, M.D. (2013). Enzymatic labeling of proteins: techniques and approaches. Bioconjug. Chem. *24*, 1277–1294.

Reusch, D. and Tejada, M.L. (2015). Fc glycans of therapeutic antibodies as critical quality attributes. Glycobiology *25*, 1325–1334.

Romeih, E. and Walker, G. (2017). Recent advances on microbial transglutaminase and dairy application. Trends Food. Sci. Technol. *62*, 133–140.

Santhi, D., Kalaikannan, A., Malairaj, P., and Arun Prabhu, S. (2017). Application of microbial transglutaminase in meat foods: a review. Crit. Rev. Food. Sci. Nutr. *57*, 2071–2076.

Sato, H., Hayashi, E., Yamada, N., Yatagai, M., and Takahara, Y. (2001). Further studies on the site-specific protein modification by microbial transglutaminase. Bioconjug. Chem. *12*, 701–710.

Sau, S., Alsaab, H.O., Kashaw, S.K., Tatiparti, K., and Iyer, A.K. (2017). Advances in antibody-drug conjugates: a new era of targeted cancer therapy. Drug Discov. Today *22*, 1547–1556.

Scaramuzza, S., Tonon, G., Olianas, A., Messana, I., Schrepfer, R., Orsini, G., and Caliceti, P. (2012). A new site-specific monoPEGylated filgrastim derivative prepared by enzymatic conjugation: Production and physicochemical characterization. J. Control. Release *164*, 355–363.

Schmidt, G., Selzer, J., Lerm, M., and Aktories, K. (1998). The Rho-deamidating cytotoxic necrotizing factor 1 from *Escherichia coli* possesses transglutaminase activity. Cysteine 866 and histidine 881 are essential for enzyme activity. J. Biol. Chem. *273*, 13669–13674.

Bereitgestellt von | Universitaets- und Landesbibliothek Darmstadt
Angemeldet | kolmar@biochemie-tud.de Autorenexemplar
Heruntergeladen am | 08.10.18 09:21

Schumacher, D., Helma, J., Mann, F.A., Pichler, G., Natale, F., Krause, E., Cardoso, M.C., Hackenberger, C.P., and Leonhardt, H. (2015). Versatile and efficient site-specific protein functionalization by tubulin tyrosine ligase. Angew. Chem. Int. Ed. *54*, 13787–13791.

Schumacher, D., Hackenberger, C.P., Leonhardt, H., and Helma, J. (2016). Current status: site-specific antibody drug conjugates. J. Clin. Immunol. *36*, 100–107.

Senter, P.D. and Sievers, E.L. (2012). The discovery and development of brentuximab vedotin for use in relapsed Hodgkin lymphoma and systemic anaplastic large cell lymphoma. Nat. Biotechnol. *30*, 631.

Serafini-Fracassini, D., Della Mea, M., Tasco, G., Casadio, R., and Del Duca, S. (2009). Plant and animal transglutaminases: do similar functions imply similar structures? Amino Acids *36*, 643–657.

Shen, B.Q., Xu, K., Liu, L., Raab, H., Bhakta, S., Kenrick, M., Parsons-Reponte, K.L., Tien, J., Yu, S.F., Mai, E., et al. (2012). Conjugation site modulates the in vivo stability and therapeutic activity of antibody-drug conjugates. Nat. Biotechnol. *30*, 184–189.

Shinmi, D., Taguchi, E., Iwano, J., Yamaguchi, T., Masuda, K., Enokizono, J., and Shiraishi, Y. (2016). One-step conjugation method for site-specific antibody-drug conjugates through reactive cysteine-engineered antibodies. Bioconjug. Chem. *27*, 1324–1331.

Shor, B., Gerber, H.P., and Sapra, P. (2015). Preclinical and clinical development of inotuzumab-ozogamicin in hematological malignancies. Mol. Immunol. *67*, 107–116.

Siegel, R.L., Miller, K.D., and Jemal, A. (2016). Cancer statistics, 2016. CA Cancer J. Clin. *66*, 7–30.

Siegmund, V., Schmelz, S., Dickgiesser, S., Beck, J., Ebenig, A., Fittler, H., Frauendorf, H., Piater, B., Betz, U.A., Avrutina, O., et al. (2015). Locked by design: a conformationally constrained transglutaminase tag enables efficient site-specific conjugation. Angew. Chem. Int. Ed. *54*, 13420–13424.

Siegmund, V., Piater, B., Zakeri, B., Eichhorn, T., Fischer, F., Deutsch, C., Becker, S., Toleikis, L., Hock, B., Betz, U.A., et al. (2016). Spontaneous isopeptide bond formation as a powerful tool for engineering site-specific antibody-drug conjugates. Sci. Rep. *6*, 39291.

Smith, A.J. (2015). New horizons in therapeutic antibody discovery: opportunities and challenges versus small-molecule therapeutics. J. Biomol. Screen. *20*, 437–453.

Sommer, C., Volk, N., and Pietzsch, M. (2011). Model based optimization of the fed-batch production of a highly active transglutaminase variant in *Escherichia coli*. Protein Expr. Purif. *77*, 9–19.

Spidel, J.L., Vaessen, B., Albone, E.F., Cheng, X., Verdi, A., and Kline, J.B. (2017). Site-specific conjugation to native and engineered lysines in human immunoglobulins by microbial transglutaminase. Bioconjug. Chem. *28*, 2471–2484.

Spolaore, B., Raboni, S., Ramos Molina, A., Satwekar, A., Damiano, N., and Fontana, A. (2012). Local unfolding is required for the site-specific protein modification by transglutaminase. Biochemistry *51*, 8679–8689.

Spolaore, B., Damiano, N., Raboni, S., and Fontana, A. (2014). Site-specific derivatization of avidin using microbial transglutaminase. Bioconjug. Chem. *25*, 470–480.

Spolaore, B., Raboni, S., Satwekar, A.A., Grigoletto, A., Mero, A., Montagner, I.M., Rosato, A., Pasut, G., and Fontana, A. (2016). Site-specific transglutaminase-mediated conjugation of interferon alpha-2b at glutamine or lysine residues. Bioconjug. Chem. *27*, 2695–2706.

Spolaore, B., Forzato, G., and Fontana, A. (2018). Site-specific derivatization of human interferon β-1a at lysine residues using microbial transglutaminase. Amino Acids. *50*, 923–932.

Spycher, P.R., Amann, C.A., Wehrmuller, J.E., Hurwitz, D.R., Kreis, O., Messmer, D., Ritler, A., Kuchler, A., Blanc, A., Behe, M., et al. (2017). Dual, site-specific modification of antibodies by using solid-phase immobilized microbial transglutaminase. Chembiochem *18*, 1923–1927.

Steffen, W., Ko, F.C., Patel, J., Lyamichev, V., Albert, T.J., Benz, J., Rudolph, M.G., Bergmann, F., Streidl, T., Kratzsch, P., et al. (2017). Discovery of a microbial transglutaminase enabling highly site-specific labeling of proteins. J. Biol. Chem. *292*, 15622–15635.

Strop, P. (2014). Versatility of microbial transglutaminase. Bioconjug. Chem. *25*, 855–862.

Strop, P., Liu, S.H., Dorywalska, M., Delaria, K., Dushin, R.G., Tran, T.T., Ho, W.H., Farias, S., Casas, M.G., Abdiche, Y., et al. (2013). Location matters: site of conjugation modulates stability and pharmacokinetics of antibody drug conjugates. Chem. Biol. *20*, 161–167.

Strop, P., Delaria, K., Foletti, D., Witt, J.M., Hasa-Moreno, A., Poulsen, K., Casas, M.G., Dorywalska, M., Farias, S., Pios, A., et al. (2015). Site-specific conjugation improves therapeutic index of antibody drug conjugates with high drug loading. Nat. Biotechnol. *33*, 694–696.

Sugimura, Y., Yokoyama, K., Nio, N., Maki, M., and Hitomi, K. (2008). Identification of preferred substrate sequences of microbial transglutaminase from *Streptomyces mobaraensis* using a phage-displayed peptide library. Arch. Biochem. Biophys. *477*, 379–383.

Tagami, U., Shimba, N., Nakamura, M., Yokoyama, K., Suzuki, E., and Hirokawa, T. (2009). Substrate specificity of microbial transglutaminase as revealed by three-dimensional docking simulation and mutagenesis. Protein Eng. Des. Sel. *22*, 747–752.

Taghi Gharibzahedi, S.M., Koubaa, M., Barba, F.J., Greiner, R., George, S., and Roohinejad, S. (2018). Recent advances in the application of microbial transglutaminase crosslinking in cheese and ice cream products: a review. Int. J. Biol. Macromol. *107*, 2364–2374.

Takahara, M., Hayashi, K., Goto, M., and Kamiya, N. (2013). Tailing DNA aptamers with a functional protein by two-step enzymatic reaction. J. Biosci. Bioeng. *116*, 660–665.

Takahara, M., Hayashi, K., Goto, M., and Kamiya, N. (2016). Enzymatic conjugation of multiple proteins on a DNA aptamer in a tail-specific manner. Biotechnol. J. *11*, 814–823.

Takahara, M., Wakabayashi, R., Minamihata, K., Goto, M., and Kamiya, N. (2017). Primary amine-clustered DNA aptamer for DNA-protein conjugation catalyzed by microbial transglutaminase. Bioconjug. Chem. *28*, 2954–2961.

Takazawa, T., Kamiya, N., Ueda, H., and Nagamune, T. (2004). Enzymatic labeling of a single chain variable fragment of an antibody with alkaline phosphatase by microbial transglutaminase. Biotechnol. Bioeng. *86*, 399–404.

Tanaka, T., Kamiya, N., and Nagamune, T. (2005). N-terminal glycine-specific protein conjugation catalyzed by microbial transglutaminase. FEBS Lett. *579*, 2092–2096.

Tanaka, Y., Tsuruda, Y., Nishi, M., Kamiya, N., and Goto, M. (2007). Exploring enzymatic catalysis at a solid surface: a case study with transglutaminase-mediated protein immobilization. Org. Biomol. Chem. *5*, 1764–1770.

Bereitgestellt von | Universitaets- und Landesbibliothek Darmstadt
Angemeldet | kolmar@biochemie-tud.de Autorenexemplar
Heruntergeladen am | 08.10.18 09:21

Tanaka, Y., Doi, S., Kamiya, N., Kawata, N., Kamiya, S., Nakama, K., and Goto, M. (2008). A chemically modified glass surface that facilitates transglutaminase-mediated protein immobilization. Biotechnol. Lett. *30*, 1025–1029.

Tao, M.H. and Morrison, S.L. (1989). Studies of aglycosylated chimeric mouse-human IgG. Role of carbohydrate in the structure and effector functions mediated by the human IgG constant region. J. Immunol. *143*, 2595–2601.

Tesfaw, A. and Assefa, F. (2014). Applications of transglutaminase in textile, wool, and leather processing. Int. J. Textile Sci. *3*, 64–69.

Tominaga, J., Kamiya, N., Doi, S., Ichinose, H., and Goto, M. (2004). An enzymatic strategy for site-specific immobilization of functional proteins using microbial transglutaminase. Enzyme Microb. Technol. *35*, 613–618.

Tominaga, J., Kamiya, N., Doi, S., Ichinose, H., Maruyama, T., and Goto, M. (2005). Design of a specific peptide tag that affords covalent and site-specific enzyme immobilization catalyzed by microbial transglutaminase. Biomacromolecules *6*, 2299–2304.

Tominaga, J., Kemori, Y., Tanaka, Y., Maruyama, T., Kamiya, N., and Goto, M. (2007). An enzymatic method for site-specific labeling of recombinant proteins with oligonucleotides. Chem. Commun. (Camb.) 401–403.

Trads, J.B., Torring, T., and Gothelf, K.V. (2017). Site-selective conjugation of native proteins with DNA. Acc. Chem. Res. *50*, 1367–1374.

Tsuchikama, K. and An, Z. (2018). Antibody-drug conjugates: recent advances in conjugation and linker chemistries. Protein Cell *9*, 33–46.

Umezawa, Y., Ohtsuka, T., Yokoyama, K., and Nio, N. (2002). Comparison of enzymatic properties of microbial transglutaminase from *Streptomyces* sp. Food Sci. Technol. Int. *8*, 113–118.

Valdivia, A., Villalonga, R., Di Pierro, P., Perez, Y., Mariniello, L., Gomez, L., and Porta, R. (2006). Transglutaminase-catalyzed site-specific glycosidation of catalase with aminated dextran. J. Biotechnol. *122*, 326–333.

van Geel, R., Wijdeven, M.A., Heesbeen, R., Verkade, J.M., Wasiel, A.A., van Berkel, S.S., and van Delft, F.L. (2015). Chemoenzymatic conjugation of toxic payloads to the globally conserved N-glycan of native mAbs provides homogeneous and highly efficacious antibody-drug conjugates. Bioconjug. Chem. *26*, 2233–2242.

VanBrunt, M.P., Shanebeck, K., Caldwell, Z., Johnson, J., Thompson, P., Martin, T., Dong, H., Li, G., Xu, H., and D'Hooge, F. (2015). Genetically encoded azide containing amino acid in mammalian cells enables site-specific antibody-drug conjugates using click cycloaddition chemistry. Bioconjug. Chem. *26*, 2249–2260.

Verderio, E.A., Johnson, T., and Griffin, M. (2004). Tissue transglutaminase in normal and abnormal wound healing: review article. Amino Acids *26*, 387–404.

Villalonga, M.L., Villalonga, R., Mariniello, L., Gómez, L., Di Pierro, P., and Porta, R. (2006). Transglutaminase-catalysed glycosidation of trypsin with aminated polysaccharides. World J. Microbiol. Biotechnol. *22*, 595–602.

Wacker, R. and Niemeyer, C.M. (2004). DDI-μFIA-A readily configurable microarray-fluorescence immunoassay based on DNA-directed immobilization of proteins. Chembiochem. *5*, 453–459.

Washizu, K., Ando, K., Koikeda, S., Hirose, S., Matsuura, A., Takagi, H., Motoki, M., and Takeuchi, K. (1994). Molecular cloning of the gene for microbial transglutaminase from *Streptoverticillium* and its expression in *Streptomyces lividans*. Biosci. Biotechnol. Biochem. *58*, 82–87.

Wilchek, M. and Bayer, E.A. (1990). Avidin-biotin mediated immunoassays: overview. In: Methods in Enzymology, Vol. 184, M. Wilchek and E.A. Adler, eds. (Amsterdam, The Netherlands: Elsevier), pp. 467–469.

Xu, Y., Jin, S., Zhao, W., Liu, W., Ding, D., Zhou, J., and Chen, S. (2017). A versatile chemo-enzymatic conjugation approach yields homogeneous and highly potent antibody-drug conjugates. Int. J. Mol. Sci. *18*, 2284.

Yang, M.T., Chang, C.H., Wang, J.M., Wu, T.K., Wang, Y.K., Chang, C.Y., and Li, T.T. (2011). Crystal structure and inhibition studies of transglutaminase from *Streptomyces mobaraense*. J. Biol. Chem. *286*, 7301–7307.

Yi, J.H., Kim, S.J., and Kim, W.S. (2017). Brentuximab vedotin: clinical updates and practical guidance. Blood Res. *52*, 243–253.

Yokoyama, K., Utsumi, H., Nakamura, T., Ogaya, D., Shimba, N., Suzuki, E., and Taguchi, S. (2010). Screening for improved activity of a transglutaminase from *Streptomyces mobaraensis* created by a novel rational mutagenesis and random mutagenesis. Appl. Microbiol. Biotechnol. *87*, 2087–2096.

Yu, C.M., Zhou, H., Zhang, W.F., Yang, H.M., and Tang, J.B. (2016). Site-specific, covalent immobilization of BirA by microbial transglutaminase: a reusable biocatalyst for *in vitro* biotinylation. Anal. Biochem. *511*, 10–12.

Zemskov, E.A., Janiak, A., Hang, J., Waghray, A., and Belkin, A.M. (2006). The role of tissue transglutaminase in cell-matrix interactions. Front. Biosci. *11*, 1057–1076.

Zhao, X., Shaw, A.C., Wang, J., Chang, C.C., Deng, J., and Su, J. (2010). A novel high-throughput screening method for microbial transglutaminases with high specificity toward Gln141 of human growth hormone. J. Biomol. Screen. *15*, 206–212.

Zheng, K., Bantog, C., and Bayer, R. (2011). The impact of glycosylation on monoclonal antibody conformation and stability. mAbs *3*, 568–576.

Zhou, Q., Stefano, J.E., Manning, C., Kyazike, J., Chen, B., Gianolio, D.A., Park, A., Busch, M., Bird, J., and Zheng, X. (2014). Site-specific antibody-drug conjugation through glycoengineering. Bioconjug. Chem. *25*, 510–520.

Zhou, J.Q., He, T., and Wang, J.W. (2016). PEGylation of cytochrome c at the level of lysine residues mediated by a microbial transglutaminase. Biotechnol. Lett. *38*, 1121–1129.

Zimmerman, E.S., Heibeck, T.H., Gill, A., Li, X., Murray, C.J., Madlansacay, M.R., Tran, C., Uter, N.T., Yin, G., and Rivers, P.J. (2014). Production of site-specific antibody-drug conjugates using optimized non-natural amino acids in a cell-free expression system. Bioconjug. Chem. *25*, 351–361.

Zindel, S., Ehret, V., Ehret, M., Hentschel, M., Witt, S., Kramer, A., Fiebig, D., Juttner, N., Frols, S., Pfeifer, F., et al. (2016). Involvement of a novel class C beta-lactamase in the transglutaminase mediated cross-linking cascade of *Streptomyces mobaraensis* DSM 40847. PLoS One *11*, e0149145.

Zotzel, J., Keller, P., and Fuchsbauer, H.L. (2003a). Transglutaminase from *Streptomyces mobaraensis* is activated by an endogenous metalloprotease. Eur. J. Biochem. *270*, 3214–3222.

Zotzel, J., Pasternack, R., Pelzer, C., Ziegert, D., Mainusch, M., and Fuchsbauer, H.L. (2003b). Activated transglutaminase from *Streptomyces mobaraensis* is processed by a tripeptidyl aminopeptidase in the final step. Eur. J. Biochem. *270*, 4149–4155.

Bereitgestellt von | Universitaets- und Landesbibliothek Darmstadt
Angemeldet | kolmar@biochemie-tud.de Autorenexemplar
Heruntergeladen am | 08.10.18 09:21

7.2. Directed Evolution of a Bond-Forming Enzyme: Ultrahigh-Throughput Screening of Microbial Transglutaminase Using Yeast Surface Display

Title:

Directed Evolution of a Bond-Forming Enzyme: Ultrahigh-Throughput Screening of Microbial Transglutaminase Using Yeast Surface Display

Authors:

Lukas Deweid, Lara Neureiter, Simon Englert, Hendrik Schneider, Jakob Deweid, Desislava Yanakieva, Janna Sturm, Sebastian Bitsch, Andreas Christmann, Olga Avrutina, Hans-Lothar Fuchsbauer and Harald Kolmar

Bibliographic data:

Chemistry: a European Journal

Volume 24, Issue 57, Pages 15195-15200

Article first published online: 26th Jul 2018

DOI: https://doi.org/10.1002/chem.201803485

Copyright: 2018 Wiley-VCH Verlag GmbH & Co. KGaA, Weinheim. Reproduced with permission.

Contributions by Lukas Deweid:

- Initial idea and project management together with H. Kolmar
- Performed the majority of experiments
- Preparation of the manuscript and all included graphical material
- Revised the manuscript

ChemPubSoc Europe

DOI: 10.1002/chem.201803485

CHEMISTRY
A European Journal
Communicatio

Enzyme Catalysis

Directed Evolution of a Bond-Forming Enzyme: Ultrahigh-Throughput Screening of Microbial Transglutaminase Using Yeast Surface Display

Lukas Deweid,[a] Lara Neureiter,[a] Simon Englert,[a] Hendrik Schneider,[a] Jakob Deweid,[a]
Desislava Yanakieva,[a] Janna Sturm,[a] Sebastian Bitsch,[a] Andreas Christmann,[a]
Olga Avrutina,[a] Hans-Lothar Fuchsbauer,[b] and Harald Kolmar*[a]

Abstract: Microbial transglutaminase from Streptomyces mobaraensis (mTG) has emerged as a useful biotechnological tool due to its ability to crosslink a side chain of glutamine and primary amines. To date, the substrate specificity of mTG is not fully understood, which poses an obvious challenge when mTG is used to address novel targets. To that end, a viable strategy providing an access to tailor-made transglutaminases is required. This work reports an ultrahigh-throughput screening approach based on yeast surface display and fluorescence-activated cell sorting (FACS) that enabled the evolution of microbial transglutaminase towards enhanced activity. Five rounds of FACS screening followed by recombinant expression of the most potent variants in E. coli yielded variants that possessed, compared to the wild type enzyme, improved enzymatic performance and labeling behavior upon conjugation with an engineered therapeutic anti-HER2 antibody. This robust and generally applicable platform enables tailoring of the catalytic efficiency of mTG.

Transglutaminases (TGases) belong to a family of bond-forming protein–glutamine g-glutamyltransferases (EC 2.3.2.13) and catalyze crosslinking of a glutamine side chain carboxamide to a primary amine, in most cases the e-amino group of lysine, towards isopeptide bond formation.[1] Being able to link biopolymers of peptidic nature following a Ca^{2+}- and GTP-independent mechanism,[2] transglutaminases of prokaryotic origin have found a vast spectrum of applications in biotechnology, material science and food industry.[3]

Transglutaminases are of growing interest for the development of antibody–drug conjugates (ADCs). Combining an immunoglobulin (IgG) that precisely recognizes its target with a covalently attached toxic drug, these macromolecular constructs have recently found their way to the global market of particular therapeutics.[4] In 2010, Jeger and co-workers found that aglycosylation of Asn297 at the antibody F_c-fragment exposes Gln295, which becomes addressable by transglutaminase.[5] This enabled mTG-mediated generation of single- and dual-functionalized ADCs and the application of branched linkers, thus enhancing the drug-to-antibody ratio.[6] To allow for TGase-mediated bioconjugation to glycosylated antibodies, the incorporation of specific enzyme recognition tags within loop structures or at the C-terminus of the heavy or the light chain, respectively, has been applied.[7]

Though the pool of scientific publications dealing with application of transglutaminase catalysis is enormous, only a few of them cover the challenging subject of mTG engineering. Although microbial transglutaminases have been tailored in view of thermostability, specific activity,[8] and substrate specificity,[9] the latter issue poses an obvious hurdle. Indeed, mTGs affinity in amine-bearing (referred to as an acyl acceptor) substrate strongly limits its selectivity. On the other hand, the glutamine counterpart (referred to as an acyl donor) repertoire is restricted to a rather narrow scope of peptide motifs.[10] Herein, we report on a strategy for directed evolution of microbial transglutaminase based on yeast surface display to improve its enzymatic performance. Our approach is robust, substrate-independent, and suitable to enrich mTG-presenting cells indicating that genotype–phenotype correlation is given.

For the laboratory evolution of Streptomyces mobaraensis transglutaminase, an inactive enzyme with an aminoterminal propeptide was displayed on the surface of yeast cells, being extracellularly fused to the Aga2p cell surface mating factor; the latter was disulfide-bound to the yeast cell wall protein Aga1p (Figure 1). The construct was equipped with a His_6-tag to enable immunofluorescent staining (see the Supporting Information, section 1.7). A dramatic decrease in cell growth was observed when mTG lacking its inhibitory propeptide was produced via Aga2p fusion (data not shown) and no surface display of mTG was detectable (Figure S12, Supporting Information). Clearly, the active enzyme is toxic to the host cells due to its high bond-forming affinity. Enzymes dispase and trypsin are known to preferentially cleave at the junction of the pro-

---

[a] L. Deweid, L. Neureiter, S. Englert, H. Schneider, J. Deweid, D. Yanakieva, J. Sturm, S. Bitsch, Dr. A. Christmann, Dr. O. Avrutina, Prof. Dr. H. Kolmar
Clemens-Schçpf-Institut fer Organische Chemie und Biochemie
Technische Universit-t Darmstadt, Alarich-Weiss-Straße 4
64287 Darmstadt (Germany)
E-mail: Kolmar@biochemie-tud.de

[b] Prof. Dr. H.-L. Fuchsbauer
Fachbereich Chemie- und Biotechnologie, Hochschule Darmstadt
Stephanstraße 7, 64295 Darmstadt (Germany)

Supporting information and the ORCID identification number(s) for the author(s) of this article can be found under:
https://doi.org/10.1002/chem.201803485.

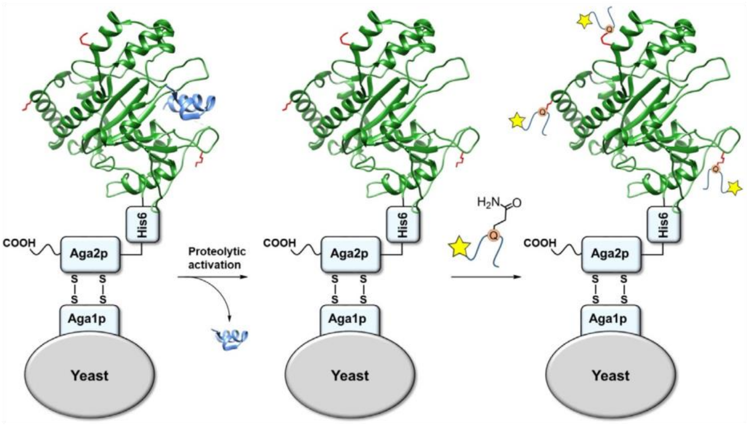

Figure 1. General scheme for the developed assay. Inactive pro-mTG constructs (**4 pro**, **5 pro**, see Table S2) are surface-displayed through genetic fusion to the N-terminus of the Aga2p. Proteolytic removal of the inhibitory propeptide results in mature, surface-bound mTG (**4**, **5**, see Table S2). When supplementing a glutamine-donor peptide attached to a biotin-handle, mTG catalyzes the surface labeling at available lysine residues, enabling the discrimination of tagged cells by FACS.

peptide and the mature TGase.[11] However, these proteases are rather unselective and, upon elongated incubation, may promote hydrolysis at other sites. To overcome this problem, an alternative pro-mTG variant (**3 pro**, Table S2) was designed that contained an enterokinase recognition sequence (DDDDK) at the propeptide-mTG junction. In the preliminary in vitro studies, the inactive, recombinantly produced proenzyme possessing either its native SFRAP cleavage site recognized by trypsin and dispase (pro-SFRAP-mTG, **2 pro**) or an engineered DDDDK motif (pro-Entero-mTG, **3 pro**) for enterokinase-mediated activation was incubated with the mentioned proteases. Specific cleavage was observed in the case of dispase (Figures S10 and S11, Supporting Information) and enterokinase (Figure 2 a), whereas treatment with trypsin led to further degradation of the active enzyme (Figure S10). Surprisingly, enterokinase is able to site-specifically cleave the inhibitory propeptide even though it has been reported to be incapable of that when the native SFRAP site is directly replaced by the DDDDK motif.[12] Though the origin of enterokinase has not been specified in the literature, the human variant of the enzyme was used in the present work. We assume certain species-dependent divergence in substrate specificity between the utilized enzymes to be responsible for the altered propeptide cleavage pattern.

Following in vitro experiments, the corresponding zymogens were fused to Aga2p, leading to presentation of the proenzyme (**4 pro**, **5 pro**, Table S2) on the surface of yeast cells as revealed by flow cytometry (Figure S13), with subsequent proteolytic cleavage of a propeptide (Figure 1).

To evaluate mTG activity in surface-bound state, 1 µM aqueous solution of an oligopeptide biotin-GSGLLQG-NH_2 (**6 a**, Table S2, see Supporting Information, section 2.1.1, Figures S1–S3) derived from the classic mTG recognition tag LLQG,[13] was used as a Gln substrate. Its incubation with the protease-treated cells within 30 min resulted in formation of covalent bonds

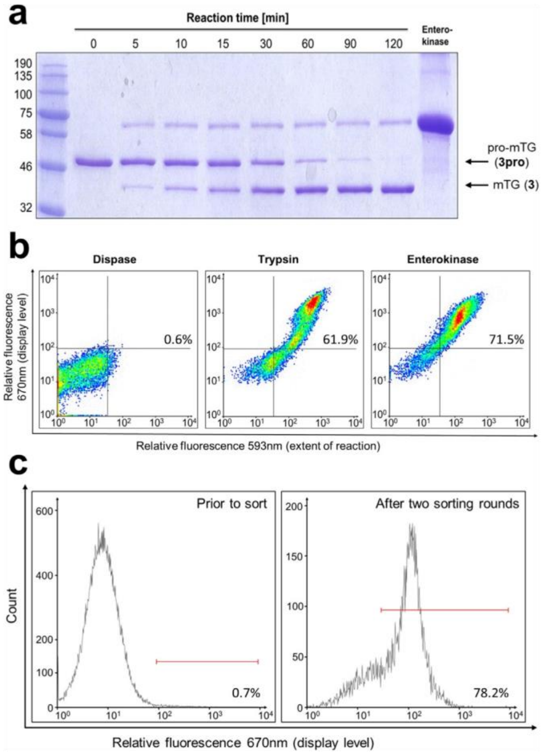

Figure 2. Yeast surface display of mTG. (a) SDS-PAGE analysis of enterokinase-mediated procession of inactive zymogen (**3 pro**) leading to mature mTG (**3**). (b) Density plot (640/670 [30] vs. 561/593 [40]. FACS analysis of protease-treated **4 pro** and **5 pro** revealed active surface-bound mTG (**4**, **5**) in the case of trypsin- and enterokinase-mediated activation. (c) FACS enrichment of transglutaminase-presenting cells (mTG$^+$) from a 1:1000 mixture with cells displaying a non-related protein (mTG$^-$).

with accessible side chains of lysins, thus enabling detection of biotinylated cells in a FACS experiment (Figure 1). Interestingly, treatment of **4 pro** with dispase led to a complete loss of surface presentation (Figure 2 b). ESI-MS analysis of the synthetic construct **2** (Table S2) revealed that dispase cleaved **2 pro** not only at its usual site, *C*-terminally from Ser in the SFRAP sequence, but also within the His_6-tag sequence (see Supporting Information, section 2.3 and Figure S11). This observation corroborates previous data.[14] Nonetheless, cells treated with either trypsin or enterokinase showed surface display of the enzyme and biotinylation, indicating that post-display procession of pro-mTG (**4 pro** and **5 pro**, Table S2) succeeded (Figure 2 b, middle and right panels).

We further localized the exact site of transamidation by incubating surface-labeled cells with 100 μM dithiothreitol (DTT) to reduce the disulfide bonds within the Aga1p-Aga2p conjugate and thereby separate the fusion protein from its surface anchor, resulting in release of mTG moiety. As a consequence, neither display nor surface decoration was observed upon flow-cytometric analysis of DTT-treated cells, indicating that conjugation occurred at surface-exposed lysines of transglutaminases **4** and **5** themselves (data not shown).

To enrich cells bearing mutants with altered properties from a library consisting of a heterogeneous pool of mutants, genotype–phenotype correlation has to be guaranteed. To ensure that the mTG-catalyzed conversion of an acyl acceptor on the enzyme's own cell surface is preferred over the undesired cross-reaction with amino functions of neighboring cells, mixture experiments were performed. To this end, mTG-displaying cells (mTG^+) were mixed in a ratio of 1:1000 with cells lacking mTG presentation (mTG^-). Although mTG^- cells bear a c-Myc epitope only, mTG^+ cells lacking this motif carry the His_6-tag and therefore can be distinguished from each other. After propeptide removal, cells were incubated with 1 μM biotinylated LLQG peptide **6 a** (Table S2) for 30 min. Biotinylated cells were fluorescently stained with streptavidin, R-phycoerythrin conjugate, isolated using FACS, and recultured (Supporting Information, section 1.7). After two rounds of a model library screening using either trypsin- or enterokinase-mediated activation of transglutaminase-containing mixtures, mTG^+ cells were successfully enriched, while the mTG^- ones were depleted (Supporting Information, section 2.6). Therefore, genotype-phenotype correlation is provided and cells bearing active mTG can be discriminated from the inactive ones (Figure 2 c).

After verification of genotype–phenotype correlation, directed evolution experiments were conducted. This approach is widely used in protein design to modulate stability, binding affinity, enzymatic activity, substrate specificity, or solvent tolerance.[15] In the present work, we generated a transglutaminase library by randomizing the gene of mature *S. mobaraensis* transglutaminase without the corresponding propeptide by error-prone PCR and transferred the mutagenized DNA into the yeast display vectors by gap repair recombination. A total of 3×10^8 individual clones were generated that contained on average 3.2 amino acid substitutions in the mTG-coding sequence, as revealed by sequencing (Supporting Information, section 1.6). To remove inactive or truncated mutants, library cells were incubated for 30 min with 1 μM of **6 a** for biotinylation of mTG^+ cells following enrichment by FACS upon fluorescent labeling (Figure 3 a, Table S7 in the Supporting Information). In the following screening rounds selective pressure was increased by stepwise reduction of substrate availability and reaction time to final conditions of 50 nM of **6 a** and 5 min incubation time in R5 (Figure 3 b, Table S7). Analysis of 150 single colonies from the fifth selection round revealed 30 clones possessing higher fluorescence intensity, indicating more efficient mTG-mediated conjugation of the acyl-donor **6 a** (Figure 3 c,d and Figure S15).

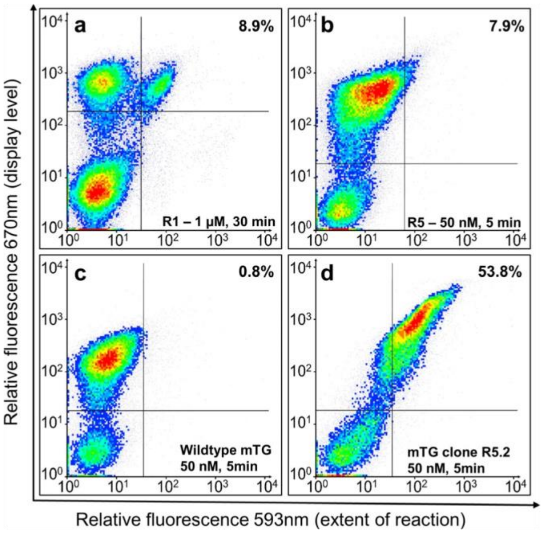

Figure 3. Density plot (640/670 [30] vs. 561/593 [40]). FACS enrichment of mTG variants. The randomized library, pre-sorted for enzymes exhibiting mTG activity (a), was screened by a stepwise selective pressure increase to enrich cells bearing mutant enzymes in sorting round 5 (b). Lower row: activity profile of clone **R5.2** (d) versus wild type mTG (c).

The genes encoding 14 mutants out of 25 unique clones that displayed the most prominent increase of labeling on the surface of yeast cells (Supporting Information, section 2.4.3) were cloned into *E. coli* expression vector pET22b(+) possessing the native SFRAP sequence instead of the engineered DDDDK one (Supporting Information, section 1.8). A total of 13 out of 14 enriched clones were produced recombinantly, whereas expression of a quadruple mutant **R5.12** failed (Supporting Information, sections 1.9, 1.10, and Table S4). One clone resembling the wildtype enzyme in view of surface activity profile served as control (**R5.4**, Table S4). Substrates **6** and **9** were incubated in the presence of the respective recombinant enzymes for a defined period of time and formation of the corresponding crosslinked product **10** (Supporting Information, section 1.11) was monitored by HPLC (Figure 4, Supporting Information, section 1.11). Thus, six transglutaminase clones showed an up to 1.36-fold increased product formation after 15 min of reaction, compared to the wild type counterpart,

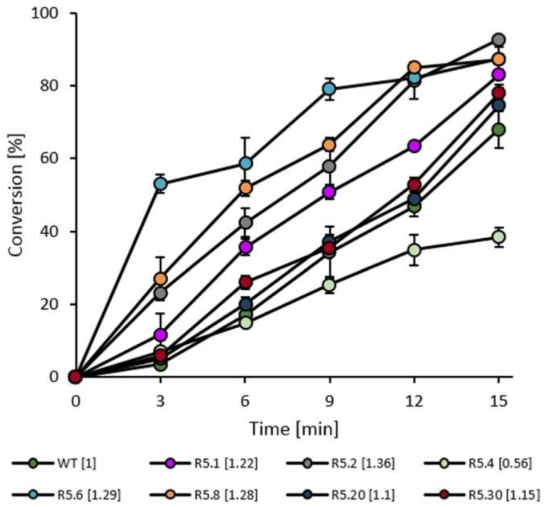

Figure 4. Crosslink of substrates **6** and **9** catalyzed by mutant transglutaminases. Product formation was monitored by HPLC and compared to the wild type enzyme after 15 min of reaction (see Supporting Information, section 1.11). Relative increase of conversion compared to the wild type enzyme is given in brackets.

whereas the reference variant **R5.4** revealed less activity (Figure 4). Noteworthy, clones **R5.10** and **R5.11** showed no transglutaminase activity as no product formation was observed. The lack of transglutaminase activity together with poor yields upon recombinant expression (Table S4) gave rise to the assumption that these mutants suffered from intrinsic instability, indicating that conformational arrangement and firmness of the Aga2p-fusion protein on the surface of yeast cells differs from the soluble counterpart.

Interestingly, mutations beneficial for catalytic performance were predominantly located within defined areas (Figure 5 a–c). Amino acid substitutions S2G and R15C combined with M234L resulted in a 1.36-fold increased product formation. Minor improvements in catalytic activity were observed upon substitution of Asp3 and Ser23 against valine and asparagine, respectively. Indeed, the N-terminal region (Asp1–Asn32) defines the active site entrance of the enzyme and is known to be highly important for substrate recognition and catalytic activity of the mature enzyme (Figure 5 b).[8,16] Moreover, single amino acid substitutions L60Q and G73A led to engineered enzymes with 1.22- and 1.28-fold enhanced substrate conversion after 15 min. Both mutations are located within a helix-loop-helix motif formed by helices α_2 and α_3 that surround the Cys64-containing loop (Figure 5 c). It is known to be involved in substrate binding, therefore mutations within this area may affect the flexibility of the active-site Cys64, thus influencing catalytic activity of the enzyme.[17] Combining amino acid substitutions G250D, S299R, and S303R, located approximately 14 Å from catalytic residues Cys64 and Asp255 at the right-side wall of the active-site cleft, lead to a 1.15-fold increased substrate consumption. This is rather predictable as G250 is known to be involved in substrate recognition.[17] Moreover,

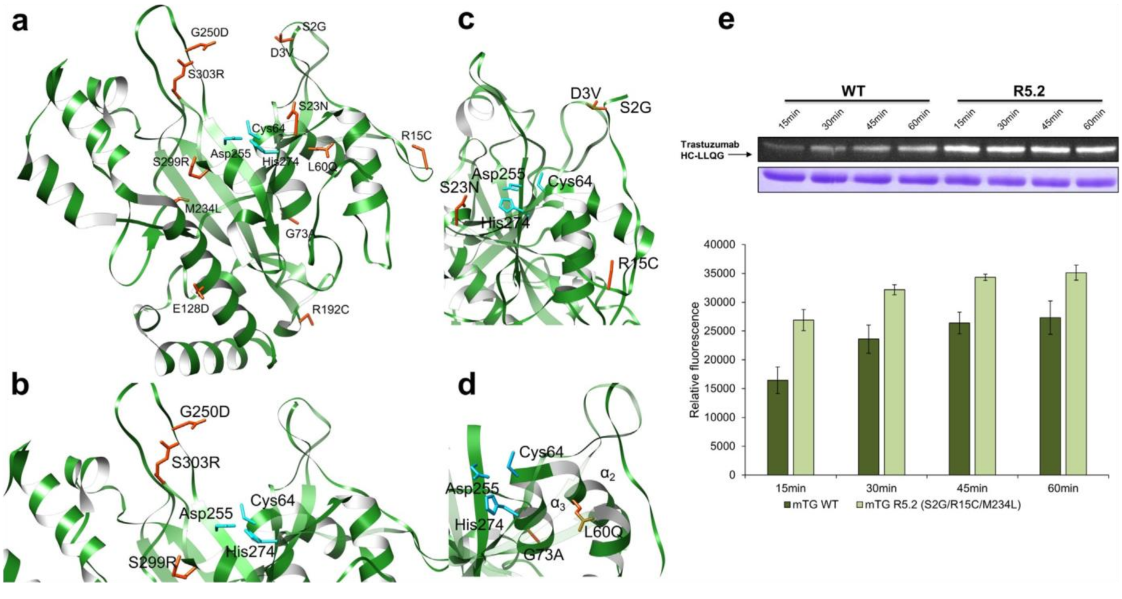
a
G250D
S2G
D3V
S303R
S23N
Cys64
R15C
S299R
Asp255
His274
L60Q
M234L
G73A
E128D
R192C
b
G250D
S303R
Asp255
Cys64
S299R
His274
c
D3V
S2G
S23N
Asp255
Cys64
His274
R15C
d
Cys64
α_2
Asp255
α_3
His274
L60Q
G73A
e
WT
R5.2
15min
30min
45min
60min
15min
30min
45min
60min
Trastuzumab HC-LLQG
40000
35000
30000
25000
20000
15000
10000
5000
0
Relative fluorescence
15min
30min
45min
60min
mTG WT
mTG R5.2 (S2G/R15C/M234L)

Figure 5. (a) Ribbon representation of mTG (PDB: 1IU4) with enriched beneficial amino acid substitutions highlighted. Active-site residues are shown in cyan, enriched amino acid substitutions in orange; (b) active-site wall involved in substrate recognition; (c) N-terminal sequence of the mature enzyme (Asp1–Asn32) that resides at the active site entrance; (d) helix-loop-helix motif formed by helices $\alpha2$ and $\alpha3$ surrounding the catalytic Cys64; (e) labelling of LLQG-tagged trastuzumab (**8**) with fluorescent handle **7** by an evolved mTG (**R5.2**) and the wildtype counterpart **2**.<

previous engineering approaches by Yokoyama et al. demonstrated minor improvements upon substitution of S299 and S303.[8] In addition, mutations E128D and R192C, located outside the catalytic cleft and the N-terminal region, led to a 1.29-fold enhanced product formation. We assume intrinsic stability effects to be responsible for this observation.

Though substrate specificity of microbial transglutaminase is not fully understood to date, it is believed to be influenced by the composition and flexibility of the glutamine-containing region as well as the tertiary structure of the addressed substrates.[18] To examine whether enriched mutants with improved catalytic activity on a peptide level also possess superior labeling of proteinaceous targets, mTG-assisted bioconjugation was undertaken using monoclonal humanized anti-HER2 antibody trastuzumab used for the treatment of breast cancer. To that end, the mAb was engineered to carry a transglutaminase recognition motif LLQG at the C-terminus of its heavy chain (construct **8**; Supporting Information, section 2.5 and Figure S16). It was incubated with a fluorescently labeled acyl acceptor peptide *TAMRA*-MRHKGS-NH_2 (**7**) (see Supporting Information, section 2.1.3, Figures S6–S9)[19] in the presence of the most potent transglutaminase mutant, **R5.2** (S2G/R15C/M234L) as well as the wild type enzyme **2**. SDS-PAGE analysis revealed that the engineered enzyme labeled the antibody more efficiently compared to the wild type counterpart (Figure 5d).

To further elucidate the performance of engineered mutant **R5.2**, kinetic parameters K_M and k_{cat}/K_M were determined and compared to the wild type enzyme (see Supporting Information, section 1.11, Table S5).[20] Surprisingly, minor improvements concerning kinetic parameters (1.4-fold decreased K_M and 1.3-fold increase in k_{cat}/K_M) seemed to be responsible for more efficient labeling of therapeutic antibody trastuzumab.

Engineering of microbial transglutaminase is a challenging topic that is barely covered by the peer-reviewed literature. Marx et al. established a microtiter plate screen based on the commonly used hydroxamate assay and isolated thermostable mutants from an error-prone randomized library. Interestingly, a single amino acid substitution S2P resulted in elevated thermal stability combined with two-fold increased activity towards the mTG-standard substrate Cbz-Gln-Gly.[16a,21] Further approaches, both rationally and randomly driven, by Yokoyama et al. resulted in mutant enzymes that exhibited an up to 1.7-fold improved turnover of Cbz-Gln-Gly. The substrate specificity of a highly homologous transglutaminase from *Streptomyces ladakanum* was optimized by Zhao et al. The engineered enzymes exclusively modified human growth hormone (hGH) at Gln141 but suffered from decreased reaction velocity.[9] In comparison to other bond-forming enzymes such as sortase A, where improvements of more than 100-fold in terms of coupling activity were achieved upon directed evolution, enhancement of mTG activity was comparably low.[22] The difference may be related to the broad substrate affinity of microbial transglutaminase with respect to both the donor and acceptor substrates, which could make tailoring of enzyme performance more difficult to achieve.

To conclude, in the present work we added microbial transglutaminase from *Streptomyces mobaraensis* to the list of enzymes whose catalytic activity can be improved upon engineering using yeast surface display.[23] However, the screening of enzymes, especially the bond-forming ones, by YSD remains challenging because an acceptor molecule within the range of the surface-displayed enzyme is required. To that end, Chen et al. established a generally applicable screening strategy and proved its viability by engineering of *Staphylococcus aureus* sortase A with respect to catalytic activity and substrate specificity.[22,24]

We adapted the mentioned strategy to microbial transglutaminase from *Streptomyces mobaraensis* and bypassed its intracellular cytotoxicity by genetic fusion of its inhibitory propeptide following subsequent proteolytic procession. In contrast to the work of Chen et al. for sortase A library screening, enzymatic immobilization of acyl–acceptor substrates is not necessary as amine groups of surface-bound transglutaminase serve as acceptors for transamidation. This finding may also facilitate the transfer of the screening strategy to other high-throughput screening formats such as phage or bacterial display. A total of 30 out of 150 isolated mTG variants yielded from combinatorial library screening possessed improved activity on the surface of yeast cells. Moreover, six out of 13 recombinantly expressed mutants revealed superior biotinylation of a peptidic substrate compared to the wildtype enzyme. Although only a 1.3-fold increase in k_{cat}/K_M was determined for the most potent variant, the results of mTG-promoted bioconjugation using a therapeutic antibody and a model TAMRA-labeled peptide clearly showed that the engineered enzyme possessed significantly faster performance compared to the wild type counterpart. It will be interesting to see whether combination of beneficial mutations, gene shuffling or site-saturation mutagenesis of identified hotspot positions will contribute to further improved enzyme performance. These results are of particular importance for the production of therapeutic antibody–drug conjugates, as catalysis with the efficient tailor-made transglutaminase should make it possible to reduce the amounts of expensive cytotoxic components upon conjugation.

Acknowledgements

This work was supported by the NANOKAT II grant from the BMBF (Bundesministerium für Bildung und Forschung) and by DFG priority program 1623.

Conflict of interest

The authors declare no conflict of interest.

Keywords: bioconjugation · directed evolution · enzyme catalysis · FACS · microbial transglutaminase · protein engineering · yeast surface display

[1] A. Shleikin, N. Danilov, *J. Evol. Biochem. Physiol.* **2011**, *47*, 1 – 14.
[2] P. Strop, *Bioconjugate Chem.* **2014**, *25*, 855 – 862.

© 2018 Wiley-VCH Verlag GmbH & Co. KGaA, Weinheim

[3] a) J. Cortez, P. L. Bonner, M. Griffin, Enzyme Microb. Technol. 2004, 34, 64–72; b) M. Kieliszek, A. Misiewicz, Folia Microbiol. 2014, 59, 241–250; c) N. M. Rachel, J. N. Pelletier, Biomolecules 2013, 3, 870–888; d) T. Li, C. Li, D. N. Quan, W. E. Bentley, L. X. Wang, Carbohydr. Res. 2018, 458–459, 77–84; e) M. Takahara, R. Wakabayashi, K. Minamihata, M. Goto, N. Kamiya, Bioconjugate Chem. 2017, 28, 2954–2961; f) A. Grigoletto, A. Mero, K. Maso, G. Pasut, Methods Enzymol. 2017, 590, 317–346.
[4] S. Sau, H. O. Alsaab, S. K. Kashaw, K. Tatiparti, A. K. Iyer, Drug Discov. Today 2017, 10, 1547–1556.
[5] S. Jeger, K. Zimmermann, A. Blanc, J. Grenberg, M. Honer, P. Hunziker, H. Struthers, R. Schibli, Angew. Chem. Int. Ed. 2010, 49, 9995–9997; Angew. Chem. 2010, 122, 10191–10194.
[6] a) Y. Anami, W. Xiong, X. Gui, M. Deng, C. C. Zhang, N. Zhang, Z. An, K. Tsuchikama, Org. Biomol. Chem. 2017, 15, 5635–5642; b) P. Spycher, C. A. Amann, J. Wehrmeller, D. R. Hurwitz, O. Kreis, A. Ritler, D. Messmer, A. Kechler, A. Blanc, P. Walde, ChemBioChem 2017, 15, 5635–5642; c) P. Dennler, A. Chiotellis, E. Fischer, D. Br8geon, C. Belmant, L. Gauthier, F. Lhospice, F. O. Romagne, R. Schibli, Bioconjugate Chem. 2014, 25, 569–578.
[7] a) V. Siegmund, S. Schmelz, S. Dickgiesser, J. Beck, A. Ebenig, H. Fittler, H. Frauendorf, B. Piater, U. A. Betz, O. Avrutina, Angew. Chem. Int. Ed. 2015, 54, 13420–13424; Angew. Chem. 2015, 127, 13618–13623; b) P. Strop, S.-H. Liu, M. Dorywalska, K. Delaria, R. G. Dushin, T.-T. Tran, W.-H. Ho, S. Farias, M. G. Casas, Y. Abdiche, Chem. Biol. 2013, 20, 161–167.
[8] K. Yokoyama, H. Utsumi, T. Nakamura, D. Ogaya, N. Shimba, E. Suzuki, S. Taguchi, Appl. Microbiol. Biotechnol. 2010, 87, 2087–2096.
[9] X. Zhao, A. C. Shaw, J. Wang, C.-C. Chang, J. Deng, J. Su, J. Biomol. Screening 2010, 15, 206–212.
[10] a) M. Malešević, A. Migge, T. C. Hertel, M. Pietzsch, ChemBioChem 2015, 16, 1169–1174; b) Y. Sugimura, K. Yokoyama, N. Nio, M. Maki, K. Hitomi, Arch. Biochem. Biophys. 2008, 477, 379–383.
[11] R. Pasternack, S. Dorsch, J. T. Otterbach, I. R. Robenek, S. Wolf, H. L. Fuchsbauer, Eur. J. Biochem. 1998, 257, 570–576.
[12] K. Wang, B. Wang, H.-L. Yang, L. Pan, Biotechnol. Lett. 2013, 35, 383–388.
[13] M. Ota, A. Sawa, N. Nio, Y. Ariyoshi, Biopolymers 1999, 50, 193–200.
[14] C. Sommer, T. C. Hertel, C. E. Schmelzer, M. Pietzsch, Amino Acids 2012, 42, 997–1006.
[15] P. A. Romero, F. H. Arnold, Nat. Rev. Mol. Cell Biol. 2009, 10, 866–876.
[16] a) C. K. Marx, T. C. Hertel, M. Pietzsch, J. Biotechnol. 2008, 136, 156–162; b) N. Shimba, M. Shinohara, K.-I. Yokoyama, T. Kashiwagi, K. Ishikawa, D. Ejima, E.-I. Suzuki, FEBS Lett. 2002, 517, 175–179.
[17] U. Tagami, N. Shimba, M. Nakamura, K. Yokoyama, E. Suzuki, T. Hirokawa, Protein Eng. Des. Sel. 2009, 22, 747–752.
[18] D. Fiebig, S. Schmelz, S. Zindel, V. Ehret, J. Beck, A. Ebenig, M. Ehret, S. Frçls, F. Pfeifer, H. Kolmar, H.-L. Fuchsbauer, A. Scrima, J. Biol. Chem. 2016, 291, 20417–20426.
[19] H. Abe, M. Goto, N. Kamiya, Chem. Eur. J. 2011, 17, 14004–14008.
[20] S. K. Oteng-Pabi, J. W. Keillor, Anal. Biochem. 2013, 441, 169–173.
[21] C. Sommer, N. Volk, M. Pietzsch, Protein Expression Purif. 2011, 77, 9–19.
[22] I. Chen, B. M. Dorr, D. R. Liu, Proc. Natl. Acad. Sci. USA 2011, 108, 11399–11404.
[23] D. Kçnning, H. Kolmar, Microb. Cell Fact. 2018, 17, 32.
[24] B. M. Dorr, H. O. Ham, C. An, E. L. Chaikof, D. R. Liu, Proc. Natl. Acad. Sci. USA 2014, 111, 13343–13348.

Manuscript received: July 6, 2018
Accepted manuscript online: July 26, 2018
Version of record online: September 10, 2018

CHEMISTRY
A European Journal

Supporting Information

Directed Evolution of a Bond-Forming Enzyme: Ultrahigh-Throughput Screening of Microbial Transglutaminase Using Yeast Surface Display

Lukas Deweid,[a] Lara Neureiter,[a] Simon Englert,[a] Hendrik Schneider,[a] Jakob Deweid,[a]
Desislava Yanakieva,[a] Janna Sturm,[a] Sebastian Bitsch,[a] Andreas Christmann,[a]
Olga Avrutina,[a] Hans-Lothar Fuchsbauer,[b] and Harald Kolmar*[a]

chem_201803485_sm_miscellaneous_information.pdf

1. Materials and Methods

1.1 Materials. If not designated otherwise, all chemical used within this work were of analytical grade and purchased from either Sigma Aldrich (Steinheim, Germany) or Carl Roth GmbH & Co. KG (Karlsruhe, Germany). Commercially available enzymes were obtained from common suppliers: Restriction enzymes, New England Biolabs, NEB (Frankfurt am Main, Germany), human enterokinase, Peprotech (Hamburg, Germany), dispase, neutral protease, Cellsystems (Troisdorf, Germany), bovine trypsin and glutamate dehydrogenase from bovine liver, Sigma Aldrich (Steinheim, Germany). For immune staining monoclonal mouse antibody specific for His_6 was obtained from Qiagen (Hilden, Germany), anti-c-Myc, monoclonal mouse antibody conjugated to fluorescein isothiocyanate (FITC) from MACS Miltenyi Biotech (Bergisch Gladbach, Germany) and rat monoclonal antibody conjugated to Allophycocyanin (APC) as well as streptavidin conjugated R-phycoerythrin (PE) were purchased from Thermo Fischer Scientific (Darmstadt, Germany).

1.1.1 Oligonucleotides

Table S1: All oligonucleotides used within his work were purchased from Sigma Aldrich.

Number	Oligonucleotide	Sequence (3'-5')	Incorporated restriction site
O1	mTG fw	5’-GCGCGCTCTAGAAATAATTTTGTTTAACTTTAAGAAGGAGATATACCATGGACAATGGTGCCGG-3’	*Xba*I
O2	mTG His6 rev	5‘-GCGCGCGAATTCTCAGTGGTGGTGGTGGTGGTGAGGCCAACCCTGTTTAACTTTATC-3’	*Eco*RI
O3	mTG overlap fw	5’- GCACTGAATGAAAGCGCACCGGCAGCAAGCAGCGCAGGTCCGGATGATGACGACAAAG -3’	
O4	mTG overlap rev	5’-CCACCACCACCAGAACCACCACCACCAGAACCACCACCACCCCATGGGTGGTGGTGGTGGTGAGGCCAACCCTGTTTAACTTTATC-3’	
O5	mTG library fw	5’-GTCCGGATGATGACGACAAA-3’	
O6	mTG SFRAP rev	5’-GCGCGCGGATCCGGCATACGATCCAGCGGTTCTGCCGGAGGGGTAACACGATCATCACTATCCGGTGCACGAAAGCTCGGACCTGCGCTGCTTGCTGCCGGTG-3’	*Bam*HI

1.2 Constructs

Table S2: Overview of synthetic constructs used within this work.

Number	Compound	Description
1	mTG-His_6	microbial transglutaminase, His_6-tagged
2pro	pro-SFRAP-mTG-His_6	recombinant, native cleavage site, His_6-tagged
3pro	pro-Entero-mTG-His_6	recombinant, engineered cleavage site, His_6-tagged
2	FRAP-mTG-His_6	dispase-activated **2pro**
3	Entero-mTG-His_6	enterokinase-activated **3pro**
4pro	pro-SFRAP-mTG-His_6-Aga2p	surface-displayed, native cleavage site, His_6-tagged
5pro	pro-Entero-mTG-His_6-Aga2p	surface-displayed, engineered cleavage site, His_6-tagged
4	AP-mTG-His_6-Aga2p	trypsin-activated **4pro**
5	Entero-mTG-His_6-Aga2p	enterokinase-activated **5pro**
6a	biotin-GSGLLQG-NH_2	Gln donor substrate derived from[1]
6	CH_3CO -GSGLLQG-NH_2	Gln donor substrate derived from[1]
7	5/6-*TAMRA*-MRHKGS-NH_2	fluorescent Lys acceptor derived from[2]
8	Trastuzumab-LLQG	monoclonal, humanized, LLQG-tag at heavy chain[3]
9	Biotin Cadaverine (*N*-(5-aminopentyl)-biotinamide)	biotinylated amine substrate for mTG
10	See section **1.11**	Coupling product of **6** and **9**

1.3 Solid-phase synthesis of peptides

1.3.1 **Automated solid-phase peptide synthesis.** Peptides were synthesized on an AmphiSpheres 40 RAM resin (Agilent, 0.35 mmol/g) by microwave-assisted Fmoc-SPPS using a Liberty Blue™ Microwave Peptide Synthesizer at a 0.25 mmol scale. Activation of the respective carboxyfunctional amino acid was performed by ethyl cyanohydroxyiminoacetate (Oxyma)/ *N,N'*-diisopropylcarbodiimide (DIC). Deprotection of the aminoterminal Fmoc-group was achieved using 20 % piperidine in *N*,*N*-dimethylformamide (DMF) in the presence of Oxyma. During the synthesis cycles all amino acids were heated to 90 °C.

1.3.2 **Manual solid-phase peptide synthesis.** Attachment of Fmoc-protected amino acids was performed as double coupling. 4 eq. of the respective amino acid, 3.98 eq. of the activator *O*-benzotriazole-*N*,*N*,*N'*,*N'*-tetramethyl-uronium-hexafluoro-phosphate (HBTU) and 8 eq. *N*,*N*-diisopropylethylamine (DIPEA), were dissolved in a minimal amount of DMF. Coupling was performed at ambient temperature for 45 min. *N*-terminal deprotection of amino acids was performed as double deprotection steps with 20 % piperidine in DMF for 10 min at ambient temperature.

1.3.3 ***N*-terminal biotinylation of peptides**. 4 eq D-biotin from Iris Biotech (Marktredwitz, Germany), 3.9 eq HBTU and 6 eq DIPEA in DMF were incubated at ambient temperature within 15 min and added to the peptide-resin. After 2 h the resin was washed trice in DMF, DCM and diethyl ether.

1.3.4 Peptide cleavage from the support. Peptides were cleaved from the resin by a standard cleavage cocktail of 94 % TFA, 2 % triethyl silane, 2 % anisole and 2 % H_2O. After 2 h of cleavage, peptides were precipitated in cold diethyl ether and washed twice with diethyl ether.

1.4 RP-HPLC. Analytic conditions are listed in Table S3. Peptides were purified by semi-preparative RP-HPLC (Varian) using a Phenomenex Luna 5u C18 LC column (250 x12.2 mm, 5 µm, 100 Å). Eluent A (water) and eluent B (90 % aq. MeCN) each contained 0.1% trifluoroacetic acid (TFA).

Table S3: Synthetic peptides used within this work were analyzed by RP-HPLC using the conditions listed below.

Peptide	HPLC Device	Column
biotin-GSGLLQG-NH_2 (**6a**)	Agilent Technologies (Santa Clara, USA) Infinity 1260 (**b**)	Phenomenex (Aschaffenburg, Germany) (Luna 5u C18 (2) 150×4.6 mm, 5 µm 100 Å) (**III**).
CH_3CO -GSGLLQG-NH_2 (**6**)	Agilent Technologies (Santa Clara, USA) Infinity 1260 (**b**)	Interchim (Montluçon, France) Uptisphere Strategy (C18-HQ 3 µm, 100×4.6 mm) (**II**)
(5/6)-*TAMRA*-MRHKGS-NH_2 (**7**)	Agilent Technologies (Santa Clara, USA) Infinity 1100 (**a**)	Agilent Eclipse Plus C18 (100×4.6 mm, 3.5 µm, 95 Å) (**I**)

1.5 ESI-MS analysis

1.5.1 Peptide mass spectrometry. ESI mass spectra were collected on a Shimadzu (Kyoto, Japan) LCMS-2020 equipped with a Phenomenex Synergy 4 *u* Fusion-RP 80 (C-18,. 250 x 4.6 mm, 2 µm, 80 Å) by using an eluent system of 0.1% aq. formic acid (eluent A) and acetonitrile containing 0.1% formic acid (eluent B).

1.5.2 Protein mass spectrometry. ESI-MS analysis of protein samples was performed using Agilent Technologies 1200 Series equipped with a Dr. Maisch HPLC GmbH (Ammerbuch, Germany) ReproSil Gold 300 (C4, 3µm) by using an eluent system of 0.03 % aq. TFA and acetonitrile containing 0.01 % TFA coupled to Bruker BioSpin GmbH, (Billerica, USA) Impact II mass spectrometer. Data analysis was performed using mMass v5.5.

1.6 Random mutagenesis and library construction. The mTG-coding gene was randomized by error-prone PCR using the GeneMorph II Kit, Agilent Genomics (Waldbronn, Germany) according to the manufacturer's instructions with oligonucleotides **O4** and **O5**. After *Dpn*I digestion, the respective PCR product was further amplified using oligonucleotides **O3** and **O4** incorporating overlaps for homologues recombination gap repair. Wizard® SV Gel and PCR Clean-up System, Promega (Mannheim, Germany) was used to purify the amplified PCR product as well as the *Nco*I and *Spe*I linearized vector pTTH-Entero-Propeptide, derived from pCT vector.[4] Purified DNA was further utilized for library construction applying the improved yeast transformation method for the generation of human antibody libraries according to Benatuil *et al*[5] followed by incubation of the cells in SD-CAA medium (6.8 g/L yeast nitrogen base without amino acids but supplemented with ammonium sulphate, 5 g/L Bacto Casamino Acids, 20 g/L dextrose, 8.6 g/L $NaH_2PO_4 \times H_2O$, and 5.4 g/L Na_2HPO_4) for 2 days at 30 °C.

1.7 Transglutaminase reaction and yeast library screening. Cells grown in SG-CAA medium (6.8 g/L yeast nitrogen base without amino acids but supplemented with ammonium sulphate, 5 g/L Bacto Casamino Acids, 20 g/L galactose, 8.6 g/L $NaH_2PO_4 \times H_2O$, and 5.4 g/L Na_2HPO_4) at 20 °C for 1 day were washed in PBS buffer. For surface-bound procession of the inactive pro-mTG, 2×10^7 cells were supplemented with 1.25 µg of the corresponding protease and incubated for 1 h at 23 °C in the case of human enterokinase or at 30 °C for bovine trypsin and dispase, respectively. Transglutaminase-mediated cell labelling was performed by incubating protease-treated cells in the presence of biotinylated glutamine donor peptide at different concentrations for a defined period of time at 30 °C. Afterwards, cells were stained for surface display using mouse monoclonal anti His_6 specific antibody (diluted 1:50 in PBS) and rat anti-mouse antibody conjugated to APC (diluted 1:100 in PBS). Enzymatic activity was visualized by streptavidin-PE (diluted 1:100 in PBS). Library screening was performed on a BD InfluxTM cell sorter and analyzed via BD FACSTM Sortware v1.0.

1.8 Reformatting of selected mTG variants. Plasmids were isolated from yeast cells using the Zymoprep™ Yeast Plasmid Miniprep II kit, Zymo Research (Freiburg, Germany) and amplified in *E. coli* cells. Isolated plasmids served as templates for PCR using oligonucleotides **O1** and **O2**. The amplified DNA was cloned into *E. coli* expression vector pET22b(+) by *Xba*I and *Eco*RI cloning. Furthermore, the enterokinase cleavage site was substituted for the native SFRAP site in a second cloning step using oligonucleotides **O1** and **O6** followed by *Xba*I and *Bam*HI cloning.

1.9 Recombinant expression and purification of selected mTG mutants. Recombinant expression of inactive pro-mTG in *E. coli* cells using isopropyl *β*-D-1-thiogalactopyranoside (IPTG) induction was performed according to Marx *et al*.[6] *E. coli* BL21(*DE3*) cells bearing the corresponding plasmid were grown in dYT medium (16 g/L trypton, 10 g/L yeast extract and 5 g/L NaCl) at 37 °C and 180 rpm to an OD_{600} of 0.7-1. Gene expression was inducted by IPTG in a final concentration of 500 µM followed by incubation at 24 °C and 180 rpm for 3 h. Cells were lysed using a Constant Systems Ltd cell disruptor (Daventry, Great Britain) and protein purification was performed by standard IMAC procedure. Purified pro-mTG was stored in standard mTG buffer (300 mM NaCl, 50 mM TRIS-HCl pH 8, 1mM $CaCl_2$ and 1 mM reduced glutathione).

1.10 Activation of pro-mTG. pro-SFRAP-mTG (**2pro**) was activated by adding dispase, solved in mTG buffer, to a final concentration of 20 µg dispase per mg pro-mTG and incubation at 37 °C for 30 min.[7] Correspondingly, pro-Entero-mTG (**3pro**) was activated by 5 µg enterokinase per mg pro-mTG at 4 °C over night. Activated mTG was separated from the utilized protease and the inhibitory propeptide by a second IMAC purification step and stored in standard mTG buffer at -80 °C.

Table S4: Overview of IMAC-purified transglutaminases produced in 1 L culture medium.

Name	Mutation	Pro-mTG (Zymogen) [mg]	mTG (active) [mg]	Recovery [%]
Wildtype		33.4	20.4	63.1
R5.1/3	L60Q	10.9	6.6	60.7
R5.2	S2G/R15C/M234L	11.9	7.6	63.6
R5.4	N176D/F221Y	4.4	2.7	61.3
R5.5	E28G/A212T	2	0.9	46
R5.6	E128D/R192C	22.3	14.9	67.2
R5.8	G73A	24.5	15.6	63.7
R5.10	S303R/D304G	1.8	0.7	41.2
R5.11	R5H/N78I	1.0	0.88	84.6
R5.12	P8L/G202C/N296K/D304G		/	
R5.13/18/20	D3V/S23N	4.6	3.3	71.73
R5.25	A173T	2.8	1.4	50
R5.30	G250D/S299R/S303R	21.7	12.6	58
R5.67	P12L/W59R/R100H/E182D/V271I	14.9	13.2	88.5
R5.102/141	K49I/A270T	16.2	9.5	58.6
R5.143	Q51R	21.7	11.8	54.3

1.11 HPLC-based assay for the performance of microbial transglutaminase. 20 µM of *N*-terminally acetylated peptide *CH_3CO*-GSGLLQG-*NH_2* (**6**) were incubated in the presence of 200 µM *N*-(5-aminopentyl)-biotin amide (**9**) and 0.2 µM transglutaminase at 30 °C in PBS. After 3, 6, 9, 12, and 15 min of reaction, samples were taken and the reaction was terminated by heat inactivation for 10 min at 98 °C. Afterwards, the enzyme was removed from the mixture by addition of 20 µL IMAC Sepharose 6 Fast Flow resin (GE Healthcare). Following centrifugation, the resulting supernatant was analyzed using HPLC (device **b**) equipped with column **II** (see Table S3) using a gradient of 10 to 60 % eluent B within 20 min. HPLC peaks of the fractions corresponding to unmodified **6** and the resulting crosslinked product **10** were compared to determine product formation catalyzed by the respective enzyme.

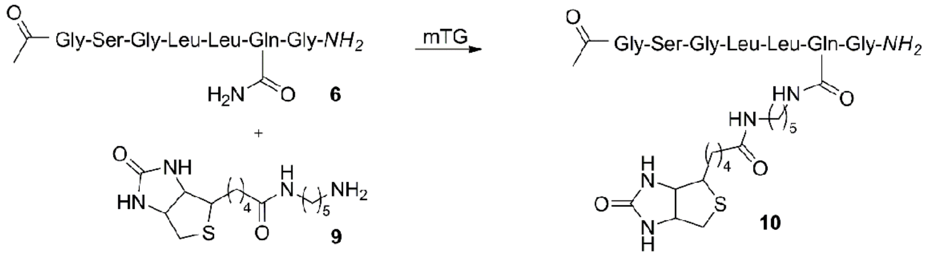
Gly-Ser-Gly-Leu-Leu-Gln-Gly-NH2
H2N
O
6
+
9
mTG
Gly-Ser-Gly-Leu-Leu-Gln-Gly-NH2
10

1.12 Glutamate dehydrogenase coupled assay for microbial transglutaminase. Initial reaction velocity of the respective transglutaminase was calculated using the recently published GDH-coupled assay.[8] Assay conditions were 200 mM MOPS buffer pH 7.2, 500 µM reduced nicotinamide adenine dinucleotide (NADH), 10 mM *α*-ketoglutarate, 10 mM glycine methyl ester, varying concentrations of glutamine donor peptide, 2 U glutamate dehydrogenase and 20 µg of the corresponding mTG in a final volume of 200 µL. Before starting the reaction by adding the enzyme, solutions were preincubated at 37 °C for 5 min. The reaction was performed in 96-well plates and the mTG-mediated reduction of NADH at 37 °C was monitored at 340 nm using BMG CLARIOstar® plate reader. All measurements were performed in triplicates. Kinetic parameters were obtained by fitting initial reaction velocities to the Michaelis-Menten equation.

Enzyme	Mutation	Vmax [nmol/s]	Kcat [s-1]	KM [mM]	kcat/KM [M-1 s-1]
FRAP-mTG Mob	Wildtype	1.766	17.17	1.158	14.82
R5.2	S2G/R15/M234L	1.618	15.73	0.8075	19.48

1.13 Enzymatic antibody conjugation using mTG. The heavy chain of monoclonal, humanized anti-HER2 antibody trastuzumab was *C*-terminal prolonged by the mTG-recognition motif LLQG using standard PCR techniques.[1] Expi293F™ cells were transiently transfected with the corresponding plasmids (pTT5-trastuzumab_hc_LLQG; pTT5-trastuzumab_lc) and the antibody was purified by protein-A affinity chromatography after 7 days of cultivation. Antibody conjugation was performed using 1 mg/mL mAb, 0.25 eq mTG and 2.5 eq amine-donor peptide (**7**) in PBS at 37 °C for 60 min. Samples were taken after 15, 30, 45 and 60 min and supplemented with Laemmli-buffer (reducing).[9] 15 % SDS-PAGE was performed and documented using UVP (Upland, USA) GelDoc-It 310 Imaging System (P/N 97-0266-02). Fluorescence intensity was quantified using ImageJ 1.8.0_112.

2. Analytical Data

2.1 Synthetic peptides

2.1.1 biotin-GSGLLQG-*NH₂* (6a)

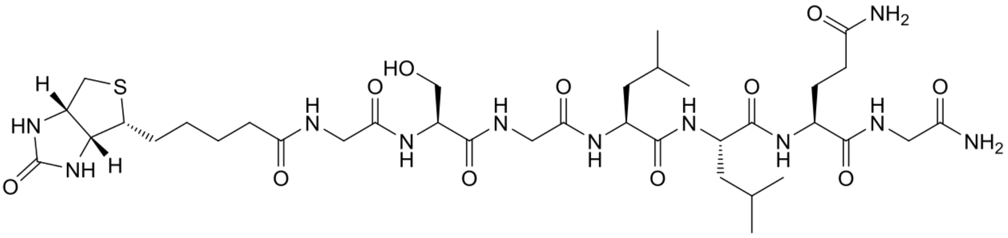

Figure S1: Structure of synthetic peptide **6a**. Synthesis was performed as described in 1.3.1. and 1.3.3.

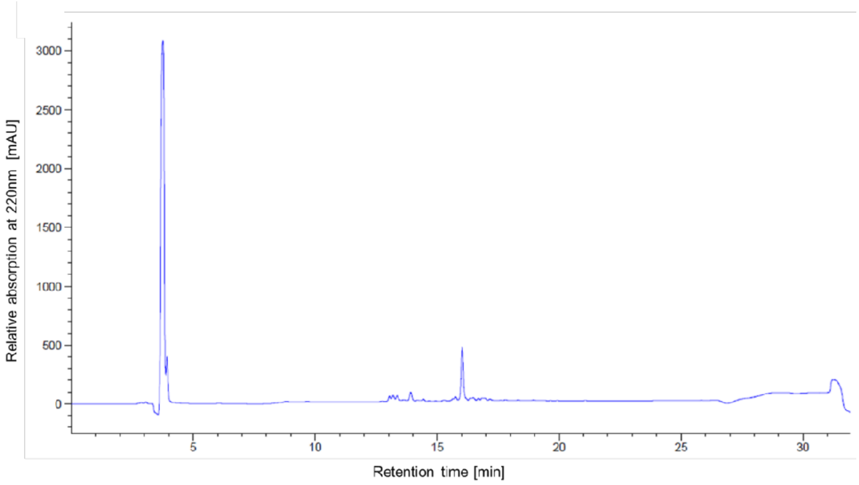

Figure S2: RP-HPLC analysis of peptide **6a** performed on device **b** equipped with column **III** (gradient 10 to 80 % eluent B within 20 min).

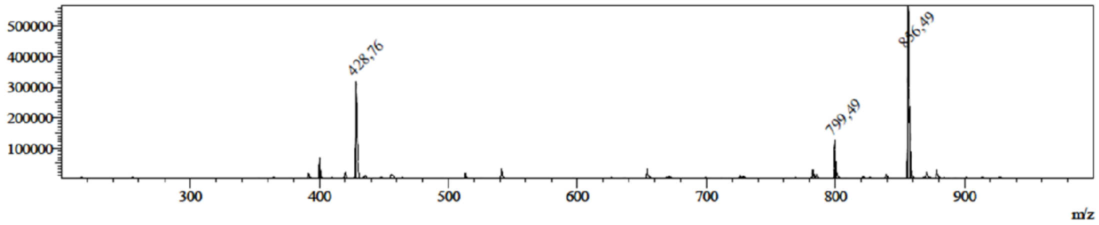

Figure S3: ESI-MS analysis of peptide **6a** according to 1.5.1. calc. mass: 855.43 g/mol; meas. m/z: 856.49 $[M+H]^+$, 428.76 $[M+2H]^{2+}$.

2.1.2 CH_3CO-GSGLLQG-NH_2 (6)

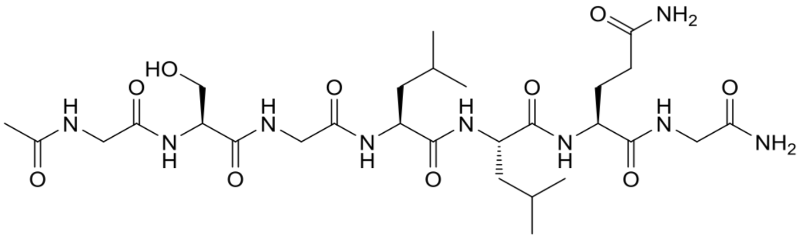

Figure S4: Structure of synthetic peptide **6**. Synthesis was performed as described in 1.3.1.

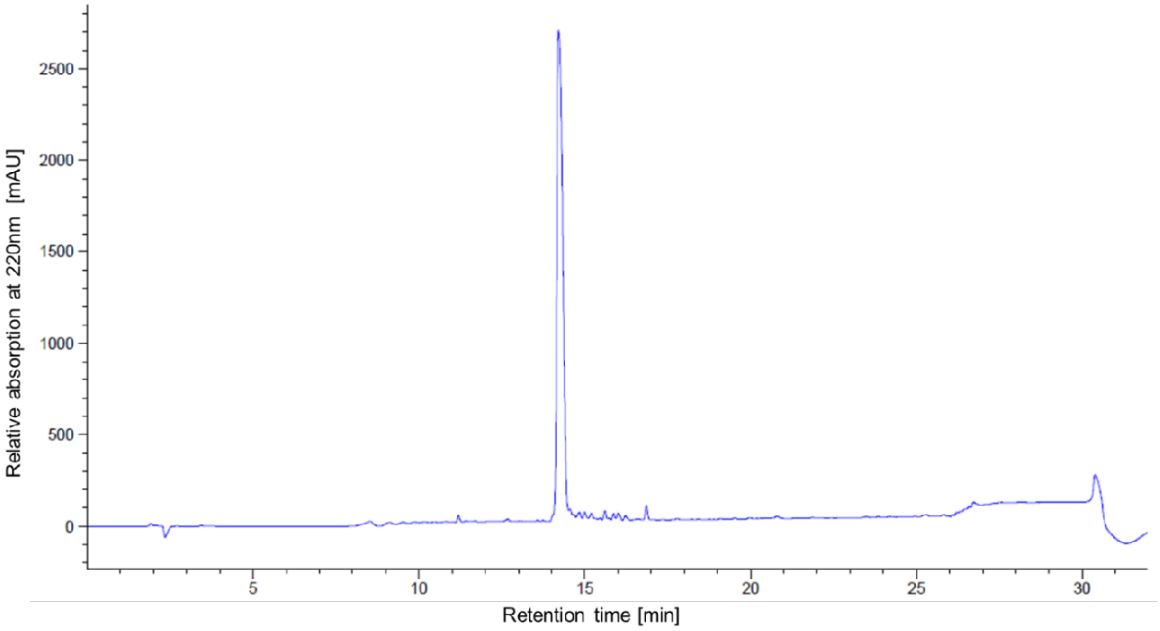

Figure S5: RP-HPLC analysis of peptide **6** performed on device **b** equipped with column **II** (gradient 10 to 80 % eluent B within 20 min).

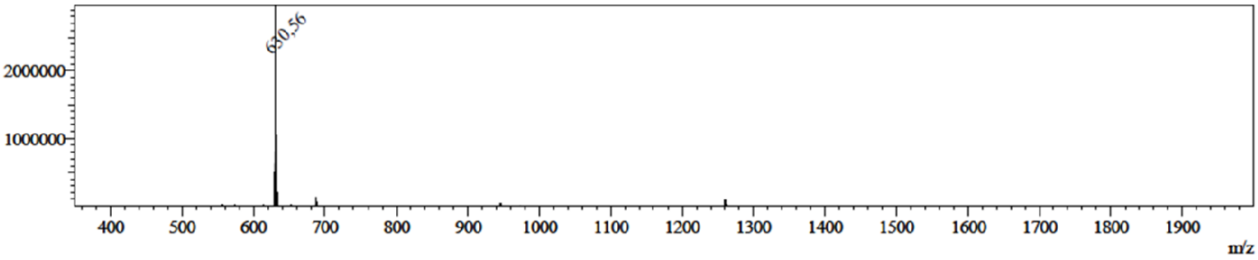

Figure S6: ESI-MS analysis of peptide **6** according to 1.5.1; calc. mass: 629.35 g/mol; meas. m/z: 630.56 $[M+H]^+$.

2.1.3 (5/6)-TAMRA-MRHKGS-*NH₂* (7)

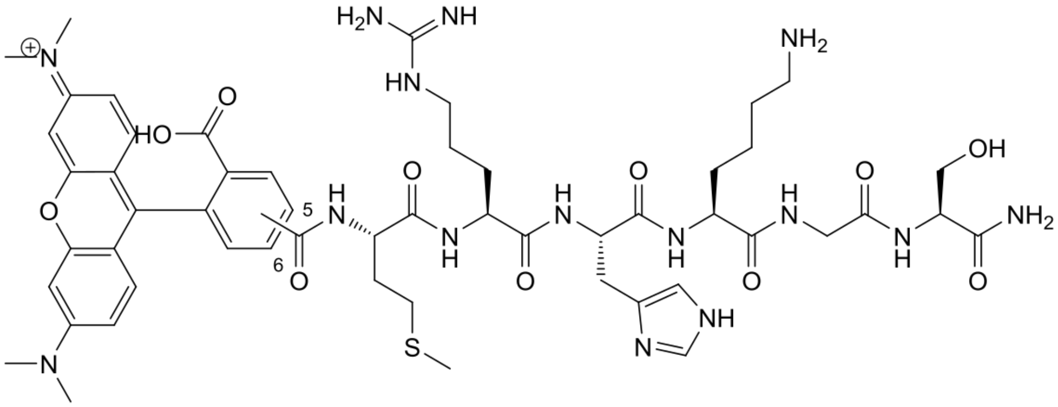

Figure S7: Structure of synthetic peptide **7**. Synthesis was performed as described in 1.3.1.

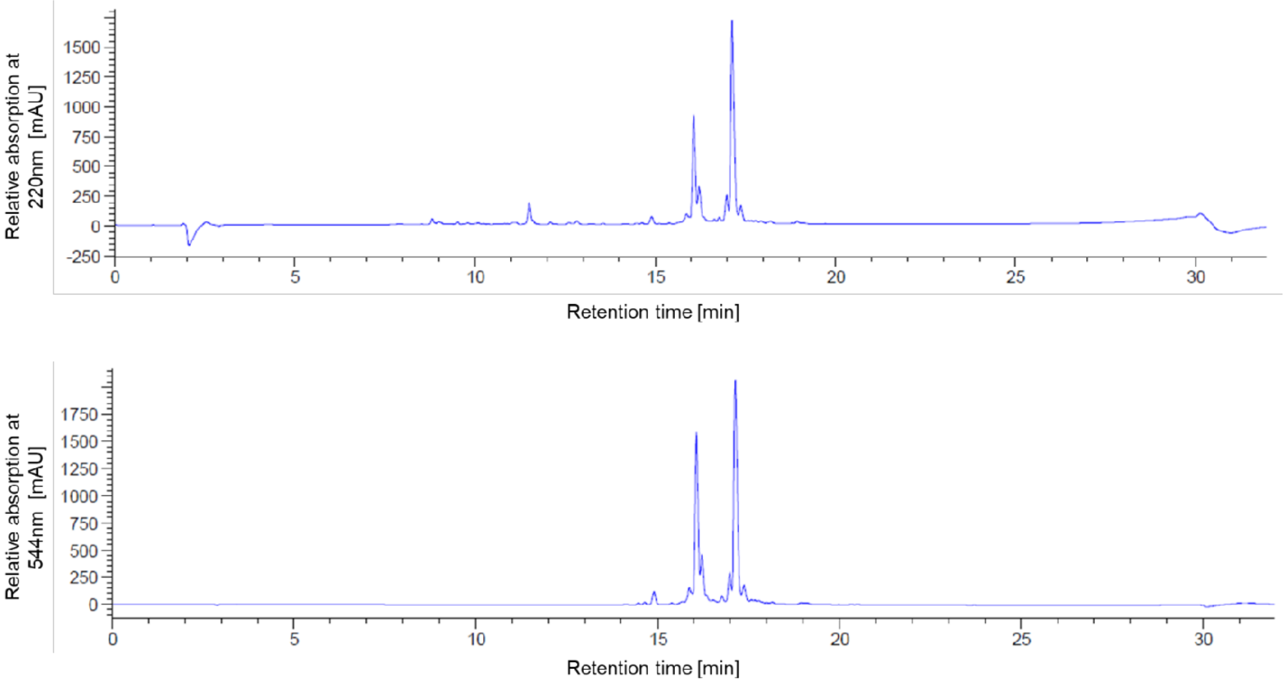

Figure S8: RP-HPLC analysis of peptide **7** performed on device **a** equipped with column **I** (gradient 10 to 80 % eluent B within 20 min).

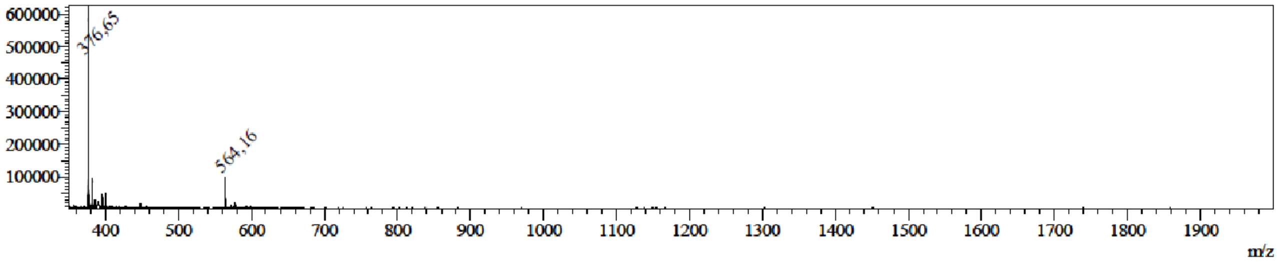

Figure S9: ESI-MS analysis of peptide **7** according to 1.5.1. calc. mass: 1126.53 g/mol; meas. m/z: 564.16 $[M+2H]^{2+}$, 376.65 $[M+3H]^{3+}$.

2.2 Proteolytic activation of pro-SFRAP-mTG (2pro)

75 µg of recombinant protein **2pro** were incubated with 6 µg of either bovine trypsin (top) or *Bacillus polymyxa* neutral protease, dispase (bottom) and incubated at 37 °C. Samples were taken after 0, 5, 10, 15, 30, 60, 90 and 120 min. The protease mediated conversion of inactive **2pro** into mature **2** was analyzed by 15 % SDS-PAGE.[7]

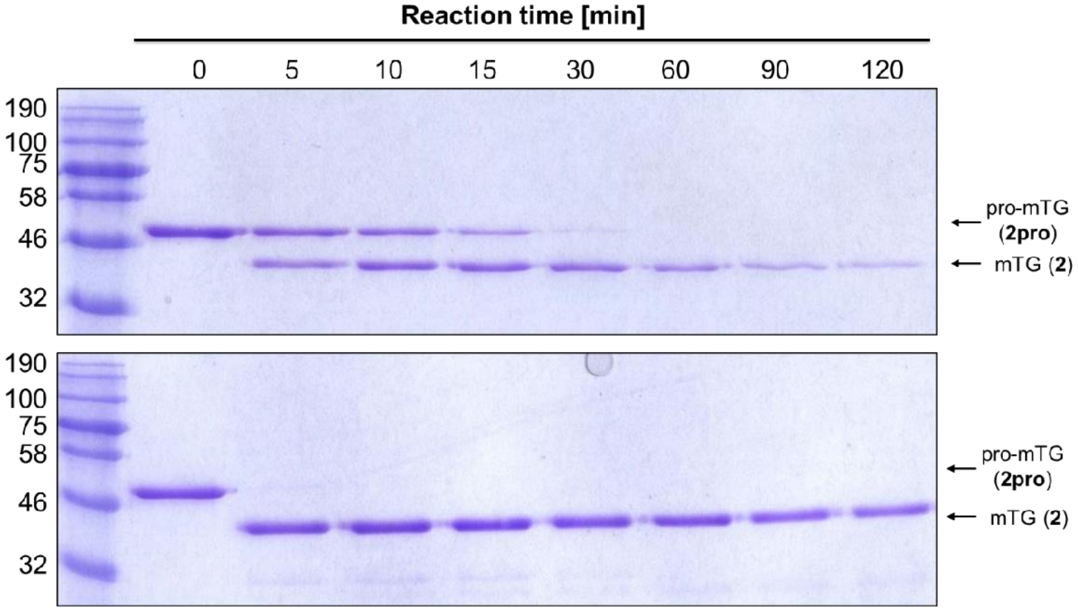
Reaction time [min]
0
5
10
15
30
60
90
120
190
100
75
58
46
32
pro-mTG (2pro)
mTG (2)
190
100
75
58
46
32
pro-mTG (2pro)
mTG (2)

Figure S10: Coomassie-stained 15% SDS-PAGE of trypsin (top) and dispase-mediated (bottom) procession of inactive pro-mTG (**2pro**)

2.3 ESI-MS analysis of 2pro and 2

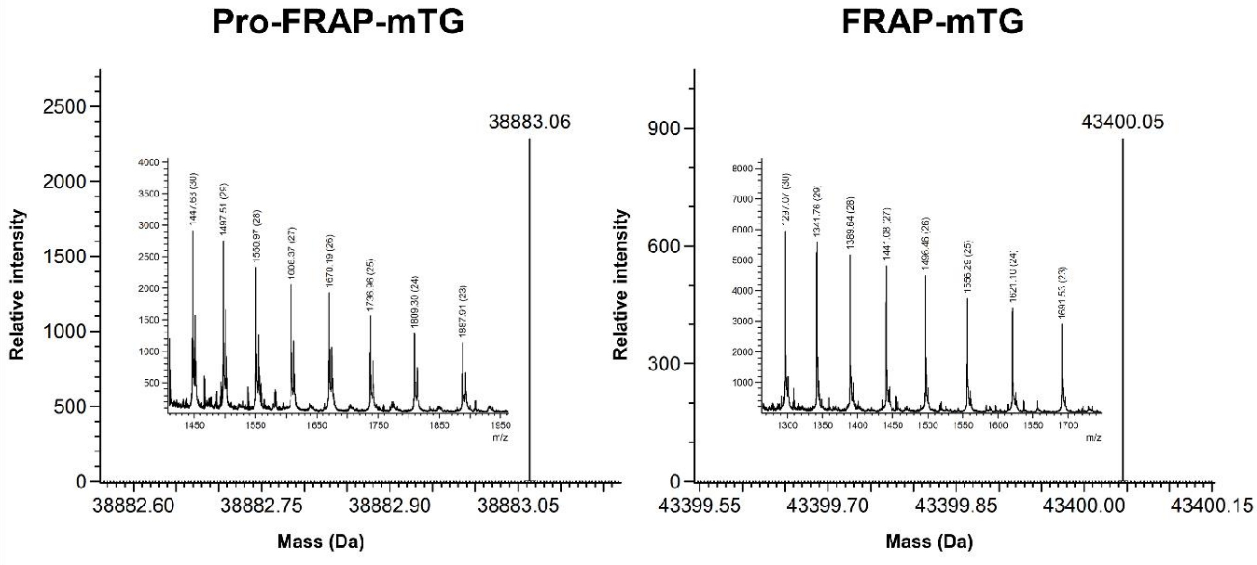

Figure S11: Recombinant proteins **2pro** and **2** were analysed by ESI-MS according to 1.5.2. Obtained raw m/z data were deconvoluted using mMass v5.5 to calculate protein masses.

Table S5: Calculated molecular weight of hypothetical FRAP-mTG constructs resulting from the treatment of pro-FRAP-mTG (**2pro**) with dispase in comparison to the measured one. Bold letters indicate the most likely product of protease cleavage.

Enyzme	Calculated mass [g/mol]	Difference between measured and calculated mass [g/mol]
Pro-FRAP-mTG-GWPHHHHHH	**43399.3**	**0.8**
FRAP-mTG-GWPHHHHHH	39156.83	-273.8
RAP-mTG-GWPHHHHHH	39009.65	-126.6
AP-mTG-GWPHHHHHH	38853.47	29.6
FRAP-mTG-GWPHHHHH	39019.69	-136.6
FRAP-mTG-GWPHHHH	**38882.55**	**0.5**
FRAP-mTG-GWP-HHH	38745.41	137.6
RAP-mTG-GWPHHHHH	38872.51	10.5
RAP-mTG-GWPHHHH	38735.37	147.7
AP-mTG-GWPHHHHH	38716.33	166.7

2.4 FACS Analysis

2.4.1 Surface display of mature mTG

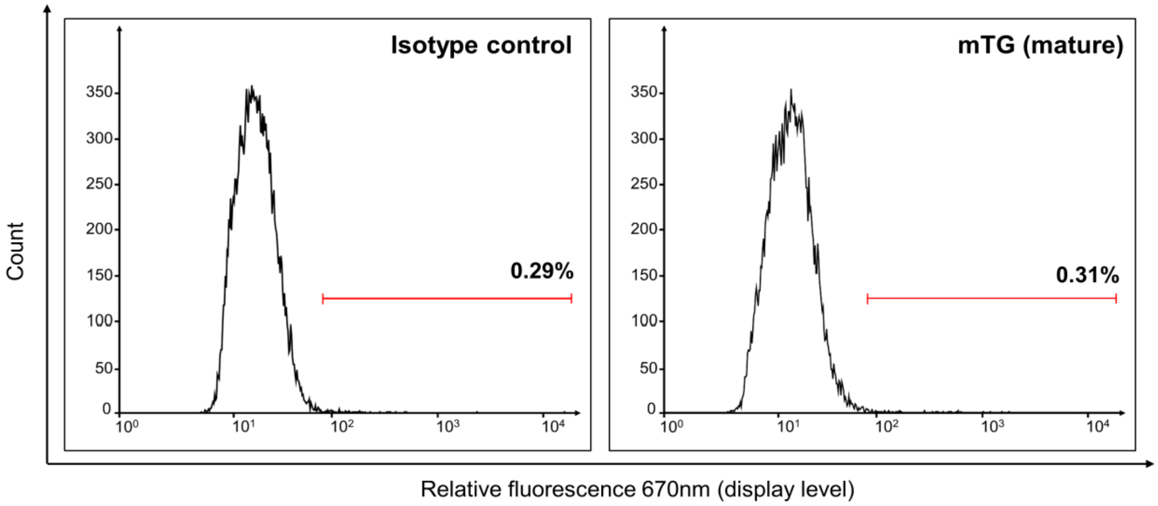

Figure S12: Histogram (640/670 [30]). Cells bearing a plasmid coding for mature mTG without its inhibitory propetide were cultivated and stained for surface presentation as described in 1.7. FACS analysis revealed no surface display of the enzyme most likely due to intracellular cytotoxicity or protein misfolding.

Surface display of 4pro and 5pro

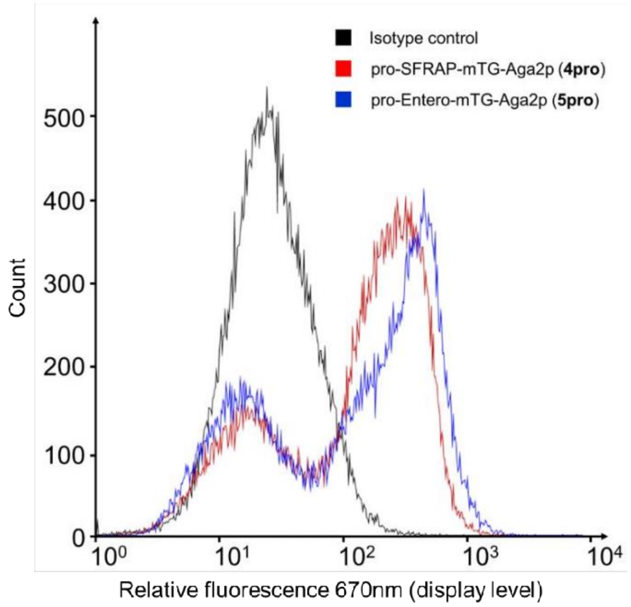

Figure S13: Histogram (640/670 [30]). Cells bearing plasmids coding for pro-mTG (**4pro**, **5pro**), containing different cleavage sites, were cultivated and stained for surface presentation as described in 1.7. FACS analysis showed that **4pro** and **5pro** were successfully displayed at the surface of yeast cells.

2.4.2 Library screening

Table S6: Overview of performed screening rounds

Screening round	Conditions	Total events	Sort count
R1 (Activity presort)	1µM **6a**, 30min	4.5×10^8	3.6×10^7
R2	100nM **6a**, 10min	1×10^8	5.1×10^6
R3	50 nm **6a**, 10min	4.7×10^7	5.5×10^5
R4	50 nm **6a**, 10min	1.2×10^7	6.1×10^5
R5	50 nm **6a**, 5min	1.3×10^7	6.4×10^5

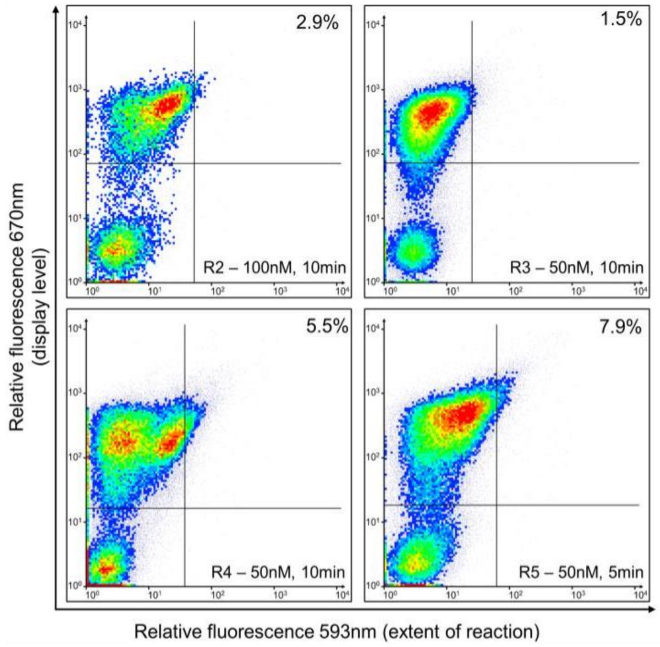

Figure S14: Density plot (640/670 [30] vs. 561/593 [40]). The randomized library, pre-sorted for enzymes exhibiting mTG activity, was screened via stepwise increasing selective pressure to enrich cells bearing mutant enzymes (see table S5).

2.4.3 Single clone analysis

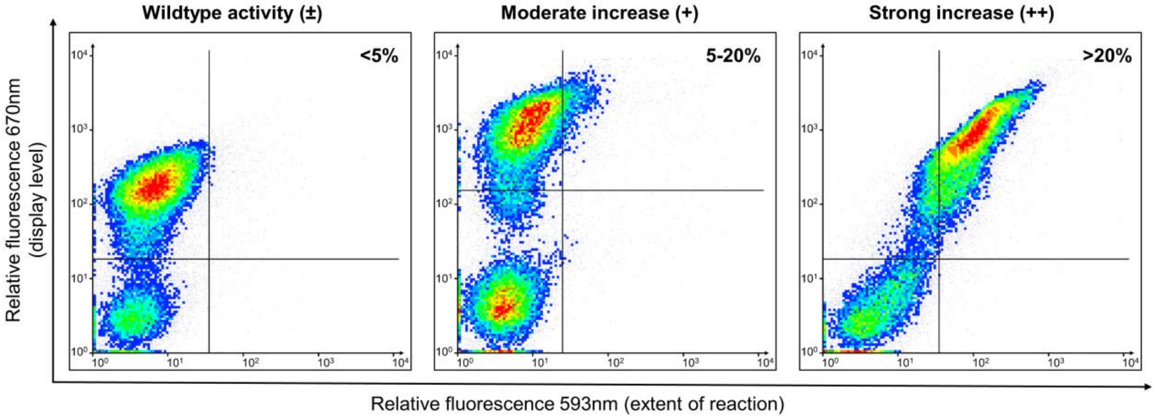

Figure S15: Density plot (640/670 [30] vs. 561/593 [40]). Individual clones were analyzed on the surface of yeast cells as described in 1.7. applying final condition of screening round 5. Cells were classified in comparison to wildtype displaying ones and cells with a moderately or strongly increased activity profile were chosen for further analysis.

2.5 Antibody purification

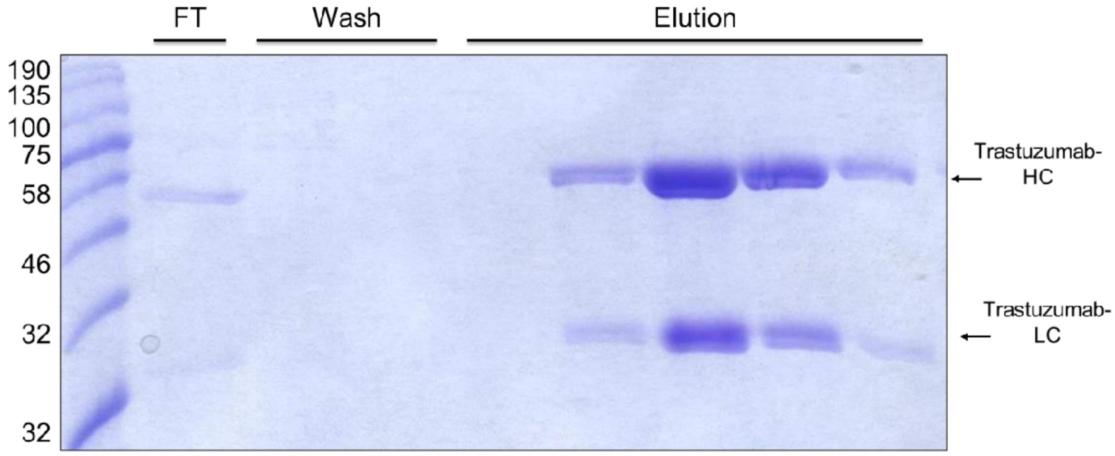

Figure S16: Coomassie stained 15 % SDS-PAGE gel analysis of purified trastuzumab-LLQG (**8**). Production was performed as described in 1.12. and **8** was purified from culture supernatant by standard protein-A affinity chromatography protocols. 60 mL cells yield 3.5 mg mAb.

2.6 Screening of model libraries

mTG-bearing cells were mixed with non-related cells in different ratios ranging from 1:10 to 1:1000 to verify that mTG^{+}-cells can be discriminated form mTG^{-} ones. After proteolytic activation (ESI 1.7.), protease-treated cells were incubated with 1 µM **6a** for 1 h at 30 °C. After one or two rounds of screening, cells were recultivated and analyzed for the presence of the mTG-coding gene by PCR using oligonucleotides **O1** and **O2**. The calculated enrichment factors are summarized in Table S8.

Table S7: Overview of performed model screen.

E-value	Sorting rounds	Enrichment factor
0.1	1	8.125
0.01	1	25
0.001	2	≥500

References

[1] M. Ota, A. Sawa, N. Nio, Y. Ariyoshi, *Biopolymers* **1999**, *50*, 193-200.
[2] H. Abe, M. Goto, N. Kamiya, *Chem. Eur. J.* **2011**, *17*, 14004-14008.
[3] C. L. Vogel, M. A. Cobleigh, D. Tripathy, J. C. Gutheil, L. N. Harris, L. Fehrenbacher, D. J. Slamon, M. Murphy, W. F. Novotny, M. Burchmore, *J. Clin. Oncol.* **2002**, *20*, 719-726.
[4] E. T. Boder, K. D. Wittrup, *Nat. Biotechnol.* **1997**, *15*, 553-557.
[5] L. Benatuil, J. M. Perez, J. Belk, C.-M. Hsieh, *Protein Eng. Des. Sel.* **2010**, gzq002.
[6] C. K. Marx, T. C. Hertel, M. Pietzsch, *Enzyme Microb. Technol.* **2006**, *40*, 1543-1550.
[7] R. Pasternack, S. Dorsch, J. T. Otterbach, I. R. Robenek, S. Wolf, H. L. Fuchsbauer, *Eur. J. Biochem.* **1998**, *257*, 570-576.
[8] S. K. Oteng-Pabi, J. W. Keillor, *Anal. Biochem.* **2013**, *441*, 169-173.
[9] U. K. Laemmli, *Nature* **1970**, *227*, 680-685.

7.3. Tailoring Activity and Selectivity of Microbial Transglutaminase

Title:

Tailoring Activity and Selectivity of Microbial Transglutaminase

Authors:

Lukas Deweid, Olga Avrutina and Harald Kolmar

Bibliographic data:

Methods in Molecular Biology

Volume 2012, Issue Enzyme-Mediated Ligation Methods, Pages 151-169

Article first published online: 4th Jun 2019

DOI: https://doi.org/10.1007/978-1-4939-9546-2_9

Publisher Name: Humana, New York, NY

Online ISBN: 978-1-4939-9546-2

Copyright: Springer Science+Business Media, LLC, part of Springer Nature 2019. Reproduced with permission.

Contributions by Lukas Deweid:

- Developed all described methods and protocols
- Preparation of the manuscript and all included graphical material
- Revised the manuscript

Chapter 9

Tailoring Activity and Selectivity of Microbial Transglutaminase

Lukas Deweid, Olga Avrutina, and Harald Kolmar

Abstract

Microbial transglutaminase (mTG), a protein-glutamine γ-glutamyltransferase from *Streptomyces mobaraensis*, is an enzyme capable of forming isopeptide bonds between the nearly inert (from the chemical point of view) γ-carboxamides present in the side chain of glutamine residues and primary amines. Its high substrate tolerance, compared to other bond-forming enzymes, makes it a versatile tool for numerous applications including food manufacturing, material science, and biotechnology. Although an mTG-mediated bioconjugation is a well-established technique, some major drawbacks of this approach need to be bypassed, with the poor substrate specificity being among the most essential ones. Especially biopharmaceutical methodologies require high subsite specificity of the utilized biocatalyst, which is often not warranted by mTG. Therefore, access to tailor-made transglutaminases is strongly desired. Herein, we describe a protocol for the generation of mTG libraries based on yeast surface display, which allow for the isolation of mutants with altered properties. Moreover, methods for cloning of respective expression vectors, recombinant expression, and in vitro procession are provided.

Key words Microbial transglutaminase, Bioconjugation, Protein engineering, Directed evolution, Fluorescence-activated cell sorting

1 Introduction

Transglutaminases are a family of enzymes that catalyze the acyl-transfer reaction of proteinaceous glutamine side chains (acyl-donor) and ε-amino groups of lysine (acyl-acceptor) under ammonia release (Fig. 1) [1]. In nature, this intermolecular or intramolecular transamidation improves stability of proteins, such as resistance against proteolytic degradation, thus participating in various cellular processes [2]. While transglutaminases from eukaryotic origin are often multidomain complexes that suffer from low intrinsic stability and cofactor dependency, their prokaryotic counterparts provide high stability and do not require any cofactors [3]. As a consequence, within the last two decades microbial transglutaminases emerged as valuable tools for molecular

Timo Nuijens and Marcel Schmidt (eds.), Enzyme-Mediated Ligation Methods, Methods in Molecular Biology, vol. 2012,
https://doi.org/10.1007/978-1-4939-9546-2_9, © Springer Science+Business Media, LLC, part of Springer Nature 2019

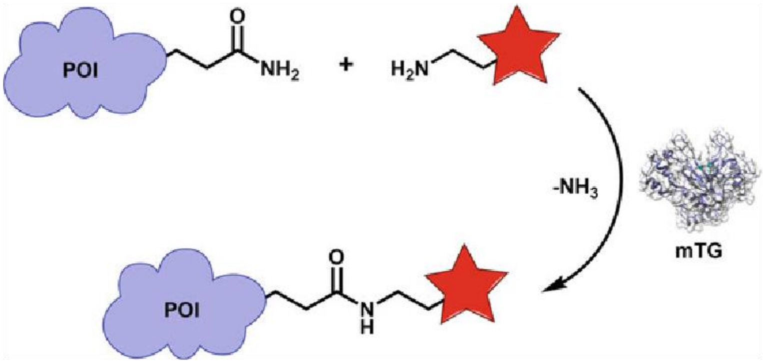

Fig. 1 Schematic illustration of the reaction catalyzed by mTG. Isopeptide bonds are formed between proteinaceous glutamine residues and primary amines under ammonia release resulting in the fluorescent labeling of the target protein. POI protein of interest

bioconjugation [4]. The most prominent enzyme from *Streptomyces mobaraensis* was recently used for the immobilization of proteins on solid support [5], construction of multifunctional protein–protein [6] or protein–nucleic acid complexes [7] and the PEGylation of small-sized proteinaceous pharmacophores to elevate their half-life in vivo [8]. Moreover, novel strategies for the mTG-mediated manufacturing of antibody–drug conjugates (ADCs), a novel class of drugs that comprises the target specificity of monoclonal antibodies and potency of small organic toxins, have been recently developed [9]. Besides its massive application in diverse biotechnological fields, discussion about the physiological role and substrate specificity of mTG are still ongoing [10]. It is believed that recognition of the acyl-donor depends on the charge and polarity of the neighboring amino acids as well as structural features of the utilized target [11]. However, predicting potential modification sites is challenging, and careful case-to-case evaluation is strongly required. The presence of various addressable sites within the same protein results in the formation of a heterogeneous mixture consisting of mono- and multi-conjugated targets [12].

To overcome these limitations, high-throughput engineering toward mutants with altered properties is of great interest [13]. To that end, a novel screening strategy for mTG, based on yeast surface display, was established. Microbial transglutaminase was anchored to the surface of yeast cells as an inactive zymogen (Pro-mTG) by genetic fusion to the aga2p-mating factor. Subsequent treatment of Pro-mTG-displaying cells with human enterokinase ensured efficient removal of the N-terminal inhibitory prosequence. When protease-treated cells were supplied with an acyl-donor substrate, surface-bound mTG catalyzed the covalent crosslinking at available lysine residues. Following immunofluorescent staining, cells bearing a mutant mTG that is capable of utilizing the supplied

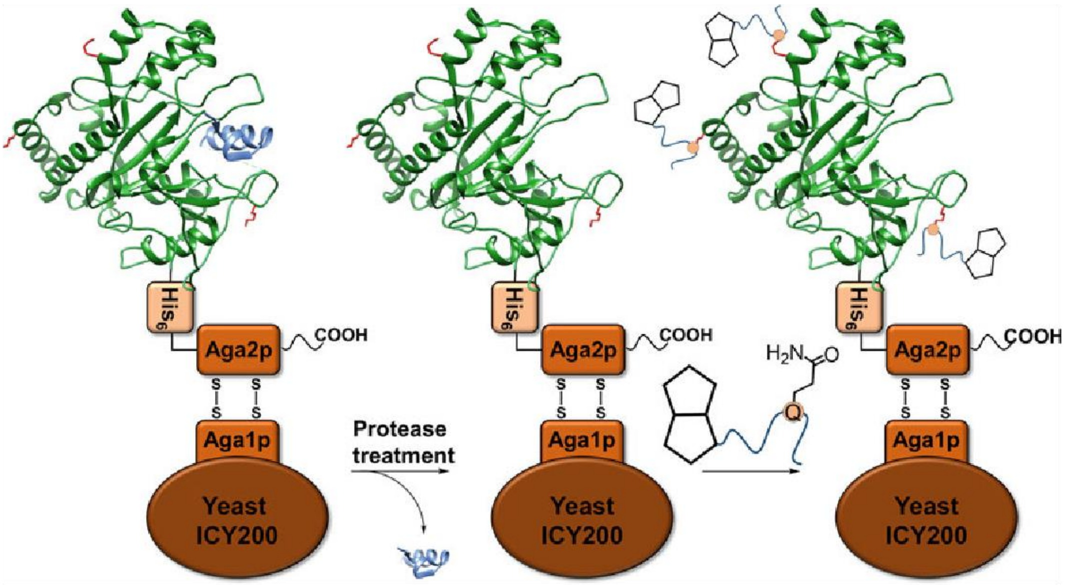

Fig. 2 Schematic illustration of the on-support transamidation. Inactive Pro-mTG is anchored on the surface of yeast cells by genetic fusion to the N-terminus of Aga2p. Subsequent protease treatment removes the inhibitory propeptide and converts the inactive zymogene into the mature enzyme. When a biotinylated acyl-donor substrate is added, mTG catalyzes the corresponding isopeptide bond formation at available lysine residues and therefore enables discrimination of active variants by FACS

substrate, were isolated by fluorescence-activated cell sorting (FACS) (Fig. 2) [14].

In this chapter, we provide a protocol for the generation and screening of mTG-libraries by yeast surface display for mutants with improved catalytic activity toward the mTG standard recognition sequence LLQG [15]. Furthermore, detailed methodologies for the cloning of corresponding *E. coli* expression vectors and recombinant expression are provided. The method is exemplified for *S. mobaraensis* transglutaminase but should be applicable to the evolutionary optimization of any other sequence-related microbial transglutaminase from different hosts.

2 Materials

2.1 Randomization of the mTG Gene by Error-Prone PCR

1. GeneMorph II Random Mutagenesis Kit (Agilent Genomics).
2. 10 μM oligonucleotides 1, 2, 3, and 4 (Table 1).
3. Plasmid pET22b(+) Pro-Entero-mTG-His_6 WT (Fig. 3).
4. Thermocycler.
5. DpnI restriction enzyme (New England Biolabs).
6. Devices and reagents for agarose gel electrophoresis.

Table 1
Oligonucleotides used for the randomization of microbial transglutaminase and subsequent library construction

Number	Oligonucleotide	Sequence (5′-3′)	Incorporated restriction site
1	mTG Library Up	GTCCGGATGATGACGACAAA	
2	mTG Library Lo	GTGGTGGTGGTGGTGGTGAGGCCAACCCTGTTTAACTTTATC	
3	mTG Library Overlap Up	GCACTGAATGAAAGCGCACCGGCAGCAAGCAGCGCAGGTCCGGATGATGACGACAAAG	
4	mTG Library Overlap Lo	AGAACCACCACCACCAGAACCACCACCACCCCATGGGTGGTGGTGGTGGTGGTGAGGCCAACCCTGTTTAACTTTATC	
5	mTG XbaI Up	GCGCGCTCTAGAAATAATTTTGTTTAACTTTAAGAAGGAGATATACCATGGACAATGGTGCCGG	XbaI
6	mTG EcoRI His_6 Lo	GCGCGCGAATTCTCAGTGGTGGTGGTGGTGGTGAGGCCAACCCTGTTTAACTTTATC	EcoRI
7	mTG FRAP BamHI Lo	GCGCGCGGATCCGGCATACGATCCAGCGGTTCTGCCGGAGGGGTAACACGATCATCACTATCCGGTGCACGAAAGCTCGGACCTGCGCTGCTTGCTGCCGGTG	BamHI
8	T7-Terminator Lo	CTGCTAACAAAGCCCGAAAG	
9	T7-Promotor Up	TAATACGACTCACTATAGG	

7. Wizard® SV Gel and PCR Clean-up System (Promega).
8. UV-Vis spectrophotometer BioSpec Nano (Shimadzu) or equivalent instrumentation.
9. Taq DNA Polymerase (New England Biolabs).
10. 10× Standard Taq Buffer (New England Biolabs).
11. Deoxynucleotide (dNTP) solution mix (New England Biolabs).

2.2 Library Construction Using Homologous Recombination in Yeast

1. Yeast strain: ICY200 [16].
2. YPD medium: 20 g/L D(+)-glucose, 20 g/L tryptone, 10 g/L yeast extract.
3. Electroporation buffer: 1 M sorbitol, 1 mM $CaCl_2$.
4. Lithium acetate buffer: 0.1 M CH_3CO_2Li, 10 mM DTT.

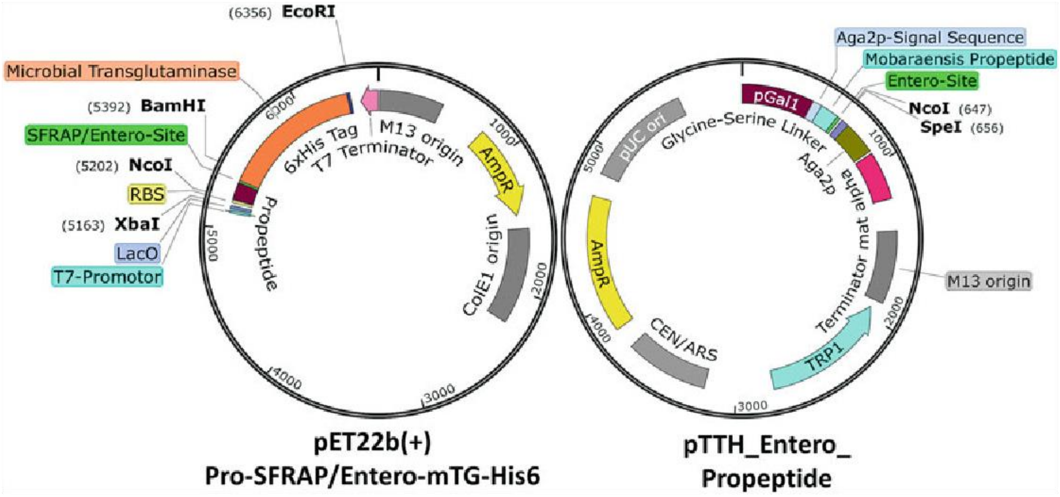
(6356) EcoRI
Microbial Transglutaminase
(5392) BamHI
SFRAP/Entero-Site
(5202) NcoI
RBS
(5163) XbaI
LacO
T7-Promotor
6xHis Tag
T7 Terminator
M13 origin
AmpR
ColE1 origin
Propeptide
1000
2000
3000
4000
5000
6000
pET22b(+)
Pro-SFRAP/Entero-mTG-His6
Aga2p-Signal Sequence
Mobaraensis Propeptide
Entero-Site
NcoI (647)
SpeI (656)
pGal1
Glycine-Serine Linker
Aga2p
alpha mat Terminator
M13 origin
TRP1
CEN/ARS
AmpR
pUC ori
1000
2000
3000
4000
5000
pTTH_Entero_
Propeptide

Fig. 3 Left: pET22b(+) Pro-SFRAP/Entero-mTG-His$_6$ for the cytoplasmic expression of microbial transglutaminase in E. coli cells. Right: E. coli/S. cerevisiae shuttle vector pTTH_Entero_Propeptide for the display of Pro-Entero-mTG on the surface of ICY200 cells derived from commonly used plasmid pCT [17]. The vector provides the transglutaminase propeptide fused to the N-terminus of Aga2p. In between, unique NcoI/SpeI endonuclease restrictions sites can be addressed to introduce artificial double-strand breaks for homologous recombination in yeast. Vector graphics were prepared using SnapGene Viewer 4.2.4

5. Sorbitol solution: 1 M sorbitol in ddH$_2$O.
6. SpeI-HF restriction enzyme (New England Biolabs).
7. NcoI-HF restriction enzyme (New England Biolabs).
8. 10 CutSmart buffer for restriction endonuclease digestion (New England Biolabs).
9. Plasmid pTTH_Entero_Propeptide derived from commercially available pCT [17] (see Fig. 3).
10. Electroporator GenePulser Xcell™ (Bio-Rad).
11. Electroporation cuvettes, 0.2 cm (Bio-Rad).
12. SD-CAA medium: 8.6 g/L NaH$_2$PO$_4$ · H$_2$O, 5.4 g/L Na$_2$HPO$_4$, 20 g/L D(+)-glucose, 6.7 g/L Yeast nitrogen base without amino acids, 5 g/L Bacto™ casamino acids.
13. SD-CAA agar plates: 8.6 g/L NaH$_2$PO$_4$ · H$_2$O, 5.4 g/L Na$_2$HPO$_4$, 20 g/L D(+)-glucose, 6.7 g/L yeast nitrogen base without amino acids, 5 g/L Bacto™ casamino acids, 10 g/L Agar-Agar Kobe 1.
14. Library storage buffer: 5%(v/v) glycerol, 0.67%(w/v) yeast nitrogen base in sterile ddH$_2$O.
15. Petri dishes, 9 cm diameter.

2.3 Library Screening

1. SG-CAA medium: 8.6 g/L $NaH_2PO_4 \cdot H_2O$, 5.4 g/L Na_2HPO_4, 20 g/L D(þ)-galactose, 6.7 g/L Yeast nitrogen base without amino acids, 5 g/L Bacto™ Casamino Acids.
2. PBS, pH 7.4: 140 mM NaCl, 10 mM KCl, 6.4 mM Na_2PO_4 and 2 mM KH_2PO_4.
3. 0.25 mg/mL Human Enterokinase (PeproTech) in phosphate-buffered saline.
4. N-terminally biotinylated substrate peptide Biotin-GSGLLQG-NH_2 (Sigma-Aldrich).
5. Mouse, monoclonal anti-His_6 IgG1 (Qiagen).
6. Rat, monoclonal anti-mouse IgG1, APC-conjugated (ThermoFisher Scientific).
7. Streptavidin, R-Phycoerythrin Conjugate (SAPE) (ThermoFisher Scientific).
8. Flow cytometer BD Influx™ (FACS) equipped with lasers Sapphire (Coherent), 56CLC100 (CVI Melles Griot), and Cobolt Jive™ (Cobolt AB) or equivalent device.

2.4 Reformatting of Selected mTG Variants

1. Zymoprep™ Yeast Plasmid Miniprep II kit (Zymo Research).
2. 10 μM oligonucleotides 5, 6, and 7 (Table 1).
3. Q5® High-Fidelity DNA polymerase (New England Biolabs).
4. 5 Q5® reaction buffer (New England Biolabs).
5. Deoxynucleotide (dNTP) solution mix (New England Biolabs).
6. Thermocycler.
7. Devices and reagents for agarose gel electrophoresis.
8. XbaI restriction enzyme (New England Biolabs).
9. DpnI restriction enzyme (New England Biolabs).
10. NcoI-HF restriction enzyme (New England Biolabs).
11. EcoRI-HF restriction enzyme (New England Biolabs).
12. BamHI-HF restriction enzyme (New England Biolabs).
13. 10 CutSmart buffer for restriction endonuclease digestion (New England Biolabs).
14. Wizard® SV Gel and PCR Clean-up System (Promega).
15. UV-Vis spectrophotometer BioSpec Nano (Shimadzu).
16. Commercially available *E. coli* expression vector pET22b(þ).
17. T4 DNA Ligase (New England Biolabs).
18. 10 T4 DNA Ligase buffer (New England Biolabs).
19. 7 M ammonium acetate solution.
20. Ethanol, pure.

21. 70% ethanol solution in ddH_2O.
22. Electrocompetent *E. coli* DH5α cells (Thermo Fisher Scientific).
23. Electroporator GenePulser Xcell™ (Bio-Rad).
24. Electroporation cuvettes, 0.2 cm (Bio-Rad).
25. DYT medium: 16 g/L tryptone, 10 g/L yeast extract, 5 g/L NaCl.
26. DYT + Amp agar plates: 16 g/L tryptone, 10 g/L yeast extract, 5 g/L NaCl, and 10 g/L Agar-Agar Kobe 1 supplemented with 100 μg/mL ampicillin.
27. Wizard® Plus SV Minipreps DNA Purification System (Promega).

2.5 Recombinant Expression and IMAC Purification of Selected mTG Variant

1. Electrocompetent *E. coli* BL21 (DE3) cells (Sigma-Aldrich).
2. DYT medium: 16 g/L tryptone, 10 g/L yeast extract, 5 g/L NaCl.
3. DYT + Amp medium: 16 g/L tryptone, 10 g/L yeast extract, 5 g/L NaCl, 10 g/L Agar-Agar Kobe 1 supplemented with 100 μg/mL ampicillin.
4. 500 mM isopropyl β-D-1-thiogalactopyranoside (IPTG) solution in ddH_2O.
5. Cell disruptor (Constant Systems Limited) or equivalent instrumentation.
6. 0.2 μm sterile filter.
7. IMAC (immobilized metal affinity chromatography)-A buffer: 600 mM NaCl, 50 mM Tris–HCl pH 8, 20 mM Imidazole, 20 mM $(NH_4)_2SO_4$, 1 mM $CaCl_2$.
8. IMAC-B buffer: 600 mM NaCl, 50 mM Tris–HCl pH 8, 500 mM Imidazole, 20 mM $(NH_4)_2SO_4$, 1 mM $CaCl_2$.
9. HisTrap HP IMAC column, 1 mL (GE Healthcare).
10. ÄKTApurifier UPC 100 (GE Healthcare) or equivalent instrumentation.
11. Dialysis membrane ZelluTrans T1, molecular weight cutoff (MWCO) 3500 Da (Carl Roth).
12. Devices and reagents for sodium dodecyl sulfate–polyacrylamide gel electrophoresis (SDS-PAGE).
13. Dispase, neutral protease (Worthington Biochemical Corporation).
14. mTG storage buffer: 300 mM NaCl, 50 mM Tris–HCl pH 8, 1 mM $CaCl_2$, 10 mM glutathione, reduced.
15. Glycerol.

3 Methods

The following protocol describes the construction of an mTG library for yeast surface display by error-prone PCR. More focused randomization procedures like gene-shuffling sexual-PCR or site saturation mutagenesis can be easily adapted [18].

The proregion of the zymogen mediates proper folding of the enzyme and suppresses intracellular activity [19]. As a consequence, randomization of microbial transglutaminase was limited to the sequence coding for the mature enzyme.

Subsequent protease treatment of the zymogen allows for the display of active mTG on the surface of yeast cells. To that end, human enterokinase was chosen to ensure highly specific cleavage of the proregion and avoid potentially toxic off-target activity.

3.1 Randomization of mTG Gene by Error-Prone PCR

Error-prone PCR relies on the biased incorporation of nucleotides into replicates of parental DNA [20]. These randomly driven exchanges will be statistically distributed over the amplified gene and the desired mutation rate can be adjusted by the utilized amount of template DNA (see Note 1). Keep in mind that the mutation frequency of the applied methodology strongly influences your results: A high mutation rate often causes intrinsic instability that drastically reduces enzymatic activity while low mutation rates barely benefit catalytic performance. Therefore, a moderate mutation rate of approximately 4–5 nucleotide exchanges per gene is recommended.

Initially, the gene coding for mature enzyme is randomized by error-prone PCR. Afterward, the reaction mixture is supplemented with DpnI aimed at digesting template DNA, followed by gel extraction of the corresponding PCR-product. These steps are crucial to obtain adequate mutation frequency of the resulting library since remaining vector from the mutagenic PCR preferentially serves as a template in following rounds of PCR amplification. In a second PCR, the purified DNA is $3'$- and $5'$-terminally extended by ~40 bp long sequences that enable gap repair cloning via homologous recombination in yeast cells [21].

1. Prepare a 50 μL error-prone reaction consisting of 41 μL ddH$_2$O, 5 μL 10× Mutazyme II reaction buffer, 1 μL 40 mM dNTP mix, 0.5 μL oligonucleotide 1, 0.5 μL oligonucleotide 2, 1 μL Mutazyme II, and 1 μL of 500 ng/μL Pro-Entero-mTG-His$_6$ WT (Fig. 3) (see Note 1).
2. Perform PCR with 2 min preincubation at 95 °C and 30 cycles with 30 s at 95 °C, 30 s at 55 °C, and 70 s at 72 °C.
3. Perform 1% (w/v) agarose gel electrophoresis to verify the presence of an amplified 1031 bp product.

4. Add 2 U DpnI per 50 μL PCR mixture and incubate for at least 1 h at 37 °C (see Note 2).
5. Perform gel extraction of the amplified and DpnI-digested PCR product from a 1% (w/v) agarose gel according to the manufacturer's instructions (Wizard® SV Gel and PCR Clean-up System) and determine the DNA concentration by UV-Vis spectroscopy.
6. The purified product serves as a template for a second PCR and is amplified to provide a suitable amount of DNA for library construction. Oligonucleotides 3 and 4 are utilized to attach homologous overlaps for gap repair cloning in yeast cells. Prepare PCR mix consisting of 407.5 μL ddH_2O, 10 μL oligonucleotide 3, 10 μL oligonucleotide 4, 10 μL dNTPs, 50 μL 10× *Taq* standard buffer, 2.5 μL *Taq* DNA Polymerase (12.5 U), and 10 μL 10 ng/μL randomized PCR product (see Note 3).
7. Conduct PCR with 5 min preincubation at 95 °C and 30 cycles with 30 s at 95 °C, 30 s at 62 °C, and 60 s at 72 °C.
8. Purify the amplified DNA according to the manufacturer's instructions (Wizard® SV Gel and PCR Clean-up System) and determine the corresponding DNA concentration on a BioSpec Nano.

3.2 Library Construction Using Homologous Recombination in Yeast

Typical libraries for yeast surface display are generated by gap repair in *Saccharomyces cerevisiae* cells. The respective mechanism relies on the precise repair of DNA double-strand breaks by homologous recombination (HR) [21]. To harness the efficiency of HR for library construction, artificial double-strand breaks need to be introduced into the target vector by restriction endonucleases. Furthermore, homologous sequences mimicking the linearized plasmid DNA have to be attached to the introduced target DNA by PCR. Upon transformation of electrocompetent *S. cerevisiae* cells, homologous DNA fragments are assembled in vivo to form a circular plasmid. Functional pTTH plasmids mediate cell growth in tryptophan-depleted medium by providing a tryptophan synthase. As a consequence, yeast cells bearing a successfully reassembled plasmid can be selected on SD-CAA agar plates. The provided methodology for the construction of randomized libraries in *Saccharomyces cerevisiae* cells is adapted from the improved yeast transformation protocol by Benatuil et al. and describes the preparation of two electroporation reactions that can be easily upscaled (see Note 4) [22].

3.2.1 Digestion of Plasmid pTTH_Entero_Propeptide

To ensure surface display of microbial transglutaminase, its inhibitory propeptide needs to be fused to the N-terminus of the mature enzyme. Following subsequent protease treatment of the surface-bound zymogen, enzymatic activity is regained. To that end, plasmid pTTH_Entero_Propeptide (Fig. 3), derived from commercially available vector pCT provides the inhibitory propeptide and a cleavage site for human enterokinase fused to the aga2p surface anchor (*see* Note 5) [17].

1. Digest 50 μg of purified pTTH_Entero_Propeptide (Fig. 3) with 60 U of SpeI-HF and NcoI-HF in CutSmart for at least 1 h at 37 °C.
2. Analyze the restriction on a 1% (w/v) agarose gel for the presence of a 5979 bp product to ensure linearization of the plasmid.
3. Purify the linearized vector using Wizard® SV Gel and PCR Clean-up System according to the manufacturer's instructions and determine the corresponding DNA concentration.

3.2.2 Library Construction

1. Incubate *Saccharomyces cerevisiae* ICY200 overnight to stationary phase in sterile YPD medium at 180 rpm and 30 °C.
2. Inoculate 100 mL of fresh YPD medium with the overnight culture to an OD_{600} of about 0.3 (*see* Note 6).
3. Incubate the cells at 30 °C and 180 rpm on a platform shaker until the OD_{600} reaches a value of about 1.4–1.6.
4. Centrifuge the cells at 4000 × g for 3 min at 4 °C and discard the resulting supernatant.
5. Wash the cells twice in 50 mL of ice-cold ddH_2O, followed by a wash step using 50 mL ice-cold electroporation buffer.
6. Resuspend the cells in 20 mL lithium acetate buffer and incubate for 30 min at 30 °C and 180 rpm.
7. Pelletize cells and wash the pellet once with 50 mL ice-cold electroporation buffer.
8. Discard the supernatant and resuspend the cells in a final volume of 1 mL electroporation buffer. This volume is sufficient for two electroporation reactions.
9. Combine 1–2 μg linearized vector with 3–6 μg randomized PCR product and add the mixture to 400 μL of electrocompetent cells.
10. Transfer the cell-DNA mixture to prechilled electroporation cuvettes (0.2 cm). Electroporate the cells at 2500 V. Transfer cells from the cuvette to 8 mL of a 1:1 (v/v) mixture of YPD and 1 M sorbitol. Incubate the cells for 1 h at 30 °C and 180 rpm.
11. Centrifuge the cells, resuspend the corresponding pellet in 10 mL SD-CAA medium, and incubate for at least 2 days at 30 °C and 180 rpm. Calculate the library diversity by dilution plating (SD-CAA plates, estimate number of colonies after 72 h).

12. For long-term storage, centrifuge the library, resuspend the cells in library storage buffer, and store them at −80 °C.
13. Determine the mutation frequency by sequencing of at least ten individual transformants.

3.3 Library Screening

To enrich yeast cells that bear mutant enzymes with altered properties, fluorescence activated cell sorting (FACS) is performed. The obtained library is incubated in SG-CAA medium to trigger expression of the Pro-mTG-Aga2p fusion protein and surface display of the inactive zymogen is verified by immunofluorescent staining. Afterward, library cells are incubated in the presence of human enterokinase to remove the inhibitory propeptide. Protease-treated cells are supplemented with a biotinylated acyl-donor target (Biotin-GSGLLQG-NH_2) that serves as a substrate for mTG. Active enzymes displayed on the surface of yeast cells label their corresponding host at available lysine residues, thus enabling separation by FACS (Fig. 2). Stepwise increase of selective pressure in following screening rounds results in the enrichment of improved variants from a mutant library [14]. Herein, we describe the screening of mTG libraries for mutants with enhanced catalytic turnover of peptide biotin-GSGLLQG-NH_2 derived from conventional transglutaminase recognition sequence LLQG [15]. However, longer peptidic sequences or proteinaceous targets can serve as acyl donors for the on-support transamidation as well.

1. Incubate library cells in SD-CAA medium at 30 °C and 180 rpm overnight to stationary phase.
2. Transfer the corresponding volume of cells to inoculate SG-CAA medium at an OD_{600} of 1 and incubate at 30 °C and 180 rpm overnight.
3. Pelletize 2×10^7 cells at 17,500 × g and wash twice with 1 mL PBS (see Note 7).
4. Resuspend cells in 1 mL PBS, add 5 μL human enterokinase (1.25 μg) and incubate the mixture on a shaker at 23 °C and 700 rpm for at least 1 h.
5. Spin down at 17,500 × g for 1 min and wash cells with 1 mL PBS.
6. Spin down at 17,500 × g for 1 min and resuspend cells in 1 mL PBS, add Biotin-GSGLLQG-NH_2 (dissolved in PBS) and incubate for a defined time at 30 °C and 700 rpm (see Note 8).
7. Spin down the cells at 17,500 × g for 1 min and wash twice with 1 mL PBS.
8. Resuspend the cells in a 1:50 (v/v) dilution of mouse, monoclonal anti-His_6 IgG1 and 1:100 dilution of SAPE in 100 μL PBS and incubate for 10 min on ice.

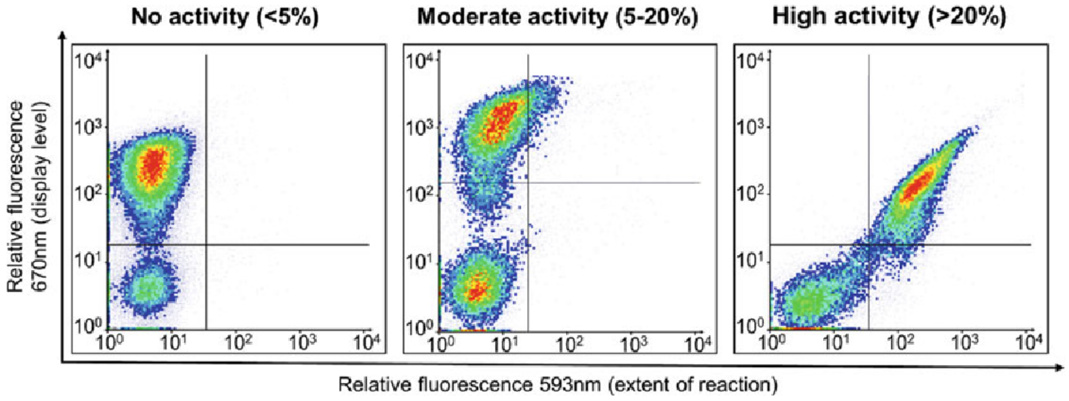

Fig. 4 Classification of on-surface activity of different individual mTG clones. If >20% cells exhibit both, surface display and transglutaminase activity (upper right panel), mutants should be chosen for in vitro characterization

9. Wash cells by centrifugation (17,500 g for 1 min) and resuspend with 1 mL PBS.
10. After centrifugation (17,500 g for 1 min) and resuspend the cells in a 1:50 dilution of rat, monoclonal anti-mouse IgG1, APC-conjugated in 100 μL PBS and incubate for 10 min on ice.
11. Wash twice by centrifugation (17,500 g, 1 min) and resuspend in 1 mL PBS.
12. Analyze cells by flow cytometry using a BD Influx™ (FACS) flow cytometer equipped with lasers Sapphire, 56CLC100, and Cobolt Jive™ and separate cells possessing desired properties (Fig. 4) (see Note 9).
13. Plate 1:10,000 of isolated cells on an SD-CAA agar plate and incubation for 48 h at 30 C.
14. Regrow isolated cells in SD-CAA medium for 48 h at 30 C and 180 rpm.
15. Calculate the respective survival rate by comparing the number of isolated cells (provided by your FACS device) to the number of colonies grown on the SD-CAA agar plate (see Note 10).

After the final round of screening has been performed, enriched clones should be analyzed on a single-clone level. Therefore, individual colonies, grown for 2 days at 30 C on SD-CAA agar plates are picked and incubated as described in Subheading 3.3. Cells are treated applying conditions of the last selection round and compared to wild type-displaying cells. Figure 4 provides an appropriate assessment about different activity levels of individual clones. Mutants with an improved on-surface activity profile are further analyzed by sequencing of the corresponding plasmid and chosen for recombinant expression in E. coli cells.

3.4 Reformatting of Selected mTG Variants

For the recombinant expression of mutant enzymes that revealed enhanced activity on the surface of yeast cells, gene transfer to an *E. coli* expression vector is required (Fig. 3). Therefore, pTTH surface-display plasmids are isolated and used as a template for an error-free PCR amplification. The utilized oligonucleotides 5 and 6 provide restriction sites for cloning of a pET22b(þ) expression vector by conventional T4-DNA ligase-mediated ligation. Afterward, the authors recommend a second cloning step in order to replace the engineered enterokinase site for SFRAP, which is the native cleavage site that is present in the wild-type enzyme. It allows for highly efficient and cost-effective in vitro procession of the inactive zymogene by *Bacillus polymyxa* dispase.

3.4.1 Cloning of pET22b(þ) Pro-Entero-mTG-His$_6$ Mut

1. Isolate pTTH plasmids of selected variant using Zymoprep™ Yeast Plasmid Miniprep II kit.
2. Prepare a 50 μL PCR reaction consisting of 35.5 μL ddH$_2$O, 10 μL 5 Q5® reaction buffer, 1 μL dNTP mix, 1 μL oligonucleotides 5, 1 μL oligonucleotide 6, 0.5 μL Q5® polymerase (1 U) and 1 μL of 10 ng/μL isolated pTTH vector (see Note 11).
3. Conduct PCR with 2 min preincubation at 95 C and 30 cycles with 30 s at 95 C, 30 s at 62 C, and 45 s at 72 C.
4. Perform 1% (w/v) agarose gel electrophoresis and verify the presence of a 1211 bp product.
5. Purify the amplified DNA using Wizard® SV Gel and PCR Clean-up System.
6. Digest the purified PCR product with 10 U of *Xba*I-HF, *Eco*RI-HF, and *Dpn*I in CutSmart for at least 1 h at 37 C.
7. Heat-inactivate restriction endonucleases for 20 min at 80 C.
8. Digest 1 μg of pET22b(þ) with 10 U of *Xba*I-HF, *Nco*I-HF, and *Eco*RI-HF in CutSmart for at least 1 h at 37 C.
9. Heat-inactivate restriction endonucleases for 20 min at 80 C.
10. Mix 320 ng digested vector and 410 ng PCR product in T4-DNA ligase buffer. Add 400 U of T4-DNA ligase and incubate for 1 h at 37 C (see Note 12).
11. Add 1/10 reaction mixture volumes of 7 M ammonium acetate and 3 volumes of 99.8% ethanol, followed by incubation at 20 C for at least 1 h.
12. Centrifuge for 30 min at 17,500 g and 4 C and discard the resulting supernatant.
13. Wash in 300 μL ice-cold 70% ethanol and centrifuge for 30 min at 17,500 g and 4 C.
14. Discard the resulting supernatant and resuspend the DNA pellet in 20 μL ddH$_2$O.

15. Add 5 μL of DNA to 50 μL of electrocompetent E. coli DH5α and transfer the resulting mixture to a prechilled electroporation cuvette (0.2 cm).
16. Electroporate the cells at 2500 V and regenerate them in 1 mL DYT at 37 C for 1 h.
17. Centrifuge for 3 min at 4000 g and discard the resulting supernatant. Resuspend the cells in approximately 50 μL PBS, spread on DYT þ Amp agar plates and incubate for 16 h at 37 C.

This highly efficient ligation strategy yields numerous colonies after 16 h of incubation. To facilitate further colony PCR screening, 1:10 or 1:100 (v/v) dilutions of cells in PBS can be plated. Afterward, colony PCR using oligonucleotides 8 and 9 to identify colonies with the correct plasmid size is performed. When the desired sequence was successfully ligated into pET22b(þ), a 1327 bp product is visible upon 1% (w/v) agarose gel electrophoresis. Otherwise, a smaller fragment of 324 bp appears. Successful cloning is confirmed by sequencing.

3.4.2 Cloning of pET22b(þ) Pro-SFRAP-mTG-His$_6$ Mut

In order to replace the engineered enterokinase cleavage site by native SFRAP, a second cloning step is performed (Fig. 3) (see Note 13).

1. Prepare a 50 μL PCR reaction consisting of 35.5 μL ddH$_2$O, 10 μL 5 Q5® reaction buffer, 1 μL dNTP mix, 1 μL oligonucleotides 5, 1 μL oligonucleotide 7, 0.5 μL Q5® polymerase (1 U), and 1 μL of 10 ng/μL pET22b(þ) Pro-Entero-mTG-His$_6$ Mut.
2. Conduct PCR with 2 min preincubation at 95 C and 30 cycles with 30 s at 95 C, 30 s at 62 C, and 15 s at 72 C.
3. Perform 2% (w/v) agarose gel electrophoresis and verify the presence of a 247 bp product.
4. Purify the amplified DNA using Wizard® SV Gel and PCR Clean-up System.
5. Digest the purified PCR product with 10 U of XbaI-HF, BamHI-HF, and DpnI per microgram DNA in CutSmart for at least 1 h at 37 C.
6. Heat-inactivate restriction endonucleases for 20 min at 80 C.
7. Digest 1 μg of pET22b(þ) Pro-Entero-mTG-His$_6$ Mut with 10 U of XbaI-HF, NcoI-HF, and BamHI in CutSmart for at least 1 h at 37 C.
8. Proceed as described in Subheading 3.4.1 [9–17].

3.5 Recombinant Expression and IMAC Purification of Selected mTG Variants

As a consequence of its high crosslinking promiscuity, mature microbial transglutaminase is toxic to its host cells, leading to insufficient yields upon recombinant expression [23]. This limitation can be bypassed applying a two-step purification protocol that relies on the expression of inactive Pro-mTG followed by proteolytic in vitro procession. To that end, multiple proteases were investigated [24]. In this protocol, dispase, an enzyme from *Bacillus polymyxa* that nonselectively hydrolyzes leucine or phenylalanine-containing peptide bonds, was chosen. We describe the recombinant expression of Pro-SFRAP-mTG in *E. coli* BL21 (DE3) cells and its purification by immobilized-metal affinity chromatography (IMAC) modified from Marx et al. [23, 25]. The purified zymogen is converted into the active enzyme by dispase treatment followed by a second IMAC purification step.

3.5.1 Recombinant Expression and Purification of Pro-mTG Mutants

1. Mix 100 ng of pET22b(+) Pro-SFRAP-mT-His$_6$ Mut and 50 µL of electrocompetent *E. coli* BL21(DE3). Transfer the mixture to a prechilled, 0.2 mm electroporation cuvette and electroporate the cells at 2500 V.
2. Add 1 mL sterile DYT-medium and incubate the cells for 1 h at 37 °C.
3. Transfer cells to a DYT + Amp agar plate, spread out and incubate for 16 h at 37 °C.
4. Use the grown colonies to inoculate 50 mL of sterile DYT + Amp medium and incubate for 16 h at 37 °C and 180 rpm.
5. Transfer overnight grown cells to inoculate 1 L of sterile DYT + Amp medium to an OD$_{600}$ of 0.3 and incubate at 37 °C and 180 rpm until an OD$_{600}$ of 0.7–1 is reached (see Note 14).
6. Add 1 mL of IPTG solution (500 µM final concentration) and incubate for 3 h and 180 rpm at 24 °C.
7. Pelletize cells for 20 min at 4000 × g and 4 °C.
8. Discard supernatant and resuspend cells in a maximum volume of 50 mL IMAC-A buffer.
9. Lyse cells on a cells disrupter or by sonication according to the manufacturer's instructions.
10. Pelletize cell debris for 30 min at 17,500 × g at 4 °C and filtrate the resulting supernatant (0.2 µm filter).
11. Equip ÄKTApurifier UPC 100 (GE Healthcare) with an 1 mL HisTrap HP column and calibrate with 5 column volume (CV) of IMAC-A buffer (recommended flow rate: 1 mL/min).
12. Apply the filtered supernatant to the column (recommended flow rate: 1 mL/min).

13. Wash out nonspecifically binding protein by 10 CV of 10% IMAC-B.
14. Elute target protein applying a linear gradient of 10–100% IMAC-B over 30 CV.
15. Confirm the presence of a 43 kDa protein by SDS-PAGE.
16. Pool protein-containing fractions and dialyze for 16 h in 4 L mTG storage buffer at 4 °C using ZelluTrans T1, MWCO 3500 Da.
17. Determine protein concentration using an extinction coefficient of 74,830 M^{-1} cm^{-1} on a BioSpec Nano and calculate the corresponding yield (see Note 15).
18. For long time storage add 10% glycerol and store at −80 °C.

3.5.2 Dispase-Mediated In Vitro Procession of Purified Pro-mTG

1. Add 75 μg of dispase per milligram Pro-mTG to the purified zymogene and incubate at 37 °C for 30 min (see Note 16).
2. Perform a second IMAC purification step according to Subheading 3.5.1 to remove the propeptide and the utilized protease (see Note 17).
3. Confirm the presence of a 38 kDa protein by SDS-PAGE (see Note 18).
4. Pool protein-containing fractions and dialyze for 2 h in 4 L mTG storage buffer at 4 °C using ZelluTrans T1 with a MWCO of 3500 Da (see Note 19).
5. Determine protein concentration using an extinction coefficient of 71,850 M^{-1} cm^{-1} on a BioSpec Nano and calculate the corresponding yield (see Note 20).
6. Add 10% glycerol and store at −80 °C.

4 Notes

1. The lower the initial DNA concentration, the higher the resulting mutation frequency. Consequently, mutations frequencies can be adjusted by utilizing different amounts of template DNA.
2. This step is crucial since incomplete digestion of the utilized template results in enrichment of the wild-type sequence in following rounds of PCR amplification. DpnI digestion can be performed overnight if necessary.
3. We recommend amplification by Taq-Polymerase since lack of proof-reading introduces further mutations. However, proof-reading polymerases like Q5® High-Fidelity DNA Polymerase (New England Biolabs) or Phusion® High-Fidelity DNA

Polymerase (New England Biolabs) are recommended for more focused randomization studies.

4. Keep in mind that the resulting library size strongly depends on the amount of conducted electroporation reactions. A larger library potentially bears variants that are more interesting. However, screening of a library with a diversity larger than 10^9 is time-consuming. As a consequence, a maximum of 20 electroporation reactions is recommended that results in the generation of approximately 10^8–10^9 variants.
5. Due to the cytotoxic character of mTG, intracellular inhibition followed by proteolytic activation of the surface-bound zymogen is necessary. To provide surface display of the mature enzyme upon protease treatment, mTG must be fused to the N-terminal site of the aga2p anchor instead of the C-terminal one, originally provided by the pCT vector. Otherwise, cleavage occurs at the aga2p-mTG junction, resulting in loss of surface presentation [14].
6. Avoid using antibiotics at this step since commonly used antibiotics decelerate growth of yeast cells.
7. Measure the optical density (OD_{600}) of overnight grown cells at 600 nm to calculate the respective cell count. An OD_{600} of 1 represents 10^7 yeast cells/mL.
8. Though temperature optimum for mTG is reported to be 50 °C, conditions of the surface-bound transamidation reaction should not exceed 30 °C to avoid temperature-induced killing of yeast cells [26].
9. We strongly recommend comparing the mutant library with the cells displaying the wild-type enzyme in order to discriminate improved variants from the wild-type phenotype.
10. Due to the harmful conditions applied during FACS, usually a portion of cells perishes. Calculating from a 1/10,000 dilution, at least 50%of cells should survive the process.
11. Usage of a proof-reading polymerase like Q5® High-Fidelity DNA Polymerase is recommended to avoid incorporation of undesired nucleotide exchanges.
12. The T4 ligase-mediated phosphodiester bond formation requires ATP, which is provided within the supplied buffer. Repeating freeze-thaw cycles impair ATP stability. Therefore, aliquoting the buffer after the initial usage is recommended.
13. Please note that oligonucleotide 7, which is used to substitute protease cleavage sites on a genetic level, also codes for the N-terminal region of the enzyme (Asp1-Asp18). In case sequencing revealed amino acid exchanges in said area, oligonucleotide 7 has to be adapted to retain these mutations.

14. The usage of 3 L Erlenmeyer baffled flasks is strongly recommended to facilitate proper cell growth and improve expression yields.
15. Depending on the intrinsic stability of the respective mutant, yields of 10–20 mg purified zymogen are expected. However, much lower yields of ~1 mg were observed in certain cases.
16. A small amount of Pro-mTG should be taken apart before the addition of dispase to confirm the cleavage reaction by SDS-PAGE afterward.
17. Besides the addressed propeptide–mTG junction, dispase is known to truncate the hexahistidine motif at the C-terminus of the enzyme [27]. Though the modified His-tag mediates proper IMAC purification, binding to the column material is slightly impaired. Consequently, washing with 10%IMAC-B must be avoided.
18. After two consecutive purification steps, purities of 95% should be achieved. Comparison to the untreated proenzyme is recommended to visualize the conducted cleavage reaction.
19. The authors recommend avoiding dialysis overnight since precipitation due to autocross-linking of the active enzyme that drastically diminishes yields might occur.
20. Typical yields of 5–15 mg mature enzyme are expected after two steps of purification. However, much lower yields of ~1 mg were observed in certain cases.

Acknowledgments

This work was supported by the NANOKAT II grant from the BMBF (Bundesministerium für Bildung und Forschung) and by DFG priority program 1623.

References

1. Greenberg CS, Birckbichler PJ, Rice RH (1991) Transglutaminases: multifunctional cross-linking enzymes that stabilize tissues. FASEB J 5(15):3071–3077
2. Griffin M, Casadio R, Bergamini CM (2002) Transglutaminases: nature's biological glues. Biochem J 368(Pt 2):377–396
3. Strop P (2014) Versatility of microbial transglutaminase. Bioconjug Chem 25(5):855–862
4. Yokoyama K, Nio N, Kikuchi Y (2004) Properties and applications of microbial transglutaminase. Appl Microbiol Biotechnol 64 (4):447–454
5. Li T, Li C, Quan DN, Bentley WE, Wang LX (2018) Site-specific immobilization of endoglycosidases for streamlined chemoenzymatic glycan remodeling of antibodies. Carbohydr Res 458-459:77–84
6. Bhokisham N, Pakhchanian H, Quan D, Tschirhart T, Tsao CY, Payne GF, Bentley WE (2016) Modular construction of multisubunit protein complexes using engineered tags and microbial transglutaminase. Metab Eng 38:1–9
7. Takahara M, Wakabayashi R, Minamihata K, Goto M, Kamiya N (2017) Primary amine-Clustered DNA aptamer for DNA-protein

conjugation catalyzed by microbial transglutaminase. Bioconjug Chem 28(12):2954–2961

8. Spolaore B, Forzato G, Fontana A (2018) Site-specific derivatization of human interferon beta-1a at lysine residues using microbial transglutaminase. Amino Acids 50(7):923–932
9. Siegmund V, Schmelz S, Dickgiesser S, Beck J, Ebenig A, Fittler H, Frauendorf H, Piater B, Betz UA, Avrutina O, Scrima A, Fuchsbauer HL, Kolmar H (2015) Locked by design: a conformationally constrained transglutaminase tag enables efficient site-specific conjugation. Angew Chem Int Ed Engl 54 (45):13420–13424
10. Fiebig D, Schmelz S, Zindel S, Ehret V, Beck J, Ebenig A, Ehret M, Frols S, Pfeifer F, Kolmar H, Fuchsbauer HL, Scrima A (2016) Structure of the dispase autolysis-inducing protein from streptomyces mobaraensis and glutamine cross-linking sites for transglutaminase. J Biol Chem 291(39):20417–20426
11. Juettner NE, Schmelz S, Bogen JP, Happel D, Fessner WD, Pfeifer F, Fuchsbauer HL, Scrima A (2018) Illuminating structure and acyl donor sites of a physiological transglutaminase substrate from Streptomyces mobaraensis. Protein Sci 27(5):910–922
12. Mero A, Spolaore B, Veronese FM, Fontana A (2009) Transglutaminase-mediated PEGylation of proteins: direct identification of the sites of protein modification by mass spectrometry using a novel monodisperse PEG. Bioconjug Chem 20(2):384–389
13. Zhao X, Shaw AC, Wang J, Chang CC, Deng J, Su J (2010) A novel high-throughput screening method for microbial transglutaminases with high specificity toward Gln141 of human growth hormone. J Biomol Screen 15 (2):206–212
14. Deweid L, Neureiter L, Englert S, Schneider H, Deweid J, Yanakieva D, Sturm J, Bitsch S, Christmann A, Avrutina O, Fuchsbauer HL, Kolmar H (2018) Directed evolution of a bond-forming enzyme: ultrahigh-throughput screening of microbial transglutaminase using yeast surface display. Chem A Eur J 24:15195
15. Tanaka Y, Tsuruda Y, Nishi M, Kamiya N, Goto M (2007) Exploring enzymatic catalysis at a solid surface: a case study with transglutaminase-mediated protein immobilization. Org Biomol Chem 5(11):1764–1770
16. Chen I, Dorr BM, Liu DR (2011) A general strategy for the evolution of bond-forming enzymes using yeast display. Proc Natl Acad Sci U S A 108(28):11399–11404
17. Boder ET, Wittrup KD (1997) Yeast surface display for screening combinatorial polypeptide libraries. Nat Biotechnol 15(6):553–557
18. Neylon C (2004) Chemical and biochemical strategies for the randomization of protein encoding DNA sequences: library construction methods for directed evolution. Nucleic Acids Res 32(4):1448–1459
19. Rachel NM, Pelletier JN (2013) Biotechnological applications of transglutaminases. Biomolecules 3(4):870–888
20. McCullum EO, Williams BA, Zhang J, Chaput JC (2010) Random mutagenesis by error-prone PCR. Methods Mol Biol 634:103–109
21. Swers JS, Kellogg BA, Wittrup KD (2004) Shuffled antibody libraries created by in vivo homologous recombination and yeast surface display. Nucleic Acids Res 32(3):e36
22. Benatuil L, Perez JM, Belk J, Hsieh CM (2010) An improved yeast transformation method for the generation of very large human antibody libraries. Protein Eng Des Sel 23(4):155–159
23. Marx CK, Hertel TC, Pietzsch M (2006) Soluble expression of a pro-transglutaminase from Streptomyces mobaraensis in Escherichia coli. Enzyme Microb Technol 40(6):1543–1550
24. Pasternack R, Dorsch S, Otterbach JT, Robenek IR, Wolf S, Fuchsbauer HL (1998) Bacterial pro-transglutaminase from Streptoverticillium mobaraense--purification, characterisation and sequence of the zymogen. Eur J Biochem 257(3):570–576
25. Marx CK, Hertel TC, Pietzsch M (2008) Purification and activation of a recombinant histidine-tagged pro-transglutaminase after soluble expression in Escherichia coli and partial characterization of the active enzyme. Enzyme Microb Technol 42(7):568–575
26. Ando H, Adachi M, Umeda K, Matsuura A, Nonaka M, Uchio R, Tanaka H, Motoki M (1989) Purification and characteristics of a novel transglutaminase derived from microorganisms. Agric Biol Chem 53(10):2613–2617
27. Sommer C, Hertel TC, Schmelzer CE, Pietzsch M (2012) Investigations on the activation of recombinant microbial pro-transglutaminase: in contrast to proteinase K, dispase removes the histidine-tag. Amino Acids 42(2-3):997–1006

7.4. Recent Progress in Transglutaminase-Mediated Assembly of Antibody-Drug Conjugates

Title:

Recent Progress in Transglutaminase-Mediated Assembly of Antibody-Drug Conjugates

Authors:

Hendrik Schneider,* Lukas Deweid,* Olga Avrutina and Harald Kolmar

*These authors contributed equally to this work

Bibliographic data:

Analytical Biochemistry

Article first published online: 5th Feb 2020

DOI: https://doi.org/10.1016/j.ab.2020.113615

Copyright: 2020 Elsevier Inc. All rights reserved. Reproduced with permission.

Contributions by Lukas Deweid:

- Initial idea and literature research together with H. Schneider
- Preparation of the manuscript and included graphical material together with H. Schneider
- Revised the manuscript

Recent Progress in Transglutaminase-mediated Assembly of Antibody-Drug Conjugates

Hendrik Schneider[†], Lukas Deweid[†], Olga Avrutina and Harald Kolmar[*]

Institute for Organic Chemistry and Biochemistry, Technische Universität Darmstadt, Alarich-Weiss-Straße 4, D-64287 Darmstadt, Germany

[†]These authors contributed equally to this work

[*]To whom correspondence should be addressed:

Harald Kolmar: Institute for Organic Chemistry and Biochemistry, Technische Universität Darmstadt, Alarich-Weiss-Straße 4, D-64287 Darmstadt, Germany

Email: Kolmar@Biochemie-TUD.de

Abstract

Antibody-drug conjugates (ADCs) are hybrid molecules intended to overcome the drawbacks of conventional small molecule chemotherapy and therapeutic antibodies by merging beneficial characteristics of both molecule classes to develop more efficient and patient-friendly options for cancer treatment. During the last decades a versatile bioconjugation toolbox that comprises numerous chemical and enzymatic technologies was developed to covalently attach a cytotoxic cargo to a tumor-targeting antibody. Being one of the approaches, microbial transglutaminase (mTG) that catalyzes isopeptide bond formation between proteinaceous or peptidic glutamines and lysines, bears plenty favored properties that are beneficial for the manufacturing of these conjugates. However, to efficiently utilize the enzyme for the constructions of ADCs, different drawbacks had to be overcome that originate from the enzyme's insufficiently understood substrate specificity. Within this review, pioneering methodologies, recent achievements and remaining limitations of mTG-assisted assembly of ADCs will be highlighted.

Keywords: Transglutaminase; Bioconjugation; Protein labeling; Antibody-Drug Conjugates; Site-Specific Conjugation; Antibodies

1. Introduction

Despite obvious scientific and therapeutic progress, treatment of cancer is still a major challenge. Indeed, malignant tumors represent the second leading cause of death in the United States with over 1.7 million new cases and 600,000 cancer-related deaths predicted for 2019, which corresponds to nearly 1,700 deaths per day.[1] In the twentieth century, chemotherapy alone or in combination with radiotherapy was the predominant approach for tumor treatment.[2-4] For decades, every effort has been exerted by oncologists to develop chemotherapeutics with enhanced anticancer efficacy, which do not affect healthy tissues.[4, 5] The combination of different anticancer agents possessing diverse modes of action and toxicity profiles led to synergistic effects that positively influenced anti-tumor activity.[2, 5, 6] Thus, multidrug treatment became a standard therapy to fight most tumor types.[2, 4] Further, highly potent cytotoxins, e.g. tubulin inhibitors (dolastatin 10, dolastatin 15, maytansin, cryptophycins), DNA alkylators (pyrrolobenzodiazepine, CC-1065, adozelesin) were employed as chemotherapeutics.[2, 5] However, their clinical efficacy was rather limited due to the lack of a sufficient therapeutic window, conditioned by the inability to kill tumor cells without causing systemic toxicity to the healthy ones.[2, 5]

In addition to commonly known chemotherapeutic approaches, numerous therapeutic antibodies have been developed that act as tailor-made drugs to specifically address tumor-associated antigens. Upon intravenous administration, these engineered macromolecules accumulate at the tumor and activate the patient's immune defense to neutralize the degenerated cells.[7] The impressive number of FDA-approved therapeutic antibodies highlights the success of this class of drugs.[8] Though their potency has been demonstrated in hundreds of clinical trials, full cancer remission through antibody treatment is challenging as antibodies often possess limited anti-tumor activity.[2, 9] To address this issue, combination of the cytotoxic potency of small-molecule cytotoxins and the remarkable targeting properties of an antibody yielded a novel class of tumor therapeutics referred to as antibody-drug conjugates (ADCs). In these constructs, a monoclonal antibody is equipped with a potent antitumor toxin *via* a cleavable or non-cleavable covalent linker. After entering the tumor tissue from the vasculature, the antibody part of the ADC is capable to recognize and bind specifically to the target antigen overexpressed on the cell-surface. Following internalization through the endosome-lysosome pathway either the linker is cleaved and/or the antibody is degraded to release the payload, which then diffuses into the cytoplasm to interact with its target: e.g. tubulin, DNA (Figure 1).[5]

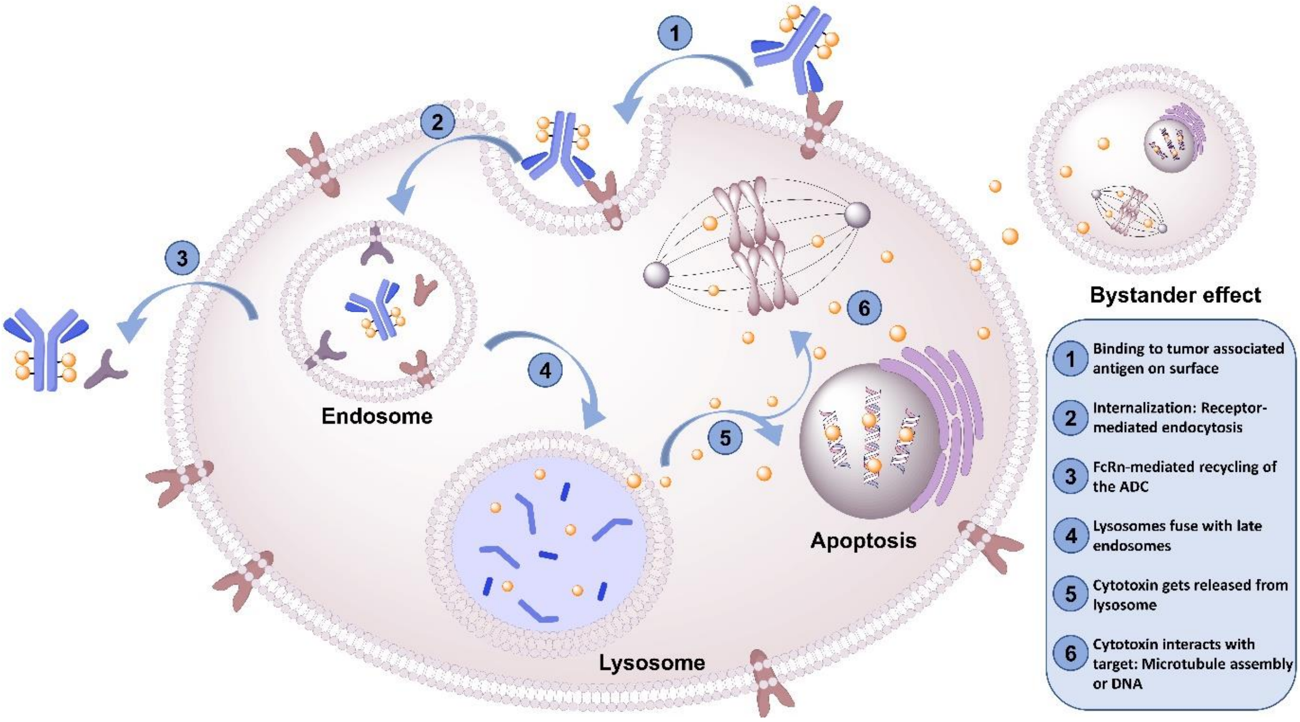
1
2
3
4
5
6
Endosome
Lysosome
Apoptosis
Bystander effect
1 Binding to tumor associated antigen on surface
2 Internalization: Receptor-mediated endocytosis
3 FcRn-mediated recycling of the ADC
4 Lysosomes fuse with late endosomes
5 Cytotoxin gets released from lysosome
6 Cytotoxin interacts with target: Microtubule assembly or DNA

Figure 1: Mechanism of action of antibody-drug conjugates: ADC are internalized through receptor-mediated endocytosis.

This strategy was envisioned to overcome the shortcomings of both conjugation partners, e.g. the small therapeutic window of the highly toxic payload and the rather low efficacy of solitaire antitumor antibodies, possibly gathering synergistic benefits.[9] Recently, different ADCs have reached the market, namely brentuximab vedotin (Adcetris®)[10, 11] from Seattle Genetics, gemtuzumab ozogamicin (Mylotarg®)[12, 13] and inotuzumab ozogamicin (Besponsa®)[14, 15] from Pfizer, as well as ado-trastuzumab emtansin (Kadcyla®)[16, 17] from Roche, all targeting hematologic malignancies or solid tumors.[5, 18] Furthermore, more than 60 ADCs are in clinical trials.[19] In most of them, the cytotoxic payload is either an antimitotic microtubule inhibitor (auristatin[20] or maytansin derivatives[21]) or a DNA-damaging agent (pyrrolobenzodiazepine dimers,[22] duocarmycin,[23] calichemicin,[24] indolino benzodiazepine dimers[25]), which alkylates, crosslinks, or breaks the DNA double strands.[5]

Most ADCs that are currently in clinical trials or are marketed rely on the stoichiometrically controlled chemical conjugation of the toxin moiety to endogenous thiols exposed by reduction of interchain disulfides, or to primary amines in lysine side chains.[4, 5] However, ADCs obtained by conventional conjugation yielded heterogenous mixtures of products, representing several species with different pharmacokinetics.[18] Therefore, a drug-to-antibody ratio (DAR) in the range of 3.5-4.0 was chosen for most ADCs, aimed at minimizing the fraction of non-conjugated antibodies and also avoiding species with high DAR.[5] However, FDA-approved ADC Kadcyla®, for example, is assembled from HER2 (human epidermal growth factor receptor 2)-targeting monoclonal antibody trastuzumab that contains

88 lysine residues, from which 70 were shown to be accessible to conjugation with tubulin inhibitor DM1.[26] As a consequence, despite maintaining the DAR at a relatively low value, a vast spectrum of variants is generated due to random conjugation to different attachment sites that results in an increased heterogeneity, which is disadvantageous in terms of the pharmacokinetic profile of the drug.[27] To overcome these deficiencies, numerous site-specific conjugation methods have been introduced, and different studies demonstrated improved therapeutic indices (TI) of the resulting constructs compared to their statistically conjugated counterparts.[28] Addressable moieties for site-specific conjugation have been introduced upon glycoengineering,[29-34] incorporation of additional cysteines (Thiomab®),[35-38] selenocysteines,[39] and non-natural amino acids.[40-42] In addition, re-bridging of natural thiols,[43, 44] metallopeptide-based catalysis,[45] redox-based methionine bioconjugation[46] as well as auto-catalytic attachment of the toxin to a reactive antibody lysine were applied.[47] In addition, various enzyme-mediated approaches, among them tubulin tyrosine ligase (TTL),[27, 48] formylglycine-generating enzyme (FGE),[49-51] SpyLigase,[52] phosphopantetheinyl transferase,[53] sortase A,[54-56] and mushroom tyrosinase[57] as well as microbial transglutaminase[58] were successfully utilized for the generation of site-specific ADCs.

Transglutaminases belong to a class of protein γ-glutamyltransferases found in microorganisms, plants, invertebrates, amphibians, fishes, and birds.[59] These bond-forming enzymes catalyze the attachment of primary amines to γ-carboxamides via release of ammonia, whereof both counterparts could be located in either a protein or a peptide.[59] In nature, transamidation occurs between the glutamine side chain as acyl donor and the ε-amino group of lysine as acyl acceptor, generating either intramolecularly cross-linked proteins or intermolecular isopeptide linkages (Figure 2).[59, 60] While transglutaminases possess certain specificity towards glutamine residues, their promiscuity in view of amine-containing acyl-donors opens space for modifications.[61]

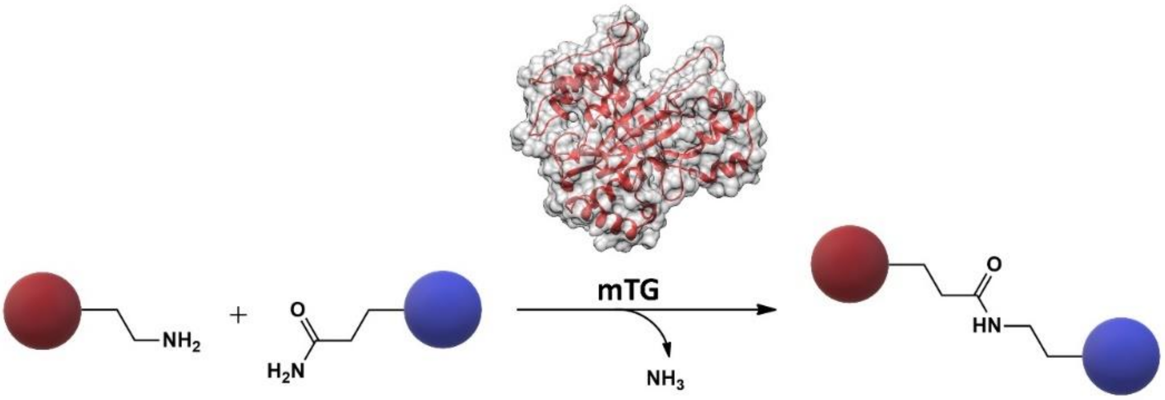

Figure 2: Reaction catalyzed by mTG. Protein- or peptide-bound glutamine side-chains are covalently crosslinked to lysine residues or primary amines. An isopeptide bond is formed under the release of ammonia.

The demand for homogeneity of ADCs for cancer treatment has put site-specific transglutaminase-catalyzed conjugation with cytotoxic payloads into the focus of research. This review will highlight recent achievements in the field of transglutaminase-mediated antibody modification and discuss the limitations of different strategies as well as unsolved challenges that need to be addressed in future work.

Despite the fact that transglutaminases are widely distributed in multiple phylogenetic species, not all of them are suitable for biotechnological applications.[62] mTG derived from the Gram-positive actinobacterium *Streptomyces mobaraensis* emerged as the one most employed transglutaminase for industrial purposes due to its high stability and pH tolerance combined with an excellent activity.[62] The enzyme is intensively used for food processing in order to texture meat and dairy products (Figure 3). Later, its remarkable properties made it a versatile tool for the posttranslational modification of various proteins.[62] PEGylation of small proteinaceous drugs to elevate their half-life *in vivo*, immobilization of aggregation-prone biocatalysts to increase their overall stability or the covalent attachment of nucleic acids to proteins to combine the beneficial properties of both biomolecules, are only a few examples for the diverse applications of the enzyme (Figure 3).[60]

The following paragraphs will introduce key methodologies that allow for the mTG-mediated modification of antibodies. Based on each of the three strategies, multiple studies that demonstrate recent achievements will be described. Moreover, their advantages and disadvantages will be compared and general remaining limitations of the mTG-technology will be discussed to provide a comprehensive overview to the reader.

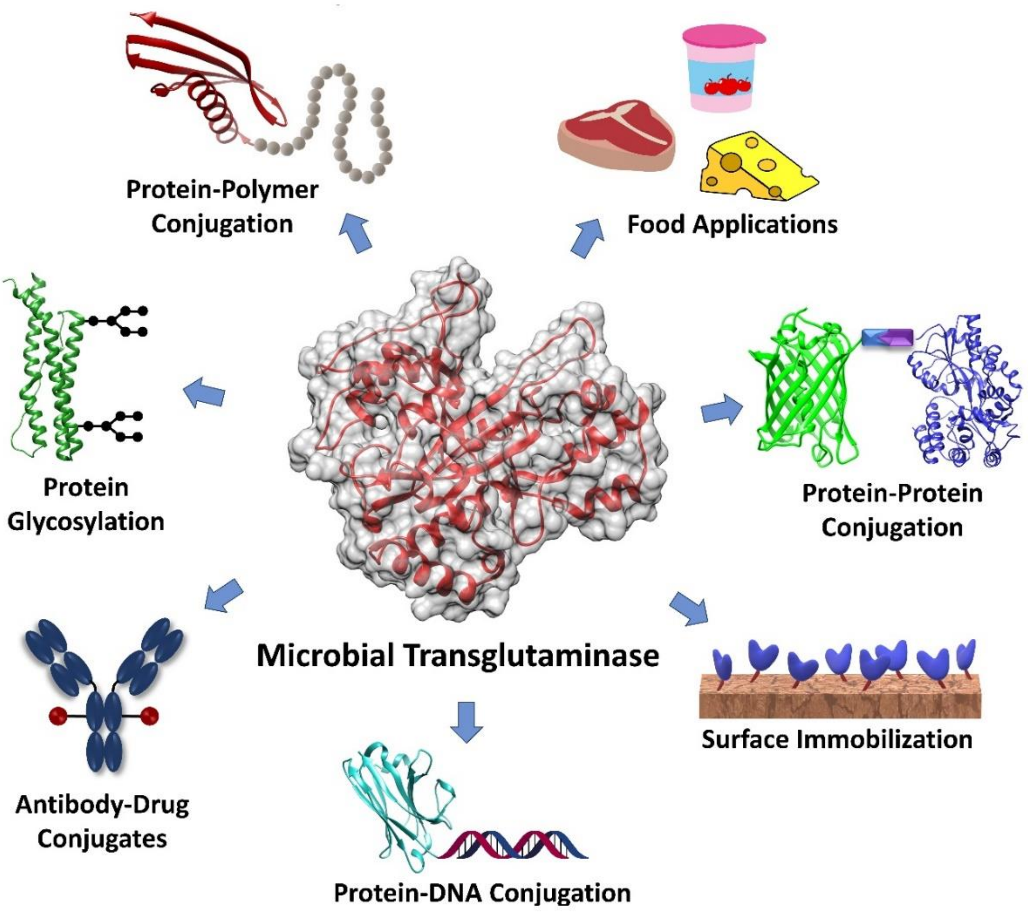
Protein-Polymer Conjugation
Food Applications
Protein Glycosylation
Protein-Protein Conjugation
Microbial Transglutaminase
Surface Immobilization
Antibody-Drug Conjugates
Protein-DNA Conjugation

Figure 3: Overview of biotechnological and industrial applications of microbial transglutaminase.

2. ADCs generated from deglycosylated and aglycosylated antibodies

At the beginning of the 21st century, Josten and colleagues were the first to report on the conjugation of a monoclonal IgG antibody mediated by microbial transglutaminase.[63] They used amine derivatives of biotin to label an anti-2,4-dichlorophenoxyacetic acid (2-4D) antibody with up to 1.9 biotin moieties per antibody and demonstrated by ELISA that enzymatic modification did not interfere with the target-binding properties of the immunoglobulin. However, further studies did not confirm these results.[58] In 2008, researchers of the Schibli group investigated the reactivity of mTG at intrinsic lysine and glutamine sites of different antibodies.[64] Their studies showed only minor modification of lysine residues with glutamine-containing peptides with an average antibody/label ratio of 0.3 – 0.5. Almost no labeling of native anti-L1Cam antibody chCE7 and a bovine IgG was observed when glutamine sites were addressed (antibody/label ratio: 0.1) with a fluorophore equipped with cadaverine. Interestingly, a significantly improved labelling was observed when a genetically aglycosylated variant of chCE7 (Asn297 replaced by Gln) was applied.[64] This phenomenon was studied in the following work and MALDI-TOF analysis proved that stoichiometric labelling of aglycosylated chCE7 in a ratio of 4:1 at positions Gln295 and Gln297 was achieved (see Table 1 for an overview of conjugation sites employed in mTG-assisted assembly of ADCs).[65] Furthermore, enzymatic deglycosylation by PNGase F was applied to native chCE7 and commercially available anti-CD20 antibody rituximab, followed by mTG-promoted ligation of different acyl-acceptor substrates. Again, specific modification of the heavy chain at position Gln295 was confirmed by mass spectrometry and the authors concluded that an increased flexibility of the C/E loop (Q295–T299) of the antibodies Fc region upon deglycosylation renders glutamine residues within this loop amenable to mTG-mediated isopeptide formation.[65] These results gave access to a powerful methodology for the mTG-assisted construction of homogeneous ADCs with a defined DAR and outlined a key technology for various follow-up studies (Figure 4).

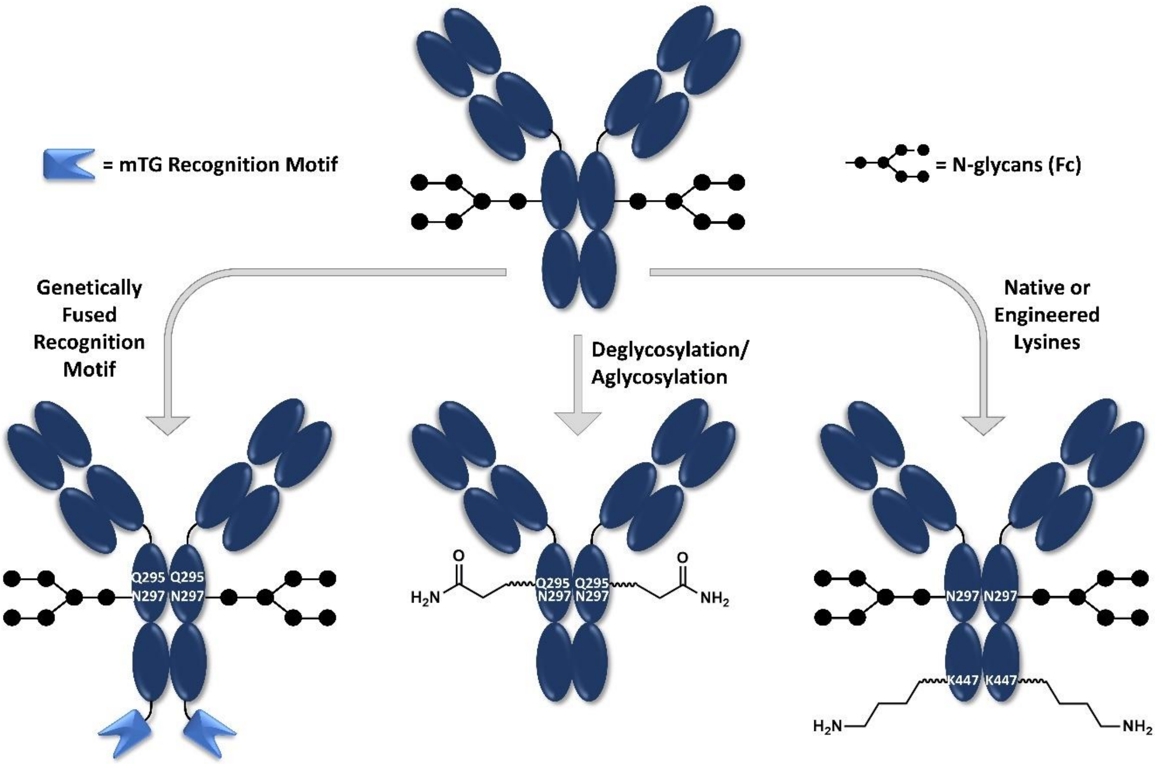
= mTG Recognition Motif
= N-glycans (Fc)
Genetically Fused Recognition Motif
Deglycosylation/ Aglycosylation
Native or Engineered Lysines
Q295 Q295
N297 N297
O
H_2N
NH_2
K447 K447

Figure 4: Harnessing transglutaminase activity for site-specific ADC generation. (top) Native, fully glycosylated antibodies are no substrate of mTG. The following strategies allow for its transamidation: (left) genetic incorporation of specific peptidyl linker sequences; (middle) genetic or enzymatic truncation of the CH2 glycan moiety to expose Gln295; (right) engineering of reactive lysines or additional C-terminal residues to prevent Lys447 from intracellular processing.

Dennler and colleagues reported a chemoenzymatic approach using deglycosylated HER2-targeting antibody trastuzumab yielding homogenous ADC in a two-step procedure.[66] Thus, PNGase F treatment, followed by enzymatic conjugation of different chemical handles suitable for maleimide-thiol coupling or strain-promoted azide-alkyne cycloaddition (SPAAC) by mTG was conducted. Subsequent conjugation of monomethyl auristatin F (MMAF) via a protease-cleavable linker gave rise to potent homogenous ADCs comprising DARs ranging from 1.8 to 2 (the different warheads, linker chemistries and click compounds applied for the construction of ADC under mTG catalysis are overviewed in Table 2). Within this study, the authors took advantage of the remarkable selectivity and kinetics of bioorthogonal conjugation by "click-chemistry" or thiol-maleimide coupling. Ready-to-use building blocks are available from commercial suppliers and can be applied for mTG catalysis at low cost. Subsequent installation of a pricey payload is achieved in a quantitative manner by adding only a slight excess of the respective molecule. Consequently, the authors achieved their DARs employing only a 2.5-fold excess of the corresponding toxin, which represents a major advantage in terms of cost-effective ADC manufacturing.[66] When employing a two-step chemoenzymatic approach, it should be considered that removal of non-coupled compounds is necessary to enable specific labelling of the desired target in the following reaction. Additional purification steps however, might diminish the yield of the overall process.

In 2015, Lhospice and co-workers further investigated the applicability of this approach and reported superior pharmacokinetic properties of an mTG generated drug conjugate of the anti-CD30 antibody brentuximab in rodent lymphoma models compared to state-of-the-art ADC ADCETRIS.[67] A genetically mutated version of brentuximab (N297Q) comprising two distinct addressable glutamines (Q295 and Q297) was functionalized with derivatives of monomethyl auristatin E (MMAE) under mTG catalysis. Employing different linker chemistries, four different ADCs were assembled by either direct enzymatic coupling of the warhead or in a two-step approach using SPAAC. Biodistribution experiments in mice revealed better tumor uptake and lower nontargeted liver and spleen uptake of the chemo-enzymatically conjugated ADC compared to ADCETRIS. Moreover, pharmacokinetic studies in rats demonstrated an elevated maximal tolerated dose and decelerated clearance of the homogenously labelled ADCs. The authors attribute these observations to the absence of species with DAR > 4, which suffer from faster catabolism and reduced binding to Fcγreceptors (FcγRs) and surface mannose receptors.[67]

In further research, Grünberg and co-workers applied different aglycosylated variants of anti-L1CAM antibody chCE7 and the chelator 1,4,7,10- tetraazacyclododecane-1,4,7,10-tetraacetic acid (DOTA) for the generation of radioimmunoconjugates (RIC).[68] Decalysines bearing 1, 3 or 5 DOTA pendants were site-specifically conjugated to each heavy chain of the genetically aglycosylated antibodies (N297D, N297Q) by mTG catalysis to generate uniform conjugates with high DOTA loading. Moreover, preferred biodistribution compared to heterogeneous, chemically modified constructs was demonstrated in mice bearing ovarian tumor xenografts. Interestingly, aglycosylated antibody chCE7agl (N297Q) with two accessible glutamines was conjugated with only one DOTA-polylysine per heavy chain as conjugation occurred at two lysine residues of the same polylysine chain simultaneously. The site-specific RIC generated by mTG catalysis with the highest DOTA/antibody ratio revealed the best tumor-to-liver ratios. Based on their results, the authors hypothesized that other properties - polarity, pI of the immunoconjugate, but not the antibody-to-ligand ratio alone - stipulate its biodistribution.[68]

As outlined above, removal of the CH2 polysaccharide moiety makes Gln295 accessible for mTG-mediated modification. This straight-forward strategy was further adopted by different research groups. Thus, Puthenveetil and co-workers reported a site-specific conjugation strategy for dual antibody labeling on solid support based on the above-mentioned chemoenzymatic procedure.[69] An engineered variant of trastuzumab (kK183c) bearing an additional cysteine at the light chain was deglycosylated using PNGase F and captured on solid support via binding to immobilized protein A. Subsequent mTG-catalyzed conjugation of NH_2-PEG_2-bicyclo[6.1.0]nonyne (NH_2-PEG_2-BCN), reduction and mild reoxidation generated an antibody bearing two orthogonal reaction handles, namely a strained alkyne (BCN) at each heavy and a thiol at each light chain. Subsequent labeling of these moieties with different fluorophores gave rise to a dual-labeled antibody, confirmed by in-gel fluorescence of a reduced antibody-fluorophore conjugate.[69] This procedure paves the way for the high-throughput generation of site-specific ADCs on solid support, utilizing mTG-mediated conjugation in a two-step procedure.

Recently, a chemoenzymatic strategy for the one-pot dual labeling of antibodies that relies on the orthogonal reactivates of microbial transglutaminase and lipoic acid ligase (LplA) was envisioned. [70] LplA is capable of ligating different derivatives of valeric acid site-specifically to a lysine residue within the 13 amino acids long amino acid motif GFEIDKVWYDLDA (LAP-tag). In the first place, a LAP-tag was engineered to the C-terminus of the heavy and light chains of trastuzumab and picolyl-azide (pAz) or trans-cyclooctene (TCO) substrates were attached under LplA-catalyzation. Light chain (LC) modification proceeded with 86% with pAz and 88% with TCO while modification of the heavy chain (HC) yielded 82% with pAz and 69% with TCO, respectively. Following “click”-reactions using either dibenzocyclooctyne-amine (DBCO)- or *methyl-tetrazine (*MeTz)-modified PEG5000 resulted in a significant shift to higher masses of the corresponding protein band in SDS-PAGE analysis. Further, a dual-labelling approach for spatially controlled cargo release in the tumor environment was investigated. TCO-modified valeric acid was conjugated to the engineered LAP-tag by LplA and NH_2-PEG_3-N_3 to Q295 of PNGase F-deglycosylated trastuzumab by mTG. The two different click chemistry handles were subsequently modified with MeTz-PEG_4-Valine-Citrulline(VC)-PAB-PEG_2-fluorescein and DBCO-PEG_4-PVGLIG-PEG_2-Rhodamine to yield dual labeled antibodies. The peptidic sequences PVGLIG and VC allowed for the controlled payload release in SK-BR-3 breast cancer cells mediated by extracellularly overexpressed matrix metalloproteinase II (MMP-2) and intracellular lysosomal cysteine protease cathepsin B (CatB), as demonstrated by *in vitro* cleavage assays and confocal laser scanning microscopy.[70]

In a proof-of-concept study, researchers of the Zentel group used mTG-mediated conjugation combined with SPAAC to attach anti-DEC205 antibodies, specific for dendritic immune cells, to an azide-modified block copolymer P(Lys)-*b*-P(HPMA) aimed at the delivery of tumor antigen-encoding plasmid DNA (pDNA) to dendritic cells for the generation of pDNA vaccines.[71] After PNGase F-mediated deglycosylation, a DBCO reaction handle bearing an ε-amino group of lysine was introduced to Q295 of DEC205 antibody by mTG catalysis. Subsequent reaction of DEC205 with a polyplex consisting of pDNA and a statistically azide-modified P(Lys)-*b*-P(HPMA) lead to successful conjugation. It should be mentioned that a large excess of DEC205-DBCO was crucial for conjugation, presumably due to the low diffusivity of two macromolecular reaction partners and the low DBCO-loading of the DEC205-DBCO compound (1-2).[71]

In 2017, researches of the Tsuchikama group employed branched PEG linkers to attach multiple payloads to antibodies.[72] Different formats of these linkers, containing one primary amine and two azide moieties for SPAAC, were synthesized and enzymatically conjugated to Q295 (N297A) or Q295 and Q297 (N297Q) of a mutated non-glycosylated HER2-trageting antibody, respectively. A comparison of cleavable linear and branched linkers was conducted. Förster resonance energy transfer (FRET) assays for cathepsin-mediated cleavage were exploited for different linear and branched spacers. A branched, PEG-containing linker revealed a release rate comparable to a linear reference, while negligible release was observed for the branched, non-PEG bearing counterpart. For the construction of an ADC, a chemoenzymatic approach based on mTG-catalyzed linker conjugation and SPAAC for payload equipment was applied. As payload, the relatively hydrophilic tubulin inhibitor MMAF was utilized generating homogenous ADCs with an average DAR of 3.9 (N297A) and 7.4 (N297Q), respectively. The target-binding properties of these homogenous ADCs were not affected and enhanced *in vitro* cytotoxicity on HER2-expressing breast cancer cell lines was shown for the DAR 3.9 (N297A) in comparison to its linear DAR 1.9 counterpart.[72] This approach opens avenues for the generation of homogenous high-DAR ADCs. Interestingly, the potency of the DAR 7.4 ADC has not been demonstrated yet and, according to the authors, further investigations are currently ongoing. The fine-tuning of their hydrophilic branched linkers is a crucial step for further conjugation of more hydrophobic payloads e.g. MMAE, as high-DAR ADCs containing hydrophobic payloads suffer from protein aggregation and rapid clearance.[72]

Branched PEG linkers were further applied to discover cathepsin cleavable linkers with enhanced stability in mouse plasma aimed at improving efficacy and accuracy in mouse models (see also work of Dorywalska et al. [73] below).[74] Different hydrophilic amino acids were introduced at the *N*-terminus of conventional L-valyl-L-citrulline dipeptide linker (VC), as modification of this position is known to affect its plasma stability.[73] Addition of glutamic acid to the linker sequence (EVC-PABC) prohibited hydrolysis catalyzed by murine carboxylesterase 1c (Ces1c), which is reported for VC-PABC linkers applied in commonly used cleavable ADCs.[73] Furthermore, faster cathepsin-mediated cleavage as well as enhanced hydrophilicity was observed for the EVC-PABC bearing DAR 3.9 ADCs.[74]

As collectively described above, the utility of de- or aglycosylated antibodies providing Gln295 as a suitable site for transamidation was consistently reported by various groups. Nevertheless, the contribution of the glycan moiety to the antibody's stability should also be considered. Lhospice *et al.* demonstrated that ADCs assembled from aglycosylated cAC10Q antibody remained stable for at least one week in human, cynomolgus monkey and rat serum.[67] Interestingly, constructs with longer linker moieties suffered from premature drug loss upon incubation in mouse plasma.[67] Though stability of their anti-CD30 ADCs was clearly proven, careful case-to-case evaluation is necessary since some studies reported aglycosylated antibodies to be more sensitive to heat and prone to aggregation.[75]

3. ADCs generated applying engineered mTG recognition motifs

Besides truncation of the antibody's native glycosylation pattern, incorporation of specific recognition tags is a common strategy to achieve efficient modification by mTG (Figure 4). One major benefit of this approach is the high flexibility in comparison to other conjugation enzymes. While the reactivity of conventional catalysts like Sortase A is limited to terminal sites, mTG also recognizes internal positions.[76] In 2013, Strop and co-workers took advantage of this capability and introduced a novel "glutamine tag" for transglutaminase-mediated conjugation that can be engineered at desired positions within the antibody.[76] This pioneering approach not only resulted in highly homogenous and reproducible ADCs but also allowed investigating the role of conjugation-site, linker and payload in frame of optimizing the drug's TI. Their engineered recognition sequence LLQG was introduced at approximately 90 surface-exposed sites of an epidermal growth factor receptor (EGFR)-targeting IgG1 antibody and screened for efficient conjugation. Twelve of the investigated positions revealed suitable biophysical properties combined with a high degree of payload loading. Further, these results were confirmed using an anti-M1S1 antibody (C16), an anti-HER2 antibody and other IgG subtypes. mTG conjugation of different amine-bearing payloads, e.g. cadaverine-Alexa488 or AcLys-VC-MMAD (monomethyl auristatin D) lead to DARs between 1.2 and 2.0, depending on the utilized conjugation site. Two distinct conjugation sites (C16 HC: C-terminal lysine replaced by LLQGA tag and C16 LC: GGLLQGA after C-terminal cysteine) were further examined; DARs approaching quantitative conjugation (1.9 and 1.8, respectively) were gained. Both generated ADCs were found highly potent *in vitro* on different M1S1-positive cell lines as well as *in vivo* upon single-dose intravenous administration in mice implanted with M1S1-positive BxPC3 pancreatic cancer cells. Interestingly, results comparable to those of a cysteine conjugate (DAR 3.6) were obtained. Moreover, their rodent models revealed that the choice of conjugation site strongly influenced the pharmacokinetic properties of an ADC. While C16-LC-AcLys-VC-MMAD remained stable in mice and rats, C16-HC-AcLys-VC-MMAD significantly suffered from premature drug loss in circulation of Sprague Dawley rats.[76]

In 2015, the same group investigated the impact of site-specific and homogenous payload attachment on the TI of ADCs with high DARs. [28] To that end, ADCs with a DAR of 2, 4, 6 or 8 were generated by site-specific conjugation of a non-cleavable MMAD on anti-M1S1 antibody C16 via mTG (N297Q, LLQG inserted at position 135 HC, LC C-terminus GGLLQGA; HC C-terminus LLQGA) and compared to cysteine-maleimide conjugates possessing comparable toxin loading (DAR4-8). *In vitro* experiments showed no significant difference in potency on BxPC3 (M1S1+++) and Colo205 (M1S1+) cells between site-specific and conventional maleimide-cysteine conjugates. However, divergence in tumor growth inhibition was obtained from *in* vivo Colo205 xenograft models with low target expression, as the conventional DAR 8 conjugate showed only minor inhibition, whereas site-selective conjugates with DAR 6 and 8 induced long-term tumor growth inhibition. Follow-up pharmacokinetic (PK) studies revealed increased exposure of the homogenous high DAR ADCs in mice (up to DAR 8) and rat (up to DAR 6). Additionally, comparable safety and tolerability was observed, widening the TI and opening avenues for addressing tumor targets with low target expression, slow internalization or intracellular processing by high DAR ADC.[28]

Likewise, Farias and co-workers investigated the site-specificity of their mTG approach by HR-MS analysis.[77] C16 anti-M1S1 antibody with the LLQGA-tag at the C-terminus of either heavy or light chain (or both) were site-specifically linked to NH_2-PEG_6-MMAD. The generated ADCs were characterized by intact mass, high resolution peptide mapping and in-source fragmentation analysis, revealing site-specific payload attachment. However, a small amount of off-target conjugation of approximately 1.3% was observed, corresponding to a small fraction of aglycosylated antibody present in the produced material. A generated C16 HC Q295N mutant lacking the off-target conjugation site, yielded highly homogenous conjugates that were more than 99.8% site-specific.[77]

Further, Dorywalska and co-workers investigated the effect of the attachment site on the stability of ADCs equipped with a cleavable linker and MMAD in rodent serum.[78] To that end, a series of different ADCs was generated by coupling of cleavable aminocaproyl-VC-PABC-MMAD to an engineered LLQG recognition site or Q295 of anti-M1S1 antibody C16 using microbial transglutaminase. While nearly no loss of payload was observed in rat, cynomolgus monkey, and human, a different linker stability was observed in mice serum, depending on the respective conjugation site. Due to steric hindrance, varying extent of enzymatic cleavage of the natural cathepsin B site was found at each investigated position. *In vitro* cytotoxicity assays upon plasma treatment of the different ADCs and *in vivo* xenograft models in mice implanted with BxPC3 cells revealed the importance of linker stability for cytotoxic potency. Interestingly, this cleavage was found to be cathepsin B-independent. These results suggest that the conjugation site plays a key role for the stability and potency of cathepsin B cleavable auristatin based ADCs. Therefore, site-directed conjugation via mTG generating homogenous ADCs is an advantageous procedure for the production of potent ADCs for preclinical trials.[78] Additionally, homogenous non-cleavable ADCs bearing PEG_6-propionyl(C2)-MMAD as a payload were investigated for stability in rodent plasma applying the same conjugation sites.[79] A position-dependent degradation of the C-terminus of MMAD was observed, which had a detrimental effect on ADC potency. Notably, an ADC bearing MMAF analog Aur3377 as a payload and the same linker did not show detectable degradation or a loss of potency.[79] In 2016, the same group identified murine serum protease carboxylesterase 1C (Ces1C) to be responsible for premature extracellular hydrolysis of the cleavable aminocaproyl-VC-PABC linker moiety of ADCs.[73] To overcome this limitation, 10 different chemical functionalities were considered at the C2 position of the C6-VC-PABC-Aur0101 linker-payload to protect it from enzymatic degradation. Upon mTG-assisted conjugation, plasma stability assays of the resulting ADCs revealed a significant impact of the utilized linker derivatives on extracellular drug loss. Depending on the addressed glutamine site, some substitutions even accelerated Ces1C-mediated degradation while others successfully protected the linker from undesired enzymatic cleavage. Successive xenograft models demonstrated improved antitumor efficacy as a result of elevated systemic ADCs stability, originating from the superior stability of a protected linker (Anami et al.[74] further investigated these effects, see above).[73]

The therapeutic index of an antibody-drug conjugate is influenced by a plethora of physiological and pharmaceutical parameters including the location of the tumor, linker stability, the toxic warhead's mode of action and the choice of the targeted antigen.[5, 18, 19, 80, 81] Antigens that are highly overexpressed on malignant cells but almost absent in healthy tissue are usually favored to avoid undesired side-effect during treatment of the patient. However, several promising tumor markers are present on both degenerated and healthy cells differing only in the extent of antigen expression. To address these molecules, engineering antibodies with mediocre affinities that accumulate only at elevated antigen levels, is a suitable approach to improve the TI of an ADC. A group from Rinat-Pfizer applied this approach in combination with their well-established transglutaminase labelling strategy to develop homogenous ADCs with balanced efficacy and toxicity, hence enriched TI.[82-84]

In 2016 Strop and co-workers investigated a medium-affinity ADC against type I transmembrane cell-surface glycoprotein Trop-2 (trophoblast cell-surface antigen 2; also known as M1S1, TACSTD2, EGP-1, GA733-1), which is highly expressed in most human carcinomas.[83] Despite the fact that its biological role is still a matter of discussion, Trop-2 overexpression is associated with cancer growth, aggressiveness, metastasis and poor prognosis in carcinomas.[83] Unfortunately, Trop-2 is also expressed on normal epithelial cells, thus an adjustment between efficacy and safety is needed. The C-terminal lysine on the heavy chain of a humanized anti-Trop-2 hIgG1 antibody was replaced with the LLQGA motif to allow for mTG-mediated modification. Subsequent conjugation with cleavable AcLys-VC-PABC–

PF-06380101, a potent microtubule inhibitor (MTI), yielded a DAR 1.9 ADC (RN927C). The applied linker was assessed as stable in BxPC3 tumor-bearing animals and highly efficient in multiple pancreatic tumor xenograft models including cell line BxPC3 and PDX models Pan0123 (pancreatic ductal carcinoma from peritoneal biopsy), Pan0135 (pancreatic adenosquamous carcinoma), and Pan0146 (metastatic pancreatic carcinoma from liver biopsy)(0.75-1.5 mg/kg), whereas a non-binding control antibody showed no effect (up to 3 mg/kg). *In vivo* ovarian, lung and triple-negative breast cancer PDX xenograft models further showed potent inhibition of tumor growth, which was superior to standard chemotherapeutic treatment with paclitaxel or gemcitabine. It should be noted that only partial tumor growth inhibition was achieved in lung PDX model with RN927C, but RN927C was superior to paclitaxel (20 mg/kg) in a comparing study. The combination of medium-affinity binding and site-specific stable isopeptide linkage of the payload lead to reduced off-target toxicity in preclinical exploratory safety studies in non-human primates, as only fully recoverable on-target epithelial toxicity was detected with minimal, non-dose limiting off-target toxicity.[83]

The above-mentioned strategy was further applied for the preparation of a safety-enhanced ADC targeting EGFR.[84] A low-affinity parental antibody was chosen to reduce off-target toxicity and to enhance tumor penetration, which was further humanized and equipped with a transglutaminase recognition motif at the C-terminus of the light chain constant domain by addition of the sequence GGLLQGPP. Upon transglutaminase-catalyzed conjugation of AcLys-VC-PABC–PF-06380101, the generated ADC RN765C comprised a DAR of 1.93-2.0 and revealed potent cell-killing properties *in vitro* on EGFR-overexpressing HCC827 cells, and even on cells insensitive for the clinically approved anti-EGFR antibody cetuximab. Additionally, RN765C was found to be less effective in killing normal human keratinocytes that express low levels of the targeted receptor. *In vivo* xenograft models based on BxPC3 cells and PDX models of colorectal and lung cancer using 1.5-3 mg/kg of RN965C resulted in persistent tumor growth inhibition regardless of their KRAS mutation. Notably, potent tumor growth inhibition was found in non-small cell lung cancer PDX LG1049 carrying the EGFR exon 19 deletion and T790M mutation, known to drive resistance for tyrosine kinase inhibitors.[84]

In 2019 Costa and co-workers designed efficacy- and tolerability-enhanced ADCs targeting the CXC motif chemokine receptor 4 (CXCR4).[82] CXCR4 has multiple functions in hematopoietic progenitor cells, e.g. maintenance of quiescence, protection of oxidative stress in adult tissues, and retention of granulocytes and neutrophils in bone marrow. Though first approaches applying small molecules have advanced into clinical trials, these compounds often comprise unfavorable PK profiles and require combinatorial treatment to achieve therapeutical benefit.[82] Thus, the first anti-CXCR4 ADC effective in xenograft models of haemopoietic cancers resistant to standard of care and anti-CXCR4 antibodies was developed. Different types of linker-payloads, DARs, affinities and Fc formats were investigated to carefully evaluate the TI of the resulting drugs. Twenty-two ADCs were generated upon site-specific mTG-mediated conjugation to engineered antibodies with different mTG-recognition motifs. Auristatins were chosen as cytotoxic payloads, as these cell division-blocking tubulin polymerization inhibitors mediated significant loss of viability in tumor cells (Ramos and OPM2) and leaved peripheral blood mononuclear cells (PBMCs, CXCR4-positive) untouched. The lead ADC 713 comprised a low-affinity antibody with reduced Fc-effector functions armed with 4 non-cleavable auristatin payloads conjugated to an LLQG tag at position 135 in the CH1 and to the accessible Q295 of N297A-mutated CH2. It was found active in hematological and solid tumors presenting a favorable TI and therefore demonstrating the possibility to generate an ADC with improved TI through empiric studies for targets with broad normal-tissue expression.[82]

The incorporation of genetically encoded mTG recognition motifs was further employed for the generation of non-cleavable ADCs with improved lysosomal trafficking.[85] ADCs bearing non-cleavable toxic payloads are hypothesized to possess enhanced stability in circulation and release their payloads upon ADC degradation in the lysosome. To investigate whether the intracellular trafficking pathway can modulate potency of an ADC, two different constructs were generated targeting two different tumor markers with comparable internalization rates: Amyloid Precursor Like Protein 2 (APLP2), which is known to efficiently deliver its interacting partners to lysosomes, and Trop-2, whose expression is often associated with poor prognosis of diseases, but is less effective in lysosomal trafficking compared to APLP2. Trop-2- and APLP2-targeting antibodies were conjugated with NH_2-PEG_6-MMAD via transglutaminase to generate ADCs with DAR 2 (C-terminal GGLLQGPP transglutaminase tag of the light chain) or 4 (N297Q mutation for conjugation to Q295 and Q297 in the heavy chain). *In vitro* potency was determined on SKOV3 and Colo205 cells that expressed different ratios of APLP2 to Trop-2 of 1:2 and 1:13, respectively. The lysosomally targeted APLP2-binding ADC induced cell killing more effectively than the one directed against Trop-2; Colo205 xenograft models further demonstrated superior *in vivo* efficacy.[85] HER2 is a prominent tumor target that is overexpressed on different types of ovarian and breast cancers but suffers from rapid recycling back to the cell surface upon endocytosis.[85] In a following approach, HER2/APLP2-targeting bispecific ADCs where investigated to merge the advantages of elevated HER2 expression and the lysosome-directing properties of APLP2. In these constructs, one Fab arm of the antibody mediates binding to the HER2 receptor, while the other arm binds APLP2. Potent growth inhibition of low HER2-expressing MCF7 cells was achieved while a bivalent anti-HER2 ADC lacking APLP2 binding showed no effect. On cell lines expressing medium (JIMT-1) and high (N87) levels of HER2, similar IC50 values were determined, but the HER2/APLP2-addressing molecule exhibited improved maximal cell killing compared to its monospecific counterpart. Unfortunately, this effect was not observed *in vivo* as JIMT-1 orthotopic breast cancer models revealed a lower anti-tumor efficacy of the bispecific ADC than the monospecific reference at two different investigated doses. The authors claim that multiple factors influence the potency of non-cleavable ADC, among them receptor copy number, DAR, internalization and lysosomal trafficking. Therefore, further studies in the field are needed, but nevertheless this bispecific approach redirecting intracellular trafficking is promising for targeted tumor therapy.[85]

In 2018, the group of Graziani introduced DNA-intercalating natural product bis-intercalator depsipeptides (NPBIDs) as a novel class of ADC payloads leading to highly efficient anti-HER2 ADCs.[86] NPBIDs are head-to-tail dimeric C2-symmetrical polypeptides primarily isolated from *Streptomyces*, which bear a bicyclic heteroaromatic chromophore on each monomer. Their intercalation into the minor groove of DNA occurs via hydrogen bonding between the polypeptide core of the NPBID and the nucleobases of the DNA. These (in principle reversible) binding properties may result in a bystander effect upon cell lysis that could be beneficial for the treatment of solid tumors. A set of nine different NPBIDs was analyzed for their *in vitro* potency in a number of human cancer cell lines (N87, MDA-MB361, HT29; IC_{50} <0.1-20 nM). Furthermore, generation of seven different ADCs either by standard maleimide coupling or mTG-catalyzed conjugation applying different PEGylated and non-PEGylated linkers resulted in the lead ADC PF-06888667, consisting of the bis-intercalator, SW-163D conjugated with *N*-acetyl-lysine-valine-citrulline-*p*-aminobenzylalcohol-*N,N*-dimethylethylenediamine linker to an engineered variant of trastuzumab (LC C-Terminus tag GGLLQGA and mutation N297A for conjugation on Q295). PF-06888667 exhibited complete regression in a N87 tumor xenograft model in mice at 1 mg/kg and a cytostatic effect at 0.3 mg/kg. Interestingly, a previous study applying the same mouse model reported complete tumor regression only at a dose of 10 mg/kg of commercially available ADC T-DM1. Optimization of the employed linker and the attachment site as well as the conjugation method were revealed to be key factors for the success of their work. Thus, an SW-163 based ADC obtained by maleimide coupling to engineered cysteines C183/290, bearing a PEG spacer showed significantly lower efficacy compared to the mTG generated ADC comprising an *N*-acetyl-lysine linker.[86]

According to calculations, 75-80% of the human proteome are considered to be undruggable by small molecules or biotherapeutics due to a lack of suitable hydrophobic pockets or their absence from the cell surface.[87] Nucleic acid therapeutics (NAT) bear great potential to address these challenging targets that are involved in multiple kinds of cancers and genetic disorders. By binding of antisense oligonucleotides or siRNAs to the mRNA off the "undruggable" protein, its translation by the ribosome is inhibited and its total concentration is downregulated. Unfortunately, unfavorable pharmacokinetics, short half-life and target-indiscrimination strongly limits the application of NAT in therapy. Through coupling of NATs to monoclonal antibodies, Huggins *et al.* intended to overcome these limitations. To that end, a chemoenzymatic approach was developed that employed mTG for the attachment of a SPAAC-reactive acyl-acceptor peptide $\underline{K}$-PEG_6-SG-K-N_3 to an engineered LL$\underline{Q}$GA motif at the C-terminus of an anti-CD33 mAb. Subsequently, a 5’ DBCO-modified siRNA was synthesized and coupled to the mAb-linker conjugate to form an antibody-siRNA conjugate with a DAR of approximately 2 and unaltered binding properties. The authors report on a straight-forward approach that allows for the assembly of antibody-nucleic acid conjugates by applying mTG catalysis and SPAAC without undesired off-target conjugation. Modification of their approach towards construction of higher or lower DAR conjugates are discussed as well as a potential application in drug-delivery of therapeutic oligonucleotides. However, cell killing experiments and *in vivo* data to further demonstrate the impact of their approach are missing.[88]

Transglutaminases are present in a vast number of different microorganisms, but besides the most prominent one from *Streptomyces mobaraensis* only a few of them were applied for biotechnological purposes even though homologs bearing novel properties would be of great value. A promising example is the newly described KalbTG from Gram-positive actinobacterium *Kutzneria albida*. In 2017, researchers from Roche identified the enzyme that comprises 32% sequence identity and a conserved active site residues by sequence alignments using the *S. mobaraensis* enzyme as a query.[89] The hypothetical gene coded for the smallest transglutaminase known to date (26.4 kDa) and a strategy for the recombinant expression in *E. coli* cells was established that employed ammonia, the inhibitory byproduct of the catalyzed transamidation, to suppress the enzyme’s cytotoxic intracellular crosslinking activity. KalbTG exhibited no cross-reactivity with known mTG substrates and ultra-high throughput screening of 1.4 million different 5-mer peptides using the NimbleGen peptide array technology revealed YRYRQ and RYESK as favored glutamine and lysine sequences. Interestingly, KalbTG was found orthogonal to mTG, making dual labeling of a 7-kDa substrate bearing a YRYRQ KalbTG site and an DYALQ mTG recognition sequence possible. Antibody conjugates were generated via mTG or KalbTG catalysis applying recognition motifs YRYRQ and LLQGA that are C-terminally fused to the heavy chain of a mouse, monoclonal anti-TSH (thyroid stimulating hormone) antibody. Site-specific conjugation by both transglutaminases was found with no labelling of mTG recognition sequence LLQGA by KalbTG. In the scope of that work, no antibody-drug conjugates were presented, but the demonstrated results provided a powerful tool for the dual-labelling of antibody employing orthogonal transglutaminases.[89]

Among others, the coupling efficiency of the used ligation strategy is a key factor for the generation of ADCs since inefficient conjugation results in heterogeneous product formation. In our group, we are interested in developing novel recognition motifs for microbial transglutaminase that facilitate highly efficient labelling of therapeutic antibodies. In 2015, we unveiled a rationally designed sequence GECTYFQAYGCTE (GEC) that was derived from a natural mTG substrate dispase-autolysis inducing protein (DAIP).[90] The motif comprised the amino acids that surround reactive Q298 of DAIP, which is located within a type II βturn connecting two beta strands, and lacks similarity with known linear recognition motifs. To precisely mimic the native structure of the loop region, an intramolecular disulfide bridge was introduced that locked both termini at 4 Å distance. On a peptide level, the conformationally constrained molecule outperformed a linear control in terms of mTG-catalyzed labelling. Fused to the heavy chain of EGFR-targeting antibody cetuximab, both sequences mediated site-specific biotinylation of the immunoglobulin as revealed by Western blot and MALDI TOF-MS analysis. Microscopic studies and flow cytometry using EGFR positive EBC-1 cells demonstrated that target binding of biotinylated constructs was not impaired upon bioconjugation by mTG. [90]

In recent research, we further employed the demonstrated approach based on deriving efficient bioconjugation tags from native mTG substrates and revealed the sequence DIPIGQGMTG (SPI7G) from Streptomyces papain inhibitor (SPI_P).[91] SPI_P is a 12 kDa protein that is secreted by *S. mobaraensis* and previous studies showed that substitution of Lys7 massively influenced transamidation of the only mTG-reactive glutamine Gln6 by mTG.[92] A small set of peptides that mimicked the *N*-terminus of SPI_P and different regions of DAIP was synthesized and investigated towards their reactivity under mTG catalysis. Interestingly, SPI7G in which the native Lys7 was replaced by glycine, outperformed previously identified sequence GEC. A similar trend was observed in a biotinylation experiment that addressed a *C*-terminally fused tag at the heavy chain of trastuzumab. To further demonstrate the practical applicability of the approach, HER2-targeting ADCs were assembled from SPI7G- and LLQG-decorated trastuzumab in a chemoenzymatic two-step procedure. NH_2-PEG_2-BCN was coupled to the heavy chains of the immunoglobulins under mTG catalysis and further modified using SPAAC to arm the respective antibody with N_3-PEG_3-VC-PAB-MMAE for targeted cancer therapy. Within a strictly contracted reaction time of 1 h, the ADC assembled from the novel tag SPI7G revealed a 4-fold increased DAR of 1.81 compared to its counterpart synthesized from conventional sequence LLQG (DAR: 0.48). Consequently, the former ADC exhibited 12.6-fold more potent killing on HER2-overexpressing SK-BR-3 cells. These studies demonstrated that mimicking the native pattern of intrinsic mTG substrates is a powerful strategy to isolate potent recognition tags for the site-specific labelling of antibodies.[91]

Besides the development of novel bioconjugation tags, mTG was also used for the generation of hydrophilic high-DAR ADCs to overcome the challenge of maintaining hydrophilicity of a conjugate equipped with numerous hydrophobic toxins.[93] To compensate the hydrophobicity of most commonly applied cytotoxins, which may negatively affects formulation, manufacturing and the biophysical properties of an ADC, 10 kDa dextran, a clinically and FDA-approved biocompatible polysaccharide consisting of repeating α(1-6)-linked oligo-D-glucose units, was applied as a modular multimerization scaffold.[5, 93-95] Dextran equipped with a single amine moiety at the reducing end and numerous azides at the glucose repeating units, was conjugated to the HER2-targeting antibody trastuzumab bearing the C-terminal mTG-recognition motif LLQG. Subsequent SPAAC of hydrophobic DBCO-PEG_3-VC-PABC-MMAE yielded novel hybrid molecules, dextramabs, comprising DARs of 2-11. Compared to the unmodified parent antibody, the hybrid ADCs revealed similar binding to its target and potent target-dependent killing (IC_{50}= 0.1 nM)on SK-BR-3 (HER2++) cells *in vitro*. HER2-negative CHO-K1 cells were not affected by all dextramabs indicating a HER2-dependent cellular uptake. Hydrophobic interaction chromatography demonstrated that dextramabs were at least as hydrophilic as the unmodified parental antibody trastuzumab, indicating that the hydrophilicity of the conjugated toxins was compensated by the introduced hydrophilic polysaccharide scaffold. This approach may open avenues towards the application of milder toxins in higher density; follow-up animal studies will reveal if the enriched hydrophilicity could assure longer half-life and less immunogenicity *in vivo*.[93]

The versatility of the mTG-mediated site-specific conjugation in combination with the multivalent dextran scaffold was further used in another approach, where dextran bearing different amounts of addressable azides on the repeating glucose units and a single amine at the reducing end was conjugated with death receptor 5 targeting peptide (DR5TP) by copper(I)-catalyzed azide alkyne cycloaddition (*CuAAC*). [96]Death receptor 5 (DR5) which is overexpressed on various cancer cells has recently become a promising target in tumor therapy. Clustering of DR5 leads to the formation of the death-inducing signal cascade (DISC) triggering apoptosis of the targeted cell. A flexible multivalent compound was assembled that effectively triggered apoptosis upon receptor clustering on DR5-positive COLO205 and Jurkat cells *in vitro*. mTG-catalyzed conjugation of the azide-modified polysaccharide to an aglycosylated human Fc fragment (N297A) bearing Q295 as a conjugation site resulted in a protein-sugar hybrid compound bearing multiple addressable azide moieties, which were further equipped with DR5TP in different copies. Conjugation of the scaffold to the Fc fragment did not impair potency. Furthermore, no toxicity was found for all constructs on DR5-negative HEK293 cells, revealing a DR5-dependent toxicity. Interestingly, in these constructs targeting is not mediated by the antibody part, but rather by the multivalent dextran-DR5TP scaffold. This may allow for the prospective attachment of a second targeting moiety, e.g. a full-size antibody, for bispecific targeting of overexpressed tumor markers, among them HER2/ErbB2, Trop-2 or EGFR, which may result in synergistic effects.[96]

4. ADCs addressing natural or engineered lysines

All previously envisioned approaches exclusively employed the addressed antibody as the acyl-donor substrate for the catalyzed transamidation. This arrangement takes advantage of the enzyme's remarkable acyl-acceptor promiscuity that allows it to handle numerous aminated toxins. However, some studies reported the reverse procedure that targets lysine side chains of the respective antibody for payload attachment by mTG catalysis (Figure 4). mTG that was non-covalently immobilized onto glass microbeads was able to modify K288/290 and K340 of aglycosylated cAC10 antibody with azide-decorated heptapeptide FGLQRPY in > 70% yield, as shown by Spycher and coworkers.[97] Subsequent bioorthogonal SPAAC using DBCO-PEG$_4$-5/6-carboxyfluorescein (5/6-FAM) resulted in quantitative fluorescent labelling of the immunoglobulin. After establishing lysine conjugation by immobilized mTG, a dual-labeling strategy was developed. In the first step, NH$_2$-PEG$_3$-*trans*-cyclooctene (TCO) was coupled to Q295 of the aglycosylated antibody (>95% yield) followed by the attachment of FGLQRPYGK-(N$_3$) to the side chain of K340 (38% yield). Again, SPAAC was applied to functionalize the antibody with tetrazine(Tz)-PEG$_4$-DOTAGA and DBCO-PEG$_4$-5/6-FAM in a straightforward one-pot reaction; the success was confirmed by SDS-PAGE and LC-MS.[97]

In a different approach, researchers from Morphotek Inc./Eisai Inc. investigated varying antibodies including human-mouse chimeric, humanized, and fully human variants comprising either κ or λ light chains towards their reactivity in mTG-catalyzed reactions.[98] Since none of the approximately 80 present lysine sites reacted with biotin-modified standard substrate carboxybenzyl group-Gln-Gly (ZQG), they engineered a K-tag GGSTKHKIPGGS at the C-terminus of a heavy or a light chain, respectively. While the light chain was dually labeled with ZQG as expected, ESI-MS analysis revealed triple modification of the heavy chain. The authors concluded that cleavage of Lys447 by carboxypeptidase B during recombinant expression in HEK293 cells is prevented by additional C-terminal amino acids facilitating mTG-mediated transamidation. Engineering of dipeptides or single amino acids at the C-terminus (position448) confirmed their hypothesis as efficient conjugation to Lys447 was demonstrated for all non-acidic and non-proline amino acids. Of note, positively charged amino acids arginine and lysine failed to prevent cleavage of Lys447 since they are substrate of carboxypeptidase B themselves. Moreover, the authors screened IgG1 antibodies for solitaire residues that allowed for transamidation upon substitution against lysine and provided a detailed protocol therefore.[99] This approach applying minimal transglutaminase recognition tags would reduce the risk of perturbing the immunoglobulin's native structure and causing an undesired response of the patient immune system.[98, 100] To that end, multiple different sites within the light chain, heavy chain and hinge region were identified and their reactivity in mTG catalysis was investigated employing different acyl-donor substrates (ZQG-biotin, ZQG-N$_3$, ZQG-PEG$_2$-BCN, ZQG-PEG$_2$-auristatin F). Interestingly, the choice of the acyl-donor, as well as the conjugation site strongly influenced the degree of transamidation. Further, the identified sites were combined and reacted with previously employed acyl-donor substrates. However, a defined and homogenous DAR of 4, 6 or 8 was not achieved as combination of otherwise efficiently modified sites resulted in suboptimal overall conjugation.[98]

5. Conclusions and Outlook

The concept of targeted therapeutics bears the potential to improve the TI of tumor treatment compared to classical chemotherapy. Hence, ADCs that combine the targeting properties of an antibody with the cytotoxic potential of a payload are widely studied in a still growing number of clinical trials and publications. Besides drugs, linkers and target selection the homogeneity of ADCs has become a promising field for ADC refinement. Site-specific conjugation is a widely distributed strategy to post-translationally customize the properties of target proteins towards different applications in pharmaceutical and biotechnological research e.g. arming tumor-specific antibodies with cytotoxic small molecules to yield antibody-drug conjugates. Numerous studies demonstrated the considerable impact of mTG from *Streptomyces mobaraensis* for the site-specific construction of homogeneous ADCs. In comparison to traditional conjugation methodologies, mTG-assisted catalysis bears certain advantages. The reactivity of other frequently employed conjugation enzymes is often limited to terminal sites (e.g. Sortase A)[54] or requires incorporation of >10 amino acids-long motifs that might interfere with mAb stability (e.g. lipoic acid ligase).[70] Comparably short mTG-recognitions tags though, provide high flexibility since they can be inserted into various regions of a mAb to efficiently mediate its labelling.[76] Additionally, the remarkable stability of the formed isopeptide bond prevents premature drug loss in circulation and therefore minimizes systemic toxicity, an issue that is often observed when payloads are installed at cysteine residues via maleimide-chemistry.[101, 102] Unfortunately, native human immunoglobulins do not serve as a substrate for mTG-mediated ligation. Thus, additional genetic engineering or glycosidase treatment are still necessary to achieve efficient modification and are accompanied by distinct advantages and disadvantages. Enzymatic deglycosylation to expose Gln295 can be applied to virtually any antibody in a straight-forward manner. However, glycan truncation increases the antibody's hydrophobicity and its tendency to pH- and temperature-induced aggregation.[75] Incorporation of peptidyl-linker sequences into varying sites of the antibody allows for the careful fine-tuning of ADC pharmacokinetics but presupposes genetic modification and might interfere with the stability and overall polarity of the mAb. Engineering of a solitaire lysine residue (acyl-acceptor) minimizes the risk of impairing the intrinsic stability and polarity of the mAb. However, laborious organic synthesis of the corresponding reaction partner is required because the commercial selection of pharmaceutically relevant acyl-donor substrates is limited. To overcome these limitations, efforts are currently ongoing to engineer mTG towards altered properties and fruitful results were obtained in terms of thermostability,[103] catalytic activity[104, 105] and substrate specificity.[106] Moreover, functionally homologous enzymes from alternative hosts beyond *Streptomyces mobarae*nsis are being investigated as tools for site-specific antibody modification.[89, 107] Notwithstanding, cytotoxin-armed antibodies that were generated via mTG conjugation showed very promising results in preclinical studies as illustrated in this review.

Conflicts of interest

Authors declare that they have no conflict of interest.

Acknowledgments

This work was supported by the Deutsche Forschungsgemeinschaft through grant SPP 1623 and by the NANOKAT II grant from the BMBF (Bundesministerium für Bildung und Forschung).

References

[1] R.L. Siegel, K.D. Miller, A. Jemal, Cancer statistics, 2019, CA: A Cancer Journal for Clinicians, 69, (2019), 7-34. https://doi.org/10.3322/caac.21551

[2] R.V. Chari, M.L. Miller, W.C. Widdison, Antibody–drug conjugates: an emerging concept in cancer therapy, Angewandte Chemie International Edition, 53, (2014), 3796-3827. https://doi.org/10.1002/anie.201307628

[3] V.T. DeVita, E. Chu, A History of Cancer Chemotherapy, Cancer Research, 68, (2008), 8643. https://doi.org/10.1158/0008-5472.CAN-07-6611

[4] J.M. Lambert, C.Q. Morris, Antibody–drug conjugates (ADCs) for personalized treatment of solid tumors: A review, Advances in therapy, 34, (2017), 1015-1035. https://doi.org/10.1007/s12325-017-0519-6

[5] J.M. Lambert, A. Berkenblit, Antibody–drug conjugates for cancer treatment, Annual review of medicine, 69, (2018). https://doi.org/10.1146/annurev-med-061516-121357

[6] E. Frei, Combination Cancer Therapy: Presidential Address, Cancer Research, 32, (1972), 2593.

[7] R.A. Beckman, L.M. Weiner, H.M. Davis, Antibody constructs in cancer therapy, Cancer, 109, (2007), 170-179. https://doi.org/10.1002/cncr.22402

[8] J.M. Reichert, Marketed therapeutic antibodies compendium, mAbs, 4, (2012), 413-415. https://doi.org/10.4161/mabs.19931

[9] K.C. Nicolaou, S. Rigol, The Role of Organic Synthesis in the Emergence and Development of Antibody–Drug Conjugates as Targeted Cancer Therapies, Angewandte Chemie International Edition, 0, (2019). https://doi.org/10.1002/anie.201903498

[10] J.H. Yi, S.J. Kim, W.S. Kim, Brentuximab vedotin: clinical updates and practical guidance, Blood Res, 52, (2017), 243-253. https://doi.org/10.5045/br.2017.52.4.243

[11] P.D. Senter, E.L. Sievers, The discovery and development of brentuximab vedotin for use in relapsed Hodgkin lymphoma and systemic anaplastic large cell lymphoma, Nature Biotechnology, 30, (2012), 631. https://doi.org/10.1038/nbt.2289

[12] J.K. Lamba, L. Chauhan, M. Shin, M.R. Loken, J.A. Pollard, Y.-C. Wang, R.E. Ries, R. Aplenc, B.A. Hirsch, S.C. Raimondi, R.B. Walter, I.D. Bernstein, A.S. Gamis, T.A. Alonzo, S. Meshinchi, CD33 Splicing Polymorphism Determines Gemtuzumab Ozogamicin Response in De Novo Acute Myeloid Leukemia: Report From Randomized Phase III Children's Oncology Group Trial AAML0531, Journal of clinical oncology : official journal of the American Society of Clinical Oncology, 35, (2017), 2674-2682. https://doi.org/10.1200/JCO.2016.71.2513

[13] F.R. Appelbaum, I.D. Bernstein, Gemtuzumab ozogamicin for acute myeloid leukemia, Blood, 130, (2017), 2373. https://doi.org/10.1182/blood-2017-09-797712

[14] B. Shor, H.-P. Gerber, P. Sapra, Preclinical and clinical development of inotuzumab-ozogamicin in hematological malignancies, Molecular Immunology, 67, (2015), 107-116. https://doi.org/10.1016/j.molimm.2014.09.014

[15] Y.N. Lamb, Inotuzumab Ozogamicin: First Global Approval, Drugs, 77, (2017), 1603-1610. https://doi.org/10.1007/s40265-017-0802-5

[16] I. Niculescu-Duvaz, Trastuzumab emtansine, an antibody-drug conjugate for the treatment of HER2+ metastatic breast cancer, Current opinion in molecular therapeutics, 12, (2010), 350-360.

[17] P.M. LoRusso, D. Weiss, E. Guardino, S. Girish, M.X. Sliwkowski, Trastuzumab Emtansine: A Unique Antibody-Drug Conjugate in Development for Human Epidermal Growth Factor Receptor 2–Positive Cancer, Clinical Cancer Research, 17, (2011), 6437. https://doi.org/10.1158/1078-0432.CCR-11-0762

[18] T. Kline, A.R. Steiner, K. Penta, A.K. Sato, T.J. Hallam, G. Yin, Methods to Make Homogenous Antibody Drug Conjugates, Pharmaceutical Research, 32, (2015), 3480-3493. https://doi.org/10.1007/s11095-014-1596-8
[19] A. Beck, L. Goetsch, C. Dumontet, N. Corvaïa, Strategies and challenges for the next generation of antibody–drug conjugates, Nature Reviews Drug Discovery, 16, (2017), 315. https://doi.org/10.1038/nrd.2016.268
[20] S.O. Doronina, B.E. Toki, M.Y. Torgov, B.A. Mendelsohn, C.G. Cerveny, D.F. Chace, R.L. DeBlanc, R.P. Gearing, T.D. Bovee, C.B. Siegall, J.A. Francisco, A.F. Wahl, D.L. Meyer, P.D. Senter, Development of potent monoclonal antibody auristatin conjugates for cancer therapy, Nature Biotechnology, 21, (2003), 778-784. https://doi.org/10.1038/nbt832
[21] W.C. Widdison, S.D. Wilhelm, E.E. Cavanagh, K.R. Whiteman, B.A. Leece, Y. Kovtun, V.S. Goldmacher, H. Xie, R.M. Steeves, R.J. Lutz, R. Zhao, L. Wang, W.A. Blättler, R.V.J. Chari, Semisynthetic Maytansine Analogues for the Targeted Treatment of Cancer, Journal of Medicinal Chemistry, 49, (2006), 4392-4408. https://doi.org/10.1021/jm060319f
[22] M.S. Kung Sutherland, R.B. Walter, S.C. Jeffrey, P.J. Burke, C. Yu, H. Kostner, I. Stone, M.C. Ryan, D. Sussman, R.P. Lyon, W. Zeng, K.H. Harrington, K. Klussman, L. Westendorf, D. Meyer, I.D. Bernstein, P.D. Senter, D.R. Benjamin, J.G. Drachman, J.A. McEarchern, SGN-CD33A: a novel CD33-targeting antibody–drug conjugate using a pyrrolobenzodiazepine dimer is active in models of drug-resistant AML, Blood, 122, (2013), 1455. https://doi.org/10.1182/blood-2013-03-491506
[23] R.C. Elgersma, R.G.E. Coumans, T. Huijbregts, W.M.P.B. Menge, J.A.F. Joosten, H.J. Spijker, F.M.H. de Groot, M.M.C. van der Lee, R. Ubink, D.J. van den Dobbelsteen, D.F. Egging, W.H.A. Dokter, G.F.M. Verheijden, J.M. Lemmens, C.M. Timmers, P.H. Beusker, Design, Synthesis, and Evaluation of Linker-Duocarmycin Payloads: Toward Selection of HER2-Targeting Antibody–Drug Conjugate SYD985, Molecular Pharmaceutics, 12, (2015), 1813-1835. https://doi.org/10.1021/mp500781a
[24] A.L. Smith, K.C. Nicolaou, The Enediyne Antibiotics, Journal of Medicinal Chemistry, 39, (1996), 2103-2117. https://doi.org/10.1021/jm9600398
[25] M.L. Miller, N.E. Fishkin, W. Li, K.R. Whiteman, Y. Kovtun, E.E. Reid, K.E. Archer, E.K. Maloney, C.A. Audette, M.F. Mayo, A. Wilhelm, H.A. Modafferi, R. Singh, J. Pinkas, V. Goldmacher, J.M. Lambert, R.V.J. Chari, A New Class of Antibody–Drug Conjugates with Potent DNA Alkylating Activity, Molecular Cancer Therapeutics, 15, (2016), 1870. https://doi.org/10.1158/1535-7163.MCT-16-0184
[26] M.T. Kim, Y. Chen, J. Marhoul, F. Jacobson, Statistical Modeling of the Drug Load Distribution on Trastuzumab Emtansine (Kadcyla), a Lysine-Linked Antibody Drug Conjugate, Bioconjugate Chemistry, 25, (2014), 1223-1232. https://doi.org/10.1021/bc5000109
[27] D. Schumacher, C.P.R. Hackenberger, H. Leonhardt, J. Helma, Current Status: Site-Specific Antibody Drug Conjugates, Journal of Clinical Immunology, 36, (2016), 100-107. https://doi.org/10.1007/s10875-016-0265-6
[28] P. Strop, K. Delaria, D. Foletti, J.M. Witt, A. Hasa-Moreno, K. Poulsen, M.G. Casas, M. Dorywalska, S. Farias, A. Pios, V. Lui, R. Dushin, D. Zhou, T. Navaratnam, T.-T. Tran, J. Sutton, K.C. Lindquist, B. Han, S.-H. Liu, D.L. Shelton, J. Pons, A. Rajpal, Site-specific conjugation improves therapeutic index of antibody drug conjugates with high drug loading, Nature Biotechnology, 33, (2015), 694. https://doi.org/10.1038/nbt.3274
[29] X. Li, T. Fang, G.-J. Boons, Preparation of Well-Defined Antibody–Drug Conjugates through Glycan Remodeling and Strain-Promoted Azide–Alkyne Cycloadditions, Angewandte Chemie International Edition, 53, (2014), 7179-7182. https://doi.org/10.1002/anie.201402606
[30] Z. Zhu, B. Ramakrishnan, J. Li, Y. Wang, Y. Feng, P. Prabakaran, S. Colantonio, M.A. Dyba, P.K. Qasba, D.S. Dimitrov, Site-specific antibody-drug conjugation through an engineered glycotransferase and a chemically reactive sugar, mAbs, 6, (2014), 1190-1200. https://doi.org/10.4161/mabs.29889
[31] B. Ramakrishnan, E. Boeggeman, P.K. Qasba, Applications of glycosyltransferases in the site-specific conjugation of biomolecules and the development of a targeted drug delivery system and contrast agents for MRI, Expert Opinion on Drug Delivery, 5, (2008), 149-153. https://doi.org/10.1517/17425247.5.2.149

[32] P.K. Qasba, Glycans of Antibodies as a Specific Site for Drug Conjugation Using Glycosyltransferases, Bioconjugate Chemistry, 26, (2015), 2170-2175. https://doi.org/10.1021/acs.bioconjchem.5b00173

[33] Q. Zhou, J.E. Stefano, C. Manning, J. Kyazike, B. Chen, D.A. Gianolio, A. Park, M. Busch, J. Bird, X. Zheng, H. Simonds-Mannes, J. Kim, R.C. Gregory, R.J. Miller, W.H. Brondyk, P.K. Dhal, C.Q. Pan, Site-Specific Antibody–Drug Conjugation through Glycoengineering, Bioconjugate Chemistry, 25, (2014), 510-520. https://doi.org/10.1021/bc400505q

[34] R. van Geel, M.A. Wijdeven, R. Heesbeen, J.M.M. Verkade, A.A. Wasiel, S.S. van Berkel, F.L. van Delft, Chemoenzymatic Conjugation of Toxic Payloads to the Globally Conserved N-Glycan of Native mAbs Provides Homogeneous and Highly Efficacious Antibody–Drug Conjugates, Bioconjugate Chemistry, 26, (2015), 2233-2242. https://doi.org/10.1021/acs.bioconjchem.5b00224

[35] D. Shinmi, E. Taguchi, J. Iwano, T. Yamaguchi, K. Masuda, J. Enokizono, Y. Shiraishi, One-Step Conjugation Method for Site-Specific Antibody–Drug Conjugates through Reactive Cysteine-Engineered Antibodies, Bioconjugate Chemistry, 27, (2016), 1324-1331. https://doi.org/10.1021/acs.bioconjchem.6b00133

[36] N. Dimasi, R. Fleming, H. Zhong, B. Bezabeh, K. Kinneer, R.J. Christie, C. Fazenbaker, H. Wu, C. Gao, Efficient Preparation of Site-Specific Antibody–Drug Conjugates Using Cysteine Insertion, Molecular Pharmaceutics, 14, (2017), 1501-1516. https://doi.org/10.1021/acs.molpharmaceut.6b00995

[37] B.-Q. Shen, K. Xu, L. Liu, H. Raab, S. Bhakta, M. Kenrick, K.L. Parsons-Reponte, J. Tien, S.-F. Yu, E. Mai, D. Li, J. Tibbitts, J. Baudys, O.M. Saad, S.J. Scales, P.J. McDonald, P.E. Hass, C. Eigenbrot, T. Nguyen, W.A. Solis, R.N. Fuji, K.M. Flagella, D. Patel, S.D. Spencer, L.A. Khawli, A. Ebens, W.L. Wong, R. Vandlen, S. Kaur, M.X. Sliwkowski, R.H. Scheller, P. Polakis, J.R. Junutula, Conjugation site modulates the in vivo stability and therapeutic activity of antibody-drug conjugates, Nature Biotechnology, 30, (2012), 184. https://doi.org/10.1038/nbt.2108

[38] J.R. Junutula, H. Raab, S. Clark, S. Bhakta, D.D. Leipold, S. Weir, Y. Chen, M. Simpson, S.P. Tsai, M.S. Dennis, Y. Lu, Y.G. Meng, C. Ng, J. Yang, C.C. Lee, E. Duenas, J. Gorrell, V. Katta, A. Kim, K. McDorman, K. Flagella, R. Venook, S. Ross, S.D. Spencer, W. Lee Wong, H.B. Lowman, R. Vandlen, M.X. Sliwkowski, R.H. Scheller, P. Polakis, W. Mallet, Site-specific conjugation of a cytotoxic drug to an antibody improves the therapeutic index, Nature Biotechnology, 26, (2008), 925. https://doi.org/10.1038/nbt.1480

[39] X. Li, C.G. Nelson, R.R. Nair, L. Hazlehurst, T. Moroni, P. Martinez-Acedo, A.R. Nanna, D. Hymel, T.R. Burke, C. Rader, Stable and Potent Selenomab-Drug Conjugates, Cell Chemical Biology, 24, (2017), 433-442.e436. https://doi.org/10.1016/j.chembiol.2017.02.012

[40] M.P. VanBrunt, K. Shanebeck, Z. Caldwell, J. Johnson, P. Thompson, T. Martin, H. Dong, G. Li, H. Xu, F. D'Hooge, L. Masterson, P. Bariola, A. Tiberghien, E. Ezeadi, D.G. Williams, J.A. Hartley, P.W. Howard, K.H. Grabstein, M.A. Bowen, M. Marelli, Genetically Encoded Azide Containing Amino Acid in Mammalian Cells Enables Site-Specific Antibody–Drug Conjugates Using Click Cycloaddition Chemistry, Bioconjugate Chemistry, 26, (2015), 2249-2260. https://doi.org/10.1021/acs.bioconjchem.5b00359

[41] E.S. Zimmerman, T.H. Heibeck, A. Gill, X. Li, C.J. Murray, M.R. Madlansacay, C. Tran, N.T. Uter, G. Yin, P.J. Rivers, A.Y. Yam, W.D. Wang, A.R. Steiner, S.U. Bajad, K. Penta, W. Yang, T.J. Hallam, C.D. Thanos, A.K. Sato, Production of Site-Specific Antibody–Drug Conjugates Using Optimized Non-Natural Amino Acids in a Cell-Free Expression System, Bioconjugate Chemistry, 25, (2014), 351-361. https://doi.org/l10.1021/bc400490z

[42] J.Y. Axup, K.M. Bajjuri, M. Ritland, B.M. Hutchins, C.H. Kim, S.A. Kazane, R. Halder, J.S. Forsyth, A.F. Santidrian, K. Stafin, Y. Lu, H. Tran, A.J. Seller, S.L. Biroc, A. Szydlik, J.K. Pinkstaff, F. Tian, S.C. Sinha, B. Felding-Habermann, V.V. Smider, P.G. Schultz, Synthesis of site-specific antibody-drug conjugates using unnatural amino acids, Proceedings of the National Academy of Sciences, 109, (2012), 16101. https://doi.org/10.1073/pnas.1211023109

[43] P. Bryant, M. Pabst, G. Badescu, M. Bird, W. McDowell, E. Jamieson, J. Swierkosz, K. Jurlewicz, R. Tommasi, K. Henseleit, X. Sheng, N. Camper, A. Manin, K. Kozakowska, K. Peciak, E. Laurine, R. Grygorash, A. Kyle, D. Morris, V. Parekh, A. Abhilash, J.-w. Choi, J. Edwards, M. Frigerio, M.P. Baker, A. Godwin, In Vitro and In Vivo Evaluation of Cysteine Rebridged Trastuzumab–MMAE Antibody Drug

Conjugates with Defined Drug-to-Antibody Ratios, Molecular Pharmaceutics, 12, (2015), 1872-1879. https://doi.org/10.1021/acs.molpharmaceut.5b00116

[44] C.R. Behrens, E.H. Ha, L.L. Chinn, S. Bowers, G. Probst, M. Fitch-Bruhns, J. Monteon, A. Valdiosera, A. Bermudez, S. Liao-Chan, T. Wong, J. Melnick, J.-W. Theunissen, M.R. Flory, D. Houser, K. Venstrom, Z. Levashova, P. Sauer, T.-S. Migone, E.H. van der Horst, R.L. Halcomb, D.Y. Jackson, Antibody–Drug Conjugates (ADCs) Derived from Interchain Cysteine Cross-Linking Demonstrate Improved Homogeneity and Other Pharmacological Properties over Conventional Heterogeneous ADCs, Molecular Pharmaceutics, 12, (2015), 3986-3998. https://doi.org/10.1021/acs.molpharmaceut.5b00432

[45] J. Ohata, Z.T. Ball, A Hexa-rhodium Metallopeptide Catalyst for Site-Specific Functionalization of Natural Antibodies, Journal of the American Chemical Society, 139, (2017), 12617-12622. https://doi.org/10.1021/jacs.7b06428

[46] S. Lin, X. Yang, S. Jia, A.M. Weeks, M. Hornsby, P.S. Lee, R.V. Nichiporuk, A.T. Iavarone, J.A. Wells, F.D. Toste, C.J. Chang, Redox-based reagents for chemoselective methionine bioconjugation, Science, 355, (2017), 597. https://doi.org/10.1126/science.aal3316

[47] A.R. Nanna, X. Li, E. Walseng, L. Pedzisa, R.S. Goydel, D. Hymel, T.R. Burke Jr, W.R. Roush, C. Rader, Harnessing a catalytic lysine residue for the one-step preparation of homogeneous antibody-drug conjugates, Nature Communications, 8, (2017), 1112. https://doi.org/10.1038/s41467-017-01257-1

[48] D. Schumacher, J. Helma, F.A. Mann, G. Pichler, F. Natale, E. Krause, M.C. Cardoso, C.P.R. Hackenberger, H. Leonhardt, Versatile and Efficient Site-Specific Protein Functionalization by Tubulin Tyrosine Ligase, Angewandte Chemie International Edition, 54, (2015), 13787-13791. https://doi.org/10.1002/anie.201505456

[49] P.M. Drake, A.E. Albers, J. Baker, S. Banas, R.M. Barfield, A.S. Bhat, G.W. de Hart, A.W. Garofalo, P. Holder, L.C. Jones, R. Kudirka, J. McFarland, W. Zmolek, D. Rabuka, Aldehyde Tag Coupled with HIPS Chemistry Enables the Production of ADCs Conjugated Site-Specifically to Different Antibody Regions with Distinct in Vivo Efficacy and PK Outcomes, Bioconjugate Chemistry, 25, (2014), 1331-1341. https://doi.org/10.1021/bc500189z

[50] T. Krüger, T. Dierks, N.J.B.c. Sewald, Formylglycine-generating enzymes for site-specific bioconjugation, Biological chemistry(2019), pp. 289-297.

[51] T. Krüger, S. Weiland, G. Falck, M. Gerlach, M. Boschanski, S. Alam, K.M. Müller, T. Dierks, N. Sewald, Two-fold Bioorthogonal Derivatization by Different Formylglycine-Generating Enzymes, Angewandte Chemie International Edition, 57, (2018), 7245-7249. https://doi.org/10.1002/anie.201803183

[52] V. Siegmund, B. Piater, B. Zakeri, T. Eichhorn, F. Fischer, C. Deutsch, S. Becker, L. Toleikis, B. Hock, U.A.K. Betz, H. Kolmar, Spontaneous Isopeptide Bond Formation as a Powerful Tool for Engineering Site-Specific Antibody-Drug Conjugates, Scientific Reports, 6, (2016), 39291. https://doi.org/10.1038/srep39291

[53] J. Grünewald, H.E. Klock, S.E. Cellitti, B. Bursulaya, D. McMullan, D.H. Jones, H.-P. Chiu, X. Wang, P. Patterson, H. Zhou, J. Vance, E. Nigoghossian, H. Tong, D. Daniel, W. Mallet, W. Ou, T. Uno, A. Brock, S.A. Lesley, B.H. Geierstanger, Efficient Preparation of Site-Specific Antibody–Drug Conjugates Using Phosphopantetheinyl Transferases, Bioconjugate Chemistry, 26, (2015), 2554-2562. https://doi.org/10.1021/acs.bioconjchem.5b00558

[54] R.R. Beerli, T. Hell, A.S. Merkel, U. Grawunder, Sortase Enzyme-Mediated Generation of Site-Specifically Conjugated Antibody Drug Conjugates with High In Vitro and In Vivo Potency, PLOS ONE, 10, (2015), e0131177. https://doi.org/10.1371/journal.pone.0131177

[55] L. Chen, J. Cohen, X. Song, A. Zhao, Z. Ye, C.J. Feulner, P. Doonan, W. Somers, L. Lin, P.R. Chen, Improved variants of SrtA for site-specific conjugation on antibodies and proteins with high efficiency, Scientific Reports, 6, (2016), 31899. https://doi.org/10.1038/srep31899

[56] Y. Xu, S. Jin, W. Zhao, W. Liu, D. Ding, J. Zhou, S. Chen, A Versatile Chemo-Enzymatic Conjugation Approach Yields Homogeneous and Highly Potent Antibody-Drug Conjugates, International Journal of Molecular Sciences, 18, (2017). https://doi.org/10.3390/ijms18112284

[57] J.J. Bruins, A.H. Westphal, B. Albada, K. Wagner, L. Bartels, H. Spits, W.J.H. van Berkel, F.L. van Delft, Inducible, Site-Specific Protein Labeling by Tyrosine Oxidation–Strain-Promoted (4 + 2)

Cycloaddition, Bioconjugate Chemistry, 28, (2017), 1189-1193. https://doi.org/10.1021/acs.bioconjchem.7b00046

[58] P. Strop, Versatility of Microbial Transglutaminase, Bioconjugate Chemistry, 25, (2014), 855-862. https://doi.org/10.1021/bc500099v

[59] M. Griffin, R. Casadio, C.M. Bergamini, Transglutaminases: nature's biological glues, The Biochemical journal, 368, (2002), 377-396. https://doi.org/10.1042/BJ20021234

[60] L. Deweid, O. Avrutina, H. Kolmar, Microbial transglutaminase for biotechnological and biomedical engineering, Biological chemistry(2018).

[61] G. Falck, M.K. Müller, Enzyme-Based Labeling Strategies for Antibody–Drug Conjugates and Antibody Mimetics, Antibodies, 7, (2018). https://doi.org/10.3390/antib7010004

[62] M.J. Arrizubieta, Transglutaminases, in: J. Polaina, A.P. MacCabe (Eds.) Industrial Enzymes: Structure, Function and Applications, Springer Netherlands, Dordrecht, (2007), pp. 567-581.

[63] A. Josten, L. Haalck, F. Spener, M. Meusel, Use of microbial transglutaminase for the enzymatic biotinylation of antibodies, Journal of Immunological Methods, 240, (2000), 47-54. https://doi.org/10.1016/S0022-1759(00)00172-1

[64] T.L. Mindt, V. Jungi, S. Wyss, A. Friedli, G. Pla, I. Novak-Hofer, J. Grünberg, R. Schibli, Modification of Different IgG1 Antibodies via Glutamine and Lysine using Bacterial and Human Tissue Transglutaminase, Bioconjugate Chemistry, 19, (2008), 271-278. https://doi.org/10.1021/bc700306n

[65] S. Jeger, K. Zimmermann, A. Blanc, J. Grünberg, M. Honer, P. Hunziker, H. Struthers, R. Schibli, Site-Specific and Stoichiometric Modification of Antibodies by Bacterial Transglutaminase, Angewandte Chemie International Edition, 49, (2010), 9995-9997. https://doi.org/10.1002/anie.201004243

[66] P. Dennler, A. Chiotellis, E. Fischer, D. Brégeon, C. Belmant, L. Gauthier, F. Lhospice, F. Romagne, R. Schibli, Transglutaminase-Based Chemo-Enzymatic Conjugation Approach Yields Homogeneous Antibody–Drug Conjugates, Bioconjugate Chemistry, 25, (2014), 569-578. https://doi.org/10.1021/bc400574z

[67] F. Lhospice, D. Brégeon, C. Belmant, P. Dennler, A. Chiotellis, E. Fischer, L. Gauthier, A. Boëdec, H. Rispaud, S. Savard-Chambard, A. Represa, N. Schneider, C. Paturel, M. Sapet, C. Delcambre, S. Ingoure, N. Viaud, C. Bonnafous, R. Schibli, F. Romagné, Site-Specific Conjugation of Monomethyl Auristatin E to Anti-CD30 Antibodies Improves Their Pharmacokinetics and Therapeutic Index in Rodent Models, Molecular Pharmaceutics, 12, (2015), 1863-1871. https://doi.org/10.1021/mp500666j

[68] J. Grünberg, S. Jeger, D. Sarko, P. Dennler, K. Zimmermann, W. Mier, R. Schibli, DOTA-Functionalized Polylysine: A High Number of DOTA Chelates Positively Influences the Biodistribution of Enzymatic Conjugated Anti-Tumor Antibody chCE7agl, PLOS ONE, 8, (2013), e60350. https://doi.org/10.1371/journal.pone.0060350

[69] S. Puthenveetil, S. Musto, F. Loganzo, L.N. Tumey, C.J. O'Donnell, E. Graziani, Development of Solid-Phase Site-Specific Conjugation and Its Application toward Generation of Dual Labeled Antibody and Fab Drug Conjugates, Bioconjugate Chemistry, 27, (2016), 1030-1039. https://doi.org/10.1021/acs.bioconjchem.6b00054

[70] D.N. Thornlow, E.C. Cox, J.A. Walker, M. Sorkin, J.B. Plesset, M.P. DeLisa, C.A. Alabi, Dual Site-Specific Antibody Conjugates for Sequential and Orthogonal Cargo Release, Bioconjugate Chemistry, 30, (2019), 1702-1710. https://doi.org/10.1021/acs.bioconjchem.9b00244

[71] S. Beck, J. Schultze, H.-J. Räder, R. Holm, M. Schinnerer, M. Barz, K. Koynov, R. Zentel, Site-Specific DBCO Modification of DEC205 Antibody for Polymer Conjugation, Polymers, 10, (2018). https://doi.org/10.3390/polym10020141

[72] Y. Anami, W. Xiong, X. Gui, M. Deng, C.C. Zhang, N. Zhang, Z. An, K. Tsuchikama, Enzymatic conjugation using branched linkers for constructing homogeneous antibody–drug conjugates with high potency, Organic & Biomolecular Chemistry, 15, (2017), 5635-5642. https://doi.org/10.1039/C7OB01027C

[73] M. Dorywalska, R. Dushin, L. Moine, S.E. Farias, D. Zhou, T. Navaratnam, V. Lui, A. Hasa-Moreno, M.G. Casas, T.-T. Tran, K. Delaria, S.-H. Liu, D. Foletti, C.J. Donnell, J. Pons, D.L. Shelton, A. Rajpal, P. Strop, Molecular Basis of Valine-Citrulline-PABC Linker Instability in Site-Specific ADCs and Its Mitigation by Linker Design, Molecular Cancer Therapeutics, 15, (2016), 958. https://doi.org/10.1158/1535-7163.MCT-15-1004

[74] Y. Anami, C.M. Yamazaki, W. Xiong, X. Gui, N. Zhang, Z. An, K. Tsuchikama, Glutamic acid–valine–citrulline linkers ensure stability and efficacy of antibody–drug conjugates in mice, Nature Communications, 9, (2018), 2512. https://doi.org/10.1038/s41467-018-04982-3

[75] D. Reusch, M.L. Tejada, Fc glycans of therapeutic antibodies as critical quality attributes, Glycobiology, 25, (2015), 1325-1334. https://doi.org/10.1093/glycob/cwv065

[76] P. Strop, S.-H. Liu, M. Dorywalska, K. Delaria, Russell G. Dushin, T.-T. Tran, W.-H. Ho, S. Farias, Meritxell G. Casas, Y. Abdiche, D. Zhou, R. Chandrasekaran, C. Samain, C. Loo, A. Rossi, M. Rickert, S. Krimm, T. Wong, Sherman M. Chin, J. Yu, J. Dilley, J. Chaparro-Riggers, Gary F. Filzen, Christopher J. O'Donnell, F. Wang, Jeremy S. Myers, J. Pons, David L. Shelton, A. Rajpal, Location Matters: Site of Conjugation Modulates Stability and Pharmacokinetics of Antibody Drug Conjugates, Chemistry & Biology, 20, (2013), 161-167. https://doi.org/10.1016/j.chembiol.2013.01.010

[77] S.E. Farias, P. Strop, K. Delaria, M. Galindo Casas, M. Dorywalska, D.L. Shelton, J. Pons, A. Rajpal, Mass Spectrometric Characterization of Transglutaminase Based Site-Specific Antibody–Drug Conjugates, Bioconjugate Chemistry, 25, (2014), 240-250. https://doi.org/10.1021/bc4003794

[78] M. Dorywalska, P. Strop, J.A. Melton-Witt, A. Hasa-Moreno, S.E. Farias, M. Galindo Casas, K. Delaria, V. Lui, K. Poulsen, C. Loo, S. Krimm, G. Bolton, L. Moine, R. Dushin, T.-T. Tran, S.-H. Liu, M. Rickert, D. Foletti, D.L. Shelton, J. Pons, A. Rajpal, Effect of Attachment Site on Stability of Cleavable Antibody Drug Conjugates, Bioconjugate Chemistry, 26, (2015), 650-659. https://doi.org/10.1021/bc5005747

[79] M. Dorywalska, P. Strop, J.A. Melton-Witt, A. Hasa-Moreno, S.E. Farias, M. Galindo Casas, K. Delaria, V. Lui, K. Poulsen, J. Sutton, G. Bolton, D. Zhou, L. Moine, R. Dushin, T.-T. Tran, S.-H. Liu, M. Rickert, D. Foletti, D.L. Shelton, J. Pons, A. Rajpal, Site-Dependent Degradation of a Non-Cleavable Auristatin-Based Linker-Payload in Rodent Plasma and Its Effect on ADC Efficacy, PLOS ONE, 10, (2015), e0132282. https://doi.org/10.1371/journal.pone.0132282

[80] N. Jain, S.W. Smith, S. Ghone, B. Tomczuk, Current ADC Linker Chemistry, Pharmaceutical Research, 32, (2015), 3526-3540. https://doi.org/10.1007/s11095-015-1657-7

[81] S. Panowski, S. Bhakta, H. Raab, P. Polakis, J.R. Junutula, Site-specific antibody drug conjugates for cancer therapy, mAbs, 6, (2014), 34-45. https://doi.org/10.4161/mabs.27022

[82] M.J. Costa, J. Kudaravalli, J.-T. Ma, W.-H. Ho, K. Delaria, C. Holz, A. Stauffer, A.G. Chunyk, Q. Zong, E. Blasi, B. Buetow, T.-T. Tran, K. Lindquist, M. Dorywalska, A. Rajpal, D.L. Shelton, P. Strop, S.-H. Liu, Optimal design, anti-tumour efficacy and tolerability of anti-CXCR4 antibody drug conjugates, Scientific Reports, 9, (2019), 2443. https://doi.org/10.1038/s41598-019-38745-x

[83] P. Strop, T.-T. Tran, M. Dorywalska, K. Delaria, R. Dushin, O.K. Wong, W.-H. Ho, D. Zhou, A. Wu, E. Kraynov, L. Aschenbrenner, B. Han, C.J. Donnell, J. Pons, A. Rajpal, D.L. Shelton, S.-H. Liu, RN927C, a Site-Specific Trop-2 Antibody–Drug Conjugate (ADC) with Enhanced Stability, Is Highly Efficacious in Preclinical Solid Tumor Models, Molecular Cancer Therapeutics, 15, (2016), 2698. https://doi.org/10.1158/1535-7163.MCT-16-0431

[84] O.K. Wong, T.-T. Tran, W.-H. Ho, M.G. Casas, M. Au, M. Bateman, K.C. Lindquist, A. Rajpal, D.L. Shelton, P. Strop, S.-H. Liu, RN765C, a low affinity EGFR antibody drug conjugate with potent anti-tumor activity in preclinical solid tumor models, Oncotarget, 9, (2018), 33446-33458. https://doi.org/10.18632/oncotarget.26002

[85] R.M. DeVay, K. Delaria, G. Zhu, C. Holz, D. Foletti, J. Sutton, G. Bolton, R. Dushin, C. Bee, J. Pons, A. Rajpal, H. Liang, D. Shelton, S.-H. Liu, P. Strop, Improved Lysosomal Trafficking Can Modulate the Potency of Antibody Drug Conjugates, Bioconjugate Chemistry, 28, (2017), 1102-1114. https://doi.org/10.1021/acs.bioconjchem.7b00013

[86] A.S. Ratnayake, L.-p. Chang, L.N. Tumey, F. Loganzo, J.A. Chemler, M. Wagenaar, S. Musto, F. Li, J.E. Janso, T.E. Ballard, B. Rago, G.L. Steele, W. Ding, X. Feng, C. Hosselet, V. Buklan, J. Lucas, F.E. Koehn, C.J. O'Donnell, E.I. Graziani, Natural Product Bis-Intercalator Depsipeptides as a New Class of Payloads for Antibody–Drug Conjugates, Bioconjugate Chemistry, 30, (2019), 200-209. https://doi.org/10.1021/acs.bioconjchem.8b00843

[87] G.L. Verdine, L.D. Walensky, The Challenge of Drugging Undruggable Targets in Cancer: Lessons Learned from Targeting BCL-2 Family Members, Clinical Cancer Research, 13, (2007), 7264. https://doi.org/10.1158/1078-0432.CCR-07-2184

[88] I.J. Huggins, C.A. Medina, A.D. Springer, A. van den Berg, S. Jadhav, X. Cui, S.F.J.M. Dowdy, Site Selective Antibody-Oligonucleotide Conjugation via Microbial Transglutaminase, Molecules, 24, (2019), 3287. https://doi.org/10.3390/molecules24183287
[89] W. Steffen, F.C. Ko, J. Patel, V. Lyamichev, T.J. Albert, J. Benz, M.G. Rudolph, F. Bergmann, T. Streidl, P. Kratzsch, M. Boenitz-Dulat, T. Oelschlaegel, M. Schraeml, Discovery of a microbial transglutaminase enabling highly site-specific labeling of proteins, Journal of Biological Chemistry, 292, (2017), 15622-15635. https://doi.org/10.1074/jbc.M117.797811
[90] V. Siegmund, S. Schmelz, S. Dickgiesser, J. Beck, A. Ebenig, H. Fittler, H. Frauendorf, B. Piater, U.A.K. Betz, O. Avrutina, A. Scrima, H.-L. Fuchsbauer, H. Kolmar, Locked by Design: A Conformationally Constrained Transglutaminase Tag Enables Efficient Site-Specific Conjugation, Angewandte Chemie International Edition, 54, (2015), 13420-13424. https://doi.org/10.1002/anie.201504851
[91] A. Ebenig, N.E. Juettner, L. Deweid, O. Avrutina, H.-L. Fuchsbauer, H. Kolmar, Efficient Site-Specific Antibody–Drug Conjugation by Engineering a Nature-Derived Recognition Tag for Microbial Transglutaminase, ChemBioChem, 0, (2019). https://doi.org/10.1002/cbic.201900101
[92] N.E. Juettner, S. Schmelz, J.P. Bogen, D. Happel, W.-D. Fessner, F. Pfeifer, H.-L. Fuchsbauer, A. Scrima, Illuminating structure and acyl donor sites of a physiological transglutaminase substrate from Streptomyces mobaraensis, Protein Science, 27, (2018), 910-922. https://doi.org/10.1002/pro.3388
[93] H. Schneider, L. Deweid, T. Pirzer, D. Yanakieva, S. Englert, B. Becker, O. Avrutina, H. Kolmar, Dextramabs: A Novel Format of Antibody-Drug Conjugates Featuring a Multivalent Polysaccharide Scaffold, ChemistryOpen, 8, (2019), 354-357. https://doi.org/10.1002/open.201900066
[94] E.E. Hong, H. Erickson, R.J. Lutz, K.R. Whiteman, G. Jones, Y. Kovtun, V. Blanc, J.M. Lambert, Design of Coltuximab Ravtansine, a CD19-Targeting Antibody–Drug Conjugate (ADC) for the Treatment of B-Cell Malignancies: Structure–Activity Relationships and Preclinical Evaluation, Molecular Pharmaceutics, 12, (2015), 1703-1716. https://doi.org/10.1021/acs.molpharmaceut.5b00175
[95] X. Sun, J.F. Ponte, N.C. Yoder, R. Laleau, J. Coccia, L. Lanieri, Q. Qiu, R. Wu, E. Hong, M. Bogalhas, L. Wang, L. Dong, Y. Setiady, E.K. Maloney, O. Ab, X. Zhang, J. Pinkas, T.A. Keating, R. Chari, H.K. Erickson, J.M. Lambert, Effects of Drug–Antibody Ratio on Pharmacokinetics, Biodistribution, Efficacy, and Tolerability of Antibody–Maytansinoid Conjugates, Bioconjugate Chemistry, 28, (2017), 1371-1381. https://doi.org/10.1021/acs.bioconjchem.7b00062
[96] H. Schneider, D. Yanakieva, A. Macarrón, L. Deweid, B. Becker, S. Englert, O. Avrutina, H. Kolmar, TRAIL-inspired multivalent dextran conjugates efficiently induce apoptosis upon DR5 receptor clustering, ChemBioChem, 0, (2019). https://doi.org/10.1002/cbic.201900251
[97] P.R. Spycher, C.A. Amann, J.E. Wehrmüller, D.R. Hurwitz, O. Kreis, D. Messmer, A. Ritler, A. Küchler, A. Blanc, M. Béhé, P. Walde, R. Schibli, Dual, Site-Specific Modification of Antibodies by Using Solid-Phase Immobilized Microbial Transglutaminase, ChemBioChem, 18, (2017), 1923-1927. https://doi.org/10.1002/cbic.201700188
[98] J.L. Spidel, B. Vaessen, E.F. Albone, X. Cheng, A. Verdi, J.B. Kline, Site-Specific Conjugation to Native and Engineered Lysines in Human Immunoglobulins by Microbial Transglutaminase, Bioconjugate Chemistry, 28, (2017), 2471-2484. https://doi.org/10.1021/acs.bioconjchem.7b00439
[99] J.L. Spidel, E.F. Albone, Efficient Production of Homogeneous Lysine-Based Antibody Conjugates Using Microbial Transglutaminase, in: S. Massa, N. Devoogdt (Eds.) Bioconjugation: Methods and Protocols, Springer New York, New York, NY, (2019), pp. 53-65.
[100] K. Terpe, Overview of tag protein fusions: from molecular and biochemical fundamentals to commercial systems, Applied Microbiology and Biotechnology, 60, (2003), 523-533. https://doi.org/10.1007/s00253-002-1158-6
[101] C. Wei, G. Zhang, T. Clark, F. Barletta, L.N. Tumey, B. Rago, S. Hansel, X. Han, Where Did the Linker-Payload Go? A Quantitative Investigation on the Destination of the Released Linker-Payload from an Antibody-Drug Conjugate with a Maleimide Linker in Plasma, Analytical Chemistry, 88, (2016), 4979-4986. https://doi.org/10.1021/acs.analchem.6b00976
[102] R.J. Christie, R. Fleming, B. Bezabeh, R. Woods, S. Mao, J. Harper, A. Joseph, Q. Wang, Z.-Q. Xu, H. Wu, C. Gao, N. Dimasi, Stabilization of cysteine-linked antibody drug conjugates with N-aryl maleimides, Journal of Controlled Release, 220, (2015), 660-670. https://doi.org/10.1016/j.jconrel.2015.09.032

[103] B. Böhme, B. Moritz, J. Wendler, T.C. Hertel, C. Ihling, W. Brandt, M. Pietzsch, Enzymatic activity and thermoresistance of improved microbial transglutaminase variants, Amino Acids, (2019). https://doi.org/10.1007/s00726-019-02764-9

[104] K. Yokoyama, H. Utsumi, T. Nakamura, D. Ogaya, N. Shimba, E. Suzuki, S. Taguchi, Screening for improved activity of a transglutaminase from Streptomyces mobaraensis created by a novel rational mutagenesis and random mutagenesis, Applied Microbiology and Biotechnology, 87, (2010), 2087-2096. https://doi.org/10.1007/s00253-010-2656-6

[105] L. Deweid, L. Neureiter, S. Englert, H. Schneider, J. Deweid, D. Yanakieva, J. Sturm, S. Bitsch, A. Christmann, O. Avrutina, H.-L. Fuchsbauer, H. Kolmar, Directed Evolution of a Bond-Forming Enzyme: Ultrahigh-Throughput Screening of Microbial Transglutaminase Using Yeast Surface Display, Chemistry – A European Journal, 24, (2018), 15195-15200. https://doi.org/10.1002/chem.201803485

[106] X. Zhao, A.C. Shaw, J. Wang, C.-C. Chang, J. Deng, J. Su, A Novel High-Throughput Screening Method for Microbial Transglutaminases with High Specificity toward Gln141 of Human Growth Hormone, Journal of Biomolecular Screening, 15, (2010), 206-212. https://doi.org/10.1177/1087057109356206

[107] S. Hu, L. Allen, Homogenous antibody drug conjugates via enzymatic methods, (2019), US10471037B10471032.

Table 2: Conjugation sites applied for mTG-generated ADCs.

Author	Year	Conjugation motif(s)	Native Glycosylation removal	Targeted antigen	Ref.
Steffen et al.	2017	HC C-terminal LLQGA, HC C-terminal GGGSYRQGGS	–	TSH	[89]
Dennler et al.	2014	Q295, Q297	PNGase F, N297Q	HER2/NEU	[66]
Lhospice et al.	2015	Q295, Q297	N297Q	CD30	[67]
Spidel et al.	2017	K447, engineered lysines	–	n.D.	[98]
Josten et al.	2000	Native lysines	–	2,4-D	[63]
Mindt et al.	2008	native Lysines(failed), Q295	N297Q	L1CAM	[64]
Jeger et al.	2010	Q295, Q297	PNGase F, N297Q	L1CAM	[65]
Grünberg et al.	2013	Q295, Q297	N297Q, N297A	L1CAM	[68]
Spycher et al.	2017	Q295, Q297, K288/290, K340	N297A, N297Q	CD30	[97]
Anami et al.	2017	Q295	N297A	HER2/NEU	[72]
Anami et al.	2018	Q295	N297A	HER2/NEU	[74]
Schneider et al.	2019	Q295	N297A	DR5	[96]
Schneider et al.	2019	HC C-terminal LLQG	–	HER2/NEU	[93]

Siegmund et al.	2016	GEN-, GEC-tag C-Terminus HC	–	EGFR/HER1	[52]
Ebenig et al.	2019	HC C-terminal (SPI7G) DIPIGQGMTG	–	HER2/NEU	[91]
Strop et al.	2013	12 sites (terminal or internal)	–	EGFR/HER1, HER2/NEU, TROP-2	[76]
Strop et al.	2015	LLQG inserted 135 HC, Q295, Q297, LC C-terminal GGLLQGA, HC C-terminal LLQGA	–	Trop-2/M1S1	[28]
Strop et al.	2016	HC C-terminal LLQGA	–	Trop-2/M1S1	[83]
Wong et al.	2018	LC C-terminal GGLLQGPP	N297Q, N297A	EGFR/HER1	[84]
Costa et al.	2019	LLQG inserted 135 HC, HC C-terminal LLQGA, LC C-terminal GGLLQGPP, Q295, Q297	N297A, N297Q	CXCR4	[82]
DeVay et al.	2017	LC C-terminal GGLLQGPP, Q295, Q297	N297Q	Trop-2/M1S1	[85]
Dorywalska et al.	2015	9 sites (terminal or internal)	N297A, N297Q	Trop-2/M1S1	[78]
Dorywalska et al.	2015	9 sites (terminal or internal)	N297A, N297Q	Trop-2/M1S1	[79]
Dorywalska et al.	2016	9 sites (terminal or internal)	N297A, N297Q	Trop-2/M1S1	[73]
Farias et al.	2013	LC C-terminal GGLLQGA, HC C-terminal LLQGA	natural observed aglycosylated, N297A	Trop-2/M1S1	[77]
Ratnayake et al.	2018	LC C-terminal GGLLQGA, Q295	–	HER2/NEU	[86]
Puthenveetil et al.	2016	Q295	PNGase F	HER2/NEU	[69]
Beck et al.	2019	Q295	PNGase F	DEC205/ CD205/ LY75	[71]
Thornlow et al.	2019	Q295	PNGase F	HER2/NEU	[70]

Abbreviations: 2,4-D, 2,4-dichlorophenoxyacetic; TSH, thyrotropin receptor; HER2/Neu, human epidermal growth factor receptor 2; CD3; DR5, death receptor 5, CXCR4, chemokine receptor type 4; EGFR, epidermal growth factor receptor; Trop-2 also known as TACSTD2, Tumor-associated calcium signal transducer 2; CD205, cluster of differentiation 205; LY75, Lymphocyte antigen 75.

Table 3: Cytotoxic payloads and linkers published for ADCs generated via mTG.

Mode of Action	Applied Toxins	References
DNA intercalator	NPBIDs: SW163D Luzopeptin A Sandramycin	[86]
Tubulin Inhibitor	MMAD	[28, 73, 76-79, 85]
	MMAE	[66, 67, 91, 93]
	MMAF	[72, 74]
	Aur0131	[82]
	Aur0101	[73, 78, 79, 82]
	Aur337	[79]
	Auristatin F	[98]
	PF-06380101	[83, 84]

Acyl donor side	Chemistry	References
PEGylated	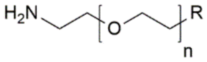	[28, 63, 66-70, 72, 74, 76, 77, 79, 82, 85, 91]
Non-PEGylated	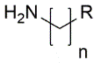	[63, 65-67, 71, 73, 76, 78, 82-84, 86, 93, 96]

Applied Linker	Chemistry	References
stable	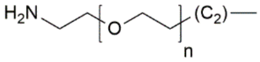	[28, 76, 77, 79, 82, 85]
cleavable	**Cathepsin B** (X)VC-PABC	[66, 67, 72-74, 76, 78, 82-84, 86, 91, 93, 96]
	MMP-2 PVGLIG	[70]

Chemoenzymatic Mechanism	Reaction handles	References
SPAAC	N_3; BCN; DBCO	[66, 67, 69-72, 74, 91, 93, 96]
Michael-Addition	thiol; Maleimide	[66]

Abbreviations: BCN, Bicyclononyne; DBCO, dibenzocyclooctyne; MMAD/E/F, monomethyl auristatin D/E/F; MMP-2, matrix metallo-proteinase II; NPBIDs, Natural Product Bis-Intercalator Depsipeptides; PABC, *p*-amino-benzyloxy-carbonyl; PEG, polyethylenglycol; VC, valine-citrulline; XVC, different R-groups on C2 position of valine-citrulline linker.

7.5. Efficient Site-Specific Antibody-Drug Conjugation by Engineering of a Nature-Derived Recognition Tag for Microbial Transglutaminase

Title:

Efficient Site-Specific Antibody-Drug Conjugation by Engineering of a Nature-Derived Recognition Tag for Microbial Transglutaminase

Authors:

Aileen Ebenig,* Norbert Egon Juettner,* Lukas Deweid,* Olga Avrutina, Hans-Lothar Fuchsbauer and Harald Kolmar

*These authors contributed equally to this work

Bibliographic data:

ChemBioChem

Volume 20, Issue 18, Pages 2411-2419

Article first published online: 2nd May 2019

DOI: https://doi.org/10.1002/cbic.201900101

Copyright: 2019 Wiley-VCH Verlag GmbH & Co. KGaA, Weinheim. Reproduced with permission.

Contributions by Lukas Deweid:

- Performed the described peptide kinetics
- Construction and biochemical analysis of antibody-drug conjugates
- Preparation of the manuscript and graphical material together with A. Ebenig and N. Juettner

ChemPubSoc Europe
DOI: 10.1002/cbic.201900101
CHEMBIOCHEM
Full Papers

Efficient Site-Specific Antibody–Drug Conjugation by Engineering a Nature-Derived Recognition Tag for Microbial Transglutaminase

Aileen Ebenig+,[a] Norbert Egon Juettner+,[b, c] Lukas Deweid+,[a] Olga Avrutina,[a] Hans-Lothar Fuchsbauer,[b] and Harald Kolmar*[a]

Microbial transglutaminase (mTG) has recently emerged as a powerful tool for antibody engineering. In nature, it catalyzes the formation of amide bonds between glutamine side chains and primary amines. Being applied to numerous research fields from material sciences to medicine, mTG enables efficient site-specific conjugation of molecular architectures that possess suitable recognition motifs. In monoclonal antibodies, the lack of native transamidation sites is bypassed by incorporating specific peptide recognition sequences. Herein, we report a rapid and efficient mTG-catalyzed bioconjugation that relies on a novel recognition motif derived from its native substrate Streptomyces papain inhibitor (SPI$_P$). Improved reaction kinetics compared to commonly applied sequences were demonstrated for model peptides and for biotinylation of Her2-targeting antibody trastuzumab variants. Moreover, an antibody–drug conjugate assembled from trastuzumab that was C-terminally tagged with the novel recognition sequence revealed a higher payload-antibody ratio than the reference antibody.

Introduction

In recent years, numerous antibody-engineering techniques have emerged that have extensive applications in the fields of immunology, biotechnology, diagnostics, and therapy. For example, site-specifically biotinylated or fluorophore-labeled antibodies are now common tools that enable specific visualization of proteins in a number of analytical platforms, among them western blot, ELISA, and flow cytometry.[1] Furthermore, synthetic antibody–drug conjugates (ADCs) have become useful tools for treating disease as they combine the specific binding of monoclonal antibodies (mAbs) with the cytotoxicity of a warhead. To enable the required covalent linkage, preferably at sites that do not interfere with function, a comprehensive toolbox of modification/conjugation methods has been established,[2] with the formation of amide bonds upon isothiocyanate- or succinimidyl-ester activation of carboxylates and thiol-ene coupling of maleimide-bearing payloads being the most prominent examples.[3] Despite having obvious advantages in view of high reactivity towards functional groups, chemical strategies possess some shortcomings owing to the lack of orthogonal addressability, which often leads to heterogeneous products with a broad spectrum of biophysical properties. As a consequence, particularly for pharmaceutical applications, site-specificity is desired. Several studies have reported increased stability, a prolonged half-life, and an improved therapeutic index of site-specifically modified drugs compared to conjugates obtained from statistical chemical distribution.[4] In addition, as the removal of undesired side products is often cumbersome and cost intensive,[5] restricting the reactivity of an organic compound to a single site within proteinaceous targets is obviously the preferred, if challenging, route for protein modification.

To date, a wide range of bond-forming enzymes has been applied to the site-specific modification/conjugation of biomacromolecules, among them phosphopantetheinyl transferase,[6] sortase A,[7] lipoic acid ligase,[8] SpyLigase,[9] or formylglycine-generating enzyme (FGE).[10] Microbial transglutaminase (mTG), a protein-glutamine g-glutamyl-transferase from Streptomyces mobaraensis, has recently been added to the toolbox of enzymatic bioconjugations due to its ability to form stable isopeptide bonds between the chemically inert g-carboxamide group of glutamine (acyl donor) and primary amines (acyl acceptor).[11] Its crosslinking activity is commonly used in the food processing industry to produce reconstructed meat[12] and to increase the texture of dairy products.[13] In biotechnology, multi-subunit protein hybrids, as well as protein–oligonucleotide, –polymer, or –small molecule conjugates were successfully assembled by applying mTG catalysis.[14] Though the enzyme is massively used for various applications, its native function and substrate specificity are still under discussion.[15]

---

[a] A. Ebenig,+ L. Deweid,+ Dr. O. Avrutina, Prof. Dr. H. Kolmar
Institute for Organic Chemistry and Biochemistry
Technische Universit-t Darmstadt
Alarich-Weiss-Strasse 4, 64287 Darmstadt (Germany)
E-mail: kolmar@Biochemie-TUD.de

[b] Dr. N. E. Juettner,+ Dr. H.-L. Fuchsbauer
Department of Chemical Engineering and Biotechnology
University of Applied Sciences Darmstadt
Stephanstrasse 7, 64295 Darmstadt (Germany)

[c] Dr. N. E. Juettner+
Department of Biology, Technische Universit-t Darmstadt
Schnittspahnstrasse 10, 64287 Darmstadt (Germany)

[+] These authors contributed equally to this work.

Supporting information and the ORCID identification numbers for the authors of this article can be found under https://doi.org/10.1002/cbic.201900101.

T 2019 Wiley-VCH Verlag GmbH & Co. KGaA, Weinheim

Although primary amines are promiscuously used,[16] the choice of corresponding glutamine substrate is strongly influenced by the properties of the neighboring amino acids[17] as well as by the secondary and tertiary structure of the addressed protein.[18] Interestingly, some proteins match these requirements and can be modified by mTG without any further incorporation of specific recognition motifs.[19]

Recently, the advantages of transglutaminase catalysis were applied to the production of ADCs, a promising class of hybrid drugs for the treatment of cancer through the covalent attachment of a chemotherapeutic cargo to a highly specific immunoglobulin. To this end, numerous methodologies for the site-specific modification of therapeutic antibodies by using either enzymatic or chemical strategies have been developed.[20] Though mTG promotes the modification of intrinsic glutamines within various protein substrates, no native glutamine residues in human IgG1 antibodies are recognized.[21] However, Jeger and co-workers found that aglycosylation of Asn297 in a therapeutic antibody exposes Gln295 as an efficient site for mTG-catalyzed transamidation.[22] An ADC that targets the cell-membrane protein CD30 was manufactured according to this technique and showed superior pharmacokinetics and pharmacodynamics in rodent models to the commercially available ADC Adcetris.[23]

As an alternative, the incorporation of specific recognition motifs is a flexible strategy that has been successfully applied to the modification of antibodies. Researchers from Rinat–Pfizer inserted an LLQG motif at 90 surface-exposed sites of an anti-epidermal growth-factor receptor (EGFR) mAb and identified 12 positions that enabled highly efficient labeling by using microbial transglutaminase catalysis.[24] Further studies of the same group showed that ADCs that were generated by using this site-specific approach possessed superior pharmacokinetics to their counterparts manufactured by conventional cysteine modification.[4b] Various other designed sequence tags have been described in recent years that allowed for site-specific target-protein labeling.[25]

Apart from the evident success of mTG applications in diverse fields, the physiological role of this enzyme in its host *S. mobaraensis* is barely understood. Nevertheless, over the past decades the reactivity of glutamine sites within intrinsic substrate proteins have been thoroughly investigated.[18a, b] Our recent research revealed a novel recognition sequence for microbial transglutaminase that was derived from its natural substrate dispase autolysis-inducing protein (DAIP). The C terminus of the heavy chain of the therapeutic antibody cetuximab was extended by the Gln298-containing region of DAIP and its native structure was mimicked by bracing through an intramolecular disulfide bridge between two engineered cysteines.[21] This conformationally locked sequence allowed the efficient mTG-mediated labeling of IgG1, thus making this motif a suitable recognition tag for the construction of homogeneous ADCs. *Streptomyces* papain inhibitor (SPI$_{P}$), another well characterized native mTG substrate, is a 12 kDa protein of unknown function, secreted by *S. mobaraensis*.[18a]

In this work, we investigated the substrate preference of mTG by using synthetic peptides derived from the sequences that surround naturally transamidated glutamine sites within SPI$_{P}$ or DAIP so as to develop efficient recognition motifs for protein labeling/conjugation. We mimicked and mutated the N-terminal region of SPI$_{P}$, which contains a single mTG-reactive acyl-donor site, Gln6. Modified sequences were fused C-terminally with therapeutic mAb trastuzumab. The performance of mTG was evaluated for peptidic and proteinaceous substrates by conjugating it with different linker constructs as acyl acceptors, applying both oligopeptide and antibody substrates (Scheme 1). The most potent recognition motif identified in biotinylation experiments was chosen for the construction of a Her2-targeting ADC by mTG-promoted modification followed by strain-promoted alkyne–azide cycloaddition (SPAAC). As a consequence of the superior coupling efficiency, toxin-armed trastuzumab was found to have more than ten times the potency on SK-BR-3 tumor cells of its counterpart tagged with the conventional recognition motif LLQG.

Results and Discussion

Substrate preferences of mTG evaluated on synthetic peptides

The reactivity of mTG is influenced by the surrounding amino acids and the structural arrangement of the targeted protein. We investigated seven oligopeptides that were derived from different natural sources or de-novo designed. Substrates **P1**–**P3** (Table 1) were derived from SPI$_{P}$, a natural substrate of mTG.[18a] Gln6, the only mTG-reactive glutamine residue of SPI$_{P}$ is located at the N terminus of the protein and has Lys7 in the +1 position. Juettner et al. demonstrated that the wild-type sequence is poorly modified by mTG but substituting Lys7 for glycine highly accelerated reactivity towards mTG[18a] and also avoided possible crosslinking of this sequence tag when in spatial proximity. Substrates **P4**–**P6** were derived from two different regions of DAIP, another *S. mobaraensis* mTG substrate protein. Gln39 and Gln298 of DAIP were shown to be efficiently biotinylated by mTG in the structural context of the protein.[18b] Mimicking the native loop bearing Gln298 resulted in superior biotinylation over a linear control.[21] Substrate **P7** is a rationally designed synthetic oligopeptide for mTG-mediated coupling.[24]

Table 1. Overview of compared mTG recognition sequences derived from natural protein substrates and de-novo-designed tags. **P4**, **P5**, and **P7** are published mTG recognition sequences and served as controls. The disulfide bridge in **P5** is indicated.

Number	Name	Sequence	Origin
P1	wtSPI	DIPIGQKMTG	SPI
P2	SPI7G	DIPIGQGMTG	SPI
P3	SPI7R	DIPIGQRMTG	SPI
P4	GEN	GENTYFQAYGNTE	DAIP
P5	GEC	GECTYF**Q**AYGCTE	DAIP
P6	9mer	TGTLQSVSY	DAIP
P7	LLQG	LLQG	de novo

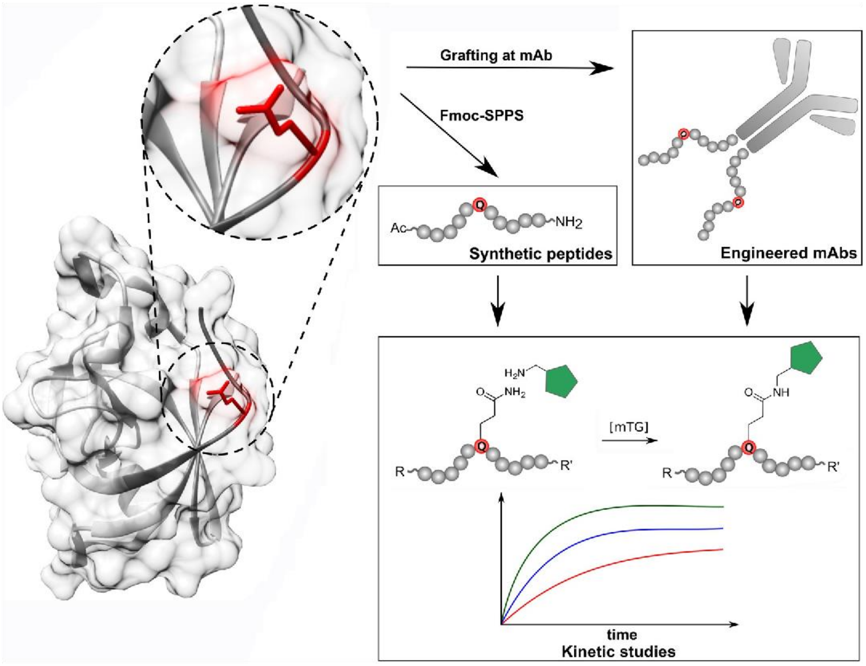

Scheme 1. General approach to efficient mTG tags. Peptides derived from sequences of natural mTG substrates were examined for their mTG reactivity as synthetic peptides and as recognition tags in engineered mAbs.

To investigate the substrate preference of mTG, peptides comprising the sequences that surround naturally transamidated glutamine sites were synthesized by Fmoc-SPPS. The N terminus was acetylated to mask the positively charged amine. The SPI$_p$-based motifs wtSPI (P1) and SPI7G (P2) were chosen as well as a Lys7Arg variant (P3) that resembles the Gln6 next to wild-type lysine both in structure and charge (Table 1). DAIP-derived sequences P4–P6, as well as the tetrapeptide P7 have been described before and were used as reference recognition sequences.[21,24,26]

The reactivity of mTG towards the substrate-derived sequences was studied by incubating the corresponding peptide and N-(biotinyl)cadaverine (1; see the Supporting Information for details) in the presence of mTG. After heat inactivation of the enzyme, the progress of the reaction was analyzed by HPLC (Figure 1). Peptides 9mer (P6) and SPI7G (P2) revealed $>80\%$ conversion after 60 min, whereas LLQG (P7) and disulfide-bridged GEC (P5) reached comparable results only after 120 min of incubation. Linear, DAIP-derived peptide GEN (P4) showed approximately 80% conversion after 180 min. Similar results were obtained for wtSPI (P1) and SPI7R (P3), thus indicating that substitution of Lys7 in SPI$_p$ by arginine had only minor effects on mTG reactivity. mTG-mediated coupling of NH_2-PEG_2-BCN (2; PEG = poly(ethylene glycol), BCN = bicyclononyne), which allows the post-translational modification of peptides and proteins by click chemistry, to peptides P1–P7 resulted in an overall slower turnover compared to the previously used model substrate 1. Again, P2 showed the highest turnover rate of $>95\%$ product formation after 180 min of reaction (Figure S16 in the Supporting Information).

mTG-mediated bioconjugation of engineered antibodies Ab1–Ab7 with bifunctional acyl acceptors

Substrate preferences of mTG evaluated on engineered antibodies

The different trastuzumab variants fused with the corresponding mTG tags were expressed in Expi293F cells and purified by protein A chromatography. Their reactivity upon mTG catalysis was studied by incubation of the antibody in presence of 1 and mTG (Figure 2). Product formation was visualized by western blot analysis and normalized to that of the overnight reaction of LLQG-decorated trastuzumab (Ab7), which was assessed as 100% conjugate yield.

Trastuzumab-SPI7G (Ab2) revealed superior labeling, reaching 110% biotinylation compared to Ab7 after 6 min and a maximum biotinylation of 120% after 12 min (Figure S17). This corresponds to a compound-to-antibody ratio (CAR) close to 2.0 (see below). Unlike in the peptide-based biotinylation assay, trastuzumab-SPI7R (Ab3) showed slightly slower but efficient reaction, reaching its maximum biotinylation of almost 120% after 30 min. The wild-type SPI-based antibody (trastuzumab-wtSPI, Ab1) showed efficient conversion, but decreasing biotinylation levels after 30 min (Figure S17, dark green curve). Only minor differences in the kinetics were observed between trastuzumab-GEN (Ab4) and trastuzumab-GEC (Ab5), which

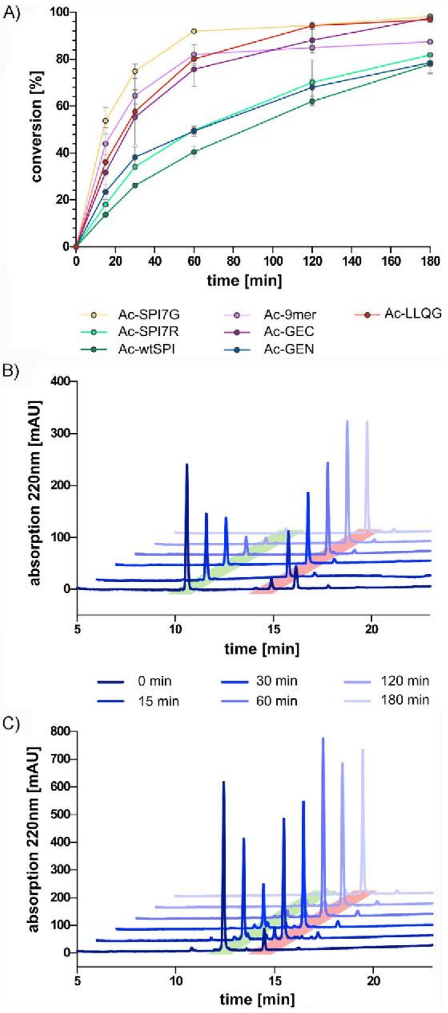

Figure 1. Comparison of the kinetics of mTG-mediated biotinylation for peptides P1–P7. The peptides were incubated in the presence of 1 and mTG at 378C. Samples were analyzed in triplicate by HPLC after different incubation times. A) Finally, the relative conversion for each peptide variant was plotted against the reaction time. HPLC analysis of mTG-promoted modification of B) P7 and C) P2 with 1 at different time points. Reactant peaks are labeled in green; product peaks are in red.

showed approximately 70% biotinylation after 120 min. Trastuzumab-9mer (Ab6) revealed almost 90% product formation after 6 min, but the terminal biotinylation was about 100% compared to the control, Ab7 (Figure S17). The four antibody variants that possessed highest biotinylation grades were further analyzed in triplicate, which confirmed previous results. However, Ab3 had slower reaction kinetics, reaching its maximum biotinylation after 60 min (Figure 3A). Comparison of Ab2 with a variant bearing the SPI7G tag at the C terminus of the light chain of trastuzumab (Ab8) revealed slightly increased labeling efficiency for the light-chain variant (Figure S18). Moreover, the stability of both biotinylated antibody variants (Ab2.1/Ab8.1) was evaluated in human serum and compared to that of the LLQG-bearing antibody (Ab7.1), as previously described by Toda et al.[27] After incubation of the antibody conjugates for 72 h at 378C, at least > 78% of the respective antibody conjugates remained intact, whereas 47% of Ab7.1 was recovered (Figure S19).

Chemoenzymatic synthesis of trastuzumab-based ADCs by applying an engineered mTG tag

Trastuzumab-SPI7G (Ab2), which revealed superior labeling in preliminary biotinylation experiments, was chosen for the construction of an ADC to further demonstrate the general applicability of our approach. A SPAAC-addressable BCN was conjugated to Ab7 or Ab2 by mTG. The BCN moiety allowed site-specific incorporation of monomethyl auristatin E by a copper-free cycloaddition through an azide-bearing linker as a second conjugation step. The BCN building block was decorated with a primary amine to make it addressable by microbial transglutaminase (Figure 2B). Following mTG-mediated condensation with successive isolation by protein A chromatography, modified antibodies were armed with the antimitotic agent monomethyl auristatin E for targeted tumor delivery, and the potency of each resulting conjugate was investigated on Her2-positive SK-BR-3 breast cancer cells.

To make the trastuzumab variants accessible for SPAAC, 2 was ligated to the corresponding recognition motif by mTG. Thus, engineered mAbs were modified with 2 in the presence of mTG for a limited incubation time (1 h), and the coupling efficiency was determined by hydrophobic interaction chromatography (HIC; Figure 4A). In the case of LLQG-tagged trastuzumab (Ab7.2), a CAR of 0.4 was obtained. Note: the low conjugation efficiency compared to previous experiments is most likely due to the fact that a different acyl-acceptor (amino-BCN vs. 1) was used and incubation time was restricted to one hour. Surprisingly, a approximately fivefold improved CAR of 1.95 was achieved when using the novel SPI7G-tag (Ab2.2). After overnight incubation, a comparable CAR of & 1.7 (data not shown) was obtained for both constructs; this indicated that rapid labeling efficiency is mediated by the newly introduced tag.

After purification of the antibodies by protein A chromatography, BCN-modified trastuzumab variants were equipped with N_3-PEG$_3$-vc-PAB-MMAE PAB = para-aminobenzyl, MMAE = monomethyl auristatin E (3) for targeted growth inhibition of Her2-positive tumor cells by SPAAC (Figure 4B). Upon HIC, a drug-to-antibody ratio (DAR) of 0.48 for the ADC assembled from trastuzumab-LLQG (Ab7.3) was calculated, whereas an approximately fourfold increased DAR of 1.81 was obtained for the SPI7G-tagged antibody (Ab2.3).

Flow cytometry was used to determine dissociation constants (K_D) on Her2-positive SK-BR-3 cells. No difference in K_D was observed upon chemoenzymatic modification of the antibodies. The K_D value of wild-type trastuzumab was determined to be 4.9 nm, whereas the toxin-loaded antibody variants revealed K_D values of 5.5 (Ab2.3) and 8.0 nm (Ab7.3; Figure S20).

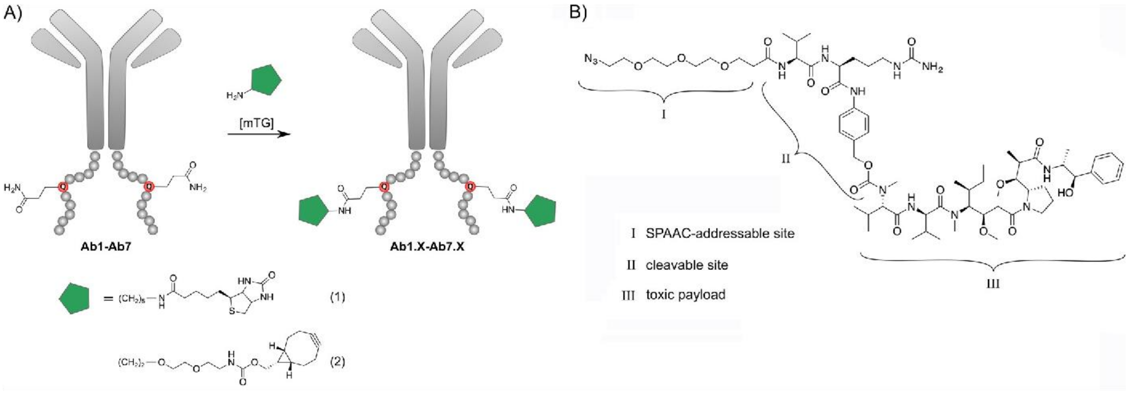

Figure 2. A) mTG-mediated bioconjugation of engineered antibodies Ab1–Ab7 with bifunctional acyl acceptors. B) Chemical structure of a cytotoxic payload with functional elements indicated.

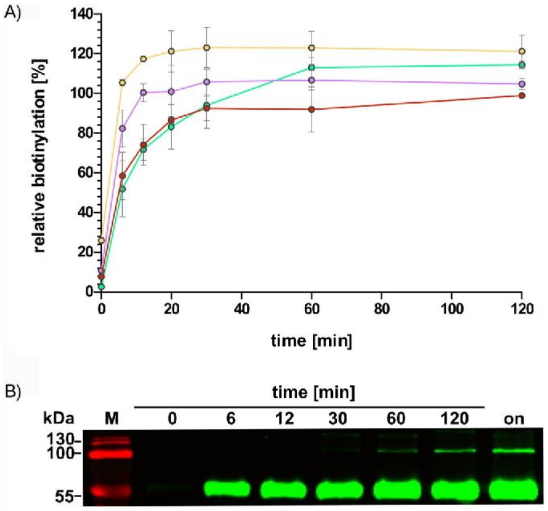

Figure 3. The kinetics of mTG-mediated biotinylation of trastuzumab variants with the corresponding mTG recognition sites (● :Ab2, ● :Ab3, ● :Ab6, ● :Ab7). The antibodies were incubated in the presence of 1 and mTG at 378C. Aliquots were analyzed after different incubation times by reducing SDS-PAGE and western blotting by using a fluorescent IRDye 800CW streptavidin conjugate in combination with the Odyssey Sa Infrared Imaging System. A) The degree of biotinylation was normalized to that of the overnight reaction of trastuzumab-LLQG and plotted against the time. mTG reactivity was analyzed in triplicate. B) Western blot of the conjugation reaction of trastuzumab-wtSPI (Ab1) showed heavy-chain–heavy-chain dimer formation.

Synthetic antibody–drug conjugates Ab2.3 and Ab7.3 were investigated in cell-proliferation assays to determine their cytotoxicity and specificity towards different cell lines. The ADCs were incubated with cells for 72 h before cell viability was evaluated by standard MTS assay. For Her2-negative CHO-K1 cells, none of the investigated constructs showed growth inhibition up to the highest applied concentration. Compared to the wild-type trastuzumab, Ab2.3 mediated efficient cell killing of Her2-overexpressing SK-BR-3 cells. Thus, the IC_{50} value of Ab2.3 was determined to be 151 pm, whereas Ab7.3 showed a 12.6-fold higher IC_{50} value of 1.9 nm on the same cell line. However, the observed improved cell toxicity of Ab2.3 resulted solely from higher achieved DAR (Figure 5).

Discussion

Though widely used in numerous scientific and industrial applications, microbial transglutaminase as a tool for protein modification often suffers from suboptimal enzymatic efficacy as its performance is significantly influenced by the spatial arrangement of the addressed target and the chemical nature of the payload used. Consequently, specific motifs of peptidic nature that are able to assure proper modification by mTG catalysis are strongly desired. We examined multiple recognition sequences from intrinsic mTG substrates for their accessibility for mTG, both as solitaire peptides and as an amendment to the C terminus of the heavy chain of the therapeutic antibody trastuzumab.

Synthetic peptide wtSPI (P1) derived from *Streptomyces* papain inhibitor, revealed only moderate conversion (& 70%) after 180 min. Biotinylation of the trastuzumab variant (Ab1) proceeded insufficiently, most likely as a result of heavy-chain–heavy-chain dimerization (Figure 3B). This is in line with previous observations, as lysine residues next to the addressed glutamine site are reported to disrupt mTG activity.[17a,18a] Peptide SPI7R (P3), which has a Lys7Arg substitution, revealed scanty modification by mTG; this corroborates previous data.[17a,18a] Surprisingly, antithetic results were obtained when the sequence was fused to the therapeutic antibody trastuzumab (Ab3). Accelerated biotinylation and an enhanced activity compared to the LLQG-bearing reference (Ab7) were observed.

In our group's previous work, substitution of Lys7 by glycine efficiently modified SPI_p in the structural context of the native protein.[18a] Similar results were obtained in this study: an SPI7G-tagged trastuzumab (Ab2) was labeled remarkably efficiently, and the corresponding peptide revealed rapid con-

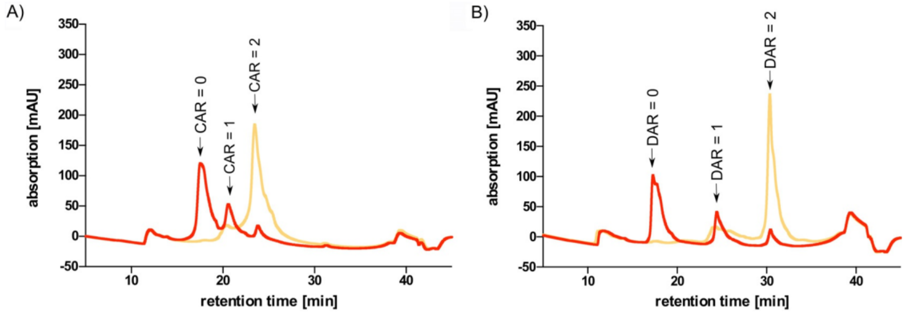

Figure 4. Determination of CAR and DAR of modified trastuzumab variants by HIC. Antibodies (—: **Ab2**, —: **Ab7**) were incubated at 37 °C with **2** in the presence of mTG. A) After 1 h, the reaction was terminated by the addition of a mTG inhibitor, and the antibody (**Ab2.2**, **Ab7.2**) was purified by protein A spin column. B) Subsequently, BCN-modified antibodies were incubated with azide-bearing MMAE, and the final ADC (**Ab2.3**, **Ab7.3**) was purified by protein A spin column.

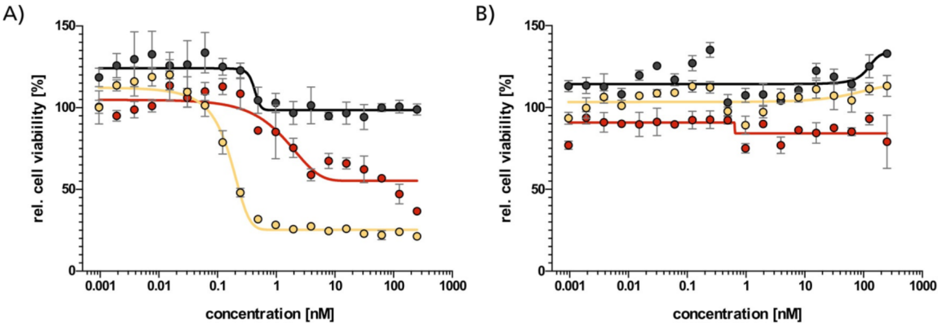

Figure 5. In vitro cell toxicity of trastuzumab–MMAE conjugates on A) Her2-positive SK-BR-3 cells and B) Her2-negative CHO-K1 cells. Cells were seeded in 96-well plates. After 24 h, cells were treated with different concentrations of trastuzumab-LLQG (—), trastuzumab-SPI7G (—), or the antibody alone (—). After another 72 h of incubation, triplicates of each concentration were analyzed by standard cell-proliferation assay (Promega). Normalized values were plotted against the concentration, and the IC_{50} value was calculated by using GraphPad Prism 5. The IC_{50} value of **Ab2.3** was determined to be 151 pm, whereas **Ab7.3** had an IC_{50} value of 1.9 nm.

sumption, >90% after 60 min. Fiebig and co-workers claimed that small amino acids in close proximity to the addressed glutamine site accelerate the modification of proteinaceous targets.[18b] With its addressable glutamine flanked by two glycine residues, substrate SPI7G supports this assumption. DAIP-derived peptide sequence **Ab6** mediated biotinylation of trastuzumab in a comparable manner to **Ab7**, but turnover of the respective peptide **P6** stagnated after 60 min for unknown reasons. Disulfide-bridged peptide GEC (**P5**) was properly labeled and mediated modification that proceeded faster than the linear GEN counterpart (**P4**). These observations confirm previous studies.[21] Fusion of both motifs to trastuzumab (**Ab4**, **Ab5**) led to an almost similar labeling efficiency of ≈80% biotinylation after 180 min, thus indicating that proper disulfide bond formation within the GEC tag did not occur during protein expression.

Surprisingly, although the majority of our results corroborated antecedent studies, some findings contradicted those concerning motifs identified in intrinsic substrate proteins or predicted by library screening. Thus, Gln39 of DAIP was strongly biotinylated when located within the protein (loop region),[18b] but revealed only moderate modification when grafted at the C terminus of a therapeutic immunoglobulin. Mimicking the native pattern of the Gln298-containing loop by introducing an intramolecular disulfide accelerated peptide consumption in comparison to a linear counterpart.[21] However, no beneficial effect was observed when the motif was grafted at an antibody. In contrast, SPI7R was efficiently conjugated, being fused to an antibody, but poorly accepted by mTG as a linear oligopeptide. These findings support the hypothesis that modification of glutamine sites by the microbial enzyme is influenced by a combination of different parameters, among them the properties of the surrounding amino acids as well as the spatial arrangement of the targeted protein.

Nonetheless, we successfully grafted recognition sequences from intrinsic transglutaminase substrates that enabled remarkably fast modification of trastuzumab. Motif SPI7G mediated highly efficient biotinylation of immunoglobulin as well as the introduction of a SPAAC-reactive site, thus enabling chemoenzymatic synthesis of an ADC equipped with a cytotoxic module for targeted tumor therapy. HIC revealed fourfold improved labeling of trastuzumab-SPI7G (**Ab2.2**) compared to the LLQG-tagged counterpart (Ab7.2). An MMAE-armed ADC assembled by SPAAC induced a more than tenfold increased DAR-dependent growth inhibition of Her2-positive cells. A significantly reduced reaction time required for the efficient modification of trastuzumab-SPI7G (Ab2) is an advantageous trait over traditionally applied sequences. From an antibody-manufacturing perspective, a short reaction time at 378C is desired to minimize any thermal stress that might contribute to protein aggregation and particularly deamidation or oxidation, protein modifications that might lay the ground work for unwanted immunogenicity issues.[28] Thus, faster reaction kinetics would be particularly useful for ADCs that are prone to aggregation upon extended incubation at 378C. For example, we observed some aggregation of aglycosylated trastuzumab upon overnight reaction at 378C (data not shown).

The substrate specificity of mTG is still not fully understood, but our results clearly demonstrate that grafting recognition sequences mediating efficient protein labeling from intrinsic transglutaminase substrates is a fruitful approach. Investigation of promising sequences in a peptide-based assay turned out to be a time- and cost-effective strategy to pre-evaluate potential hit candidates as solid-phase peptide synthesis and HPLC analysis operate in a fully automated manner. Nevertheless, a careful case-to-case evaluation is necessary because the modification of peptidic substrates and full-length proteins by mTG differs in some situations. Interestingly, as mTG transamidates some native glutamine sites in various targets, examining the reactive residues of unrelated proteins could yield powerful recognition tags. Our results illustrate a straightforward approach for the identification of potent motifs towards mTG-assisted bioconjugation and might contribute to the tightly controlled and cost-effective construction of ADCs for targeted cancer therapy.

Experimental Section

Materials: All chemicals and solvents for automated peptide synthesis, analysis and isolation were purchased from Iris Biotech, Agilent Technologies, Sigma–Aldrich, Roth and Thermo Fisher Scientific. They were used without further purification. Microbial transglutaminase from S. mobaraensis was produced as described previously.[29] N-(Biotinyl)cadaverine was purchased from Zedira (Darmstadt, Germany). N_3-PEG_3-vc-PAB-MMAE was purchased from MedChemExpress (Sollentuna, Sweden). N-[(1R,8S,9S)-Bicyclo[6.1.0]non-4-yn-9-ylmethyloxycarbonyl]-1,8-diamino-3,6-dioxaoctane (2) was purchased from Sigma–Aldrich. mTG-Blocker C102 was purchased from Zedira.

Solid-phase peptide synthesis: All peptides were synthesized as previously described[21] on AmphiSpheres 40 RAM resin (0.3 mmol g$^{@1}$, Agilent) by using microwave-assisted Fmoc SPPS in a Liberty blue Microwave Peptide Synthesizer on a 0.1 mmol scale.[21] Peptides' N termini were acetylated by using CH_2Cl_2 (10 mL, 50% (v/v)), acetic anhydride (30%, v/v), and N,N-diisopropylethylamine (20%, v/v) for 30 min at room temperature.

RP-HPLC: Peptides were analyzed by analytical RP-HPLC by using an Infinity 1100 (Agilent) system and an Agilent Eclipse Plus C_{18} column (4.6V100 mm, 3.5 mn, 95 a). Peptides were isolated by preparative RP-HPLC (PuriFlash 4250) on an Interchim C_{18}-HQ column (250V21.2 mm, 5 mn, 100 a) by using 0.1% aq. TFA (eluent A) and 90% aq. MeCN, 0.1% TFA (eluent B).

ESI-MS analysis: ESI mass analysis was performed on a Shimadzu LCMS-2020 equipped with a Phenomenex synergi 4u Hydro-RP C_{18} LC column (4.6V250 mm, 4 mn, 80 a) by using 0.1% aq. formic acid (eluent A) and acetonitrile containing 0.1% formic acid (eluent B).

Antibody expression and purification: All plasmids coding for either trastuzumab wild type (heavy and light chain) or variants containing C-terminal transglutaminase tags at the heavy chain were prepared by standard PCR techniques. The templates were kindly provided by Merck (Darmstadt, Germany). The C-terminal Lys447 was always omitted to avoid dimerization of the antibodies. Antibodies were transiently expressed in Expi293F cells by PEI transfection. Conditioned supernatants were applied on HiTrap Protein A HP 1 mL (GE Healthcare) columns and washed with sodium phosphate (20 mm, pH 7.0). Proteins were eluted with citrate buffer (100 mm, pH 3.0) and neutralized with Tris·HCl (1 m, pH 9.0). Eluted proteins were concentrated and rebuffered in PBS (pH 7.4) by using Amicon Ultra centrifugal filters and stored at @808C.

Peptide modification assay: Peptides were dissolved at DMSO (20 mm) and adjusted to a final concentration of 400 mm in PBS (pH 7.4). The peptides were incubated with acyl-acceptor substrate (5 mol equiv) and mTG (1/5000 mol equiv) at 378C. Aliquots were analyzed after 0, 15, 30, 60, 120, and 180 min. The reaction was stopped by heat inactivation at 958C for 10 min. Subsequently, the enzyme was removed by centrifugation dialysis (Microcon-10, 10.000 NMWL, Merck Millipore). Aliquots were analyzed by RP-HPLC by using a gradient from 10 to 60% eluent B (90% aq. MeCN) over 20 min at 0.6 mL min$^{@1}$. A final concentration of 2% (v/v) DMSO within the reaction mixture was not exceeded.

Transglutaminase-mediated modification of antibodies: Antibodies (adjusted to 0.5 mm) were incubated with 1 (60 mol equiv per conjugation site) and transglutaminase (0.07 mm) in Tris·HCl (50 mm, pH 8.0) containing NaCl (100 mm) at 378C. Aliquots of the reaction mixture were collected after 0, 6, 12, 20, 30, 60, 120 min and 16 h and supplemented with hot SDS loading dye. The reactions were analyzed by 15% reducing SDS-PAGE, and biotinylated heavy chains were visualized by semidry western blot by using fluorescent IRDye 800CW streptavidin conjugate in combination with the Odyssey Sa Infrared Imaging System. The degree of biotinylation was normalized to that of the overnight reaction of trastuzumab-LLQG, which was defined as 100% biotinylation.

To make antibodies accessible for SPAAC, mAbs (1 mg mL$^{@1}$) was incubated at 378C and 600 rpm in the presence of 2 (60 equiv) and mTG (0.01 mol equiv) in PBS (pH 7.4). After 1 h of reaction, MTG-Blocker C102 (20 mm; Zedira) was added to suppress transglutaminase activity. The modified antibody was separated from the remaining NH_2-PEG_2 reagents by protein A HP SpinTrap according to the manufacturer's instructions.

Strain-promoted alkyne–azide cycloaddition (SPAAC): BCN-modified antibodies were armed for targeted cell delivery by SPAAC as followed. BCN-modified mAb (3 mg mL$^{@1}$) was incubated with N_3-PEG_3-vc-PAB-MMAE 3 (5 equiv; Section 2 in the Supporting Information) per site for 16 h at 228C in PBS (pH 7.4). The final ADC was purified by protein A HP SpinTrap according to the manufacturer's instructions.

Hydrophobic interaction chromatography: HIC was performed to determine the coupling efficiencies of mTG-mediated antibody modification and SPAAC. An HPLC 1260 Infinity device (Agilent Technologies) was equipped with TSKgel butyl-NPR, 2.5 mm, 4.6 mmV3.5 cm (Tosoh Bioscience). Conjugates were separated with linear gradient of 0 to 100% B over 45 min (eluent A: 1.5m ammonium sulfate, 25 mm Tris·HCl, pH 7.5; eluent B: 25 mm Tris·HCl, pH 7.5). CARs were calculated from the area under the peak of the corresponding species.

Stability evaluation for antibody conjugates in human serum: Biotinylated antibody conjugates in PBS were mixed with an equal volume of human serum on ice. Subsequently the mixtures were incubated at 378C for 72 h. Aliquots were collected after 0, 24, 48, and 72 h and stored at @808C until SDS-PAGE and western blot analysis. The half-life of the respective trastuzumab variant was calculated by using GraphPad Prism.

Cell binding experiments: Cell binding experiments were performed by using Her2-overexpressing SK-BR-3 and Her2-negative CHO-K1 cells in combination with flow cytometry. Washing and incubation steps were performed on ice with PBS (pH 7.4) containing 1% BSA. 2V10^5 viable cells (vc)/well were incubated with the respective antibody conjugate (250 nm). Goat anti-human IgG (Fab specific), FITC-conjugated antibody (Sigma, dilution 1:20) was used to detect bound antibody at the cell surface. Cell fluorescence was determined by using a BD Influx cell sorter and BD FACS Software with detection of 1V10^4 events. To determine the dissociation constant (K_D) on Her2-positive SK-BR-3 cells, serial dilutions (1:2) between 250 and 0.49 nm were analyzed by using flow cytometry.

Cytotoxicity assay: Her2-positive SK-BR-3 cells were seeded with a cell density of 6V10^3 vc/well in a 96-well plate. For Her2-negative CHO-K1 cells, a cell density of 5V10^3 vc/well was used. The day after, cells were treated with serial dilutions (1:2) of between 0.9 pm and 250 nm of the respective antibody conjugate and incubated for three days at 378C under 5% CO_2. Cell viability was investigated by using a CellTiter96 AQ$_{ueous}$ One Solution Cell Proliferation Assay (Promega) according to the manufacturer's instructions.

Acknowledgements

This work was supported by a NANOKAT II grant from the Bundesministerium fer Bildung und Forschung (BMBF).

Conflict of Interest

The authors declare no conflict of interest.

Keywords: antibody–drug conjugates · bioconjugation · microbial transglutaminase · protein labeling

[1] a) S. Vira, E. Mekhedov, G. Humphrey, P. S. Blank, Anal. Biochem. 2010, 402, 146–150; b) R. P. Haugland, Curr. Protoc. Cell Biol. 2000, 6, 16.5.1–16.5.22.
[2] Chemoselective and Bioorthogonal Ligation Reactions: Concepts and Applications, Vol. 2 (Eds.: W. R. Algar, P. Dawson, I. L. Medintz), Wiley-VCH, Weinheim, 2017.
[3] C. P. Toseland, J. Chem. Biol. 2013, 6, 85–95.
[4] a) J. R. Junutula, H. Raab, S. Clark, S. Bhakta, D. D. Leipold, S. Weir, Y. Chen, M. Simpson, S. P. Tsai, M. S. Dennis, Y. Lu, Y. G. Meng, C. Ng, J. Yang, C. C. Lee, E. Duenas, J. Gorrell, V. Katta, A. Kim, K. McDorman, K. Flagella, R. Venook, S. Ross, S. D. Spencer, W. L. Wong, H. B. Lowman, R. Vandlen, M. X. Sliwkowski, R. H. Scheller, P. Polakis, W. Mallet, Nat. Biotechnol. 2008, 26, 925–932; b) P. Strop, K. Delaria, D. Foletti, J. M. Witt, A. Hasa-Moreno, K. Poulsen, M. G. Casas, M. Dorywalska, S. Farias, A. Pios, V. Lui, R. Dushin, D. Zhou, T. Navaratnam, T. T. Tran, J. Sutton, K. C. Lindquist, B. Han, S. H. Liu, D. L. Shelton, J. Pons, A. Rajpal, Nat. Biotechnol. 2015, 33, 694–696.
[5] G. T. Hermanson, Bioconjugate Techniques, Academic Press, San Diego, 2013.
[6] J. Grenewald, H. E. Klock, S. E. Cellitti, B. Bursulaya, D. McMullan, D. H. Jones, H. P. Chiu, X. Wang, P. Patterson, H. Zhou, J. Vance, E. Nigoghossian, H. Tong, D. Daniel, W. Mallet, W. Ou, T. Uno, A. Brock, S. A. Lesley, B. H. Geierstanger, Bioconjugate Chem. 2015, 26, 2554–2562.
[7] B. Valldorf, H. Fittler, L. Deweid, A. Ebenig, S. Dickgiesser, C. Sellmann, J. Becker, S. Zielonka, M. Empting, O. Avrutina, H. Kolmar, Angew. Chem. Int. Ed. 2016, 55, 5085–5089; Angew. Chem. 2016, 128, 5169–5173.
[8] M. Best, A. Degen, M. Baalmann, T. T. Schmidt, R. Wombacher, ChemBioChem 2015, 16, 1158–1162.
[9] V. Siegmund, B. Piater, B. Zakeri, T. Eichhorn, F. Fischer, C. Deutsch, S. Becker, L. Toleikis, B. Hock, U. A. Betz, H. Kolmar, Sci. Rep. 2016, 6, 39291.
[10] S. Dickgiesser, N. Rasche, D. Nasu, S. Middel, S. Horner, O. Avrutina, U. Diederichsen, H. Kolmar, ACS Chem. Biol. 2015, 10, 2158–2165.
[11] L. Deweid, L. Neureiter, S. Englert, H. Schneider, J. Deweid, D. Yanakieva, J. Sturm, S. Bitsch, A. Christmann, O. Avrutina, H. L. Fuchsbauer, H. Kolmar, Chem. Eur. J. 2018, 24, 15195–15200.
[12] D. Santhi, A. Kalaikannan, P. Malairaj, S. A. Prabhu, Crit. Rev. Food Sci. Nutr. 2017, 57, 2071–2076.
[13] S. M. Taghi Gharibzahedi, M. Koubaa, F. J. Barba, R. Greiner, S. George, S. Roohinejad, Int. J. Biol. Macromol. 2018, 107, 2364–2374.
[14] L. Deweid, O. Avrutina, H. Kolmar, Biol. Chem. 2019, 400, 257–274.
[15] S. Zindel, V. Ehret, M. Ehret, M. Hentschel, S. Witt, A. Kramer, D. Fiebig, N. Juttner, S. Frols, F. Pfeifer, H. L. Fuchsbauer, PLoS One 2016, 11, e0149145.
[16] M. T. Gundersen, J. W. Keillor, J. N. Pelletier, Appl. Microbiol. Biotechnol. 2014, 98, 219–230.
[17] a) M. Malesevic, A. Migge, T. C. Hertel, M. Pietzsch, ChemBioChem 2015, 16, 1169–1174; b) Y. Sugimura, K. Yokoyama, N. Nio, M. Maki, K. Hitomi, Arch. Biochem. Biophys. 2008, 477, 379–383.
[18] a) N. E. Juettner, S. Schmelz, J. P. Bogen, D. Happel, W. D. Fessner, F. Pfeifer, H. L. Fuchsbauer, A. Scrima, Protein Sci. 2018, 27, 910–922; b) D. Fiebig, S. Schmelz, S. Zindel, V. Ehret, J. Beck, A. Ebenig, M. Ehret, S. Frols, F. Pfeifer, H. Kolmar, H. L. Fuchsbauer, A. Scrima, J. Biol. Chem. 2016, 291, 20417–20426; c) N. E. Juettner, S. Schmelz, A. Kraemer, S. Knapp, B. Becker, H. Kolmar, A. Scrima, H. L. Fuchsbauer, FEBS J. 2018, 285, 4684–4694.
[19] J. Buchardt, H. Selvig, P. F. Nielsen, N. L. Johansen, Biopolymers 2010, 94, 229–235.
[20] D. Y. Jackson, Org. Process Res. Dev. 2016, 20, 852–866.
[21] V. Siegmund, S. Schmelz, S. Dickgiesser, J. Beck, A. Ebenig, H. Fittler, H. Frauendorf, B. Piater, U. A. Betz, O. Avrutina, A. Scrima, H. L. Fuchsbauer, H. Kolmar, Angew. Chem. Int. Ed. 2015, 54, 13420–13424; Angew. Chem. 2015, 127, 13618–13623.
[22] S. Jeger, K. Zimmermann, A. Blanc, J. Grunberg, M. Honer, P. Hunziker, H. Struthers, R. Schibli, Angew. Chem. Int. Ed. 2010, 49, 9995–9997; Angew. Chem. 2010, 122, 10191–10194.
[23] F. Lhospice, D. Bregeon, C. Belmant, P. Dennler, A. Chiotellis, E. Fischer, L. Gauthier, A. Boedec, H. Rispaud, S. Savard-Chambard, A. Represa, N. Schneider, C. Paturel, M. Sapet, C. Delcambre, S. Ingoure, N. Viaud, C. Bonnafous, R. Schibli, F. Romagne, Mol. Pharm. 2015, 12, 1863–1871.
[24] P. Strop, S. H. Liu, M. Dorywalska, K. Delaria, R. G. Dushin, T. T. Tran, W. H. Ho, S. Farias, M. G. Casas, Y. Abdiche, D. Zhou, R. Chandrasekaran, C. Samain, C. Loo, A. Rossi, M. Rickert, S. Krimm, T. Wong, S. M. Chin, J. Yu, J. Dilley, J. Chaparro-Riggers, G. F. Filzen, C. J. O'Donnell, F. Wang, J. S. Myers, J. Pons, D. L. Shelton, A. Rajpal, Chem. Biol. 2013, 20, 161–167.
[25] a) W. Steffen, F. C. Ko, J. Patel, V. Lyamichev, T. J. Albert, J. Benz, M. G. Rudolph, F. Bergmann, T. Streidl, P. Kratzsch, M. Boenitz-Dulat, T. Oelschlaegel, M. Schraeml, J. Biol. Chem. 2017, 292, 15622–15635; b) P. Dennler, L. K. Bailey, P. R. Spycher, R. Schibli, E. Fischer, ChemBioChem 2015, 16, 861–867; c) S. K. Oteng-Pabi, C. Pardin, M. Stoica, J. W. Keillor, Chem. Commun. 2014, 50, 6604–6606.
[26] Y. Tanaka, Y. Tsuruda, M. Nishi, N. Kamiya, M. Goto, Org. Biomol. Chem. 2007, 5, 1764–1770.

[27] N. Toda, S. Asano, C. F. Barbas III, Angew. Chem. Int. Ed. 2013, 52, 12592–12596; Angew. Chem. 2013, 125, 12824–12828.
[28] Q. Luo, M. K. Joubert, R. Stevenson, R. R. Ketchem, L. O. Narhi, J. Wypych, J. Biol. Chem. 2011, 286, 25134–25144.
[29] R. Pasternack, S. Dorsch, J. T. Otterbach, I. R. Robenek, S. Wolf, H. L. Fuchsbauer, Eur. J. Biochem. 1998, 257, 570–576.

Manuscript received: February 18, 2019
Revised manuscript received: April 28, 2019
Accepted manuscript online: May 2, 2019
Version of record online: August 20, 2019

CHEMBIOCHEM

Supporting Information

Efficient Site-Specific Antibody–Drug Conjugation by Engineering a Nature-Derived Recognition Tag for Microbial Transglutaminase

Aileen Ebenig+,[a] Norbert Egon Juettner+,[b, c] Lukas Deweid+,[a] Olga Avrutina,[a]
Hans-Lothar Fuchsbauer,[b] and Harald Kolmar*[a]

cbic_201900101_sm_miscellaneous_information.pdf

Supporting Information

1. Chemical compounds

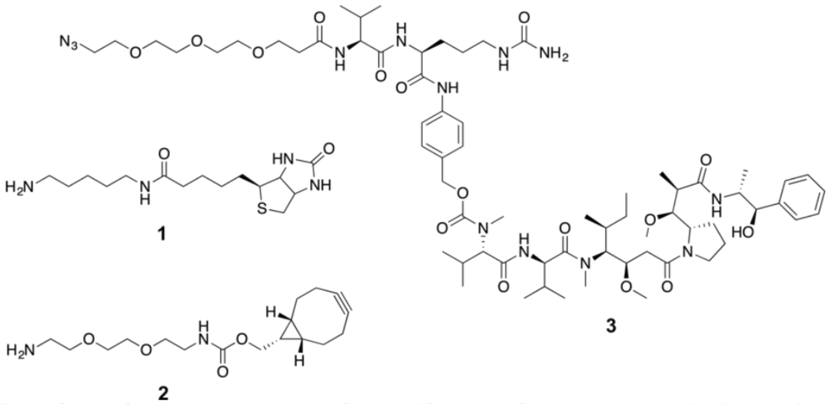

Figure-S 1: Chemical compounds for modification of engineered antibodies. N-(biotinyl)cadaverine 1; N-[(1R,8S,9s)-Bicyclo[6.1.0]non-4-yn-9-ylmethyloxycarbonyl]-1,8-diamino-3,6-dioxaoctane 2; N_3-PEG$_3$-vc-PAB-MMAE 3.

2. Analysis of synthetic peptides

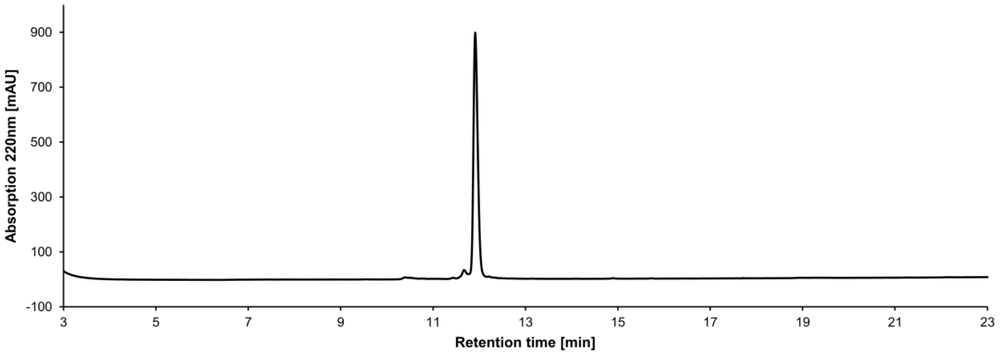

Figure-S 2: RP-HPLC analysis of acetylated peptide wtSPI (P1) (gradient 10% to 60% B in 20 min).

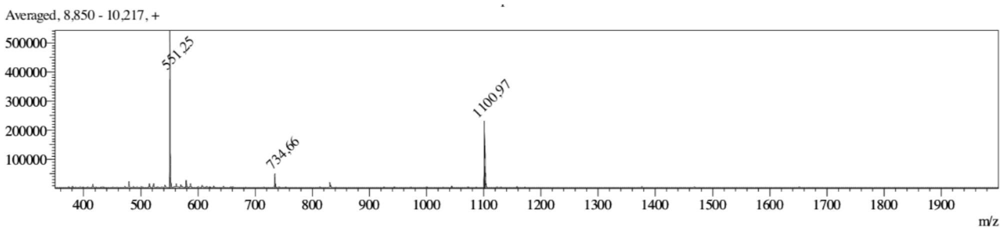

Figure-S 3: LC-MS analysis of acetylated peptide wtSPI (P1); calc. mass: 1100.30 g/mol; meas. m/z: 1100.97 $[M+H]^+$, 551.25 $[M+2H]^{2+}$.

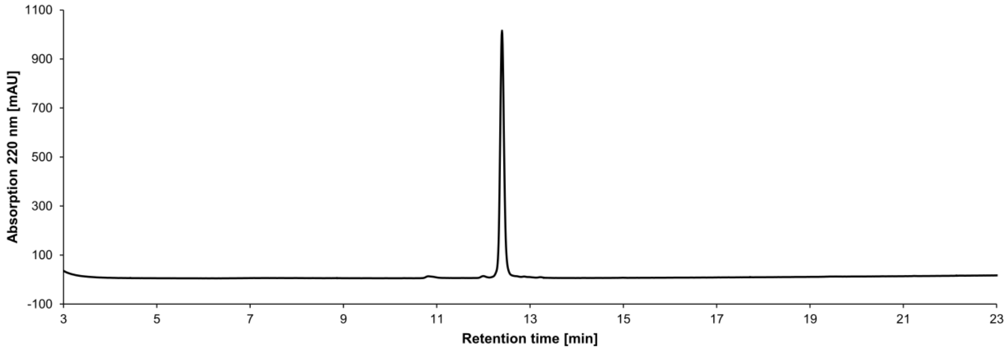

Figure-S 4: RP-HPLC analysis of acetylated peptide SPI7G (P2) (gradient 10% to 60% B in 20 min).

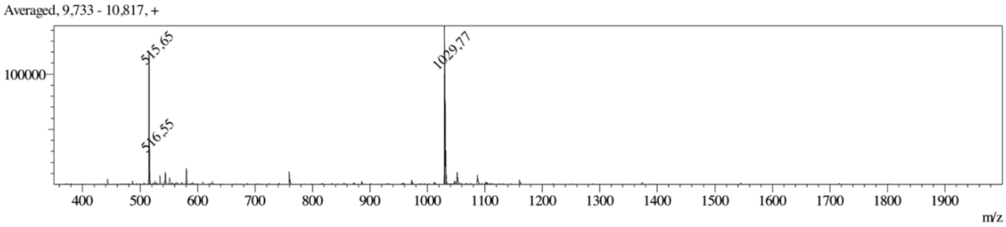

Figure-S 5: LC-MS analysis of acetylated peptide SPI7G (P2); calc. mass: 1029.18 g/mol; meas. m/z: 1029.77 $[M+H]^+$, 515.65 $[M+2H]^{2+}$.

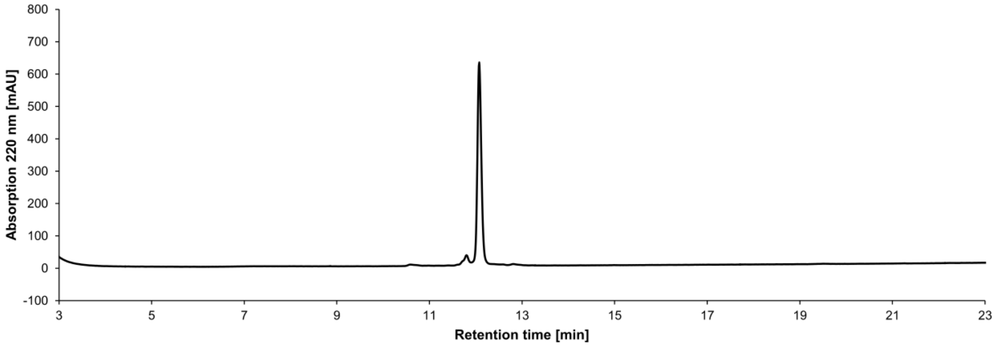

Figure-S 6: RP-HPLC analysis of acetylated peptide SPI7R (P3) (gradient 10% to 60% B in 20 min).

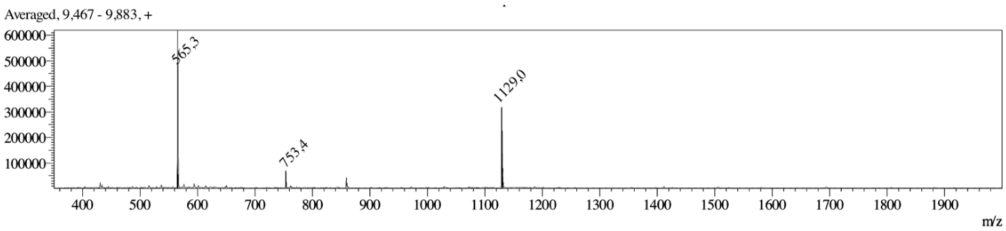

Figure-S 7: LC-MS analysis of acetylated peptide SPI7R (P3); calc. mass: 1128.32 g/mol; meas. m/z: 1129.0 $[M+H]^+$, 565.3 $[M+2H]^{2+}$.

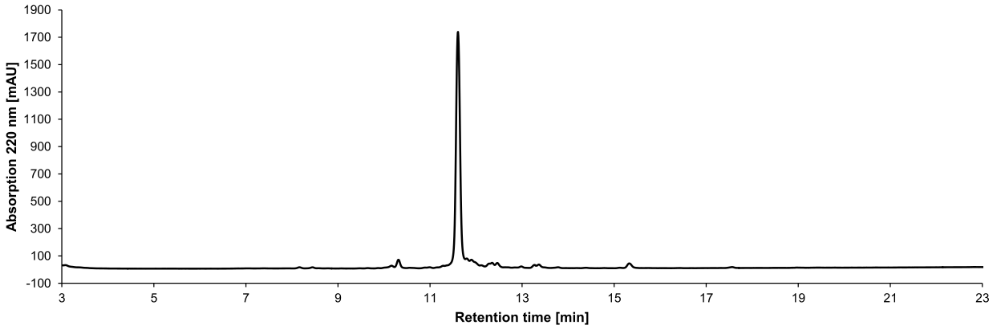

Figure-S 8: RP-HPLC analysis of acetylated peptide GEN (P4) (gradient 10% to 60% B in 20 min).

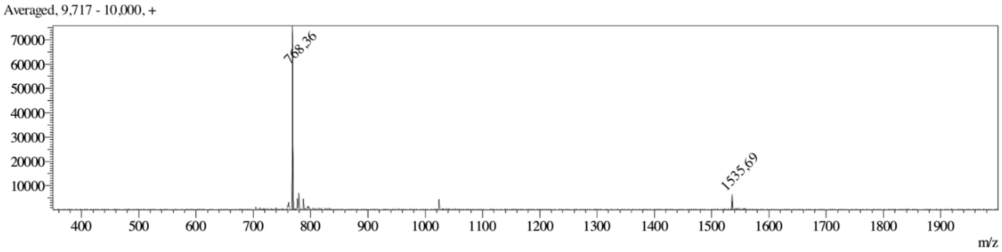

Figure-S 9: LC-MS analysis of acetylated peptide GEN (P4); calc. mass: 1534.56 g/mol; meas. m/z: 1535.69 $[M+H]^+$, 768.36 $[M+2H]^{2+}$.

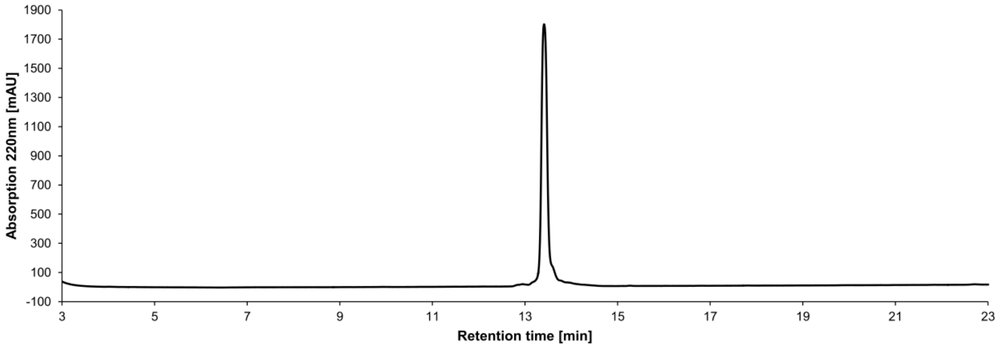

Figure-S 10: RP-HPLC analysis of acetylated peptide GEC (P5) (gradient 10% to 60% B in 20 min).

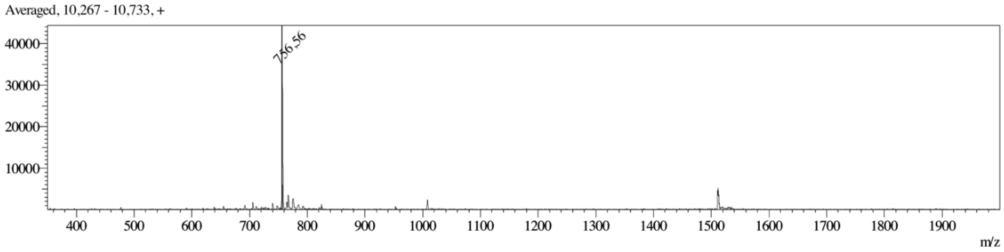

Figure-S 11: LC-MS analysis of acetylated and oxidized peptide GEC (P5); calc. mass: 1510.61 g/mol; meas. m/z: 1510.55 $[M+H]^+$, 756.56 $[M+2H]^{2+}$.

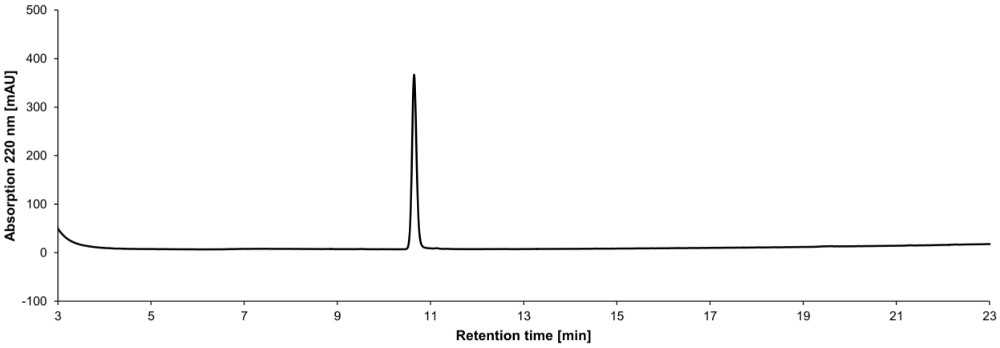

Figure-S 12: RP-HPLC analysis of acetylated peptide LLQG (P7) (gradient 10% to 60% B in 20 min).

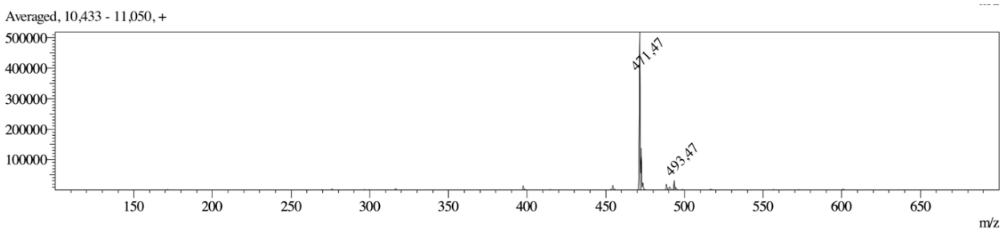

Figure-S 13: LC-MS analysis of acetylated peptide LLQG (P7); calc. mass: 470.57 g/mol; meas. m/z: 471.47 $[M+H]^+$.

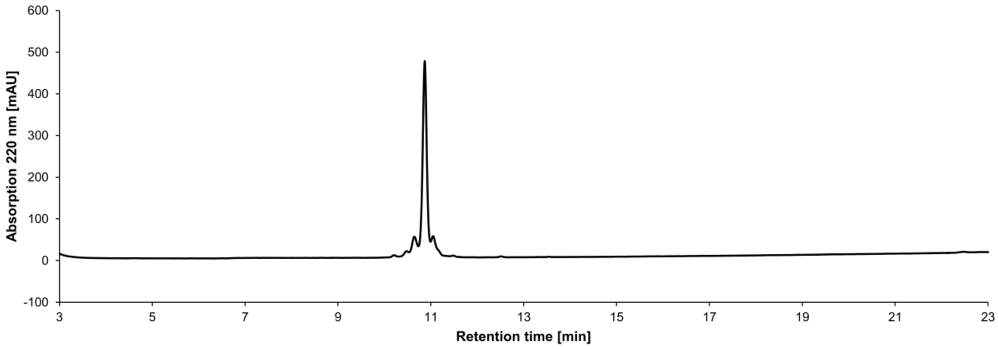

Figure-S 14: RP-HPLC analysis of acetylated peptide 9mer (P6) (gradient 10% to 60% B in 20 min).

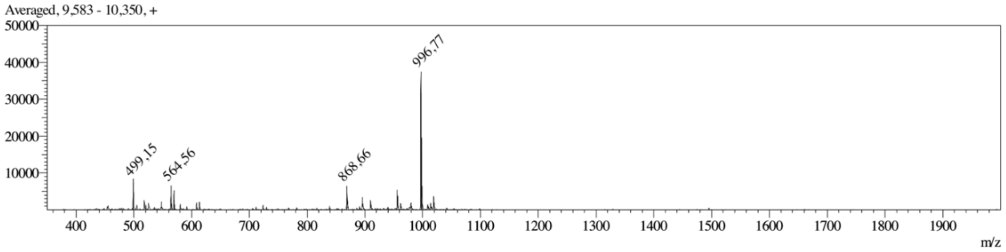

Figure-S 15: LC-MS analysis of acetylated peptide 9mer (P6); calc. mass: 995.49 g/mol; meas. m/z: 996.77 [M+H]$^+$, 499.15 [M+2H] $^{2+}$.

3. mTG-mediated functionalization of peptide P1-P7 using N-[(1R,8S,9s)-Bicyclo[6.1.0]non-4-yn-9-ylmethyloxycarbonyl]-1,8-diamino-3,6-dioxaoctane

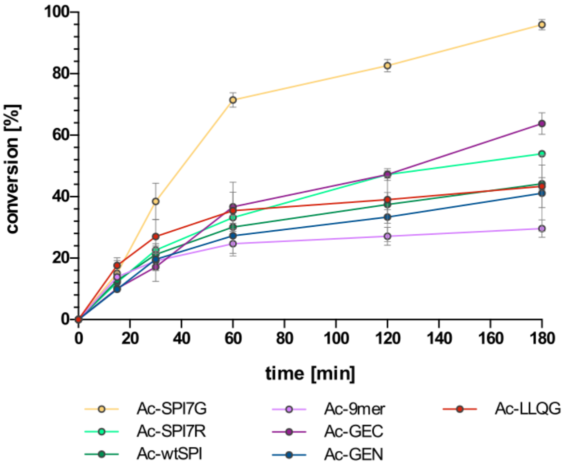

Figure-S 16: Kinetic studies of mTG-mediated modification of peptide P1-P7 using N-[(1R,8S,9s)-Bicyclo[6.1.0]non-4-yn-9-ylmethyloxycarbonyl]-1,8-diamino-3,6-dioxaoctane. Product formation was analyzed in triplicates *via* HPLC and blotted against the respective reaction time.

4. mTG-mediated biotinylation of engineered trastuzumab variants (Ab1-Ab7)

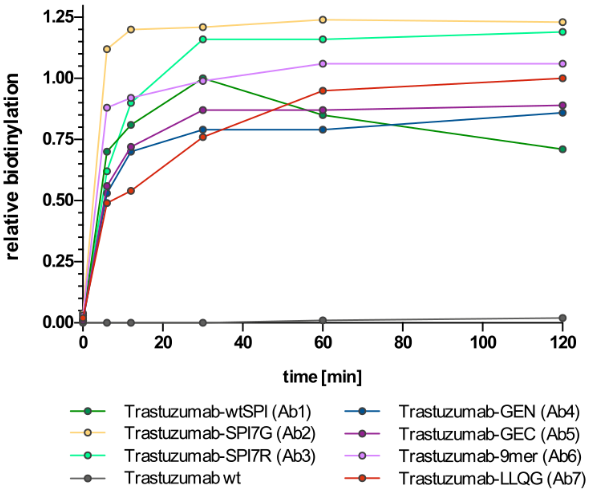

Figure-S 17*:* Kinetics of mTG-mediated biotinylation of trastuzumab variants with corresponding mTG recognition sites (Ab1-Ab7). The antibodies were incubated in the presence of *N*-(biotinyl)-cadaverine (1) and mTG at 37 °C. Aliquots were visualized after different incubation times *via* reducing SDS-PAGE and western blot analysis using fluorescent IRDye® 800CW streptavidin conjugate in combination with the Odyssey® Sa Infrared Imaging System. The biotinylation degree was normalized to the overnight reaction of trastuzumab-LLQG and plotted against the time (A).

5. mTG-mediated biotinylation of SPI7G-bearing heavy and light chain trastuzumab variants

Antibody concentrations were adjusted to 0.5 µM and incubated with 60 mol equivalents monobiotinyl cadaverine and 0.0175 µM transglutaminase per conjugation site in 50 mM Tris/HCl pH 8.0 containing 100 mM NaCl at 37°C. Aliquots of the reaction mixture were collected after 0, 6, 15, 30, 60, 120 and 180 min and 20 h and supplemented with hot SDS-loading dye. The reactions were analyzed by 15% SDS-PAGE and biotinylated heavy chain or light chain were visualized by semi-dry western blot using fluorescent IRDye® 800CW streptavidin conjugate in combination with the Odyssey® Sa Infrared Imaging System. The degree of biotinylation is normalized to the overnight reaction of trastuzumab-SPI7G which was defined as 100% biotinylation.

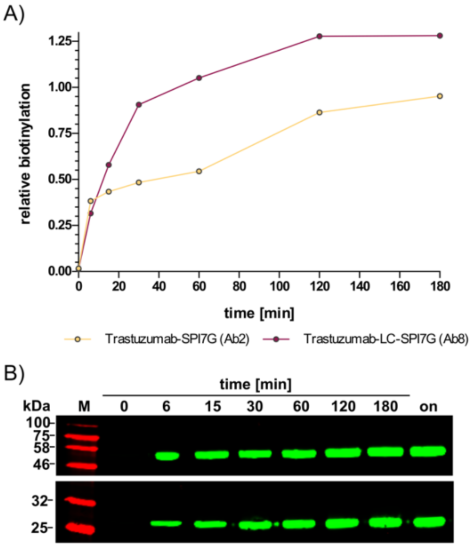

Figure-S 18: Kinetics of mTG-mediated biotinylation of trastuzumab variants bearing the SPI7G sequence at the C-terminus of either the light (B, lower picture) or the heavy chain (B, upper picture).

6. Stability of the Trastuzumab-SPI7G and Trastuzumab-LC-SPI7G in human serum

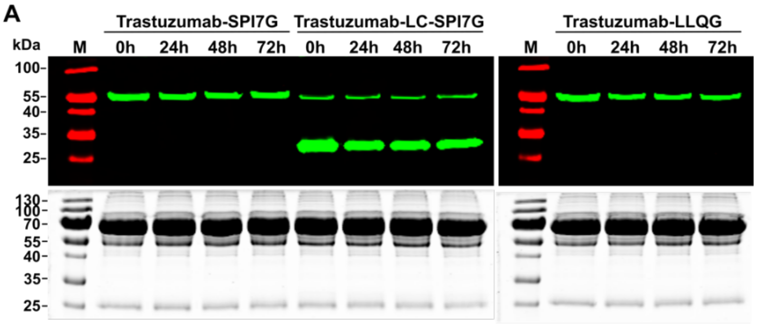
A
Trastuzumab-SPI7G
Trastuzumab-LC-SPI7G
Trastuzumab-LLQG
kDa
M
0h
24h
48h
72h
0h
24h
48h
72h
M
0h
24h
48h
72h
100
55
40
35
25
130
100
70
55
40
35
25

B

h	Trastuzumab-SPI7G	Trastuzumab-LC-SPI7G	Trastuzumab-LLQG
0	100.0 %	100.0 %	100.0 %
24	82.7 %	79.1 %	53.9 %
48	78.2 %	78.7 %	48.1 %
72	79.6 %	77.9 %	47.6 %

Figure-S 19: Stability of biotinylated trastuzumab-SPI7G heavy and light chain variants in human serum at 37°C for 72 h. Remaining conjugates were analyzed using western blot analysis.

7. Determination of the dissociation constant of toxin loaded trastuzumab variants

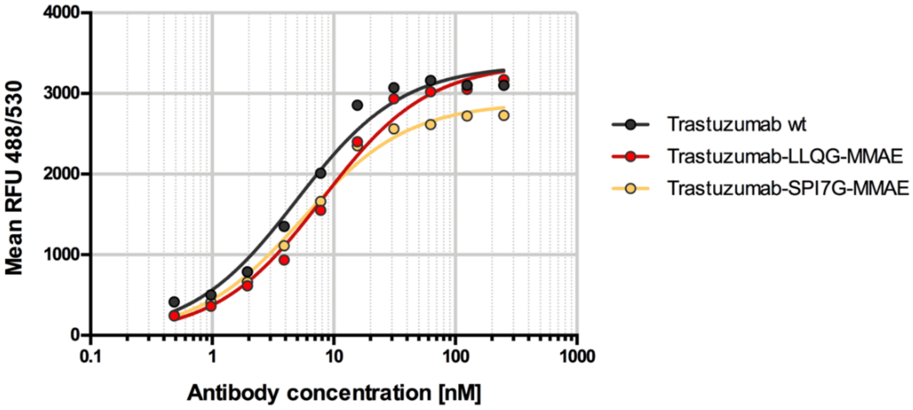

Figure-S 20: Determination of the dissociation constant of trastuzumab-LLQG-MMAE (Ab7.2.3, 8.0 nM) and trastuzumab-SPI7G-MMAE (Ab2.2.3, 5.5 nM) on Her2-positive SK-BR-3 cells.

7.6. Glutamine Scanning Towards Transglutaminase-Mediated Modification of an Antibody Fragment Crystallisable

Title:

Glutamine Scanning Towards Transglutaminase-Mediated Modification of an Antibody Fragment Crystallisable

Authors:

Lukas Deweid, Adem H.-Parisien, Sebastian Bitsch, Kiana Lafontaine, Irina Sagamanova, André B. Charette, Harald Kolmar and Joelle Pelletier

Bibliographic data:

Unpublished data. The following data was generated in the scope of an international corporation between the groups of Prof. Kolmar (TU Darmstadt) and Prof. Pelletier (Université de Montréal) as a part of this doctoral study. The presented study has not been published yet but represent an important contribution to the field of transglutaminase-mediated bioconjugation of antibodies. Further data that significantly improves the resulting publication will be obtained during a follow-up internship of A. Parisien and J. Pelletier in Darmstadt in Q1, 2020.

Contributions by Lukas Deweid:

- Initiated the cooperation between the groups of Prof. Kolmar (TU Darmstadt) and Prof. Pelletier (Université de Montréal)
- Project management together with H. Kolmar and J. Pelletier
- Performed initial experiments presented in this study
- Preparation of the manuscript and all included graphical material

Glutamine Scanning Towards Transglutaminase-Mediated Modification of an Antibody Fragment Crystallisable

Lukas Deweid[a], Adem H.-Parisien[b], Sebastian Bitsch[a], Kiana Lafontaine[b,d], Irina Sagamanova[c,d], André B. Charette[c,d], Harald Kolmar[a]* and Joelle N. Pelletier[c,d,e]*

Abstract: Beating cancer is a major challenge for modern medicine and antibody-drug conjugates (ADCs) were lately approved by the Food and Drug Administration (FDA) to reach a step closer to this ambitious goal. Microbial transglutaminase (mTG) from *Streptomyces mobaraensis* catalyses the formation of amide bonds between glutamine residues and primary amines and has been proven to be a useful tool for the assembly of antibody-drug conjugates. However, in the absence of native reactivity of antibodies with mTG, elaborate manipulation of the antibody is required to transform it into a suitable substrate for the enzyme. We hypothesized that these modifications could be minimized by identifying sites that allow for mTG-mediated modification upon single amino acid substitution. To this effect, we individually substituted 30 surface exposed residues of a human IgG1 fragment crystallisable (Fc) with glutamine and investigated their reactivity in mTG-promoted bioconjugation using a fluorescent assay. Incorporation of unique reactive sites reduces the risk of causing immunogenicity or interfering with the therapeutics' intrinsic stability compared to bulky recognition sequences. The results presented in this study will contribute to the straightforward construction of homogenous ADCs with the use of microbial transglutaminase.

Introduction

Cancer is a fickle disease that was recognized as far back as ancient Egypt and still harms modern society today.[1] In 2018, approximately 18.1 million new patients were diagnosed with cancer while 9.6 million cancer-related deaths were registered worldwide.[2] Recent studies estimate that ~600,000 US citizens will pass away as a result of cancer in 2019,[3] vividly illustrating the societal cost of this disease. Though long-term survival rates are constantly improving, progress in biomedical research is necessary to provide access to more effective and patient-friendly therapeutic options. In particular, targeted therapies can increase treatment efficacy and reduce toxicity to healthy tissues and organs, improving outcome. Antibody-drug conjugates address this need by combining the remarkable target specificity of monoclonal antibodies and the high cytotoxicity of organic compounds, and have been recently launched on the world market.[4] In the context of these promising therapeutic agents, the immunoglobulin is used as a vehicle that site-specifically delivers the potent toxin to the tumour environment. This results in a widened therapeutic window of the drug, such that undesired site-effects of conventional chemotherapy may be reduced.[5]

This breakthrough concept has stimulated research worldwide to develop methodologies to covalently link toxic payloads to antibodies.[6] Initial approaches relied on the remarkable reactivity of chemical compounds towards intrinsic lysine or cysteine residues of the targeted antibody.[7] However, controlling the drug-to-antibody ratio (DAR) and the corresponding conjugation sites is challenging, since multiple amino acids of similar reactivity are present within typical human IgG1 molecules.[8] For instance, the therapeutic antibody trastuzumab, that is applied for the treatment of Her2-positive breast cancer, contains 88 lysine residues and 4 *N*-terminal primary amines among which 70 were demonstrated to be reactive towards an NHS-activated SMCC-linker (succinimidyl-4-(*N*-maleimidomethyl)cyclohexane-1-carboxylate).[9] To overcome this limitation, multiple chemical and biological strategies for the site-specific modification of antibodies have been developed[10] and demonstration has been made of the improved pharmacokinetic and pharmacodynamic properties of these precisely assembled drugs compared to their heterogeneously conjugated counterparts.[8, 11]

Among enzymatic methods for antibody modification, microbial transglutaminase has recently been demonstrated to be a versatile tool for the site-specific modification of immunoglobulins.[12] In nature, mTG catalyses the posttranslational transamidation of glutamine and lysine residues to form isopeptide bonds, resulting in protein crosslinks (see Figure 1A)[13]. Whereas the glutamine-bearing moiety is obligatory, it has been recognized that the lysine side-chain can be replaced by a variety of non-proteinaceous primary amines.[14] Multiple biotechnological applications take advantage of this substrate promiscuity, ranging from PEGylation of small proteinaceous drugs to increase their half-life *in vivo*[15] and conjugation of nucleic acids to proteins to combine their beneficial properties,[16] to surface immobilization of biocatalysts to improve their cost-efficiency via their reuse.[17]

Although human IgG1 molecules natively possess a number of surface-exposed glutamines, none serves as a substrate of

---

[a] Institute for Organic Chemistry and Biochemistry
Technische Universität Darmstadt
Alarich-Weiss-Straße 4, D-64287 Darmstadt

[b] Département de biochimie
Université de Montréal
2900 Boulevard Edouard-Montpetit, Montréal, H3T 1J4, Canada

[c] Département de chimie
Université de Montréal
2900 Boulevard Edouard-Montpetit, Montréal, H3T 1J4, Canada

[d] CGCC, the Center in Green Chemistry and Catalysis, Montréal, H3A 0B8, Canada

[e] PROTEO, the Québec Network for Protein Function, Structure and Engineering, Québec, G1V 0A6, Canada

* To whom correspondence should be addressed

E-mail: kolmar@Biochemie-TUD.de
E-mail: joelle.pelletier@umontreal.ca

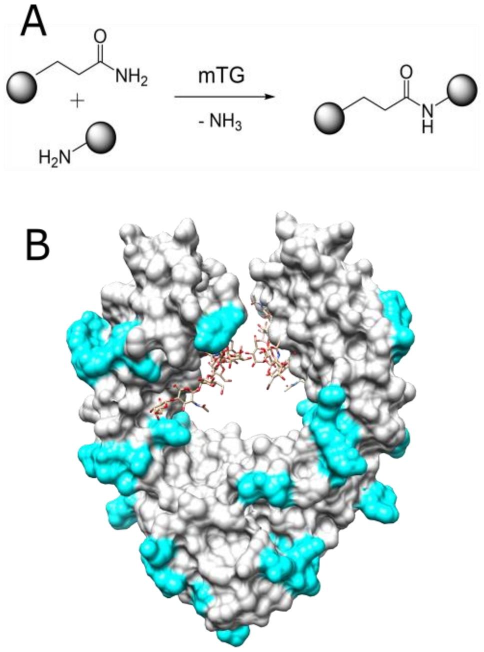

Figure 1: (A) Schematic representation of the reaction catalysed by mTG. **(B)** Crystal structure of human IgG1 Fc portion according to PDB:3DO3. Proposed sites for mutagenesis are highlighted in cyan. Glycosylation of the CH2 domain at Asn297 is indicated as sticks.

the mTG.[12] Jeger and coworkers recognized that genetic substitution of the glycosylation site, Asn297, or enzymatic truncation of the Fc glycan moiety exposes the neighbouring Gln295 as an efficient site for transamidation by mTG.[18] They further demonstrated in rodent models that this strategy is suitable for the construction of potent ADCs[19] and this key technology paved the way for follow-up applications.[20] Nonetheless, the contribution of the glycan moiety to antibody stability is still a topic of investigation: aglycosylated antibodies are more prone to aggregation and suffer from increased thermal sensitivity compared to their native counterparts.[21]

As an alternative to removing the glycan chain from the antibody, genetic incorporation of recognition tags is a powerful strategy to engineer antibodies into suitable substrates for mTG. The efficiency of this approach has been demonstrated in multiple applications.[22] Though specific, glutamine-bearing peptidic recognition motifs can promote rapid labelling by mTG, incorporation of heterologous peptide sequences into full-length antibodies can lead to undesired consequences. Substitution of the native amino acid pattern with recognition motifs at internal sites of an immunoglobulin may lead to decreased stability. Moreover, the risk of causing undesired immunogenicity upon intravenous administration increases with the length of the tag.[23]

In this work, we overcome these limitations by incorporating individual glutamine residues into surface-exposed regions of a human Fc to identify positions that are efficiently modified by mTG. To that end, a strategy for the recombinant expression of a human Fc in *E. coli* cells was established. Upon purification of the respective Fc variants, reactivity of the enzyme towards the substituted residues was investigated in a fluorescent assay using different acyl-acceptor substrates.[24]

Results and Discussion

EGFR-targeting Cetuximab is a representative therapeutic antibody in that it possesses 64 intrinsic glutamine residues. Despite many being surface-exposed, none are modified by mTG.[22c] This obstacle to the mTG-mediated modification of human antibodies can only be bypassed by deglycosylation of the immunoglobulin CH2 domain or by incorporation of specific mTG recognition motifs. Both methodologies bear certain disadvantages in terms of either stability or immunogenicity of the resulting antibody-drug conjugate. We speculated that this risk would be minimized by introducing individual glutamine residues that can be addressed by the enzyme. It is not known why certain surface-exposed glutamines serve as substrates for mTG and others do not: no clear motif or signature has emerged from studies using diverse protein and peptide substrates.[24-25] Since rational creation of a mTG-reactive glutamine is not feasible, we individually mutated and screened 29 surface-exposed residues of a human Fc to identify sites that allow for efficient labelling upon substitution against glutamine (Figure 1; Appendix, Table 1). Of note, residues M252, E283, A287, K288, K290, K340, P343, G385, G420, H433 and P445 were previously identified as suitable lysine-acceptor sites for mTG in previous applications and were therefore included for substitution to glutamine in our approach.[23a, 26]

In a first step, a recombinant expression system that allows for the cost-effective and straightforward production of a human Fc in *E. coli* was developed. The gene of interest was cloned into vector pET22b(+) for periplasmic expression by in-frame fusion with an *N*-terminal pelB signal sequence (*Xba*I/*Xho*I-mediated ligation), or without the pelB signal sequence for cytoplasmic expression (*Nco*I/*Xho*I). Periplasmic expression in *E. coli* BL21(DE3) resulted in poor yields of monomeric and incorrectly assembled Fc as revealed

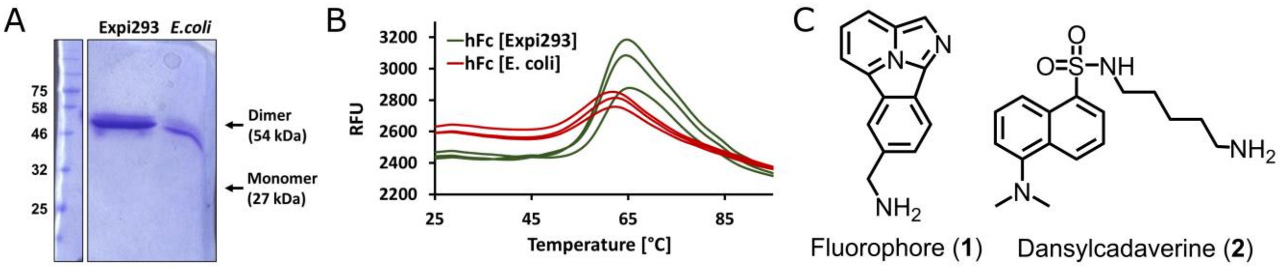

Figure 2: (A) Non-reducing SDS-PAGE of a human Fc portion purified by IMAC from E. coli SHuffle T7 cells or purified by ProteinA affinity chromatography from Expi293 human cells. **(B)** Thermal shift assay using SYPRO™ Orange to reveal T_m of 62.3 ± 0.2 and 64.8 ± 0.5°C for the human Fc purified from E. coli or from eukaryotic cells, respectively. **(C)** Structure of the aminated fluorophores used for labelling of glutamine-substituted Fc variants.

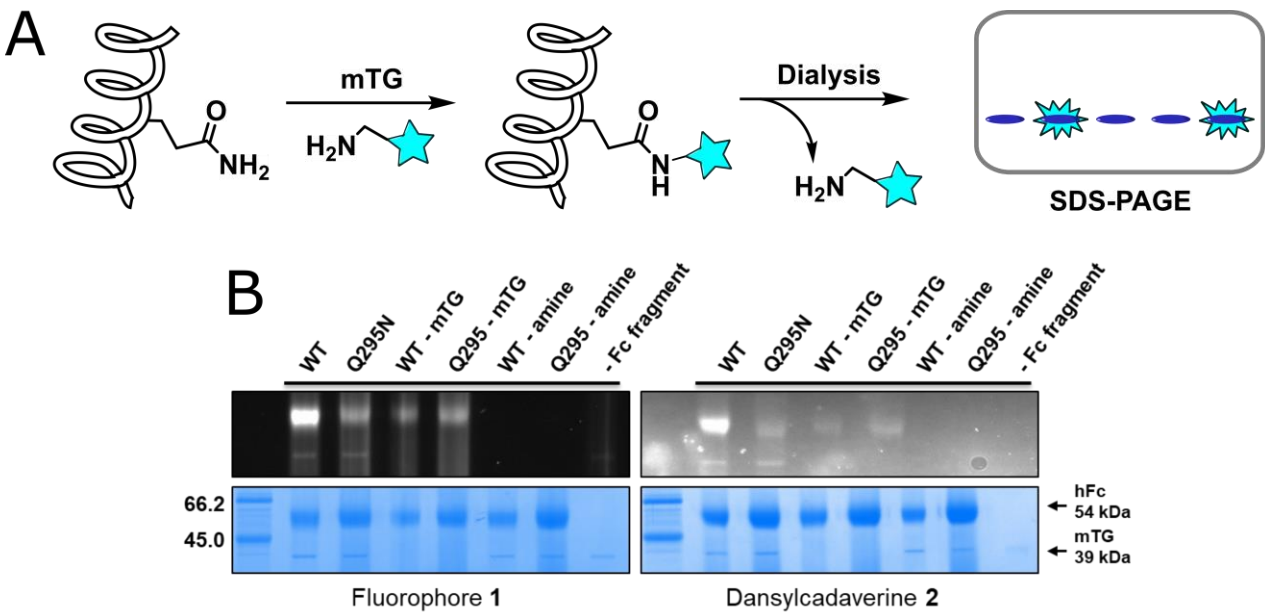

Figure 3: (**A**) General scheme of the fluorescent assay according to Rachel *et al*.[23] Human Fc variants were incubated in the presence of mTG and fluorescent acyl-acceptor probes **1** or **2**. Excess fluorophore was removed by microdialysis and the extent of reaction was visualised by non-reducing SDS-PAGE. (**B**) Protein samples (2µg) were resolved on gel and analysed for fluorescence using a Cy2 filter and an exposure time of 15s, prior to Coomassie staining (**1**). Samples incubated with **2** were visualised using a SYBR™ Green filter and an exposure time of 12.5s. Mutant Q295N displayed only background activity while the wildtype Fc was strongly labelled by mTG. No reactivity was observed for references lacking either mTG, a fluorescent amine or the target Fc.

by non-reducing SDS-PAGE (data not shown). However, co-expression of sulfhydryl oxidase Erv1p and *E. coli* isomerase DsbC in the cytoplasm of *E. coli* SHuffle® T7 Express yielded soluble, dimeric Fc in good yield (see Figure 2A, Appendix Table 1 and Experimental section).[27] We investigated the correct assembly of the fragment in thermal shift assays and compared its melting point to a reference purified from eukaryotic HEK Expi293® cells. Melting points of 64.8 ± 0.5°C (Expi293) and 62.3 ± 0.2°C (*E. coli*) were measured (Figure 2B). We further performed LC-MS analysis (see Experimental section) and observed a molecular weight of 54228.0 Da (data not shown) for the dimeric WT Fc, which is +4.6 Da larger as the calculated mass for the molecule with all six (four intramolecular and two interchain) disulfides closed (M=54223.4 Da). Consequently, ~2 disulfide bridges of the *E. coli*-purified Fc are not accurately formed. These results are most likely responsible for the minor difference of 2.5°C in melting temperature between the fragments purified from prokaryotic and eukaryotic sources. Of note, the investigated Fc still comprises Cys220 of the hinge region, which is usually responsible for light chain pairing within the full-length antibody. Expression of C220S mutant resulted in poor yields (data not shown). In our approach, these residues are supposed to be unpaired, however undesired disulfide formation at Cys220 is possible. These results indicate that the Fc purified from a bacterial source adopts its natural fold and serves as a suitable model antibody for our labelling studies.

Gln295 of IgG molecules is known to be efficiently modified by mTG when the CH2 sugar moiety is absent.[18] Since prokaryotic hosts lack posttranslational glycosylation, bacterially-expressed Fc would be labelled by mTG at Gln295. This can serve as a positive control for reactivity, but would interfere with the search for new reactive glutamine sites upon expression in prokaryotic systems. Thus, Gln295 was substituted with Asn by site-directed mutagenesis PCR to eliminate background signal during fluorescent screening (see Experimental section). The resulting Gln295Asn Fc mutant served as a negative control and was compared to the wildtype Fc counterpart in a fluorescent assay performed according to Rachel *et al*.[24] To this end, we incubated the Fc variants with mTG in the presence of either fluorophore **1** or dansylcadaverine **2** (see Figure 2C), which are known acyl-acceptor substrates. The extent of reactivity was visualised by non-reducing SDS-PAGE (see Figure 3A and Experimental section).[28] A distinct fluorescent signal was observed when the wildtype Fc served as a glutamine-donor substrate. Low levels of background signal were observed for the Gln295Asn Fc mutant as well as in the corresponding controls lacking mTG (Figure 3B). These results are consistent with previous reports[12, 18, 22c, 22d] and therefore represent an additional hint towards correct dimeric assembly of the utilized Fc.

We applied the established assay to 30 out of 32 designated glutamine-substituted Fc mutants (cloning of 2 variants failed) to identify positions that allow for efficient modification. The reactivity was compared to the non-glycosylated wildtype Fc that served as a positive control. Among the investigated variants, we identified 2 glutamine substitution, namely I253Q and Y296Q that served as substrate for labelling of the immunoglobulin domain, at levels comparable to or greater than the wildtype Fc reference (Figure 4A). I253Q is located at the CH2/CH3 interface in a moderately flexible region of the protein and its side-chain is orientated to the exterior of the molecule (Figure 4B). Interestingly, the glutamine side-chains of M252, S254 and R255 that are neighbouring reactive I253Q, point toward the interior of the protein and are poorly or not reactive upon substitution against glutamine. We hypothesise that steric hindrance prevents reactivity.

Substitution Y296Q is located within the C/E loop of the CH2 domain and an immediate neighbour of Q295. We assume that the increased flexibility of the loop, caused by the absence of the glycan moiety, enabled the labelling of Y296Q, similarly to native Q295 of deglycosylated antibodies.

Moreover, 11 site (M252Q, R255Q, V282Q, N286Q, K288Q, T289Q, K290Q, A339Q, K340Q, N361Q and P445Q) were identified that mediated lower labelling intensity than the wildtype. These positions might suffer from suboptimal properties for transamidation and are probably not suitable for efficient construction of immune-conjugates.

We have demonstrated that single residue substitution within an antibody Fc enables its effective modification by mTG. To that end, an efficient purification protocol and a straightforward fluorescence assay were established and we successfully identified two sites (I253Q and Y296Q) that allowed for mTG-mediated labelling.

The data presented in this study has to be confirmed in further experiments before being considered scientifically valid. The Fc variants used in our approach were purified from prokaryotic host *E. coli* SHhuffle Express T7 to facilitate cost-effective and rapid screening but the flawless assembly of the dimeric protein is still debatable. A melting point comparable to a reference purified from HEK Expi293 cells and LC-MS analysis indicated near-native assembly but binding of the fragment to its receptors has not been demonstrated yet. ELISA assays to prove the binding of the Fc to its native receptors would further substantiate these preliminary results. Posttranslational modification of eukaryotic hosts is a crucial quality attribute of therapeutic proteins to avoid undesired reactivity of the patients' immune system. For instance, aglycosylation of a human IgG antibody increases the flexibility of its CH2 C/E loop (Q295–T299), which results in efficient labelling of Gln295 by mTG.[18] Consequently, promising mutations that were identified in this study have to be confirmed with a fully glycosylated antibody originating from a eukaryotic host to ensure that glycosylation does not interfere with the reactivity observed in absence of glycosylation. Particular attention should be given to sites that are closely located to the C/E loop and the hinge region. They require careful evaluation since they might be sterically inaccessible in the context of a full-length antibody. Therefore, the hexa-histidine tag should be removed and purification should be performed by Protein A affinity chromatography instead. Antibodies in general are highly stable molecules but substitution of certain stabilising residues might alter their overall folding. Peptide mass fingerprinting should be used to verify that conjugation occurred at the mutated site rather than residues exposed by mutagenesis-induced misfolding. Though further investigations are required, these results lay the cornerstone for mTG-mediated construction of antibody-drug conjugates upon single residue substitution.

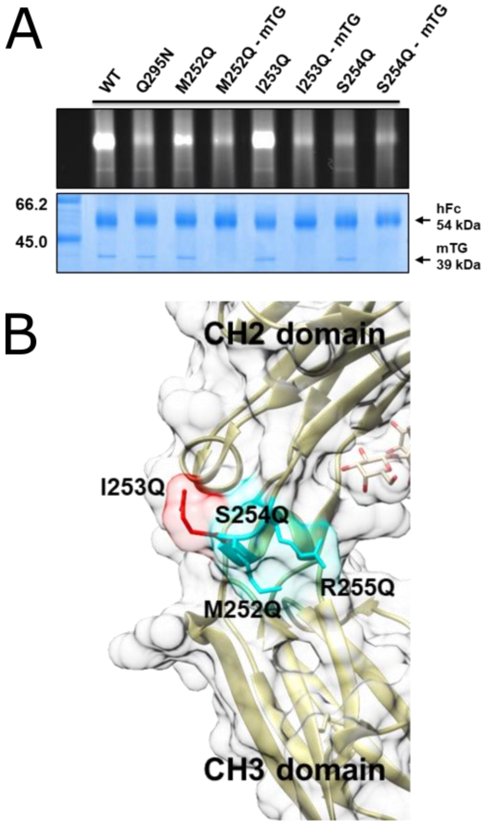

Figure 4: (A): Exemplary results of the conducted conjugation assay shown for mutants Q252M (moderately reactive), I253Q (highly reactive) and S254Q (nonreactive). Fluorophore **1** served as an acyl-acceptor and non-reducing SDS-PAGE was performed to resolve excess **1**. The extent of reaction was visualized using a Cy2 filter and an exposure time of 15 s, prior to Coomassie staining. Wildtype Fc was used a positive control and Q295N as a negative control, respectively. References that lack mTG (-mTG) were performed to determine background fluorescence. (**B**) Mutation I253Q has high reactivity compared to the wildtype positive control. I253Q (shown in red) is located in a moderately flexible region of the Fc at the interface of the CH2 and CH3 domain. Its sidechain is orientated towards the exterior of the Fc while less or non-reactive residues M252Q, S254Q and R255Q (shown in cyan) point toward the interior. PDB:3DO3.

Experimental Section

Material: All chemicals and materials used in this report were of analytical grade and purchased from BioShop Canada Inc. Dansylcadaverine (**2**) was purchased from Sigma Aldrich and fluorophore **1** (Benzo[a]imidazo[2,1,5-c,d] indolizin-7-ylmethanaminium chloride was synthesised in-house.[28a] Phusion® polymerase was purchased from Thermo Fischer Scientific and all restriction enzymes were from New England Biolabs. Pierce™ 96-well Microdialysis Plate, 3.5K MWCO were purchased from Thermo Fischer Scientific.

Production of microbial transglutaminase: mTG from *Streptomyces mobaraensis* was produced as previously described.[24] Briefly, *E. coli* BL21(DE3)-pET20-mTG cells, grown in 50 mL LB+Amp (final concentration: 100 µg/mL) overnight at 37°C and 230 rpm were used to inoculate 500 mL of sterile LB+Amp medium to an OD_{600} of 0.1. Cells were grown at 37°C and 230 rpm to an OD_{600} of 0.7 – 1 and gene expression was induced by the addition of IPTG in a final concentration of 500 µM. Cells were incubated at 24°C and 230 rpm for 3h and afterwards pelleted by centrifugation for 30 min at 4°C and 3000 rpm (rotor: Sorvall SLA-3000). The supernatant was discarded and the resulting cell pellet was resuspended in 30 mL IMAC-A buffer (600 mM NaCl, 50 mM Tris-HCl pH 8, 1 mM $CaCl_2$ and 20 mM imidazole). Cells were lysed in a Constant Systems Cell Disruptor according to the manufacturer's instructions. Cell debris was pelleted by centrifugation for 30 min at 14000 rpm (rotor: Sorvall SS34) and 4°C. The resulting supernatant was sterile filtered and supplemented with 111 µg/mL trypsin (final concentration) to cleave the inhibitory propeptide of mTG. After incubation for 30 min at 30°C, IMAC was performed to separate the mature enzyme from the cell lysate. Purified fractions were pooled and dialysed against PBS pH 7.2 overnight at 4°C. Absorption at 280 nm was measured and the protein concentration was calculated using a molar extinction coefficient of

71850 L×mol^{-1}×cm^{-1} and a molecular weight of 39095.74 g/mol. For long term storage at -70°C, 10% glycerol was added.

Production of human Fc in *E. coli* cells: *E. coli* Shuffle T7 Express cells were co-transformed with pET22b(+)-hFc and SOX-plasmid[27] and were grown in 50 mL LB+Ampicillin/Chloramphenicol (final concentration: Amp: 100 µg/mL and Cm: 50 mg/mL, respectively) overnight at 37°C and 230 rpm. The preculture was used to inoculate 500 mL of sterile LB+Amp/Cm medium to an OD_{600} of 0.1 and cells were grown at 37°C and 230rpm to an OD_{600} of 0.7 – 1. Gene expression of DsbC isomerase and Erv1p sulfhydryl oxidase was induced by the addition of 0.1% (w/v) sterile arabinose (final concentration) and the cells were incubated for 1h at 18°C and 230 rpm. Afterwards, expression of the human Fc was induced by the addition of IPTG in a final concentration of 500 µM and cells were incubated at 18°C and 230 rpm overnight. Cell were centrifuged for 30 min at 4°C and 3000 rpm (rotor Sorvall SLA-3000) and the resulting supernatant was discarded. The corresponding cell pellet was resuspended in 30 mL IMAC-A buffer (600 mM NaCl, 50 mM Tris-HCl pH 8, 1 mM $CaCl_2$ and 20 mM imidazole) and lysed in a Constant Systems Cell Disruptor according to the manufacturer's instructions. Cell debris was pelleted by microcentrifugation for 30 min at 14000 rpm (rotor: Sorvall SS-34) and 4°C. The resulting supernatant was sterile filtered and applied to a 1 mL HisTrap Crude column (GE Healthcare) to purify the Fc from the cell lysate. Protein-containing fractions were pooled and an equal volume of buffer was added prior to dialysis against PBS pH 7.2 overnight at 4°C. Proteins were concentrated to a final concentration of 5 mg/mL using Merck Millipore Amico® 10kDa MWCO filter units. Non-reducing SDS-PAGE was performed to verify the presence of a 54 kDa protein band that corresponds to the correctly assembled Fc. Absorption at 280 nm was measured and the protein concentration was calculated using a molar extinction coefficient of 71695 L×mol^{-1}×cm^{-1} and a molecular weight of 54217.39 g/mol. For long term storage at -70°C, 10% glycerol was added. Yields typically ranged between 20-40 mg/mL. However, drastically lower yields were observed for certain mutant Fc variants.

Site-directed mutagenesis: Single amino acids substitutions were introduced into the Fc on a genetic level by site-directed mutagenesis PCR. To this end, oligonucleotides were designed in a non-overlapping, back-to-back manner.[28] A 50 µL PCR reaction consisted of 35 µL of ddH_2O, 10 µL of 5 × HF-Buffer, 1 µL of dNTPs (10 mM stock), 1 µL per oligonucleotide (10 µM stock), 1 µL of template (50-100 ng/µL stock) and 1 µL of Phusion® polymerase. PCR reactions were conducted with 5 min pre-incubation at 95°C and 30 cycles with 30 s at 95°C (denaturing), 30 s at 58°C (annealing) and 5min at 68°C (elongation), followed by a final elongation step for 5 min at 68°C. PCR products (8µL) were analysed by 1% agarose gel electrophoresis and the presence of a band with a size of ~6000 bp confirms the successful amplification of the template.

Afterwards, 2 µL of *Dpn*I were added per reaction and incubated for at least 1h at 37°C to digest the methylated template DNA while the non-methylated PCR product remains. *Dpn*I was inactivated by incubation at 80°C for 20 min and sodium acetate/ethanol precipitation was used to remove all salts from the reaction. To this effect, 1/10 volume of 3 M sodium acetate and 3 volumes of pure ethanol were added and incubated at -20°C for 30 min. Precipitated nucleic acids were pelleted by microcentrifugation for 30 min at 14000 rpm and 4°C. The supernatant was discarded and the pellet was washed with 200 µL ice-cold 70% ethanol by microcentrifugation at 14000 rpm and 4°C for 30 min. The pellet was resuspended in 20 µL ddH_2O and 5 µL were transformed into competent *E. cloni* cells by electroporation and grown overnight at 37°C on LB+Amp agar plates.

Single colonies were picked to inoculate 5 mL of LB+Amp medium and propagated overnight at 37°C and 230 rpm. Plasmids were isolated using the NEB Monarch® Miniprep Kit according to the manufacturer's instructions. Correct incorporation of the desired mutation was confirmed by DNA sequencing.

mTG-mediated bioconjugation: To investigate the reactivity of mTG towards the mutant Fc variants, conjugation assays were performed. 25 µM of the respective target protein (Fc variants) were incubated for 16h at 37°C in the presence of 2.5 mM of fluorophore **1** or **2** and 2.5 µM mTG in PBS pH 7.2. Excess unreacted fluorophore was removed using a Pierce™ 96-well Microdialysis Plate, 3.5K MWCO for 2h in PBS pH 7.2 according to the manufacturer's instructions.

Resolution on 15% non-reducing SDS-PAGE was performed. Prior to Coomassie staining, a Cy2 filter and an exposure time of 5-12.5s were used to visualise fluorophore **1**. For **2**, a SYBR® Green filter and an exposure time of 5-12.5s were applied.

Intact protein LC-MS analysis: LC-MS separation of intact proteins was carried out on a 6224A TOF instrument coupled to an HPLC 1260 Infinity both from Agilent Technologies. The chromatographic column was an Aeris widepore XB-C8, 3.6 µm, 4.6 × 100 mm from Phenomenex. Eluents consisted of 0.1% formic acid in water (eluent A) and Acetonitrile (eluent B). Elution was performed at 0.4 mL/min with a gradient going from 10% B to 70% B over 9 min and a total run time of 15 min. The electrospray ionisation source was operated in positive ion mode and mass spectra were acquired from m/z 100 to 3200. Agilent's Mass Hunter software was used for instrument control, data acquisition and data analysis (Bioconfirm module).

Acknowledgements

This work was supported by the NANOKAT II grant from the BMBF (Bundesministerium für Bildung und Forschung) and NSERC: LD and KL were supported by awards from The Fonds de Recherche Nature et Technologie du Québec and the CGCC (Center in Green Chemistry and Catalysis).

Keywords: Microbial transglutaminase • Bioconjugation • Protein labeling • Antibody-drug conjugates

References

[1] G. B. Faguet, *Int J Cancer* **2015**, *136*, 2022-2036.

[2] F. Bray, J. Ferlay, I. Soerjomataram, R. L. Siegel, L. A. Torre, A. Jemal, *CA Cancer J Clin* **2018**, *68*, 394-424.

[3] R. L. Siegel, K. D. Miller, A. Jemal, *CA Cancer J Clin* **2019**, *69*, 7-34.

[4] J. M. Lambert, A. Berkenblit, *Annu Rev Med* **2018**, *69*, 191-207.

[5] T. Kline, A. R. Steiner, K. Penta, A. K. Sato, T. J. Hallam, G. Yin, *Pharm Res* **2015**, *32*, 3480-3493.

[6] A. Beck, L. Goetsch, C. Dumontet, N. Corvaia, *Nat Rev Drug Discov* **2017**, *16*, 315-337.

[7] K. C. Nicolaou, S. Rigol, *Angew Chem Int Ed Engl* **2019**, *58*, 11206-11241.

[8] J. R. Junutula, H. Raab, S. Clark, S. Bhakta, D. D. Leipold, S. Weir, Y. Chen, M. Simpson, S. P. Tsai, M. S. Dennis, Y. Lu, Y. G. Meng, C. Ng, J. Yang, C. C. Lee, E. Duenas, J. Gorrell, V. Katta, A. Kim, K. McDorman, K. Flagella, R. Venook, S. Ross,

S. D. Spencer, W. Lee Wong, H. B. Lowman, R. Vandlen, M. X. Sliwkowski, R. H. Scheller, P. Polakis, W. Mallet, *Nat Biotechnol* **2008**, *26*, 925-932.

[9] M. T. Kim, Y. Chen, J. Marhoul, F. Jacobson, *Bioconjug Chem* **2014**, *25*, 1223-1232.

[10] C. R. Behrens, B. Liu, *MAbs* **2014**, *6*, 46-53.

[11] P. Strop, K. Delaria, D. Foletti, J. M. Witt, A. Hasa-Moreno, K. Poulsen, M. G. Casas, M. Dorywalska, S. Farias, A. Pios, V. Lui, R. Dushin, D. Zhou, T. Navaratnam, T. T. Tran, J. Sutton, K. C. Lindquist, B. Han, S. H. Liu, D. L. Shelton, J. Pons, A. Rajpal, *Nat Biotechnol* **2015**, *33*, 694-696.

[12] P. Strop, *Bioconjug Chem* **2014**, *25*, 855-862.

[13] J. Zotzel, R. Pasternack, C. Pelzer, D. Ziegert, M. Mainusch, H. L. Fuchsbauer, *Eur J Biochem* **2003**, *270*, 4149-4155.

[14] M. T. Gundersen, J. W. Keillor, J. N. Pelletier, *Appl Microbiol Biotechnol* **2014**, *98*, 219-230.

[15] A. Grigoletto, A. Mero, I. Zanusso, O. Schiavon, G. Pasut, *Macromol Biosci* **2016**, *16*, 50-56.

[16] M. Takahara, R. Wakabayashi, K. Minamihata, M. Goto, N. Kamiya, *Bioconjug Chem* **2017**, *28*, 2954-2961.

[17] T. Li, C. Li, D. N. Quan, W. E. Bentley, L. X. Wang, *Carbohydr Res* **2018**, *458-459*, 77-84.

[18] S. Jeger, K. Zimmermann, A. Blanc, J. Grunberg, M. Honer, P. Hunziker, H. Struthers, R. Schibli, *Angew Chem Int Ed Engl* **2010**, *49*, 9995-9997.

[19] F. Lhospice, D. Bregeon, C. Belmant, P. Dennler, A. Chiotellis, E. Fischer, L. Gauthier, A. Boedec, H. Rispaud, S. Savard-Chambard, A. Represa, N. Schneider, C. Paturel, M. Sapet, C. Delcambre, S. Ingoure, N. Viaud, C. Bonnafous, R. Schibli, F. Romagne, *Mol Pharm* **2015**, *12*, 1863-1871.

[20] a) D. N. Thornlow, E. C. Cox, J. A. Walker, M. Sorkin, J. B. Plesset, M. P. DeLisa, C. A. Alabi, *Bioconjug Chem* **2019**, *30*, 1702-1710; b) Y. Anami, W. Xiong, X. Gui, M. Deng, C. C. Zhang, N. Zhang, Z. An, K. Tsuchikama, *Org Biomol Chem* **2017**, *15*, 5635-5642.

[21] D. Reusch, M. L. Tejada, *Glycobiology* **2015**, *25*, 1325-1334.

[22] a) H. Schneider, L. Deweid, T. Pirzer, D. Yanakieva, S. Englert, B. Becker, O. Avrutina, H. Kolmar, *ChemistryOpen* **2019**, *8*, 354-357; b) A. Ebenig, N. E. Juettner, L. Deweid, O. Avrutina, H. L. Fuchsbauer, H. Kolmar, *Chembiochem* **2019**, *20*, 2411-2419; c) V. Siegmund, S. Schmelz, S. Dickgiesser, J. Beck, A. Ebenig, H. Fittler, H. Frauendorf, B. Piater, U. A. Betz, O. Avrutina, A. Scrima, H. L. Fuchsbauer, H. Kolmar, *Angew Chem Int Ed Engl* **2015**, *54*, 13420-13424; d) P. Strop, S. H. Liu, M. Dorywalska, K. Delaria, R. G. Dushin, T. T. Tran, W. H. Ho, S. Farias, M. G. Casas, Y. Abdiche, D. Zhou, R. Chandrasekaran, C. Samain, C. Loo, A. Rossi, M. Rickert, S. Krimm, T. Wong, S. M. Chin, J. Yu, J. Dilley, J. Chaparro-Riggers, G. F. Filzen, C. J. O'Donnell, F. Wang, J. S. Myers, J. Pons, D. L. Shelton, A. Rajpal, *Chem Biol* **2013**, *20*, 161-167.

[23] a) J. L. Spidel, B. Vaessen, E. F. Albone, X. Cheng, A. Verdi, J. B. Kline, *Bioconjug Chem* **2017**, *28*, 2471-2484; b) K. Terpe, *Appl Microbiol Biotechnol* **2003**, *60*, 523-533.

[24] N. M. Rachel, D. Quaglia, E. Levesque, A. B. Charette, J. N. Pelletier, *Protein Sci* **2017**, *26*, 2268-2279.

[25] Y. Sugimura, K. Yokoyama, N. Nio, M. Maki, K. Hitomi, *Arch Biochem Biophys* **2008**, *477*, 379-383.

[26] P. R. Spycher, C. A. Amann, J. E. Wehrmuller, D. R. Hurwitz, O. Kreis, D. Messmer, A. Ritler, A. Kuchler, A. Blanc, M. Behe, P. Walde, R. Schibli, *Chembiochem* **2017**, *18*, 1923-1927.

[27] G. Veggiani, A. de Marco, *Protein Expr Purif* **2011**, *79*, 111-114.

[28] a) E. Levesque, W. S. Bechara, L. Constantineau-Forget, G. Pelletier, N. M. Rachel, J. N. Pelletier, A. B. Charette, *J Org Chem* **2017**, *82*, 5046-5067; b) R. Pasternack, H. P. Laurent, T. Ruth, A. Kaiser, N. Schon, H. L. Fuchsbauer, *Anal Biochem* **1997**, *249*, 54-60.

Appendix

Table 4: Overview of the 32 sites that were investigated for mTG-mediated conjugation of the Fc and the respective oligonucleotides used for mutagenesis/cloning. Proteins were produced in 500mL scale and corresponding yields were calculated from the final volume after concentration using Amicon® filter units.

Position	**Forward**	**Sequence 5' - 3'**	**Reverse**	**Sequence 5' - 3'**	**Yield [mg/L]**
WT	hFc XbaI Up	GCGCGCTCTAGAAATAATTTTGTTTAACTTTAAGAAG GAGATATACATATGGAGCCCAAGAGCTGCGACAA	hFc XhoI Lo	GCGCGCCTCGAGGCCGGGGCTCAG GCTCAGGG	37.4
Q295N	hFc Q295N Up	CCCGGGAGGAAAATTACGCCAGCAC	hFc Q295N Lo	GGTCAGCACGGACACCACCCGGTAG	47.2
Lys246	hFc K246Q Up	TGTTCCCCCCACAGCCCAAGGACAC	hFc K246Q Lo	TTCGGGGGTCCGGCTGATCATCAGG	10.2
Met252	hFc M252Q Up	AGGACACCCTGCAGATCAGCCGGAC	hFc M252Q Lo	CACCACCACGCAGGTCACTTCGGGG	51.7
Ile253	hFc I253Q Up	ACACCCTGATGCAGAGCCGGACCCC	hFc I253Q Lo	GTCCACCACCACGCAGGTCACTTCG	88.2
Ser254	hFc S254Q Up	CCCTGATGATCCAGCGGACCCCCGA	hFc S254Q Lo	CACGTCCACCACCACGCAGGTCACT	23.0
Arg255	hFc R255Q Up	TGATGATCAGCCAGACCCCCGAAGT	hFc R255Q Lo	GGACACGTCCACCACCACGCAGGTC	4.8
Val282	hFc V282Q Up	ATGTGGACGGCCAGGAGGTGCACAA	hFc V282Q Lo	TTCCTCCCGGGGCTTGGTCTTGGCG	27.9
Glu283	hFc E283Q Up	TGGACGGCGTGCAGGTGCACAACGC	hFc E283Q Lo	ATTTTCCTCCCGGGGCTTGGTCTTG	14.0
Val284	hFc V284Q Up	ACGGCGTGGAGCAGCACAACGCCAA	hFc V284Q Lo	GTAATTTTCCTCCCGGGGCTTGGTC	/
His285	hFc H285Q Up	GCGTGGAGGTGCAGAACGCCAAGAC	hFc H285Q Lo	GGCGTAATTTTCCTCCCGGGGCTTG	9.1
Asn286	hFc N286Q Up	TGGAGGTGCACCAGGCCAAGACCAA	hFc N286Q Lo	GCTGGCGTAATTTTCCTCCCGGGGC	7.7
Ala287	hFc A287Q Up	AGGTGCACAACCAGAAGACCAAGCC	hFc A287Q Lo	GGTGCTGGCGTAATTTTCCTCCCGG	6.3
Lys288	hFc K288Q Up	TGCACAACGCCCAGACCAAGCCCCG	hFc K288Q Lo	GTAGGTGCTGGCGTAATTTTCCTCC	59.3
Thr289	hFc T289Q Up	ACAACGCCAAGCAGAAGCCCCGGGA	hFc T289Q Lo	CCGGTAGGTGCTGGCGTAATTTTCC	6.0
Lys290	hFc K290Q Up	ACGCCAAGACCCAGCCCCGGGAGGA	hFc K290Q Lo	CACCCGGTAGGTGCTGGCGTAATTT	8.9
Tyr296	hFc Y296Q Up	GGGAGGAAAATCAGGCCAGCACCTA	hFc Y296Q Lo	CACGGTCAGCACGGACACCACCCGG	11.2
Lys338	hFc K338Q Up	AAACCATCAGCCAGGCCAAGGGCCA	hFc K338Q Lo	GGTGTACACCTGGGGTTCTCTGGGC	/
Ala339	hFc A339Q Up	CCATCAGCAAGCAGAAGGGCCAGCC	hFc A339Q Lo	CAGGGTGTACACCTGGGGTTCTCTG	7.0
Lys340	hFc K340Q Up	TCAGCAAGGCCCAGGGCCAGCCCAG	hFc K340Q Lo	GGGCAGGGTGTACACCTGGGGTTCT	38.6
Gly341	hFc G341Q Up	GCAAGGCCAAGCAGCAGCCCAGAGA	hFc G341Q Lo	GGGGGGCAGGGTGTACACCTGGGGT	7.3
Pro343	hFc P343Q Up	CCAAGGGCCAGCAGAGAGAACCCCA	hFc P343Q Lo	TCTGCTGGGGGGCAGGGTGTACACC	6.7
Thr359	hFc T359Q Up	GAGATGAGCTGCAGAAGAACCAGGT	hFc T359Q Lo	GCCCTTCACCAGGCAGGTCAGGGAC	32.2
Lys360	hFc K360Q Up	ATGAGCTGACCCAGAACCAGGTGTC	hFc K360Q Lo	GAAGCCCTTCACCAGGCAGGTCAGG	47.6
Asn361	hFc N361Q Up	AGCTGACCAAGCAGCAGGTGTCCCT	hFc N361Q Lo	GTAGAAGCCCTTCACCAGGCAGGTC	27.0
Asn384	hFc N384Q Up	AGTGGGAGAGCCAGGGCCAGCCTGA	hFc N384Q Lo	AGGGGGGGTGGTCTTGTAGTTGTTC	16.4
Gly385	hFc G385Q Up	GGGAGAGCAACCAGCAGCCTGAGAA	hFc G385Q Lo	CACAGGGGGGGTGGTCTTGTAGTTG	20.4
Ser400	hFc S400Q Up	CTGTGCTGGACCAGGACGGCAGCTT	hFc S400Q Lo	CACGGTCAGTTTGGAGTACAGGAAG	12.6
Asp401	hFc D401Q Up	TGCTGGACAGCCAGGGCAGCTTCTT	hFc D401Q Lo	GTCCACGGTCAGTTTGGAGTACAGG	41.6
Gly420	hFc G420Q Up	GGTGGCAGCAGCAGAACGTGTTCAG	hFc G420Q Lo	CAGGGCCTCGTGCATCACGCTGCAG	15.6
Asn421	hFc N421Q Up	GGCAGCAGGGCCAGGTGTTCAGCTG	hFc N421Q Lo	GTGCAGGGCCTCGTGCATCACGCTG	17.1
His433	hFc H433Q Up	ACGAGGCCCTGCAGAACCACTACAC	hFc H433Q Lo	GGGGCTCAGGCTCAGGGACTTCTGG	23.5
Asn434	hFc N434Q Up	AGGCCCTGCACCAGCACTACACCCA	hFc N434Q Lo	GCCGGGGCTCAGGCTCAGGGACTTC	26.7
Pro445	hFc P445Q Up	TGAGCCTGAGCCAGGGCCTCGAGCA	hFc P445Q Lo	CGGATCTCAGTGGTGGTGGTGGTGG	14.0

8. Danksagung

An dieser Stelle würde ich gerne die Gelegenheit nutzen um allen Menschen, die mich auf meinem bisherigen Weg und besonders während der Anfertigung dieser Arbeit sowohl privat als auch beruflich begleitet haben, von ganzem Herzen zu danken!

An erster Stelle möchte ich meinem Doktorvater **Prof. Dr. Harald Kolmar** danken. In deiner Gruppe und unter deiner Federführung bin ich vom ungeschickten Bachelorpraktikanten zum immer noch ungeschickten aber halbwegs passablen Wissenschaftler gereift. Danke für spannende und produktive wissenschaftliche Diskussion, die auch gerne mal hitzig und zäh sein konnten. Für die äußerst produktiven letzten Jahren und die vielen Möglichkeiten, die du mir eröffnet hast. Danke Harald!

Prof. Dr. Beatrix Süß, **Prof. Dr. Siegfried Neumann** und **Prof. Dr. Hans-Lothar Fuchsbauer** für viele hilfreiche Anregungen und die Übernahme der 2. Korreferentin bzw. der Fachprüfung meiner Disputation.

Besonderer Dank gilt **meiner Familie** für ihre bedingungslose Unterstützung während meiner gesamten akademischen Ausbildung und persönlichen Entwicklung. Ohne euch wäre nichts davon auch nur ansatzweise möglich gewesen. Vielen herzlichen Dank!

Ganz besonders meiner Freundin **Franziska Ott**, für ihre Geduld, Verständnis und die vielen aufbauenden Worte in guten sowie schlechten Phasen. Danke, dass du immer an mich glaubst!

Dr. Andreas Christmann, der mir bei zahlreichen Problemstellungen mit Rat und Tat zur Seite stand. Wie oft du für mich das FACS reparierst hast, nachdem ich es verunstaltet habe, habe ich mittlerweile aufgehört zu zählen.

Dr. Olga Avrutina, dafür, dass sie mir englisches Schreiben beigebracht und meine sprachlichen Ergüsse in stilistische Meisterwerke verwandelt hat.

Allen meinen Co-Autoren und besonders **Dr. Aileen Ebenig**, **Dr. Norbert Egon Jüttner** und **Hendrik Schneider** für die gute und spannende Zusammenarbeit während unseren gemeinsamen Projekten.

Janna Sturm, Sebastian Bitsch, Sebastian Jäger, und allen anderen von mir betreuten Bachelor- und Masterstudenten. Ich hatte viel Spaß und unsere Zusammenarbeit sehr genossen!

Dr. Thomas Pirzer, Arturo Macarron, Ata Ali, Hendrik Schneider, Jan Habermann, Bastian Becker, Sebastian Bitsch und allen anderen Tischkicker-Spielern für viele spannende und nervenaufreibende Matches.

Den **Biochemical Borthers and Sisters** für eine unvergessene kämpferische Leistung, die mit dem Gewinn des ChemCups 2017, dem Höhepunkt meiner sportlichen Karriere, belohnt wurde.

Barbara Distelmann für ihre unermüdliche Hilfe bei allen bürokratischen und dokumentarischen Angelegenheiten. Ohne dich würde bei uns das Chaos ausbrechen.

Cecilia "Cilli" Gorus, deren unfassbar wichtige Rolle für unsere Gruppe immer dann bemerkbar wird, wenn sie ihren wohlverdienten Urlaub nimmt.

Dr. Julius Grzeschik für exzellente Beschallung während später Stunden im Labor, dem erweitert meines musikalischen Horizontes und unzähligen verstörenden Videos!

Dem Rest der Ferring Crew, **Jan Bogen, Dr. David Fiebig** und **Dr. Benjamin Mates** für die familiäre Zusammenarbeit in unserer kleinen Gruppe. Es macht jeden Tag Spaß mit euch zu arbeiten und ich freue mich auf unsere gemeinsame berufliche Zukunft!

Steffen Hinz, Simon Englert, Desislava Yanakieva, Adrian Elter, Dominic Happel, Lara Neureiter, Dana Schmidt, Anja Hofmann, Valentina Hilberg Dr. Doreen Könning, Dr. Christina Uth, Dr. Niklas Koch und dem gesamten Rest der Arbeitsgruppe Kolmar für technische Unterstützung, organisatorische Hilfe, obligatorische Mittagspausen um Punkt 11:15 Uhr und die vielen gemeinsamen Stunden auf Feiern, Radtouren, Alexander Marcus-konzerten und im KWT. Danke für die tolle Zeit!

I would also like to thank **Prof. Dr. Joelle Pelletier** for giving me the opportunity to do my research internship in her laboratory in Montréal. She and her group welcomed me with wide open arms and I had the most wonderful time during my stay in Canada. Thank you very much, I'm already looking forward to welcome you in Darmstadt!

Lorea Alejaldre and the other Chimuelos **Ferran Sanchjo** and **Ingrid Pulido** for introducing me to countless great people, showing me around in Montréal and teaching me a little Spanish. For our awesome trip to Quebec, hot yoga on Fridays, Game of Thrones Mondays, bicycle and hiking trips, poutine or sushi dinners and nights of heavy drinking. Thank you for the wonderful memories!

Kina Lafontaine for our great fun in the laboratory, trash bin-basketball in Kobe style, NBA final nights and always having an open ear, merci beaucoup!

Jonathan Besna, Ali Fendri, Adem Parisien and **Charlotte Skye** for fun times in the lab, at lunch and at the soccer field, for beer-and-chips and trips to the botanical garden. Thank you for being an awesome part of my journey!

9. Affirmations

Ludwig Lukas Deweid
Waldstraße 93
64319 Pfungstadt
Deweid@Biochemie-TUD.de
017632698275

Darmstadt, 29.11.2019

Erklärung

Ich erkläre hiermit, dass ich meine Dissertation selbstständig und nur mit den angegebenen Hilfsmitteln angefertigt habe.

Ludwig Lukas Deweid

Ludwig Lukas Deweid
Waldstraße 93
64319 Pfungstadt
Deweid@Biochemie-TUD.de
017632698275

Darmstadt, 29.11.2019

Erklärung

Ich erkläre hiermit, noch keinen Promotionsversuch unternommen zu haben.

Ludwig Lukas Deweid

Ludwig Lukas Deweid
Waldstraße 93
64319 Pfungstadt
Deweid@Biochemie-TUD.de
017632698275

Darmstadt, 29.11.2019

Erklärung

Ich erkläre hiermit, dass die elektronische Version der Doktorarbeit mit der schriftlichen Version übereinstimmt. Die elektronische Version liegt dem Prüfungssekretariat vor.

Ludwig Lukas Deweid